Title
New Mechanisms for Regeneration of Visual Pigments in the Vertebrate Retina

Author
Xu, Tongzhou

Publication Date
2017

Peer reviewed|Thesis/dissertation

UNIVERSITY OF CALIFORNIA

Los Angeles

New Mechanisms for Regeneration of Visual Pigments in the Vertebrate Retina

A dissertation submitted in partial satisfaction of the requirements for the degree Doctor of Philosophy

in Molecular, Cellular, and Integrative Physiology

by

Tongzhou Xu

2017

ABSTRACT OF THE DISSERTATION

New Mechanisms for Regeneration of Visual Pigments in the Vertebrate Retina

by

Tongzhou Xu

Doctor of Philosophy in Molecular, Cellular, and Integrative Physiology

University of California, Los Angeles, 2017

Professor Gabriel H. Travis, Chair

Vision begins when a photon is captured by a visual pigment in a photoreceptor cell. For most vertebrates, the light-sensitive chromophore in the visual pigment is 11-*cis*-retinaldehyde (11-*cis*-retinal), which is covalently bound to the protein moiety, opsin, through a Schiff base linkage. The absorption of a photon isomerizes 11-*cis*-retinal to its all-*trans*-isomer and activates the visual pigment. In vertebrate ciliary photoreceptors, after a brief activation, the pigment decays to yield apo-opsin and free all-*trans*-retinal. Light sensitivity restoration in photoreceptor cells occurs following re-isomerization of all-*trans*-retinal to 11-*cis*-retinal by enzymatic pathways termed “visual cycles”. At present, two visual cycles have been established: (1) A well understood canonical visual cycle between RPE cells and photoreceptors, with RPE65 as its retinoid isomerase (Isomerase I); (2) A relatively under characterized alternate visual cycle between Müller cells and cones, with an unknown retinoid isomerase (Isomerase II). Recently, we have identified dihydroceramide desaturase-1 (DES1) as a novel retinoid isomerase and a strong candidate for Isomerase II. In this dissertation, follow-up biochemical

characterizations of DES1 were performed. Our results suggest that DES1 coimmunoprecipitates with cellular retinaldehyde-binding protein (CRALBP). Its retinoid isomerase activity appears to (1) rely on the cytochrome b5 electron transport chain, (2) involve a free radical intermediate(s) and (3) an iron (iii) co-factor **(Chapter 2.1)**. A Des1-/- mouse model was also investigated. Although neither obvious retina morphological abnormality nor significant reduction of visual chromophore after overnight dark-adaptation was observed in Des1-/- mice, the key point, their ability to recover cone sensitivity after bleach, has not been tested. Further studies are needed to address the physiological role of DES1 in the alternate visual cycle **(Chapter 2.2)**. Furthermore, attempts were made to identify a putative retinol dehydrogenase in cones that enable them to utilize the alternate visual cycle for pigment regeneration exclusively. But this enzyme remains unidentified despite our efforts **(Chapter 2.3)**. Besides the two known enzymatic visual cycles, we also identified a novel non-enzymatic photoisomerization pathway for functional visual pigment regeneration in the vertebrate retina with a photoactive intermediate, N-retinylidene-phosphatidylethanolamine (N-ret-PE) **(Chapter 3)**. Our findings greatly promote the current understanding of visual pigment regeneration mechanisms.

The dissertation of Tongzhou Xu is approved.

Alapakkam P. Sampath

Hui Sun

Xianjie Yang

Gabriel H. Travis, Committee Chair

University of California, Los Angeles

2017

DEDICATION

I dedicate this dissertation with the deepest gratitude to my beloved parents, grandparents and relatives. It would have been impossible for me to make this achievement without their unconditional love and constant encouragement!

I also dedicate this dissertation to all my previous teachers for their hard work of teaching and inspiring, and all my friends for their kind help and support!

Thank you all so much!

TABLE OF CONTENTS

LIST OF FIGURES

LIST OF TABLE(S)

LIST OF ABBREVIATIONS

4-hydroxy-TEMPO (4HT)	4-hydroxy-2,2,6,6-tetramethylpiperidine-1-oxyl
A2E	N-retinylidene-N-retinylethanolamine
ADH7	Alcohol dehydrogenase 7
ARAT	Acyl CoA: retinol acyltransferase
BIPY	2,2'- bipyridyl
BSA	Bovine serum albumin
CRALBP	Cellular retinaldehyde-binding protein
CRBP	Cellular retinol-binding protein
COO	Carotenoid cleavage oxygenase
DA	Dark-adapted
DCPIP	2,6-Dichloroindophenol
DES1	Dihydroceramide desaturase-1
DHRS1,3	Dehydrogenase/reductase member 1,3
DMPIO	2,2-dimethyl-4-phenyl-2H-imidazole-1-oxide
DMPO	5,5-dimethyl-1-pyrroline-N-oxide
DOPC	1,2-dioleoyl-sn-glycero-3-phosphocholine
DOPE	1,2-dioleoyl-sn-glycero-3-phosphoethanolamine
ENDOR	Electron-nuclear double resonance
EPR	Electron paramagnetic resonance
ER	Endoplasmic reticulum
ERG	Electroretinography
GPCR	G protein-coupled receptor
GRK-1	G protein-coupled receptor kinase 1
HMB	4-(hydroxymercuri) benzoic acid
HPLC	High-performance liquid chromatography
IRBP	Interphotoreceptor retinoid-binding protein
IS	Inner segment
LRAT	Lecithin: retinol acyltransferase
MFAT	Multifunctional O-acyltransferase

NAD	Nicotinamide adenine dinucleotide
NADP	Nicotinamide adenine dinucleotide phosphate
NCBI	National center for biotechnology information
NEM	N-ethylmaleimide
N-ret-PE	N-retinylidene-phosphatidylethanolamine
OS (ROS/COS)	Outer segment (rod/cone outer segment)
PBN	N-tert-Butyl-α-phenylnitrone
PC	Phosphatidylcholine
PCR	Polymerase chain reaction
PDE	Phosphodiesterase
PE	Phosphatidylethanolamine
PIH	Pyridoxal isonicotinoyl hydrazone
PTMIO	4-phenyl-2,2,5,5-tetramethyl-3-imidazoline-1-oxyl nitroxide
PTU	6-propyl-2-thiouracil
RDH	Retinol dehydrogenase
RGR	Retinal G protein-coupled receptor
RPE	Retinal pigment epithelium
RPE65	Retinal pigment epithelium-specific 65 kDa protein
RAL	Retinaldehyde
RT	Room temperature
ROL	Retinol
ROX	Retinaldehyde oximes
SDR	Short-chain dehydrogenase/reductase
SDS	Sodium dodecyl sulfate
TFA	Trifluoroacetic acid

ACKNOWLEDGEMENTS

My deepest gratitude goes to my Ph.D. advisor, Prof. Gabriel H. Travis. He supported me without reservation and inspired me throughout my Ph.D. studies. He provided me with constructive instructions and invaluable suggestions. He dedicated his time and efforts teaching and helping me in those days and nights during my Ph.D. life. I would not have achieved this point without his constant guidance, encouragement and support! He is my role model! Thank you so much!

My sincere gratitude goes to Dr. Joanna J. Kaylor. During these years, she enthusiastically encouraged me and patiently taught me various experimental skills. She provided me with insightful comments and suggestions in my research and closely collaborated with me in a lot of studies. She is always available and ready to help. She is an excellent teacher, fantastic colleague and great friend! Thank you so much!

My special gratitude goes to Dr. Quan Yuan. He was the person who met me the first time I came to UCLA as an exchange student and introduced me to the lab. He was the person who showed me the ropes and substantially helped me when I was new to the lab and encountered a lot of difficulties. He taught me a lot of biochemical knowledge, trained me up for many lab techniques, and instructed and collaborated with me in multiple experiments, some of which are presented in this dissertation (in **Chapter 2.1**). I would not have made such progress without him! Thank you so much!

My heartfelt gratitude goes to Prof. Roxana A. Radu. She was extremely friendly and helpful to me over these years. She helped me dissect a lot of mouse tissues, including most of the tissues used in the experiments presented here. She also provided me with

excellent scientific suggestions during lab meetings and helped me with some experiments. This dissertation would be impossible without her! Thank you so much!

My earnest gratitude goes to Dr. Jeremy D. Cook. We had a great time during these years in the lab, from the old building to the new one. He was happy to help anytime I needed. He provided me with helpful advice on my experiments and showed me the techniques of immunofluorescence and imaging with a confocal microscope. We are good friends both in the lab and outside! He made my Ph.D. life more exciting and easier! Thank you so much!

My sincere gratitude goes to Avian Tsan and Zhichun (Isabelle) Jiang. They helped me a lot during these years, especially with the maintenance of the mice colony. They provided great support in some of our experiments as well. Zhichun (Isabelle) Jiang also helped me with some RNA extractions and animal handling in a few experiments presented here. This work would never be completed without them! Thank you both so much!

My special gratitude goes to Prof. Gordon L. Fain and Norianne T. Ingram. They are great collaborators! They designed and performed the electrophysiological studies in the publication reprinted in **Chapter 3.2**. This work would be impossible without their strong support and significant contribution. Thank you both so much!

I would like to give my cordial thanks to Shannan Eddington. She significantly contributed to the morphology studies of the Des1 mice (in **Chapter 2.2**). She showed

me perfusion techniques, prepared the sections, and collected many light microscopic images with me. These data would not exist otherwise. Thank you so much!

I would like to give my earnest thanks to Jacob Makshanoff and Nicholas Bischoff. They worked in our lab previously and provided great help in our studies. Jacob showed me many lab techniques when I just joined the lab. Nicholas helped me maintain the mice colony and gave me a lot of technical assistance in several experiments. Thank you both so much!

I would like to express my special thanks to Drs. Nathaniel Roybal and Shanta Sarfare, both of whom taught me a lot at the beginning of my Ph.D. studies. Thank you both so much!

I would like to say many thanks to Hayk Hakobyan, Eunice Ng and Lily Yuan. They provided me with technical assistance and were great to work with. Thank you all so much!

I would like to give my warm thanks to Rikard Frederiksen. He is currently collaborating with us on an ongoing project and is really kind and helpful. Thank you so much! I would like to say a lot thanks to Drs. Tamara L. Lenis, and Ala Morshedian, for their suggestions and help in my Ph.D. studies. Thank you both so much!

I would like to thank my other current and previous labmates, Robert A. Valencia, Anita Kim, Jessica Gomez, Jay Yu, Cindy Ruan and Tran Nguyen, two former exchange students in the Cross-disciplinary Scholars in Science and Technology (CSST) Program, Zhanlin Zhao and Pengfei Cheng, and the undergraduate students who

worked with me, Aileen Nuñez and Sally (Won Kyung) Oh, for their support and help. Thank you all so much!

I want to express my deep gratitude to Profs. Steven Nusinowitz and Dean Bok for their helpful comments and suggestions in my research. Thank you both all so much!

I want to express my heartfelt and special thanks to my other dissertation committee members, Profs. Alapakkam P. Sampath, Hui Sun and Xianjie Yang for their continuous instructions, help and inspiration! I am eternally grateful for all your support! You are all my role models! Thank you all so much!

I want to express my sincere and special thanks to Drs. Ren Sun, Yibin Wang, Thomas M Vondriska and other professors in the CSST program. This exchange program offered me the opportunity to study abroad for the first time, opened the door to UCLA for me and changed my life and career completely! Thank you so much!

I want to express my sincere acknowledgments to Dr. Minghao Jin for his previous work which provided hints to the study in **Chapter 2.3**, as well as the generous gift of a mouse SDR9C7 cDNA clone. I want to express my sincere acknowledgements to to Dr. Vladimir J. Kefalov for the generous gift of *rd*7 mice, to Dr. Krzysztof Palczewski for the generous gift of an anti-LART antibody, to Dr. Scott A. Summers for the generous gift of an anti-DES1 antibody, to Dr. Jian-Xing Ma for the generous gift of a human RDH10 cDNA clone, to Dr. Rosalie K. Crouch for the generous gift of 11-*cis*-retinal. I want to express my sincere acknowledgments to Dr. Catherine Bowes Rickman and Dr. S. Lawrence Zipursky for sharing their unpublished data and valuable scientific opinions,

which were highly helpful to the studies presented in **Chapter 2.3**. Thank you all so much!

I want to express my profound acknowledgments again to all our collaborators/co-authors in the two publications reprinted/adapted in this dissertation (listed below). Thank you all so much!

Finally, I would like to express my sincere acknowledgements to our funding sources, which are essential to this work: US National Eye Institute R01 Grants EY011713, EY024379 and EY0001844, the National Eye Institute Core Grant P30EY00331, a Research to Prevent Blindness Unrestricted Grant to the Jules Stein Eye Institute, the Charles Kenneth Endowed Professorship (to Prof. Gabriel H. Travis). China Scholarship Council affiliated with the Ministry of Education of China also supported me with a China Scholarship Council (CSC) Scholarship.

Copyright permissions:

A portion of **Chapter 2.1** is adapted with permission from the publication: Joanna J. Kaylor, Quan Yuan, Jeremy Cook, Shanta Sarfare, Jacob Makshanoff, Anh Miu, Anita Kim, Paul Kim, Samer Habib, C. Nathaniel Roybal, Tongzhou Xu, Steven Nusinowitz, and Gabriel H. Travis (2013). Identification of DES1 as a vitamin A isomerase in Müller glial cells of the retina. *Nat Chem Biol*. 9(1):30-36. doi:10.1038/nchembio.1114.
I contributed to the experiments of coimmunoprecipitation of CRALBP with DES1 and the inhibition of DES1 isomerase activity by dihydroceramide and its analog.

Profs. Gabriel H. Travis and Steven Nusinowitz are the principal investigators. The author contributions have been stated in this publication:

> "G.H.T. conceived the project. G.H.T., J.J.K., C.N.R., Q.Y., and S.N. designed the experiments and interpreted the data. J.J.K., Q.Y., J.C., S.S., J.M., A.M., A.K., P.K., S.H., T.X., and C.N.R. performed the experiments. G.H.T. wrote the manuscript." (Kaylor, Yuan et al. 2013)

Chapter 3.2 is a reprint (with permission) of the publication: Joanna J. Kaylor, Tongzhou Xu, Norianne T. Ingram, Avian Tsan, Hayk Hakobyan, Gordon L. Fain and Gabriel H. Travis (2017). Blue light regenerates functional visual pigments in mammals through a retinyl-phospholipid intermediate. *Nat Commun*. 8(1):16. doi:10.1038/s41467-017-00018-4.

A small portion of **Chapter 3.1** is also adapted from this publication.

Profs. Gabriel H. Travis and Gordon L. Fain are the principal investigators.

The author contributions have been stated in this publication:

> "J.J.K. designed and performed the experiments on bovine OS, mouse retinas, and live mice. T.X. designed and performed experiments on photoisomerization of N-ret-PE in solution and the quantum efficiency determination. N.T.I. helped design and performed whole-retina and suction-electrode cone recording experiments. A.T. performed experiments on OS and in live mice. H.H. performed experiments on OS and mouse retinas. G.L.F. helped design the experiments in Fig. 5, analyzed data from whole-retina and suction-electrode cone recording experiments, and wrote this section of the manuscript. G.H.T.

conceptualized the study, analyzed the data, and wrote the manuscript." (Kaylor, Xu et al. 2017)

Figure 1-2 and its legend are reproduced with permission from the publication: Joanna J. Kaylor, Jeremy D. Cook, Jacob Makshanoff, Nicholas Bischoff, Jennifer Yong, and Gabriel H. Travis (2014). Identification of the 11-*cis*-specific retinyl-ester synthase in retinal Müller cells as multifunctional O-acyltransferase (MFAT). *Proc Natl Acad Sci U S A*. 111(20):7302-7307. doi: 10.1073/pnas.1319142111.

VITA

EDUCATION

Ph.D. Candidate, Molecular, Cellular, and Integrative Physiology Program
University of California, Los Angeles (UCLA), USA 2011-2017 (expected)

Exchange Student, Cross-disciplinary Scholars in Science and Technology (CSST) Program
UCLA, USA Summer 2010 and Winter 2011

Graduate Student, Zhejiang University School of Medicine, China 2010-2011

Medical Degree, Zhejiang University School of Medicine, China 2005-2010

Minor, Public Administration (UPA Program), Chu Kochen Honors College, Zhejiang University, China 2007-2010

PROFESSIONAL QUALIFICATION

National Qualification for Medical Practitioners Licensed by the Ministry of Public Health (National Health and Family Planning Commission) of China

PUBLICATIONS

Kaylor JJ, **Xu T**, Ingram NT, Tsan A, Hakobyan H, Fain GL, Travis GH (2017). Blue light regenerates functional visual pigments in mammals through a retinyl-phospholipid intermediate. *Nat Commun*. 8(1): 16. doi:10.1038/s41467-017-00018-4.

Kaylor JJ, Yuan Q, Cook J, Sarfare S, Makshanoff J, Miu A, Kim A, Kim P, Habib S, Roybal CN, **Xu T,** Nusinowitz S, Travis GH (2013). Identification of DES1 as a vitamin A isomerase in Müller glial cells of the retina. *Nat Chem Biol*. 9(1): 30-36. doi:10.1038/nchembio.1114.

PRESENTATIONS

Tongzhou Xu. Functional Mammalian Visual Pigments are Regenerated by Blue Light through a Retinyl-phospholipid Intermediate. The Biology & Chemistry of Vision, Federation of American Societies for Experimental Biology, 2017. Oral Presentation.

Tongzhou Xu, Quan Yuan, Joanna J. Kaylor, Avian Tsan and Gabriel H. Travis. The Role of Free Radicals in Thermal, Light-driven and Enzyme-catalyzed Isomerization of Retinoids. The Association for Research in Vision and Ophthalmology Annual Meeting, 2016. Poster.

TOP AWARDS/HONORS

National Scholarships in 2008 and 2009, both awarded by the Ministry of Education of China
CSC Scholarship in 2011, awarded by the China Scholarship Council (CSC) affiliated with the Ministry of Education of China

Chapter 1: Introduction to visual chromophore regeneration

1.1 Brief introduction to photoreceptor cells in the vertebrate retina

Vision is one of the most important senses to humans and animals. Through this process, light passes through the optical media and reaches the retina. There, the photons are detected by light-sensitive molecules termed visual pigments in a specialized type of cells, the photoreceptors. Subsequently, a cascade of biological and electrophysiological reactions is triggered, which finally sends signals to the visual cortex to encode the surrounding environment. A conventional camera is a common analogy used to describe the eye and the retina is likened to the film, indicating the importance and major function of the retina, which is probably still oversimplified. Considering the evolutionary relevance to human beings, this dissertation will mainly focus on the vision of vertebrates, especially mammals.

A mammalian retina is laminated into several different layers (Wilkinson-Berka 2004, Willermain, Libert et al. 2014) and contain many distinct types of neurons, including photoreceptor cells, horizontal cells, amacrine cells, bipolar cells and retinal ganglion cells (for detailed cell types, refer to (Masland 2001, Masland 2012)). Amongst them, the photoreceptor cells serve as primary light-sensors for image-forming and are the focus of this research. In addition to neurons, there are also other non-neuron cells, including the Müller cells. Müller cells are a type of neuroglia and have a variety of biological functions in the retina, including the support of retina structure, maintenance of retina homeostasis, regulation of neuronal metabolism, etc. (see (Vecino, Rodriguez et al. 2016) for a review). In addition, they contribute to visual acuity by lowering light scattering (Franze, Grosche et al. 2007, Agte, Junek et al. 2011). They are also closely related to our research, which will be discussed later. To the exterior of the retina (the

neural retina) lies the retinal pigment epithelium (RPE) cells. They are a single layer of pigmented epithelial cells and perform several crucial functions. For example, they closely interact with photoreceptors and maintain their integrity through the phagocytosis of dated outer segments; they can release neurotrophic factors and are involved in visual pigment regeneration (Strauss 2005, Strauss 2016).

The vertebrate retina can detect light with a wide range of intensities thanks to the division of work by the two major types of photoreceptor cells, rods and cones (Govardovskii, Calvert et al. 2000). Rods are highly light sensitive, capable of responding to just a single photon (Baylor, Lamb et al. 1979), but become saturated under moderate light intensity (Green 1971, Baylor, Nunn et al. 1984, Kefalov 2012). Cones, on the other hand, are less sensitive and difficult to saturate (Boynton and Whitten 1970, Baylor 1987, Kefalov 2012). Therefore, dim light vision is mainly mediated by rods while bright light vision is mediated by cones (Wang and Kefalov 2011), together extending the range of light detection by the retina.

The major light-sensing machinery in rods and cones is located in their membranous outer segments (OS). The rod outer segments (ROS) are usually cylindrically shaped and contains a stack of closed membranous discs that are discontinuous with the plasma membrane (Arikawa, Molday et al. 1992, Molday and Moritz 2015). The cone outer segments (COS), on the other hand, are usually conically shaped and shorter. They comprise a series of membranous invaginations that are continuous with the plasma membranes (Arikawa, Molday et al. 1992, Mustafi, Engel et al. 2009, Molday and Moritz 2015).

1.2 Retinoids, visual pigments and light detection

Retinoids are a class of chemicals that include vitamin A and its derivatives. They have several geometrical configurations including all-*trans*- and several *cis*- and di-*cis*-isomers (such as 11-*cis*-, 13-*cis*-, 9-*cis*-, 9,13-di-*cis*-isomers) (Kaylor, Yuan et al. 2013). The all-*trans*-isomer is sterically planar and the most stable configuration, while the *cis*- and di-*cis*-isomers contain sterically hindered conformations and are therefore less stable due to the increased conformational energy (Rowan, Warshel et al. 1974, Warshel and Huler 1974, Warshel, Huler et al. 1974, Kiser, Golczak et al. 2014). For example, there is a 4.1 kcal/mol energy difference between 11-*cis*- and all-*trans*-retinals (determined in an equilibrium reaction at 50 °C) (Rando and Chang 1983). The conformational change between retinoid isomers can be catalyzed by light and multiple chemicals (Hubbard, Bownds et al. 1965, Hubbard 1966, Kropf and Hubbard 1970, Futterman and Rollins 1973, Rando and Chang 1983).

Retinoids have multiple critical biological functions, one of which is to form light-sensing molecules in a wide range of living creatures (Zhong, Kawaguchi et al. 2012). The light-sensing molecules in vertebrate photoreceptors are visual pigments, which consist of a chromophore and a protein moiety. So far all known visual pigments are retinoid-based and almost always use 11-*cis*-retinal or its derivatives as their chromophores (Saari 2012), including 11-*cis*-retinal (vitamin A1), 11-*cis*-3-dehydroretinal (vitamin A2), 3-hydroxy-11-*cis*-retinal (vitamin A3), or 4-hydroxy-11-*cis*-retinal (vitamin A4) (Babino, Golczak et al. 2016). The chromophore is bound to the protein moiety, opsin, through a protonated Schiff base to a lysine residue (the 296th amino acid in bovine rhodopsin) and interacts with a glutamic acid as the counterion (the 113th amino acid in bovine

rhodopsin) (Sakmar, Franke et al. 1989). All the opsins in metazoans are members of the G protein-coupled receptor (GPCR) family, for the majority of which 11-*cis*-retinal (A1) is the chromophore (Nakanishi 1991, Zhong, Kawaguchi et al. 2012). Two major types of opsins exist in vertebrates, visual opsins and non-visual opsins. The former contributes to image-forming and is closely related to this study, which includes rhodopsin (the opsin in rods) and several cone opsins (the opsins predominantly in cones), such as S-, M1-, M2- and L-opsins (Shichida and Matsuyama 2009). (The latter is not the focus of this dissertation. For a review, refer to (Shichida and Matsuyama 2009)).

How is light detected by vertebrate photoreceptors? It involves an amplified signaling pathway known as visual transduction cascade. Its mechanism is similar in both rods and cones (Wang and Kefalov 2011), although many of the proteins are different. Phototransduction in rods is more intensively studied and will be described as the representative model below.

When a photon reaches the retina, it is absorbed by the visual pigment, rhodopsin, causing the isomerization of the visual chromophore, 11-*cis*-retinal (11-*cis*-RAL) to its all-*trans*-isomer (Kaylor, Yuan et al. 2013). Subsequently, a series of fast conformational changes of rhodopsin is triggered, leading to the formation of a signaling state, metarhodopsin II (Meta II) (Okada, Ernst et al. 2001). Meta II stimulates the α-subunit of transducin (a heterotrimeric G protein consisting of α, β and γ subunits), resulting in its dissociation followed by its activation of a cGMP-specific phosphodiesterase (PDE), which hydrolyzes cGMP. This causes closure of the cation

selective cGMP-gated channels in ROS, hyperpolarization of the cell and reduced release of neurotransmitter at the photoreceptor synapse. This sends signals to the second order neurons, the bipolar cells (Arshavsky, Lamb et al. 2002, Luo, Xue et al. 2008, Arshavsky and Burns 2014, Palczewski 2014).

After signal transmission, this cascade is turned off and the photoreceptor cell is returned to its dark state. Details of this process are beyond the scope of this dissertation and can be found in (Burns and Baylor 2001, Arshavsky, Lamb et al. 2002, Lamb and Pugh 2006, Molday and Moritz 2015). As for Meta II, it finally decays to all-*trans*-retinal and unliganded opsin (Wald 1968, Okada, Ernst et al. 2001) after its phosphorylation by G protein-coupled receptor kinase 1 (GRK-1) and binding by arrestin (Koch and Dell'Orco 2015).

1.3 Visual chromophore regeneration and the visual cycle(s)

As aforementioned, one molecule of 11-*cis*-retinal is consumed for each photon detected. While the total number of visual pigments in a photoreceptor is limited (it is estimated to be about 10^7 to 10^8 per rod in mammals (Kefalov 2012)), 11-*cis*-retinal must be regenerated from its photoisomerized isomer, all-*trans*-retinal (all-*trans*-RAL), to maintain the light sensitivity of photoreceptors. In vertebrates, this re-isomerization process is carried out by enzymatic pathway(s) termed “visual cycle(s)” or “retinoid cycle(s)”. Currently, two pathways of visual cycles have been established, (1) the canonical visual cycle between the RPE cells and rod/cone photoreceptors (also known as “the RPE visual cycle”) and (2) an alternate visual cycle between the Müller cells and

cones (also referred to as “the cone visual cycle”, “the retina visual cycle”, “the Müller cell visual cycle”, etc.).

The canonical visual cycle has been well-established and is described in detail by several recent review papers (Travis, Golczak et al. 2007, Saari 2012, Tang, Kono et al. 2013, Kiser and Palczewski 2016, Sahu and Maeda 2016), as well as our published article (Kaylor, Yuan et al. 2013). **Fig.1-1** is a summary of this pathway using rod photoreceptor as an example (similar biological reactions happen in both rods and cones). 11-*cis*-RAL is bound to an opsin (11-*cis*-retinylidene) in the dark state and is isomerized to all-*trans*-RAL after photon absorption, transiently converting rhodopsin to its signaling state Meta II. Meta II triggers the phototransduction cascade, then decays releasing apo-opsin and free all-*trans*-retinal. The latter is translocated from the ROS disc membranes to the cytoplasm by an ATP-binding cassette transporter (ABCA4), and is subsequently reduced by retinol dehydrogenases to all-*trans*-retinol (all-*trans*-ROL). All-*trans*-ROL is transported to RPE cells by interphotoreceptor retinoid-binding protein (IRBP), where it is transferred to cellular retinol-binding protein-1 (CRBP1) (Bok, Ong et al. 1984, Edwards and Adler 1994). The major ester synthase in RPE cells, lecithin: retinol acyltransferase (LRAT), esterifies all-*trans*-retinol to all-*trans*-retinyl ester (all-*trans*-RE) and converts the fatty acyl group donor phosphatidylcholine (PC) to lyso-PC simultaneously. All-*trans*-RE is then converted to 11-*cis*-retinol (11-*cis*-ROL) by the retinoid isomerase, retinal pigment epithelium-specific 65 kDa protein (RPE65) (Redmond, Yu et al. 1998, Jin, Li et al. 2005, Moiseyev, Chen et al. 2005, Redmond, Poliakov et al. 2005). This is an endergonic reaction (ΔG° = +4.13 kcal/mol (Rando and Chang 1983)) and is thought to be driven by the coupled hydrolysis of the all-*trans*-RE

substrate (ΔG° ≥ -5 kcal/mol approximately) (Deigner, Law et al. 1989). 11-*cis*-retinol binds to CRALBP with high affinity (Saari and Bredberg 1987, Golovleva, Bhattacharya et al. 2003), and is further oxidized to 11-*cis*-retinal by retinol dehydrogenases in RPE cells. The interaction of CRALBP/11-*cis*-retinal with acidic lipids (indicated by +/- charges in the figure) on the plasma membranes unloads 11-*cis*-retinal (Saari, Nawrot et al. 2009), which is then transported again by IRBP to rod photoreceptor where it binds to apo-opsin and forms a new visual pigment.

Several retinol dehydrogenases (RDHs) are possibly involved in the visual cycle(s). The reduction of all-*trans*-retinal to all-*trans*-retinol in photoreceptors is believed to be catalyzed by RDH8 and RDH12 (Janecke, Thompson et al. 2004, Maeda, Maeda et al. 2005, Maeda, Maeda et al. 2006, Maeda, Maeda et al. 2007, Parker and Crouch 2010, Kiser, Golczak et al. 2012, Lhor and Salesse 2014, Sahu and Maeda 2016). The study of RDH8 deficient mice found that the phenotype is only evident after bright light illumination, which includes delayed recovery of rod sensitivity and significant all-*trans*-retinal accumulation, indicating RDH8 is not the only enzyme responsible for the reduction of all-*trans*-retinal (Maeda, Maeda et al. 2005). Although RDH12 deficiency is related to childhood-onset severe retinal dystrophy in humans (Janecke, Thompson et al. 2004), studies of RDH12 deficient mice revealed only a weak phenotype (Maeda, Maeda et al. 2006, Kurth, Thompson et al. 2007, Maeda, Maeda et al. 2007). In the retina of RDH8-/- RDH12-/- double knockout mice, a significant decrease of the all-*trans*-retinal reduction activity has been observed, and it has been estimated that 30% of this reduction activity is attributed to RDH12 while 70% is attributed to RDH8 (Maeda, Maeda et al. 2007).

The oxidation of 11-*cis*-retinol to 11-*cis*-retinal is believed to be catalyzed by RDHs such as RDH5, RDH11 and perhaps also RDH10 (Driessen, Janssen et al. 1995, Yamamoto, Simon et al. 1999, Jang, Van Hooser et al. 2001, Haeseleer, Jang et al. 2002, Farjo, Moiseyev et al. 2009, Parker and Crouch 2010, Lhor and Salesse 2014, Sahu, Sun et al. 2015, Sahu and Maeda 2016). RDH5 deficient mice are still able to regenerate 11-*cis*-retinal, although delayed dark adaptation is observed under bright light, suggesting RDH5 is needed but not the only 11-*cis*-retinol oxidase (Driessen, Winkens et al. 2000). RDH11 deficient mice do not show a strong phenotype (Kasus-Jacobi, Ou et al. 2005, Kim, Maeda et al. 2005), but the study of RDH5-/- RDH11-/- double knockout mice suggests that RDH11 plays a minor role in the visual cycle and indicates that an additional RDH may exist (Kim, Maeda et al. 2005). RDH10 is another retinol dehydrogenase in RPE cells (Wu, Chen et al. 2002) which can oxidize 11-*cis*-retinol (Farjo, Moiseyev et al. 2009). RDH10 deficiency is embryonically lethal (Sandell, Sanderson et al. 2007). Delayed dark adaptation has been observed in mice with conditional RDH10 knockout in RPE cells under bright light, but the conditional disruption of RDH10 does not seem to affect retinal morphology, suggesting it plays a complementary role to other RDHs (Sahu, Sun et al. 2015). Overall, these suggest a high redundancy of RDHs in the visual cycle.

Despite the establishment of this pathway, accumulating lines of evidence challenge the concept that this is the sole source of the visual chromophore and indicate the existence of another pathway. Such evidence (also discussed in our published article (Kaylor, Yuan et al. 2013)) include but are not limited to: (1) Early studies in isolated retina suggested the possible regeneration of visual pigment without RPE (Goldstein 1967,

Goldstein 1968, Cone and Brown 1969, Baumann 1970, Goldstein 1970, Goldstein and Wolf 1973, Hood and Hock 1973). (2) It was reported that isolated salamander rods can only utilize 11-*cis*-retinal but not 11-*cis*-retinol for dark adaptation while cones can use both (Jones, Crouch et al. 1989). Similar phenomena have been observed by later studies (Ala-Laurila, Cornwall et al. 2009, Wang, Estevez et al. 2009, Wang and Kefalov 2009, Sato and Kefalov 2016). This selectivity seems to be independent of the type visual pigment (Ala-Laurila, Cornwall et al. 2009, Sato and Kefalov 2016). (3) Based on a biochemical estimation, the RPE visual cycle is too slow (about “50-fold slower”) to maintain light sensitivity in bright light condition (Mata, Radu et al. 2002). (4) As has been pointed out, cones are in a disadvantageous situation compared to rods regarding chromophore competition and transportation, and visual pigment stability, indicating the need for an alternative pathway in which cones have priority (Wang and Kefalov 2011). (5) It has been reported (Das, Bhardwaj et al. 1992) that Müller cells in the chicken retina can convert all-*trans*-retinol to 11-*cis*-retinol, 11-*cis*- and all-*trans*-retinyl palmitates, indicating the presence of a retinoid isomerase and a retinyl ester synthase activity. Retinoid isomerase activity has also been observed in the retinas of cone-dominant animals (Mata, Radu et al. 2002, Mata, Ruiz et al. 2005, Muniz, Betts et al. 2009). (6) An 11-*cis*-retinyl-ester synthase activity in the retina was reported, which utilizes palm-CoA as an acyl donor and is different from LRAT (Mata, Radu et al. 2002). This activity has been later confirmed to be an acyl CoA: retinol acyltransferase (ARAT) activity and is thought to be attributed to the Müller cells (Mata, Ruiz et al. 2005, Muniz, Villazana-Espinoza et al. 2006). (7) Several visual cycle-related proteins are expressed in Müller cells in the retina, such as RDH10 (Wu, Moiseyev et al. 2004), cellular

retinaldehyde-binding protein (CRALBP) (Bunt-Milam and Saari 1983, Das, Bhardwaj et al. 1992) and cellular retinol-binding protein (CRBP) (Bok, Ong et al. 1984, Eisenfeld, Bunt-Milam et al. 1985). (8) Physiological studies further support pigment regeneration in retinas from several rod-dominant species including mouse (Wang, Estevez et al. 2009, Wang and Kefalov 2009), human, primate (Wang and Kefalov 2009) and salamander (Wang, Estevez et al. 2009). The location of retinoid isomerization in the retina is again attributed to Müller cells by experiments using a Müller cell-specific inhibitor, L-alpha-aminoadipic acid (Wang, Estevez et al. 2009, Wang and Kefalov 2009).

The above evidence strongly suggests the existence of an alternate visual cycle in the retina supporting cone visual pigment regeneration and demonstrates its localization in the Müller cells. However, some essential components in the canonical visual cycle, such as the retinoid isomerase, RPE65 and the ester synthase, LRAT, are predominantly restricted to RPE cells and are not detected in Müller cells (Mata, Radu et al. 2002, Muniz, Betts et al. 2009). Furthermore, the new retinoid isomerase (referred to as “Isomerase II”, following RPE65 as “Isomerase I”) in the retina seems to use all-*trans*-retinol as its substrate instead of all-*trans*-retinyl esters (Das, Bhardwaj et al. 1992, Mata, Radu et al. 2002, Mata, Ruiz et al. 2005, Muniz, Betts et al. 2009). These suggest that the machinery between the alternate and the canonical visual cycles are somehow different.

Recently, our lab has been dedicated to the study of the visual cycles and the identification of the necessary components of the alternate visual cycle machinery.

Identifying the retinoid isomerase in the alternate visual cycle was our primary goal. In 2013, we identified dihydroceramide desaturase-1 (DES1) as a retinol isomerase and a strong candidate for Isomerase II (Kaylor, Yuan et al. 2013). DES1 is expressed in the Müller cells and catalyzes retinol isomerization with the ratios of different isomers similar to that catalyzed by iodine at the equilibrium phase. An i*n vivo* rescue study with Rpe65 deficient mice and RNAi knockdown experiments in cultured Müller cells all strongly suggest its role as Isomerase II in the retina visual cycle (Kaylor, Yuan et al. 2013). Shortly after, colleagues in our lab identified multifunctional O-acyltransferase (MFAT) as an 11-*cis*-specific retinyl ester synthase in Müller cells, which is an ARAT and can promote the 11-*cis*-retinol formation catalyzed DES1 through mass action (Kaylor, Cook et al. 2014).

Based on previous evidence and our two recent studies, a model of the alternate visual cycle has been proposed (Kaylor, Cook et al. 2014) (**Fig.1-2 and its legend** (reprinted with permission from (Kaylor, Cook et al. 2014)). This alternate visual cycle (or Müller-cell pathway) supports almost exclusively cone photoreceptors. Upon the absorption of a photon by a cone opsin, the bound 11-*cis*-RAL is isomerized to all-*trans*-RAL and transiently converts the opsin to Meta II. Meta II decays after a short signaling period, which yields apo-opsin and free all-*trans*-RAL. All-*trans*-RAL is translocated, and then reduced predominantly by RDH8 to all-*trans*-ROL, coupled with the converting of the cofactor NADPH to $NADP^+$. All-*trans*-ROL is transported by IRBP to Müller cells, where it is isomerized by DES1 to different *cis*-isomers. The produced 11-*cis*-retinol is either bound to CRALBP with high affinity or esterified by MFAT to 11-*cis*-retinyl esters (mainly 11-*cis*-retinyl palmitate). Either of these events is highly 11-*cis*-selective, which

separates 11-*cis*-retinol and drives the equilibrium to the direction favoring for 11-*cis*-retinol formation. 11-*cis*-retinyl esters can be hydrolyzed by a retinyl-ester hydrolase (identity still unknown, labeled as REH?), which is thought to be modulated by apo-CRALBP (Stecher, Gelb et al. 1999), to release 11-*cis*-retinol. CRALBP-bound 11-*cis*-retinol is unloaded upon the interaction with charged acidic lipids on the plasma membranes (Saari, Nawrot et al. 2009) and transported back to cones by IRBP. In cones, an actively studied (see **Chapter 2.3**) but still unidentified retinol dehydrogenase (labeled as RDH?) oxidizes 11-*cis*-ROL to 11-*cis*-RAL. The conversion of the co-factors, $NADP^+$/NADPH, by the RDH? and RDH8 may be coupled together in a "self-renewing" way. 11-*cis*-RAL is used to form a new visual pigment and enter another round of "visual cycle". (This paragraph is adapted from the **legend** of the reprinted **Fig.1-2** (Kaylor, Cook et al. 2014)).

Although DES1 has been identified as a strong candidate of Isomerase II (Kaylor, Yuan et al. 2013), what is its catalytic mechanism? Could its role be confirmed by *in vivo* studies using animal model(s)? Also, what is the identity of the "RDH?" in cones? These questions will be discussed in **Chapter 2** of this dissertation.

According to Mata et al., even though the alternate visual cycle might be "20-fold faster" than the canonical visual cycle, it may still only meet "two-thirds" of the chromophore regeneration need under bright light (Mata, Radu et al. 2002). Furthermore, a recent physiological study suggests that the alternate visual cycle may only be as equally fast as the canonical visual cycle regarding the initial cone-opsin regeneration rates. (Wang, Estevez et al. 2009). Could there be possibly other pathways or mechanisms that

regenerate 11-*cis*-RAL as well? An intriguing fact is that, unlike vertebrates, some lower invertebrate species have a different type of visual pigment, called bistable pigment. Its chromophore remains covalently bound to the opsin even after isomerized to the all-*trans*-configuration, and can be converted back to the 11-*cis*-isomer upon the absorption of another photon (Lamb 2013). Could a similar mechanism somehow also be present in vertebrates? If so, what is the biochemical mechanism? We have proposed a novel mechanism regarding this and it will be addressed in **Chapter 3** of this dissertation.

Visual cycles are indispensable to vision. A significant number of pathological conditions are related to the defects of these pathways (Travis, Golczak et al. 2007, Liu, Chen et al. 2016). What is the potential clinical significance of this study and what are the future directions? These will be discussed in the last chapter, **Chapter 4**, of this dissertation.

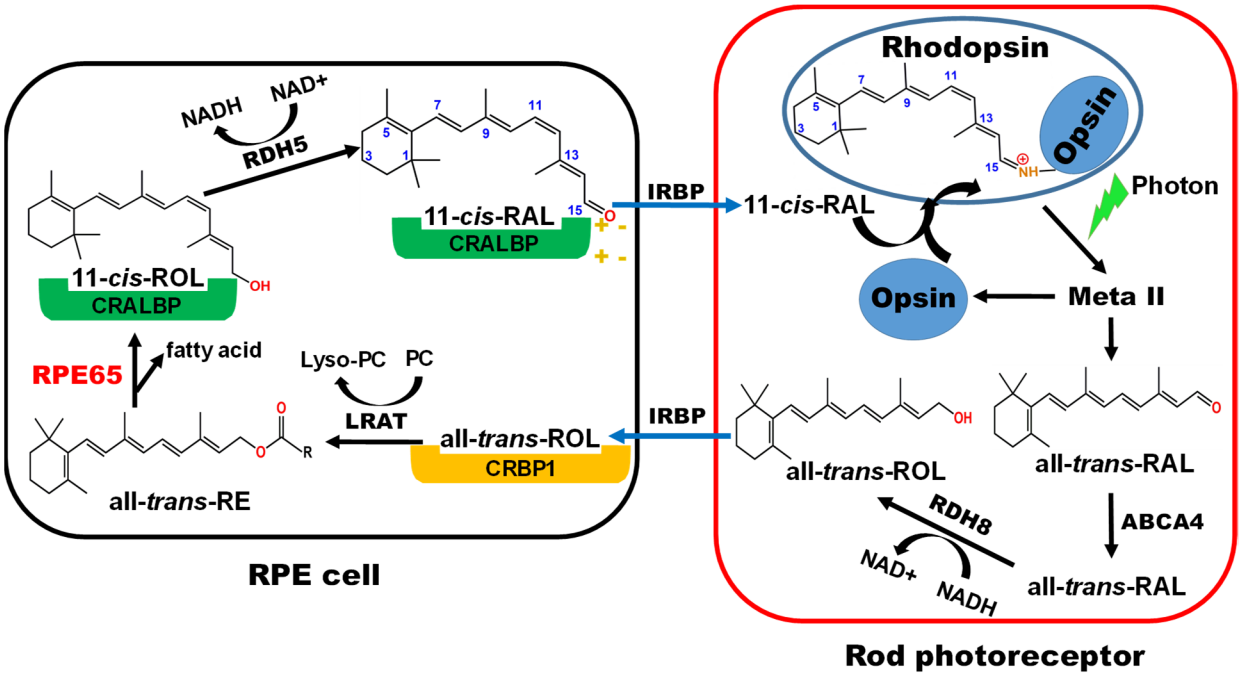

Figure 1-1. The canonical visual cycle. See text for a detailed description. (Travis, Golczak et al. 2007, Saari 2012, Kaylor, Yuan et al. 2013, Tang, Kono et al. 2013, Kiser and Palczewski 2016, Sahu and Maeda 2016)

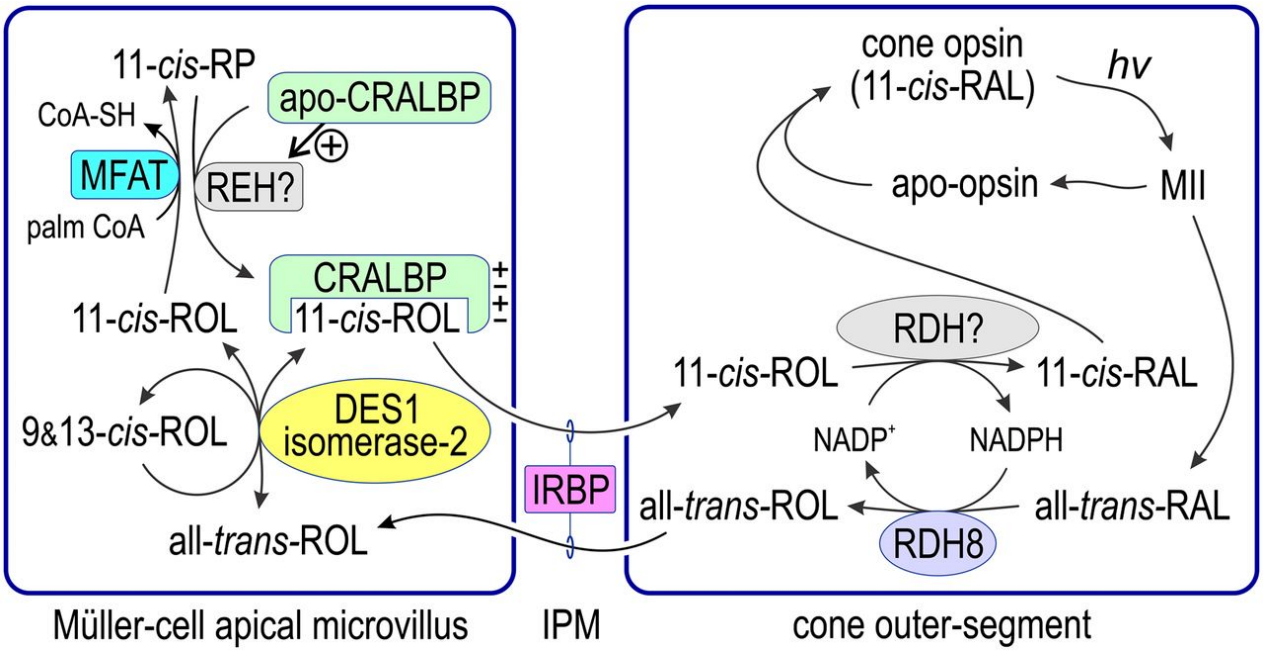

Figure 1-2. Noncanonical visual cycle in Müller cells. Cone opsins use 11-*cis*-RAL as visual chromophore. Absorption of a photon by a cone opsin isomerizes the 11-*cis*-RAL to all-*trans*-RAL, as in rods. After reduction by RDH8 in the cone OS, the all-*trans*-ROL is released into the IPM and taken up by a Müller cell. Here, the all-*trans*-ROL is isomerized by DES1 to 11-*cis*-ROL, 9-*cis*-ROL, and 13-*cis*-ROL. The 11-*cis*-ROL binds to CRALBP or is fatty acylated by MFAT to yield an 11-*cis*-RE. In either event, 11-*cis*-ROL is removed from the equilibrium reaction. The other retinol isomers are reisomerized by DES1. An as-yet unidentified 11-*cis*-retinyl-ester hydrolase (REH?) hydrolyzes 11-*cis*-RP to yield 11-*cis*-ROL and palmitic acid. The 11-*cis*-REH activity was shown to be activated by apo-CRALBP and inhibited by holo-CRALBP (Stecher, Gelb et al. 1999). Interaction with negatively charged phospholipids on the plasma membrane causes holo-CRALBP to release its 11-*cis*-ROL ligand into the IPM, where it binds IRBP and, subsequently, is taken up by a cone outer segment (Saari, Nawrot et al. 2009). Binding to CRALBP provides a mechanism to protect 11-*cis*-ROL from reverse isomerization by DES1. In the cone OS, 11-*cis*-ROL is oxidized by an unknown 11-*cis*-ROL dehydrogenase (RDH?) to 11-*cis*-RAL, which combines with apo-opsin to form a new opsin pigment. Simultaneous reduction of all-*trans*-RAL and oxidation of 11-*cis*-ROL in the cone OS provides a self-renewing supply of NADPH/$NADP^+$ cofactors. (This figure and its legend are reprinted with permission from (Kaylor, Cook et al. 2014). doi: 10.1073/pnas.1319142111.)

References

Agte, S., S. Junek, S. Matthias, E. Ulbricht, I. Erdmann, A. Wurm, D. Schild, J. A. Kas and A. Reichenbach (2011). "Muller Glial Cell-Provided Cellular Light Guidance through the Vital Guinea-Pig Retina." Biophysical Journal **101**(11): 2611-2619.

Ala-Laurila, P., M. C. Cornwall, R. K. Crouch and M. Kono (2009). "The action of 11-cis-retinol on cone opsins and intact cone photoreceptors." J Biol Chem **284**(24): 16492-16500.

Arikawa, K., L. L. Molday, R. S. Molday and D. S. Williams (1992). "Localization of peripherin/rds in the disk membranes of cone and rod photoreceptors: relationship to disk membrane morphogenesis and retinal degeneration." J Cell Biol **116**(3): 659-667.

Arshavsky, V. Y. and M. E. Burns (2014). "Current understanding of signal amplification in phototransduction." Cell Logist **4**: e29390.

Arshavsky, V. Y., T. D. Lamb and E. N. Pugh, Jr. (2002). "G proteins and phototransduction." Annu Rev Physiol **64**: 153-187.

Babino, D., M. Golczak, P. D. Kiser, A. Wyss, K. Palczewski and J. von Lintig (2016). "The Biochemical Basis of Vitamin A3 Production in Arthropod Vision." ACS Chem Biol **11**(4): 1049-1057.

Baumann, C. (1970). "Regeneration of rhodopsin in the isolated retina of the frog (Rana esculenta)." Vision Res **10**(8): 627-637.

Baylor, D. A. (1987). "Photoreceptor signals and vision. Proctor lecture." Invest Ophthalmol Vis Sci **28**(1): 34-49.

Baylor, D. A., T. D. Lamb and K. W. Yau (1979). "Responses of retinal rods to single photons." J Physiol **288**: 613-634.

Baylor, D. A., B. J. Nunn and J. L. Schnapf (1984). "The photocurrent, noise and spectral sensitivity of rods of the monkey Macaca fascicularis." J Physiol **357**: 575-607.

Bok, D., D. E. Ong and F. Chytil (1984). "Immunocytochemical localization of cellular retinol binding protein in the rat retina." Invest Ophthalmol Vis Sci **25**(8): 877-883.

Boynton, R. M. and D. N. Whitten (1970). "Visual adaptation in monkey cones: recordings of late receptor potentials." Science **170**(3965): 1423-1426.

Bunt-Milam, A. H. and J. C. Saari (1983). "Immunocytochemical localization of two retinoid-binding proteins in vertebrate retina." J Cell Biol **97**(3): 703-712.

Burns, M. E. and D. A. Baylor (2001). "Activation, deactivation, and adaptation in vertebrate photoreceptor cells." Annu Rev Neurosci **24**: 779-805.

Cone, R. A. and P. K. Brown (1969). "Spontaneous regeneration of rhodopsin in the isolated rat retina." Nature **221**(5183): 818-820.

Das, S. R., N. Bhardwaj, H. Kjeldbye and P. Gouras (1992). "Muller cells of chicken retina synthesize 11-cis-retinol." Biochem J **285 (Pt 3)**: 907-913.

Deigner, P. S., W. C. Law, F. J. Canada and R. R. Rando (1989). "Membranes as the Energy-Source in the Endergonic Transformation of Vitamin-a to 11-Cis-Retinol." Science **244**(4907): 968-971.

Driessen, C. A., B. P. Janssen, H. J. Winkens, A. H. van Vugt, T. L. de Leeuw and J. J. Janssen (1995). "Cloning and expression of a cDNA encoding bovine retinal pigment epithelial 11-cis retinol dehydrogenase." Invest Ophthalmol Vis Sci **36**(10): 1988-1996.

Driessen, C. A., H. J. Winkens, K. Hoffmann, L. D. Kuhlmann, B. P. Janssen, A. H. Van Vugt, J. P. Van Hooser, B. E. Wieringa, A. F. Deutman, K. Palczewski, K. Ruether and J. J. Janssen (2000). "Disruption of the 11-cis-retinol dehydrogenase gene leads to accumulation of cis-retinols and cis-retinyl esters." Mol Cell Biol **20**(12): 4275-4287.

Edwards, R. B. and A. J. Adler (1994). "Exchange of retinol between IRBP and CRBP." Exp Eye Res **59**(2): 161-170.

Eisenfeld, A. J., A. H. Bunt-Milam and J. C. Saari (1985). "Localization of retinoid-binding proteins in developing rat retina." Exp Eye Res **41**(3): 299-304.

Farjo, K. M., G. Moiseyev, Y. Takahashi, R. K. Crouch and J. X. Ma (2009). "The 11-cis-retinol dehydrogenase activity of RDH10 and its interaction with visual cycle proteins." Invest Ophthalmol Vis Sci **50**(11): 5089-5097.

Franze, K., J. Grosche, S. N. Skatchkov, S. Schinkinger, C. Foja, D. Schild, O. Uckermann, K. Travis, A. Reichenbach and J. Guck (2007). "Muller cells are living optical fibers in the vertebrate retina." Proc Natl Acad Sci U S A **104**(20): 8287-8292.

Futterman, S. and M. H. Rollins (1973). "The catalytic isomerization of all-trans-retinal to 9-cis-retinal and 13-cis-retinal." J Biol Chem **248**(22): 7773-7779.

Goldstein, E. B. (1967). "Early receptor potential of the isolated frog (Rana pipiens) retina." Vision Res **7**(11): 837-845.

Goldstein, E. B. (1968). "Visual pigments and the early receptor potential of the isolated frog retina." Vision Res **8**(8): 953-963.

Goldstein, E. B. (1970). "Cone pigment regeneration in the isolated frog retina." Vision Res **10**(10): 1065-1068.

Goldstein, E. B. and B. M. Wolf (1973). "Regeneration of the green-rod pigment in the isolated frog retina." Vision Res **13**(3): 527-534.

Golovleva, I., S. Bhattacharya, Z. Wu, N. Shaw, Y. Yang, K. Andrabi, K. A. West, M. S. Burstedt, K. Forsman, G. Holmgren, O. Sandgren, N. Noy, J. Qin and J. W. Crabb (2003). "Disease-causing mutations in the cellular retinaldehyde binding protein tighten and abolish ligand interactions." J Biol Chem **278**(14): 12397-12402.

Govardovskii, V. I., P. D. Calvert and V. Y. Arshavsky (2000). "Photoreceptor light adaptation. Untangling desensitization and sensitization." J Gen Physiol **116**(6): 791-794.

Green, D. G. (1971). "Light adaptation in the rat retina: evidence for two receptor mechanisms." Science **174**(4009): 598-600.

Haeseleer, F., G. F. Jang, Y. Imanishi, C. A. Driessen, M. Matsumura, P. S. Nelson and K. Palczewski (2002). "Dual-substrate specificity short chain retinol dehydrogenases from the vertebrate retina." J Biol Chem **277**(47): 45537-45546.

Hood, D. C. and P. A. Hock (1973). "Recovery of cone receptor activity in the frog's isolated retina." Vision Res **13**(10): 1943-1951.

Hubbard, R. (1966). "The stereoisomerization of 11-cis-retinal." J Biol Chem **241**(8): 1814-1818.

Hubbard, R., D. Bownds and T. Yoshizawa (1965). "The chemistry of visual photoreception." Cold Spring Harb Symp Quant Biol **30**: 301-315.

Janecke, A. R., D. A. Thompson, G. Utermann, C. Becker, C. A. Hubner, E. Schmid, C. L. McHenry, A. R. Nair, F. Ruschendorf, J. Heckenlively, B. Wissinger, P. Nurnberg and A. Gal (2004). "Mutations in RDH12 encoding a photoreceptor cell retinol dehydrogenase cause childhood-onset severe retinal dystrophy." Nat Genet **36**(8): 850-854.

Jang, G. F., J. P. Van Hooser, V. Kuksa, J. K. McBee, Y. G. He, J. J. Janssen, C. A. Driessen and K. Palczewski (2001). "Characterization of a dehydrogenase activity responsible for oxidation of 11-cis-retinol in the retinal pigment epithelium of mice with a disrupted RDH5 gene. A model for the human hereditary disease fundus albipunctatus." J Biol Chem **276**(35): 32456-32465.

Jin, M., S. Li, W. N. Moghrabi, H. Sun and G. H. Travis (2005). "Rpe65 is the retinoid isomerase in bovine retinal pigment epithelium." Cell **122**(3): 449-459.

Jones, G. J., R. K. Crouch, B. Wiggert, M. C. Cornwall and G. J. Chader (1989). "Retinoid requirements for recovery of sensitivity after visual-pigment bleaching in isolated photoreceptors." Proc Natl Acad Sci U S A **86**(23): 9606-9610.

Kasus-Jacobi, A., J. Ou, D. G. Birch, K. G. Locke, J. M. Shelton, J. A. Richardson, A. J. Murphy, D. M. Valenzuela, G. D. Yancopoulos and A. O. Edwards (2005). "Functional characterization of mouse RDH11 as a retinol dehydrogenase involved in dark adaptation in vivo." J Biol Chem **280**(21): 20413-20420.

Kaylor, J. J., J. D. Cook, J. Makshanoff, N. Bischoff, J. Yong and G. H. Travis (2014). "Identification of the 11-cis-specific retinyl-ester synthase in retinal Muller cells as multifunctional O-acyltransferase (MFAT)." Proc Natl Acad Sci U S A **111**(20): 7302-7307.

Kaylor, J. J., Q. Yuan, J. Cook, S. Sarfare, J. Makshanoff, A. Miu, A. Kim, P. Kim, S. Habib, C. N. Roybal, T. Xu, S. Nusinowitz and G. H. Travis (2013). "Identification of DES1 as a vitamin A isomerase in Muller glial cells of the retina." Nat Chem Biol **9**(1): 30-36.

Kefalov, V. J. (2012). "Rod and cone visual pigments and phototransduction through pharmacological, genetic, and physiological approaches." J Biol Chem **287**(3): 1635-1641.

Kim, T. S., A. Maeda, T. Maeda, C. Heinlein, N. Kedishvili, K. Palczewski and P. S. Nelson (2005). "Delayed dark adaptation in 11-cis-retinol dehydrogenase-deficient mice: a role of RDH11 in visual processes in vivo." J Biol Chem **280**(10): 8694-8704.

Kiser, P. D., M. Golczak, A. Maeda and K. Palczewski (2012). "Key enzymes of the retinoid (visual) cycle in vertebrate retina." Biochim Biophys Acta **1821**(1): 137-151.

Kiser, P. D., M. Golczak and K. Palczewski (2014). "Chemistry of the retinoid (visual) cycle." Chem Rev **114**(1): 194-232.

Kiser, P. D. and K. Palczewski (2016). "Retinoids and Retinal Diseases." Annu Rev Vis Sci **2**: 197-234.

Koch, K. W. and D. Dell'Orco (2015). "Protein and Signaling Networks in Vertebrate Photoreceptor Cells." Front Mol Neurosci **8**: 67.

Kropf, A. and R. Hubbard (1970). "The photoisomerization of retinal." Photochem Photobiol **12**(4): 249-260.

Kurth, I., D. A. Thompson, K. Ruther, K. L. Feathers, J. D. Chrispell, J. Schroth, C. L. McHenry, M. Schweizer, S. Skosyrski, A. Gal and C. A. Hubner (2007). "Targeted disruption of the murine retinal dehydrogenase gene Rdh12 does not limit visual cycle function." Mol Cell Biol **27**(4): 1370-1379.

Lamb, T. D. (2013). "Evolution of phototransduction, vertebrate photoreceptors and retina." Progress in Retinal and Eye Research **36**: 52-119.

Lamb, T. D. and E. N. Pugh, Jr. (2006). "Phototransduction, dark adaptation, and rhodopsin regeneration the proctor lecture." Invest Ophthalmol Vis Sci **47**(12): 5137-5152.

Lhor, M. and C. Salesse (2014). "Retinol dehydrogenases: membrane-bound enzymes for the visual function." Biochem Cell Biol **92**(6): 510-523.

Liu, X., J. Chen, Z. Liu, J. Li, K. Yao and Y. Wu (2016). "Potential Therapeutic Agents Against Retinal Diseases Caused by Aberrant Metabolism of Retinoids." Invest Ophthalmol Vis Sci **57**(3): 1017-1030.

Luo, D. G., T. Xue and K. W. Yau (2008). "How vision begins: An odyssey." Proceedings of the National Academy of Sciences of the United States of America **105**(29): 9855-9862.

Maeda, A., T. Maeda, Y. Imanishi, V. Kuksa, A. Alekseev, J. D. Bronson, H. Zhang, L. Zhu, W. Sun, D. A. Saperstein, F. Rieke, W. Baehr and K. Palczewski (2005). "Role of photoreceptor-specific retinol dehydrogenase in the retinoid cycle in vivo." J Biol Chem **280**(19): 18822-18832.

Maeda, A., T. Maeda, Y. Imanishi, W. Sun, B. Jastrzebska, D. A. Hatala, H. J. Winkens, K. P. Hofmann, J. J. Janssen, W. Baehr, C. A. Driessen and K. Palczewski (2006). "Retinol dehydrogenase (RDH12) protects photoreceptors from light-induced degeneration in mice." J Biol Chem **281**(49): 37697-37704.

Maeda, A., T. Maeda, W. Sun, H. Zhang, W. Baehr and K. Palczewski (2007). "Redundant and unique roles of retinol dehydrogenases in the mouse retina." Proc Natl Acad Sci U S A **104**(49): 19565-19570.

Masland, R. H. (2001). "The fundamental plan of the retina." Nat Neurosci **4**(9): 877-886.

Masland, R. H. (2012). "The neuronal organization of the retina." Neuron **76**(2): 266-280.

Mata, N. L., R. A. Radu, R. C. Clemmons and G. H. Travis (2002). "Isomerization and oxidation of vitamin a in cone-dominant retinas: a novel pathway for visual-pigment regeneration in daylight." Neuron **36**(1): 69-80.

Mata, N. L., A. Ruiz, R. A. Radu, T. V. Bui and G. H. Travis (2005). "Chicken retinas contain a retinoid isomerase activity that catalyzes the direct conversion of all-trans-retinol to 11-cis-retinol." Biochemistry **44**(35): 11715-11721.

Moiseyev, G., Y. Chen, Y. Takahashi, B. X. Wu and J. X. Ma (2005). "RPE65 is the isomerohydrolase in the retinoid visual cycle." Proc Natl Acad Sci U S A **102**(35): 12413-12418.

Molday, R. S. and O. L. Moritz (2015). "Photoreceptors at a glance." Journal of Cell Science **128**(22): 4039-4045.

Muniz, A., B. S. Betts, A. R. Trevino, K. Buddavarapu, R. Roman, J. X. Ma and A. T. Tsin (2009). "Evidence for two retinoid cycles in the cone-dominated chicken eye." Biochemistry **48**(29): 6854-6863.

Muniz, A., E. T. Villazana-Espinoza, B. Thackeray and A. T. Tsin (2006). "11-cis-Acyl-CoA:retinol O-acyltransferase activity in the primary culture of chicken Muller cells." Biochemistry **45**(40): 12265-12273.

Mustafi, D., A. H. Engel and K. Palczewski (2009). "Structure of cone photoreceptors." Prog Retin Eye Res **28**(4): 289-302.

Nakanishi, K. (1991). "Why 11-Cis-Retinal." American Zoologist **31**(3): 479-489.

Okada, T., O. P. Ernst, K. Palczewski and K. P. Hofmann (2001). "Activation of rhodopsin: new insights from structural and biochemical studies." Trends Biochem Sci **26**(5): 318-324.

Palczewski, K. (2014). "Chemistry and Biology of the Initial Steps in Vision: The Friedenwald Lecture." Investigative Ophthalmology & Visual Science **55**(10).

Parker, R. O. and R. K. Crouch (2010). "Retinol dehydrogenases (RDHs) in the visual cycle." Exp Eye Res **91**(6): 788-792.

Rando, R. R. and A. Chang (1983). "Studies on the Catalyzed Interconversions of Vitamin-a Derivatives." Journal of the American Chemical Society **105**(9): 2879-2882.

Redmond, T. M., E. Poliakov, S. Yu, J. Y. Tsai, Z. Lu and S. Gentleman (2005). "Mutation of key residues of RPE65 abolishes its enzymatic role as isomerohydrolase in the visual cycle." Proc Natl Acad Sci U S A **102**(38): 13658-13663.

Redmond, T. M., S. Yu, E. Lee, D. Bok, D. Hamasaki, N. Chen, P. Goletz, J. X. Ma, R. K. Crouch and K. Pfeifer (1998). "Rpe65 is necessary for production of 11-cis-vitamin A in the retinal visual cycle." Nat Genet **20**(4): 344-351.

Rowan, R., 3rd, A. Warshel, B. D. Sykes and M. Karplus (1974). "Conformation of retinal isomers." Biochemistry **13**(5): 970-981.

Saari, J. C. (2012). "Vitamin A metabolism in rod and cone visual cycles." Annu Rev Nutr **32**: 125-145.

Saari, J. C. and D. L. Bredberg (1987). "Photochemistry and stereoselectivity of cellular retinaldehyde-binding protein from bovine retina." J Biol Chem **262**(16): 7618-7622.

Saari, J. C., M. Nawrot, R. E. Stenkamp, D. C. Teller and G. G. Garwin (2009). "Release of 11-cis-retinal from cellular retinaldehyde-binding protein by acidic lipids." Mol Vis **15**: 844-854.

Sahu, B. and A. Maeda (2016). "Retinol Dehydrogenases Regulate Vitamin A Metabolism for Visual Function." Nutrients **8**(11).

Sahu, B., W. Sun, L. Perusek, V. Parmar, Y. Z. Le, M. D. Griswold, K. Palczewski and A. Maeda (2015). "Conditional Ablation of Retinol Dehydrogenase 10 in the Retinal

Pigmented Epithelium Causes Delayed Dark Adaption in Mice." J Biol Chem **290**(45): 27239-27247.

Sakmar, T. P., R. R. Franke and H. G. Khorana (1989). "Glutamic Acid-113 Serves as the Retinylidene Schiff-Base Counterion in Bovine Rhodopsin." Proceedings of the National Academy of Sciences of the United States of America **86**(21): 8309-8313.

Sandell, L. L., B. W. Sanderson, G. Moiseyev, T. Johnson, A. Mushegian, K. Young, J. P. Rey, J. X. Ma, K. Staehling-Hampton and P. A. Trainor (2007). "RDH10 is essential for synthesis of embryonic retinoic acid and is required for limb, craniofacial, and organ development." Genes & Development **21**(9): 1113-1124.

Sato, S. and V. J. Kefalov (2016). "cis Retinol oxidation regulates photoreceptor access to the retina visual cycle and cone pigment regeneration." J Physiol **594**(22): 6753-6765.

Shichida, Y. and T. Matsuyama (2009). "Evolution of opsins and phototransduction." Philos Trans R Soc Lond B Biol Sci **364**(1531): 2881-2895.

Stecher, H., M. H. Gelb, J. C. Saari and K. Palczewski (1999). "Preferential release of 11-cis-retinol from retinal pigment epithelial cells in the presence of cellular retinaldehyde-binding protein." J Biol Chem **274**(13): 8577-8585.

Strauss, O. (2005). "The retinal pigment epithelium in visual function." Physiol Rev **85**(3): 845-881.

Strauss, O. (2016). "Pharmacology of the retinal pigment epithelium, the interface between retina and body system." Eur J Pharmacol **787**: 84-93.

Tang, P. H., M. Kono, Y. Koutalos, Z. Ablonczy and R. K. Crouch (2013). "New insights into retinoid metabolism and cycling within the retina." Prog Retin Eye Res **32**: 48-63.

Travis, G. H., M. Golczak, A. R. Moise and K. Palczewski (2007). "Diseases caused by defects in the visual cycle: retinoids as potential therapeutic agents." Annu Rev Pharmacol Toxicol **47**: 469-512.

Vecino, E., F. D. Rodriguez, N. Ruzafa, X. Pereiro and S. C. Sharma (2016). "Glia-neuron interactions in the mammalian retina." Prog Retin Eye Res **51**: 1-40.

Wald, G. (1968). "Molecular basis of visual excitation." Science **162**(3850): 230-239.

Wang, J. S., M. E. Estevez, M. C. Cornwall and V. J. Kefalov (2009). "Intra-retinal visual cycle required for rapid and complete cone dark adaptation." Nat Neurosci **12**(3): 295-302.

Wang, J. S. and V. J. Kefalov (2009). "An alternative pathway mediates the mouse and human cone visual cycle." Curr Biol **19**(19): 1665-1669.

Wang, J. S. and V. J. Kefalov (2011). "The cone-specific visual cycle." Prog Retin Eye Res **30**(2): 115-128.

Warshel, A. and E. Huler (1974). "Theoretical Evaluation of Potential Surfaces, Equilibrium Geometries and Vibronic Transition Intensities of Excimers - Pyrene Crystal Excimer." Chemical Physics **6**(3): 463-468.

Warshel, A., E. Huler, D. Rabinovich and Z. Shakked (1974). "Examination of Intramolecular Potential Surfaces of Flexible Conjugated Molecules by Calculation of Crystal-Structures - Equilibrium Geometries of Chalcones and Diphenyloctatetraene in Crystal and Gaseous State." Journal of Molecular Structure **23**(2): 175-191.

Wilkinson-Berka, J. L. (2004). "Diabetes and retinal vascular disorders: role of the renin-angiotensin system." Expert Rev Mol Med **6**(15): 1-18.

Willermain, F., S. Libert, E. Motulsky, D. Salik, L. Caspers, J. Perret and C. Delporte (2014). "Origins and consequences of hyperosmolar stress in retinal pigmented epithelial cells." Front Physiol **5**: 199.

Wu, B. X., Y. Chen, Y. Chen, J. Fan, B. Rohrer, R. K. Crouch and J. X. Ma (2002). "Cloning and characterization of a novel all-trans retinol short-chain dehydrogenase/reductase from the RPE." Invest Ophthalmol Vis Sci **43**(11): 3365-3372.

Wu, B. X., G. Moiseyev, Y. Chen, B. Rohrer, R. K. Crouch and J. X. Ma (2004). "Identification of RDH10, an All-trans Retinol Dehydrogenase, in Retinal Muller Cells." Invest Ophthalmol Vis Sci **45**(11): 3857-3862.

Yamamoto, H., A. Simon, U. Eriksson, E. Harris, E. L. Berson and T. P. Dryja (1999). "Mutations in the gene encoding 11-cis retinol dehydrogenase cause delayed dark adaptation and fundus albipunctatus." Nat Genet **22**(2): 188-191.

Zhong, M., R. Kawaguchi, M. Kassai and H. Sun (2012). "Retina, retinol, retinal and the natural history of vitamin A as a light sensor." Nutrients **4**(12): 2069-2096.

Chapter 2: Characterization of DES1 and search for a specific cone retinol dehydrogenase in the alternate visual cycle

2.1 Biochemical characterization of DES1

A portion of this section (part of the Introduction, Results 2.1.2.1 and 2.1.2.2, part of the Discussion and part of the Materials and Methods) is adapted from the publication: Joanna J. Kaylor, Quan Yuan, Jeremy Cook, Shanta Sarfare, Jacob Makshanoff, Anh Miu, Anita Kim, Paul Kim, Samer Habib, C. Nathaniel Roybal, Tongzhou Xu, Steven Nusinowitz, and Gabriel H. Travis (2013). Identification of DES1 as a vitamin A isomerase in Müller glial cells of the retina. *Nat Chem Biol*. 9(1):30-36. doi: 10.1038/nchembio.1114. Author contributions are listed on the Acknowledgement page of this dissertation.

2.1.1 Introduction

Retinoid isomerases are crucial to the regeneration of visual chromophore. Recently, we have identified DES1 as a novel retinoid isomerase and an excellent candidate for Isomerase II in the retina (Kaylor, Yuan et al. 2013).

Originally, Des1 gene was cloned from *Drosophila melanogaster* by Dr. Okada and colleagues and named DEGS1 (drosophila degenerative spermatocyte 1) (Endo, Akiyama et al. 1996, Casasampere, Ordonez et al. 2016). Later, DES1 protein was found to have the function of introducing a 4,5-*trans*-double band to dihydroceramide and converting it to ceramide, the precursor of sphingolipids (Geeraert, Mannaerts et al. 1997, Michel, van Echten-Deckert et al. 1997, Savile, Fabrias et al. 2001, Larsen and Tennagels 2014). In addition to the major Δ4-desaturase activity, DES1 also exhibits minor C-4-hydroxylase activity (Ternes, Franke et al. 2002). DES1 is a member of the

membrane fatty acid desaturase family and is mainly localized to the endoplasmic reticulum (ER) (Shanklin, Whittle et al. 1994, Cadena, Kurten et al. 1997, Causeret, Geeraert et al. 2000). It was conjectured to be a multiple membrane-spanning protein that consists of four transmembrane segments (Shanklin, Whittle et al. 1994, Cadena, Kurten et al. 1997, Michel, van Echten-Deckert et al. 1997, Fabrias, Munoz-Olaya et al. 2012). It is a member of a superfamily of enzymes that contain three conserved motifs of histidines, $HX_{(3–4)}H$, $HX_{(2–3)}HH$, and $(H/Q)X_{(2–3)}HH$, which may be involved in the formation of oxo-bridged diiron binding clusters (Shanklin, Whittle et al. 1994, Ternes, Franke et al. 2002). DES1 undergoes N-terminal myristoylation, which increases its desaturase activity and targets it from ER to mitochondria (Beauchamp, Goenaga et al. 2007, Beauchamp, Tekpli et al. 2009, Rioux, Pedrono et al. 2011, Ezanno, le Bloc'h et al. 2012). DES1 is distributed quite ubiquitously in many tissues. In rats, DES1 activity has been found in liver, kidney, lung, spleen, testis, brain, etc. (Causeret, Geeraert et al. 2000)

DES1-catalyzed dihydroceramide desaturation requires NAD(P)H as an electron donor (Geeraert, Mannaerts et al. 1997, Michel, van Echten-Deckert et al. 1997, Schulze, Michel et al. 2000). DES1 desaturase activity is believed to rely on the cytochrome b5 electron-transport chain. In this chain, electrons donated by NAD(P)H are first transferred to cytochrome b5 reductase (flavoprotein), then to the cytochrome b5 haem group, and finally to DES1, which reduces oxygen (the final electron acceptor) to water and converts dihydroceramide to ceramide. (Geeraert, Mannaerts et al. 1997, Michel, van Echten-Deckert et al. 1997, Schulze, Michel et al. 2000). An iron co-factor is also believed to be involved in the DES1 desaturase activity (Geeraert, Mannaerts et al.

1997, Michel, van Echten-Deckert et al. 1997, Schulze, Michel et al. 2000, Savile, Fabrias et al. 2001, Casasampere, Ordonez et al. 2016).

The aforementioned characterizations of DES1 were mainly focused on its role as a dihydroceramide desaturase, but not as a retinoid isomerase. Given the essential role of retinoid isomerases in the visual cycles, it is crucial to characterize the retinoid isomerase function of DES1.

In parallel, as mentioned before, RPE65 is the retinoid isomerase in the canonical visual cycle. Thus, it is useful to consider RPE65 when formulating our hypothesis and performing studies for DES1. RPE65 was initially described in 1991 as a 63 kDa protein (Sagara and Hirosawa 1991, Kiser and Palczewski 2010) and is predominantly expressed in the RPE cells (Sagara and Hirosawa 1991, Bavik, Levy et al. 1993, Hamel, Tsilou et al. 1993). It belongs to the family of carotenoid cleavage oxygenases (COOs) (Kiser, Golczak et al. 2014). The crystal structure of RPE65 has been resolved and recently reviewed by Palczewski and colleagues. The basic architecture is a seven-bladed β-propeller under an α-helices cap, with an iron cofactor in its active site (Kiser, Golczak et al. 2009, Golczak, Kiser et al. 2010, Kiser, Farquhar et al. 2012, Kiser, Golczak et al. 2014, Kiser and Palczewski 2016). The enzymatic activity of RPE65 depends on iron (II) (Moiseyev, Takahashi et al. 2006, Kiser, Golczak et al. 2009, Kiser, Farquhar et al. 2012), which may act as a Lewis acid to facilitate retinyl ester cleavage during retinoid isomerization (Kiser, Farquhar et al. 2012). As reviewed (Wright, Redmond et al. 2015), several mechanisms have been proposed for RPE65-catalyzed isomerization, including a S_N2' nucleophilic substitution mechanism (Deigner, Law et al.

1989), a carbocation-based mechanism (McBee, Kuksa et al. 2000) and a radical cation-based mechanism (Poliakov, Parikh et al. 2011, Chander, Gentleman et al. 2012). The carbocation-based mechanism is supported by most recent structure-based analysis (Kiser, Zhang et al. 2015) but the possibility of a radical cation may not be completely excluded (Wright, Redmond et al. 2015).

Here, we performed several biochemical studies regarding the features of DES1-catalyzed retinoid isomerization.

2.1.2 Results

2.1.2.1 DES1 coimmunoprecipitates with CRALBP

11-*cis*-retinol is the precursor of visual chromophore, but its production is not favored in DES1-catalyzed retinol isomerization (Kaylor, Yuan et al. 2013). CRALBP is expressed in Müller cells (Bunt-Milam and Saari 1983) and has selectively high affinities with 11-*cis*-retinol and 11-*cis*-retinal (Saari and Bredberg 1987, Golovleva, Bhattacharya et al. 2003). Therefore, it may play a role in driving DES1-catalyzed isomerization towards the formation of 11-*cis*-retinol by mass action. We thus tested the coimmunoprecipitation of CRALBP with DES1. Homogenates of chicken retinas were incubated with immobilized, affinity-purified antibodies against chicken DES1. After washing, we eluted the bound proteins and analyzed all fractions by immunoblotting. Both DES1 and CRALBP were present in the eluate **(Fig.2.1-1)**. To test for non-specific binding of CRALBP to immobilized DES1 antibodies, we loaded homogenates of 293T cells expressing CRALBP onto the same column and analyzed for CRALBP immunoreactivity in the eluate. None was detectable **(Fig.2.1-1)**, ruling out the non-specific interactions

between CRALBP and immobilized DES1 antibodies. Next, we tested for reciprocal immunoprecipitation of DES1 by CRALBP using a column containing immobilized CRALBP antibodies. We observed no DES1 immunoreactivity in the eluate **(Fig.2.1-1)**, possibly owing to epitope masking or because CRALBP is much more abundant than DES1 in chicken retinas **(Fig.2.1-1)**. Finally, we tested for coimmunoprecipitation of DES1 with the Müller-cell ER protein RDH10 (Wu, Moiseyev et al. 2004). In contrast to CRALBP, RDH10 did not coimmunoprecipitate with DES1. Coimmunoprecipitation of CRALBP by DES1 suggests a direct interaction between these proteins.

2.1.2.2 DES1 isomerase activity is inhibited by dihydroceramide and its analog

Since both retinol and dihydroceramide are substrates of DES1, the presence of dihydroceramide may inhibit DES1 isomerase activity. To address that, we determined the DES1-catalyzed retinol isomerization in the presence of increasing concentrations of C8-dihydroceramide using 293T-D cells (cells we established that stably express chicken DES1) as the source of DES1. Similar experiments were also performed in the presence of C8-cyclopropenylceramide, a nondesaturable analog that competitively inhibits DES1-catalyzed ceramide synthesis (Triola, Fabrias et al. 2003). As shown in **Fig.2.1-2**, both agents inhibited DES1 isomerase activity.

2.1.2.3 DES1 isomerase activity depends on the cytochrome b5 electron transport chain

Because the dihydroceramide desaturase activity of DES1 is dependent on the cytochrome b5 electron transport chain, we hypothesized that the same electron

transport system may also be essential for its retinoid isomerase activity. If that is the case, cytochrome b5 electron transport inhibitors would inhibit the isomerase activity of DES1. To test this hypothesis, we assayed DES1 activity in the presence of various reagents that act on the cytochrome b5 electron transport chain, including ascorbic acid (ascorbate), *N*-ethylmaleimide (NEM), 2,6-Dichloroindophenol (DCPIP), 6-propyl-2-thiouracil (PTU) and 4-(hydroxymercuri) benzoic acid (HMB). Ascorbate interrupts the electron flow from the cytochrome b5 reductase to cytochrome b5 (Geeraert, Mannaerts et al. 1997). NEM (Geeraert, Mannaerts et al. 1997), HMB (Saulter, Kurian et al. 2005) and PTU (Lee and Kariya 1986, Saulter, Kurian et al. 2005, Gan, von Moltke et al. 2009) are cytochrome b5 reductase inhibitors. DCPIP interrupts the electron transfer from cytochrome b5 to DES1 (Geeraert, Mannaerts et al. 1997). As shown in **Fig.2.1-3**, DES1 isomerase activity (represented by the formation of 13-*cis*-retinol) was almost abolished by all the inhibitors except PTU, suggesting that this activity also relies on the cytochrome b5 electron transport chain.

2.1.2.4 DES1 isomerase activity seems to depend predominantly on iron (III)

Although an iron cofactor is important for the dihydroceramide desaturase activity of DES1 (Geeraert, Mannaerts et al. 1997, Michel, van Echten-Deckert et al. 1997, Schulze, Michel et al. 2000, Savile, Fabrias et al. 2001, Casasampere, Ordonez et al. 2016), its necessity and oxidation state for isomerase activity have not been studied. To address whether DES1 is an iron (II)- or iron (III)-dependent retinoid isomerase, we performed an iron chelating experiment. We determined DES1 isomerase activity using 293T-D cell homogenate in the presence of 2,2’- bipyridyl (BIPY) and pyridoxal

isonicotinoyl hydrazone (PIH). The former is an iron (II) chelator (Romeo, Christen et al. 2001) while the latter is an iron (III) chelator (Vitolo, Hefter et al. 1990). As shown in **Fig.2.1-4**, DES1 isomerase activity was significantly inhibited by PIH, indicating that DES1 seems to depend predominantly on iron (III) for its isomerase activity.

2.1.2.5 A free-radical intermediate is probably involved in DES1-catalyzed retinoid isomerization

Retinoids have a system of conjugated double bonds, which can stabilize radical or carbocation intermediates through electron delocalization. If a radical intermediate is present during DES1-catalyzed retinoid isomerization, it should be stabilized by spin trap and/or spin probe reagents (Poliakov, Parikh et al. 2011), which would thus inhibit such isomerization. If the reaction is based purely on a carbocation mechanism, no inhibition is expected.

To address that, we tested the inhibitory effects of various types of spin traps/probes on DES1 isomerase activity using 293-D cell homogenates, which include 4-hydroxy-2,2,6,6-tetramethylpiperidine-1-oxyl (4-hydroxy-TEMPO); 5,5-dimethyl-1-pyrroline-N-oxide (DMPO); 2,2-dimethyl-4-phenyl-2H-imidazole-1-oxide (DMPIO) and 4-phenyl-2,2,5,5-tetramethyl-3-imidazoline-1-oxyl nitroxide (PTMIO). As shown in **Fig.2.1-5**, DES1-catalyzed isomerization was strongly inhibited by 4-hydroxy-TEMPO and PTMIO. To further address how efficient 4-hydroxy-TEMPO and PTMIO in inhibiting DES1 isomerase activity, I also tested their effects using lower concentrations, from 5 mM to 50 μM, and included the homogenate of 293T cells as a control. The results suggest that even 50 μM of these two reagents are sufficient to significantly inhibit DES1

isomerase activity **(Fig.2.1-6)**. Such inhibition indicates the possible involvement of a free-radical intermediate in the DES1-catalyzed retinoid isomerization process.

2.1.2.6 DES1 appears to isomerize both A1 and A2 retinols, but does not catalyze the conversion of A1 retinol to A2

A visual pigment in vertebrates is composed of an opsin and a chromophore. Although usually determined by different types of opsins (such as long, middle or short wavelength-sensitive opsins), the spectral absorption properties of the visual pigment can also be altered by the chromophore, such as the shift between vitamin A1- and A2-aldehydes in vertebrates (Jokela, Vartio et al. 2003, Temple, Plate et al. 2006). The difference between A1 and A2 is that A2, formally known as 3-dehydroretinol or 3,4-didehydroretinol, has one more conjugated double bond at the 3,4-position in the β-ionone ring (Enright, Toomey et al. 2015) **(Fig.2.1-7A)**. The chromophore exchange from A1- to A2- aldehyde results in a red-shift of the λ_{max} of the pigment (Temple, Plate et al. 2006). Some vertebrates such as certain freshwater fishes, reptiles and amphibians, have vitamin A2-based pigments in addition to those based on A1, the amount of which varies based on factors such as season, migration and age (Reuter, White et al. 1971, Provencio, Loew et al. 1992, Toyama, Hironaka et al. 2008, Morshedian, Toomey et al. 2017).

Since DES1 can function both as a (dihydroceramide) desaturase and a (retinol) isomerase, we asked whether it could carry out the function of adding a double bond on the 3,4-position of A1 retinol, that is, converting A1 retinol to A2 retinol. To test this hypothesis, I first obtained and purified A2 retinol (all-*trans*-3,4-didehydroretinol), and

then determined the absorption spectra of both A1 and A2 retinols in ethanol. The λ_{max} of the A1 retinol is about 325 nm while that of A2 is about 350 nm **(Fig.2.1-7B)**, consistent with the literature (Leenheer, Lambert et al. 2000). Then I added A1 retinol (all-*trans*-retinol) to 293T-D cell homogenate in a DES1 activity assay and included samples with 293T cell homogenate or assay buffer without cell homogenate (substrate only) as controls in the presence of no cofactors, NAD^+ or $NADP^+$ **(Fig.2.1-8)**. The final extractions of the reaction products were aliquoted to two parts. One set of the aliquots was directly analyzed by high-performance liquid chromatography (HPLC) while the other set was supplemented with exogenous A2 retinol to introduce an external peak as a reference in the HPLC chromatogram. As shown in **Fig.2.1-8A-C**, no significant A2 peak was seen on the HPLC chromatograms of samples with 293T-D cell homogenate (and also other controls) using A1 retinol as the substrate, suggesting that DES1 does not convert A1 retinol to A2 in our experimental condition. On the other hand, isomerization from A1-(all-*trans*-) retinol to 13-*cis*-retinol was observed **(Fig.2.1-8D)**, indicating DES1 was properly expressed and active.

Considering the structural similarities of A1 and A2 **(Fig.2.1-7A)**, we then hypothesized that DES1 may also be able to isomerize A2 retinol, thus contributing to the regeneration of vitamin A2-based visual chromophore. To test this, I performed another DES1 activity assay using cell homogenates of 293T or 293T-D cells, or assay buffer without cell homogenate. However, instead of using A1 retinol as the substrate, I supplemented the reactions with A2 retinol and analyzed the formation of A2-*cis*-isomers based on the postulated retention time deduced from that of A1 standards and the characteristic spectrum of A2 (we did not have the authentic standards of the *cis*-

isomers of A2 retinol, because of their poor commercial availability). In the resultant HPLC chromatograms, three peaks were believed to be *cis*-isomers of A2 retinol **(Fig.2.1-9A right panels)**, which were quantified **(Fig.2.1-9B)**. It seems that certain peaks (especially peaks 1 and 2) in samples containing 293T-D cell homogenate were significantly higher than those containing 293T cell homogenate or no cell homogenate **(Fig.2.1-9B)**. These results suggest that A2 retinol is also a substrate for DES1 isomerase activity.

2.1.3 Discussion

The equilibrium isomerization catalyzed by DES1 produces minor amounts of 11-*cis*-retinol itself (Kaylor, Yuan et al. 2013), which may be a concern for efficient chromophore regeneration. Coimmunoprecipitation of CRALBP and DES1 illustrates the physical interactions of these two proteins **(Fig.2.1-1)**. The high affinity of CRALBP towards 11-*cis*-retinol (Saari and Bredberg 1987, Golovleva, Bhattacharya et al. 2003) allows for a timely removal of 11-*cis*-retinol and thus drives the equilibrium towards increased 11-*cis*-retinol formation through mass action. Later, an 11-*cis*-specific ester synthase, MFAT, has been identified, which could also contribute to the mass action by esterifying 11-*cis*-retinol to its esters (Kaylor, Cook et al. 2014). These two mechanisms promote the production of 11-*cis*-retinol.

The inhibition study of DES1 isomerase activity by C8-dihydroceramide and C8-cyclopropenylceramide confirms the functions of DES1 as both a dihydroceramide desaturase and a retinoid isomerase **(Fig.2.1-2)**.

The cytochrome b5 electron transfer chain is localized in the endoplasmic reticulum (Porter 2015). Cytochrome b5 is involved in various biological processes such as fatty acid desaturation and elongation (Bhatt, Khatri et al. 2017), and can donate electrons to lipid desaturases such as sterol C5-desaturase (Honjo, Ishibashi et al. 1985, Porter 2015). As mentioned in the introduction, DES1 is a membrane protein mainly localized to the ER (Shanklin, Whittle et al. 1994, Cadena, Kurten et al. 1997, Causeret, Geeraert et al. 2000), the same subcellular organelle as cytochrome b5. DES1 isomerase activity was significantly inhibited by four out of the five cytochrome b5 electron transport chain inhibitors tested **(Fig.2.1-3)**, suggesting an essential role of this electron transport chain in DES1-catalyzed retinoid isomerization. Considering the multiple functions of DES1, it is possible that they would share a similar mechanism. However, due to the non-specificity of these inhibitors tested, their inhibitory effects could also be due to some "off-target" effects. For example, DCPIP is an artificial electron acceptor (Dean and Miskiewicz 2003) and could potentially interrupt various electron transport systems. NEM is a thiol-reactive reagent (Jahng, David et al. 2003) and might react with cysteine residues in DES1 that may be important for its enzymatic activity. However, the use of four different inhibitors in our study lowered the chance of such non-specific effect to a large degree.

Both DES1 and RPE65 are iron-dependent enzymes (Geeraert, Mannaerts et al. 1997, Michel, van Echten-Deckert et al. 1997, Schulze, Michel et al. 2000, Savile, Fabrias et al. 2001, Moiseyev, Takahashi et al. 2006, Kiser, Golczak et al. 2009, Kiser, Farquhar et al. 2012, Casasampere, Ordonez et al. 2016). The oxidation state of iron in RPE65 has been determined to be mainly iron (II) (Moiseyev, Takahashi et al. 2006, Kiser, Golczak

et al. 2009, Kiser, Farquhar et al. 2012). It has also been reported that the dihydroceramide desaturase activity in rat liver is not inhibited by bathophenanthroline sulfonate, an iron (II) chelator (Michel, van Echten-Deckert et al. 1997, Schulze, Michel et al. 2000). No conclusive study so far, however, demonstrates the oxidation state of iron for DES1 isomerase activity. By using two different iron chelators, we showed that DES1-catalyzed retinoid isomerization is mainly dependent on iron (III) **(Fig.2.1-4)**. Previously, Savile et al. (Savile, Fabrias et al. 2001) described a model for the dihydroceramide desaturase mechanism, based on a proposed mechanism for Oleate Δ12 Desaturase (Buist and Behrouzian 1998). In this model, a diiron oxidant involving iron (III) and/or iron (IV) may be present in the catalysis process (Savile, Fabrias et al. 2001). Although our result could not confirm the existence of iron (IV) in the isomerization process, it indicates that a similar mechanism is entirely possible based on the significant inhibition of DES1 isomerase activity by the iron (III) chelator, PIH **(Fig.2.1-4)**.

In the above model Savile et al. described, a putative short-lived free radical intermediate (or its organoiron equivalent) was also proposed (Savile, Fabrias et al. 2001). A complete resolution of a carbocation-based or a radical cation-based mechanism may be very challenging, just as the case of RPE65 (see Introduction). However, the existence of a radical intermediate may be relatively more straightforward to test by spin trap/probe reagents. We tested the inhibitory effect of two hydrophilic (4-hydroxy-TEMPO and DMPO) and two hydrophobic (DMPIO and PTMIO) spin trap/probe reagents on DES1 isomerase activity. One reagent from each group, namely, 4-hydroxy-TEMPO and PTMIO, almost completely inhibited DES1 activity **(Fig.2.1-5)**,

suggesting that the inhibitory effect may not be limited to a particular group. More importantly, even 50 μM of these two reagents were sufficient to significantly inhibit DES1 isomerase activity **(Fig.2.1-6)**, strongly indicating the existence of a radical intermediate.

Both vitamin A1 and A2 can form visual pigments in certain animals, the ratio of which may vary due to several factors (Reuter, White et al. 1971, Provencio, Loew et al. 1992, Toyama, Hironaka et al. 2008, Morshedian, Toomey et al. 2017). What is the enzyme responsible for converting A1 to A2? Could it be DES1? However, based on our tests, DES1 did not exhibit such an activity **(Fig.2.1-8)**. This is not surprising, since otherwise the two activities (dehydrogenase and isomerase) towards the same substrate (A1 retinol) may compete, leaving a negative effect on either side. Moreover, since retinoid isomerization and dehydrogenation will probably require distinct catalytic processes, coordination of such two different mechanisms towards the same substrate may be difficult. The enzymatic basis for the conversion of A1- to A2-retinol was finally solved in 2015 by Enright et al., who identified Cyp27c1 (a member of the cytochrome P450 family) as the responsible enzyme (Enright, Toomey et al. 2015). This finding confirms that DES1 is not the enzyme responsible for this conversion. On the other hand, we showed that A2 retinol seems to be another substrate for DES1 isomerase activity **(Fig.2.1-9)**. Given the high structural similarity, this is quite reasonable. Therefore, DES1 may also be important for the regeneration of A2-based visual chromophore, further highlighting its biological significance.

Overall, the biochemical studies presented here demonstrate the interaction between DES1 and CRALBP, confirming the multi-function of DES1 and indicating that it can isomerize both A1 and A2 retinols. The mechanism of DES1-catalyzed isomerization appears to rely on the cytochrome b5 electron transport chain, and involves an iron (III) cofactor and a free radical intermediate.

2.1.4 Materials and Methods

2.1.4.1 Coimmunoprecipitation of CRALBP with DES1

The method of this part is from (Kaylor, Yuan et al. 2013). Chicken retinas or 293T cells transfected with a plasmid encoding chicken CRALBP, were incubated in Lysis/Wash buffer (25 mM Tris pH 7.4, 150 mM NaCl, 1 mM EDTA, 1% NP-40, 5% glycerol and complete proteinase inhibitors - Roche) at 4 °C on an orbital shaker for 30 min. The lysate was centrifuged at 13,000xg for 10 min in a 1.5 ml Eppendorf tube. The supernatant was collected and a small aliquot was removed for protein quantification by the BCA assay. 150 µL of Dynabeads Protein A suspension (30 mg/ml) (Invitrogen) was added to a 1.5 mL Eppendorf tube. The tube was placed on a magnet and the supernatant removed. The Dynabeads were washed twice with 200 µL Lysis/Wash buffer. After removal of the final lysis/wash buffer, 30 µg of affinity-purified rabbit polyclonal antiserum against chicken DES1 or rabbit polyclonal RLBP1-specific (CRALBP) antiserum (Sigma-Aldrich) in 100 µL lysis/wash buffer was added to the tube containing the washed Dynabeads and incubated for 20 min with rotational mixing at room temperature. The supernatant was removed and the Dynabeads containing the immobilized antibodies were washed twice with lysis/wash buffer. Then, 200 µL cell

extract (10 mg/ml total protein) was added to the Dynabeads–antibody complex and gently resuspended by pipetting. The tube was incubated at room temperature for 30 min. The supernatant was removed and the beads were washed three times with 200 µL Lysis/Wash buffer by gently pipetting. The beads were resuspended in 100 µL Lysis/Wash buffer and transferred to a clean Eppendorf tube. The beads were then washed with 200 µL conditioning buffer and resuspended in 20 µL of Elution buffer (200 mM glycine, pH 2.8). The suspension was incubated at room temperature for five min. The supernatant was collected for immunoblotting after placing the tube on a magnet.

2.1.4.2 Inhibition of DES1 isomerase activity by C8-dihydroceramide and C8-cyclopropenylceramide

The method of this part is from (Kaylor, Yuan et al. 2013). DES1-expressing 293T cells were homogenized in Tris buffer containing Complete EDTA-free proteinase inhibitors. Various volumes of C8-dihydroceramide or C8-cyclopropenylceramide (400 µM in ethanol) were added to the reaction tubes and dried under a stream of nitrogen. Ten µL of ethanol was added to each tube and the lipids were dissolved. Ninety µL of Tris-HCl buffer with 2% BSA was added to the ethanol solution and vortexed vigorously for 10 seconds, three times, chilling on ice in between for one min. One-hundred µL of cell homogenates containing 500 µg total protein was pre-incubated in assay buffer for 10 min at room temperature. The assay mixtures were incubated at 37°C in the dark for 20 min after addition of 5 µM all-*trans*-ROL in ethanol. The isomerase activities were calculated after subtracting background activities and normalizing to the control reaction with no inhibitors.

2.1.4.3 Inhibition of DES1 isomerase activity by multiple inhibitors

All manipulations involving retinoids were performed in dim red light unless otherwise mentioned (this is true throughout this dissertation). Generally, DES1 isomerase activity assays were performed according to the method previously published (Sun and Travis 2010, Kaylor, Yuan et al. 2013), with some modifications. Briefly, HEK 293T cells stably expressing chicken DES1 (293T-D cells) were homogenized in ice-cold 40 mM Tris buffer pH 7.2 with 150mM NaCl, 1 mM DTT and complete EDTA-free protease inhibitors (Roche Diagnostics) and used immediately. Activity assays were performed using 293T-D cell homogenate (except for no cell homogenate "all-*trans*-ROL only" controls) as the source of DES1 in the above Tris buffer supplemented with 1% bovine serum albumin (BSA), 500 μM NADPH and 500 μM palmitoyl-CoA, in the presence of various inhibitors. The reaction mixtures were pre-incubated on ice for 10-15 minutes before initiated by the addition of all-*trans*-retinol (final concentration ~ 25-29 μM, in ethanol or DMSO, less than 2% of total reaction volume) except for no substrate ("293T-D cell homogenate only") controls (added the same volume of ethanol or DMSO instead). The concentration of all-*trans*-retinol was determined using a molar extinction coefficient of 52770 $M^{-1}cm^{-1}$ at 325 nm in ethanol (Leenheer, Lambert et al. 2000). The reactions were incubated at 37 ºC for 20-30 minutes followed by immediate quenching with 100 μL 1% SDS for each 400 μL reaction mixture. 1 ml methanol per sample was then added. Retinoids were extracted twice as described (Kaylor, Yuan et al. 2013, Kaylor, Xu et al. 2017). Each time 2 ml hexane was added, and the mixture was centrifuged at 3000 g for 5 minutes to separate the phases. The pooled retinoid extractions (in the upper hexane phase) were dried under a nitrogen gas stream, resuspended in 100 μL

hexane and analyzed by normal-phase high-performance liquid chromatography (HPLC) run on an Agilent 1100 series chromatograph with a photodiode-array detector. The method for HPLC analysis and retinoid quantitation were the same as published (Kaylor, Yuan et al. 2013, Kaylor, Xu et al. 2017).

For cytochrome b5 electron transport chain inhibition study **(Fig.2.1-3)**, the inhibitors used included: 10 mM ascorbic acid (Sigma), 5 mM *N*-ethylmaleimide (NEM) (Sigma-Aldrich), 5 mM 2,6-dichloroindophenol sodium salt hydrate (DCPIP) (Sigma), 5mM 6-propyl-2-thiouracil (PTU) (Sigma) or 1 mM 4-(hydroxymercuri) benzoic acid sodium salt (HMB) (Sigma) as indicated. For iron chelation study **(Fig.2.1-4)**, the inhibitors used included 5 mM 2,2'- bipyridyl (BIPY) (Riedel-de Haën) or 5 mM pyridoxal isonicotinoyl hydrazone (PIH). For inhibition study of spin traps/probes **(Fig.2.1-5)**, the inhibitors used included: 4-hydroxy-2,2,6,6-tetramethylpiperidine-1-oxyl (4-hydroxy-TEMPO) (Aldrich); 5,5-dimethyl-1-pyrroline-N-oxide (DMPO) (Sigma); 2,2-dimethyl-4-phenyl-2H-imidazole-1-oxide (DMPIO) (Enzo Life Sciences and Alexis Biochemicals) or 4-phenyl-2,2,5,5-tetramethyl-3-imidazoline-1-oxyl nitroxide (PTMIO) (Enzo Life Sciences), all at a concentration of 10 mM.

For inhibition study of 4-hydroxy-TEMPO and PTMIO at lower concentrations (5 mM, 500 µM and 50 µM) **(Fig.2.1-6)**, 293T or 293T-D cells were homogenized in ice-cold 40 mM Tris buffer pH 7.2 with EDTA-free Halt protease inhibitor cocktail (Thermo Fisher Scientific). Aliquots of homogenates were taken and their protein concentrations were determined by a protein assay using a Micro BCA protein assay kit (Thermo Scientific) according to the protocol suggested by the manufacturer. The cell homogenates were

snap-frozen in liquid nitrogen and stored at -80 ºC until use (within a few days). DES1 isomerase activity assays were performed using cell homogenates of equal amounts of total protein (~0.4 mg) in 40 mM Tris buffer pH 7.2 with 1.3 mM DTT, 500 μM NADPH, 1% BSA and Halt protease inhibitor cocktail, in the presence of 4-hydroxy-TEMPO or PTMIO delivered in ethanol with indicated concentrations. The reactions were initiated by the addition of all-*trans*-retinol in ethanol (final concentration 25 μM, ethanol <3% of total volume) after a 10-15 minute pre-incubation on ice. The reaction mixtures were incubated at 37 ºC for 25 minutes followed by quenching with 25 μL of 5% SDS, 50 μL brine for each 500 μL of the reaction mixture. 2 ml of methanol was added and the retinoids were extracted twice with 2 ml hexane (centrifuged at 3500 g for 5 minutes), and analyzed by HPLC using the same method above.

2.1.4.4 Vitamin A2-related DES1 dehydrogenase and isomerase activity tests

3-dehydroretinol (all-*trans*-3,4-didehydroretinol) was obtained from Santa Cruz Biotechnology and purified using normal-phase HPLC with the same retinoid analysis method (Kaylor, Yuan et al. 2013). The peak of all-*trans*-3,4-didehydroretinol was eluted shortly (about 1 minute) after all-*trans*-retinol. Spectra of both all-*trans*-retinol and all-*trans*-3,4-didehydroretinol were obtained in their ethanol solutions by a UV-Vis spectrometer (UV-2401(PC), Shimazu Corporation). The concentration of all-*trans*-3,4-didehydroretinol was determined using a molar extinction coefficient of 41320 $M^{-1}cm^{-1}$ at 350 nm in ethanol (Leenheer, Lambert et al. 2000).

For the test of DES1 dehydrogenase activity to convert A1 retinol to A2 retinol **(Fig.2.1-8)**, equal numbers of 100 mm plates of 293T and 293T-D cells were homogenized in

ice-cold 40 mM Tris buffer pH 7.2 with 1 mM DTT and used immediately. The protein concentrations of the homogenates were later measured by a micro BCA assay and turned out to be almost equal (less than 5% difference). Activity assays were performed using equal volumes of either type of cell homogenate (containing about 0.4 mg total protein per reaction) or the homogenization buffer (for “no cell homogenate” controls) in 40 mM Tris buffer pH 7.2 with1 mM DTT, supplemented with 1% BSA, ± 500 μM of NAD^+ or $NADP^+$, and 25 μM of all-*trans*-retinol (added last to initiate the reactions) in DMSO (~ 2% of final volume). The reactions were incubated at 37 ºC for 25 minutes and then quenched immediately by adding 25 μL of 5% SDS and 50 μL brine to each 500 μL of the reaction mixture. Retinoids were extracted into 2 ml hexane twice (centrifuged at 3500 g for 5 minutes) after adding 2 ml of methanol. Pooled extractions were derided and re-suspended in 210 μL of chilled hexane per sample. An aliquot of 95 μL per reaction was analyzed directly by HPLC, while another aliquot of 95 μL from the same reaction was supplemented with 5 μL of a small amount of exogenous all-*trans*-3,4-didehydroretinol (A2) in hexane and then also injected into HPLC. The addition of external A2 retinol would introduce an A2 peak in the HPLC chromatogram that could be used as a reference. The retinoids were analyzed using the same method above. Only sample aliquots without the supplementation of A2 were used for quantitative analysis **(Fig.2.1-8D)**.

For the test of DES1 isomerase activity using A2 retinol as substrate **(Fig.2.1-9)**, a similar assay condition was used. The activity was tested with 293T or 293T-D cell homogenates of equal amounts of total protein (~0.3 mg protein per reaction) or homogenization buffer (for “no cell homogenate” controls) in 40 mM Tris buffer pH 7.2

with 1 mM DTT, supplemented with 1% BSA, 500 μM NADPH and 20 μM of all-*trans*-3,4-didehydroretinol (in DMSO, ~2% of total volume). The reactions were incubated at 37 ºC for 25 minutes, and then quenched, extracted and analyzed the same way as above (with the exception that each sample was resuspended in 100 μL chilled hexane and analyzed directly by HPLC without the supplementation of external A2).

2.1.4.5 Statistical analysis

Statistical significance between two groups was determined by either a two-tailed Welch's or a two-tailed Student's *t*-test (the choice is based on an F-test). Statistical significance between multiple groups was determined by a single factor ANOVA test (in **Fig.2.1-9**). A p-value of less than 0.05 was considered significant.

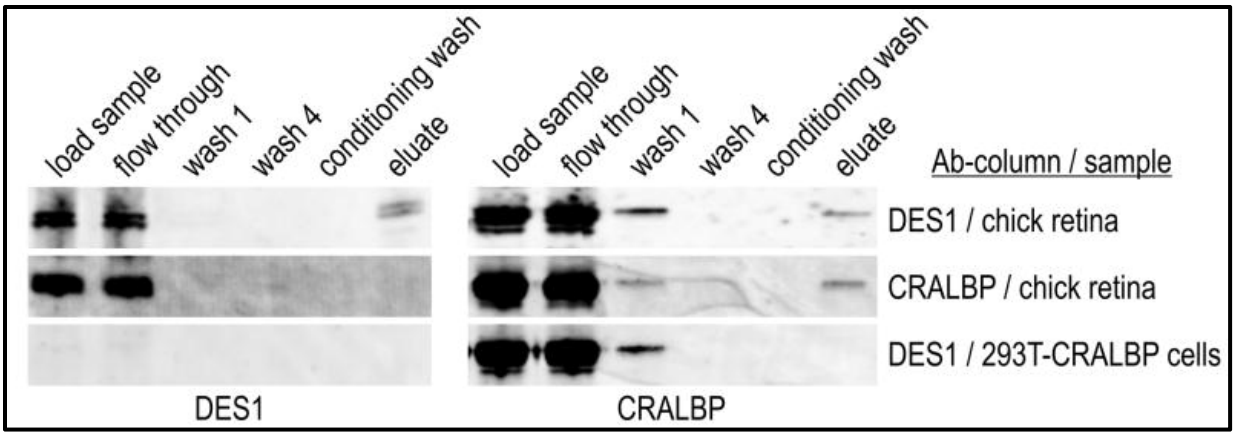

Figure 2.1-1. Co-immunoprecipitation of CRALBP with DES1. Immunoblots of protein samples detected with antibodies against chicken DES1 (left) or CRALBP (right). Samples include the starting homogenates (load sample); unbound samples after incubation with immobilized DES1 or CRALBP antibody (flow through); unbound samples after the first (wash 1) or final (wash 4) wash of the column with wash/lysis buffer; unbound samples after washing with conditioning buffer (conditioning buffer); and eluted proteins after washing with elution buffer (eluate). Homogenates were from chicken retinas (first and second rows of blots) or 293T-cells expressing CRALBP (third row of blots). (This figure and its legend are adapted from (Kaylor, Yuan et al. 2013)).

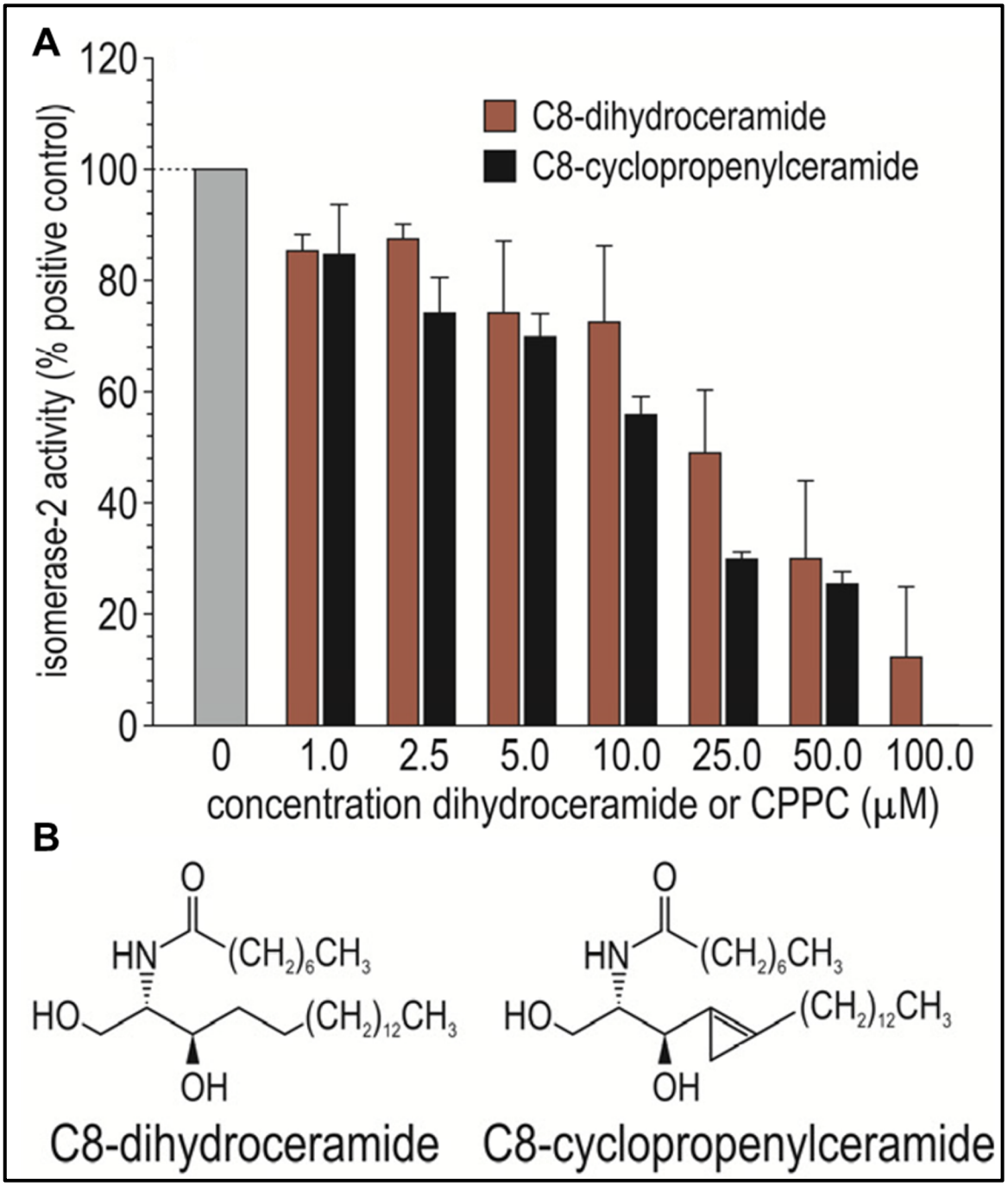

Figure 2.1-2. DES1 isomerase activity was inhibited by dihydroceramide and its analog. (A) DES1-catalyzed isomerase-2 activities at different concentrations of C8-dihydroceramide or C8-cyclopropenylceramide. Activities were expressed as percentage of activity with no inhibitor. **(B)** Molecular structures of C8-dihydroceramide, C8-cyclopropenylceramide. (This figure and its legend are adapted from (Kaylor, Yuan et al. 2013)).

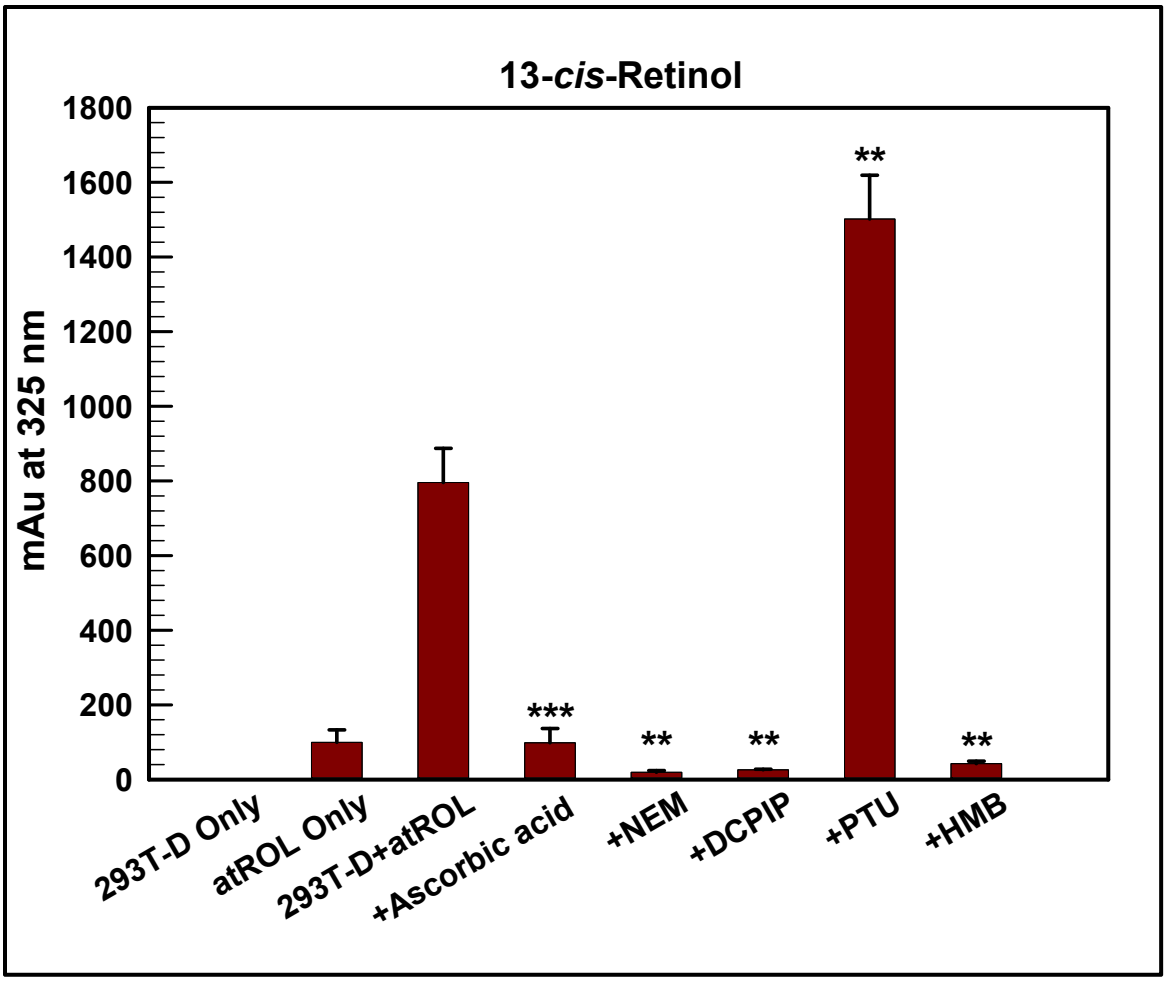

Figure 2.1-3. DES1 isomerase activity was inhibited by cytochrome b5 electron transport inhibitors. DES1 isomerase activity was assayed with the following conditions: 293T-D cell homogenate only (without adding the substrate, all-*trans*-retinol), all-*trans*-retinol (atROL) only (without 293T-D cell homogenate), the addition of both (293T-D+atROL), and the addition of both in the presence of 10 mM ascorbic acid, 5 mM NEM, 5 mM DCPIP, 5 mM PTU or 1 mM HMB. DES1 isomerase activity was represented by the formation of its major *cis*-isomer product, 13-*cis*-retinol (Kaylor, Yuan et al. 2013), in milli-Absorbance Units (mAU) read at 325 nm the in HPLC chromatograms (same below). Data were plotted as Mean ± S.D., n=3. **p<0.01, ***p<0.001, compared to the positive control, 293T-D+atROL.

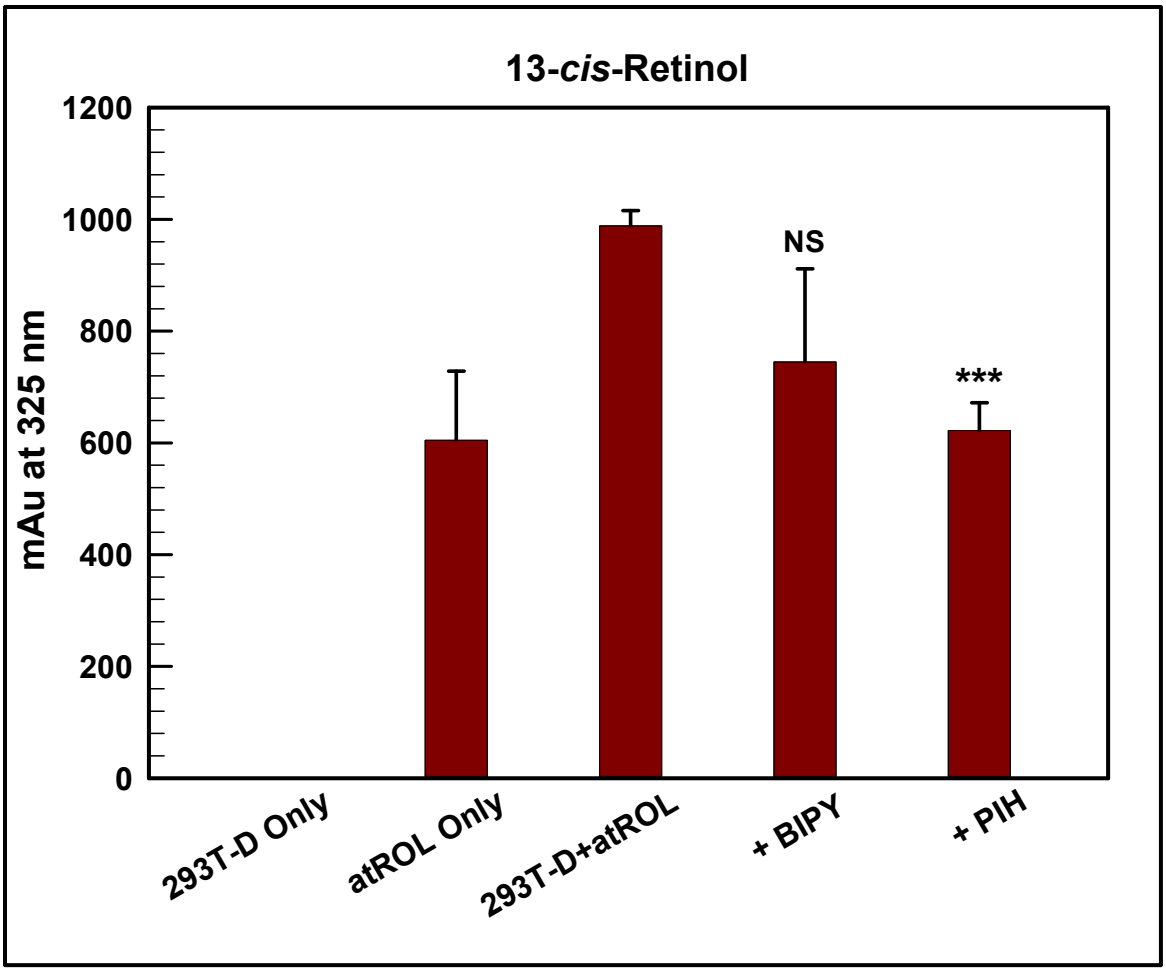

Figure 2.1-4. DES1 isomerase activity was inhibited predominantly by an iron (III) chelator, PIH. DES1 isomerase activity was assayed with the following conditions: 293T-D cell homogenate only, atROL only, the addition of both (293T-D+atROL), and the addition of both in the presence of 5 mM BIPY or 5 mM PIH. The DES1 isomerase activity was represented by the formation of 13-*cis*-retinol as above. Data were plotted as Mean ± S.D., n=3. ***p<0.001; NS, non-significant (for BIPY, p=0.123), compared to the positive control, 293T-D+atROL.

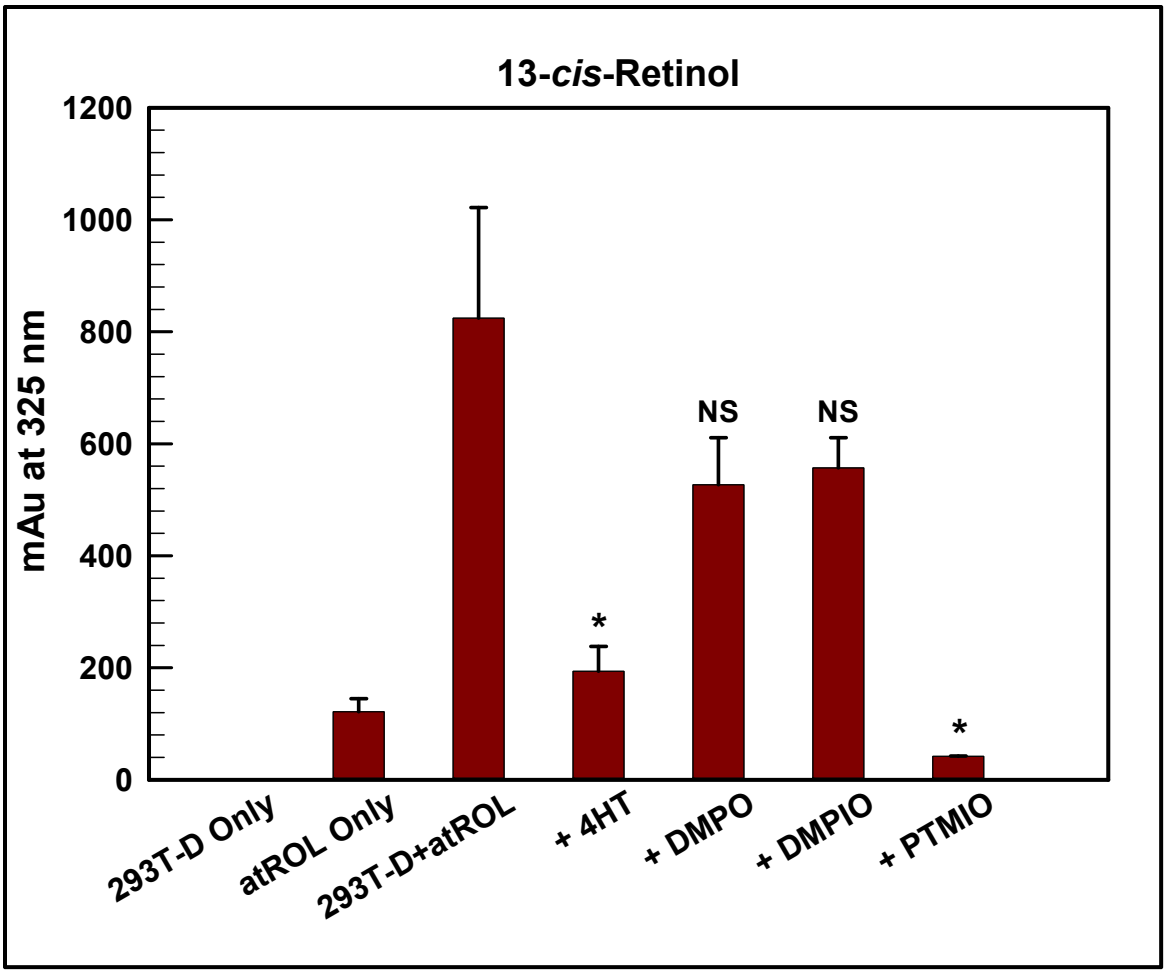

Figure 2.1-5. DES1 isomerase activity was inhibited by certain spin trap/probe reagents. DES1 isomerase activity was assayed with the following conditions: 293T-D cell homogenate only, atROL only, the addition of both (293T-D+atROL), and the addition of both in the presence of 10 mM 4-hydroxy-TEMPO (4HT), DMPO, DMPIO or PTMIO. DES1 isomerase activity was represented by the formation of 13-*cis*-retinol. Data were plotted as Mean ± S.D., n=3. *$p<0.05$; NS, non-significant (for DMPO, $p=0.074$; for DMPIO, $p=0.086$), compared to the positive control, 293T-D+atROL.

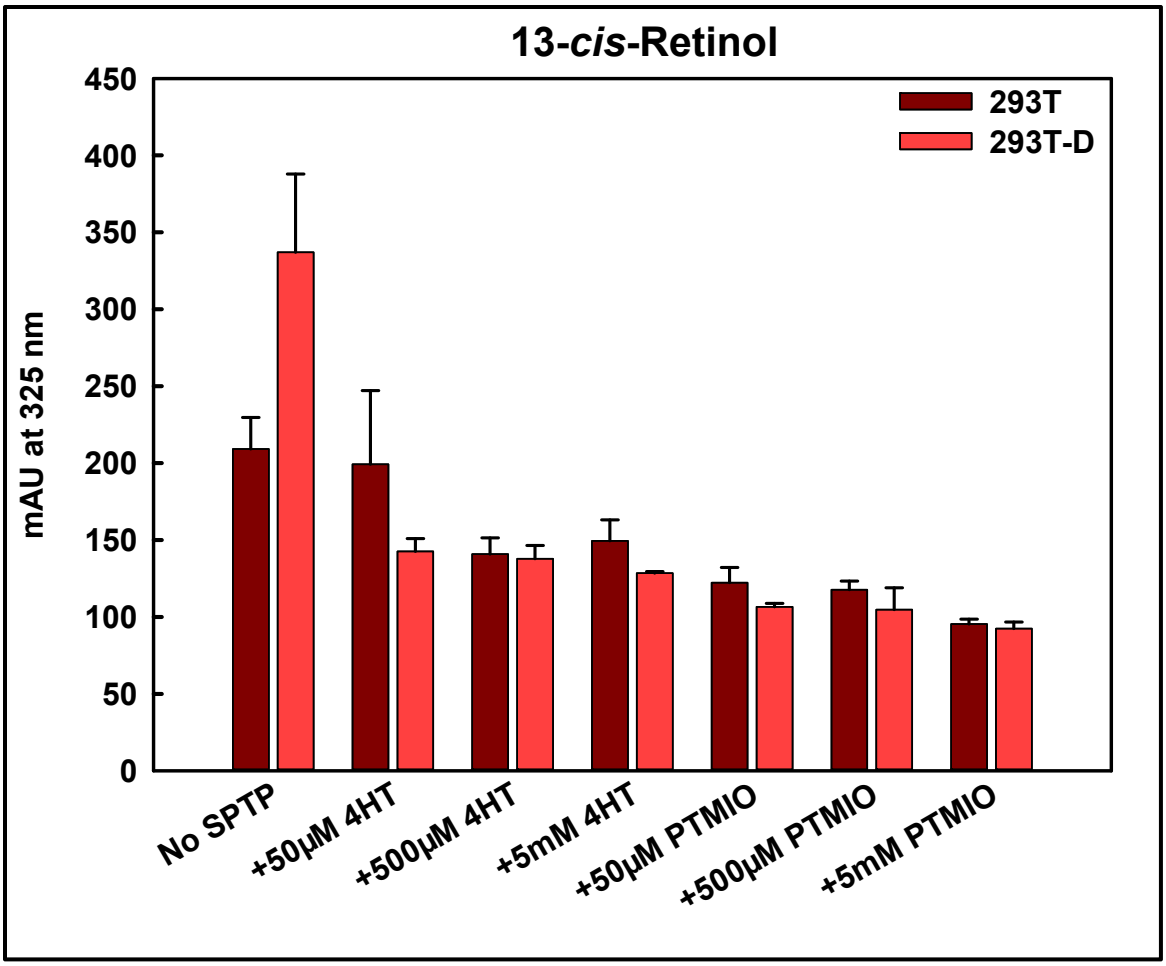

Figure 2.1-6. DES1 isomerase activity was inhibited by 4-hydroxy-TEMPO and PTMIO at lower concentrations. DES1 isomerase activity was assayed using either 293T or 293T-D cell homogenate with all-*trans*-retinol as the substrate, in the presence of no spin trap/probe reagent (No SPTP), or of a gradient concentration of 50 μM, 500 μM or 5 mM of 4-hydroxy-TEMPO (4HT) or PTMIO. DES1 isomerase activity was represented by the formation of 13-*cis*-retinol. Note the DES1-dependent formation of 13-*cis*-retinol between samples containing 293T-D versus 293T cell homogenate in the absence of spin trap/probe reagent (No SPTP). Such activity was abolished in the presence of 4HT and PTMIO at all tested concentrations. Data were plotted as Mean ± S.D., n=3.

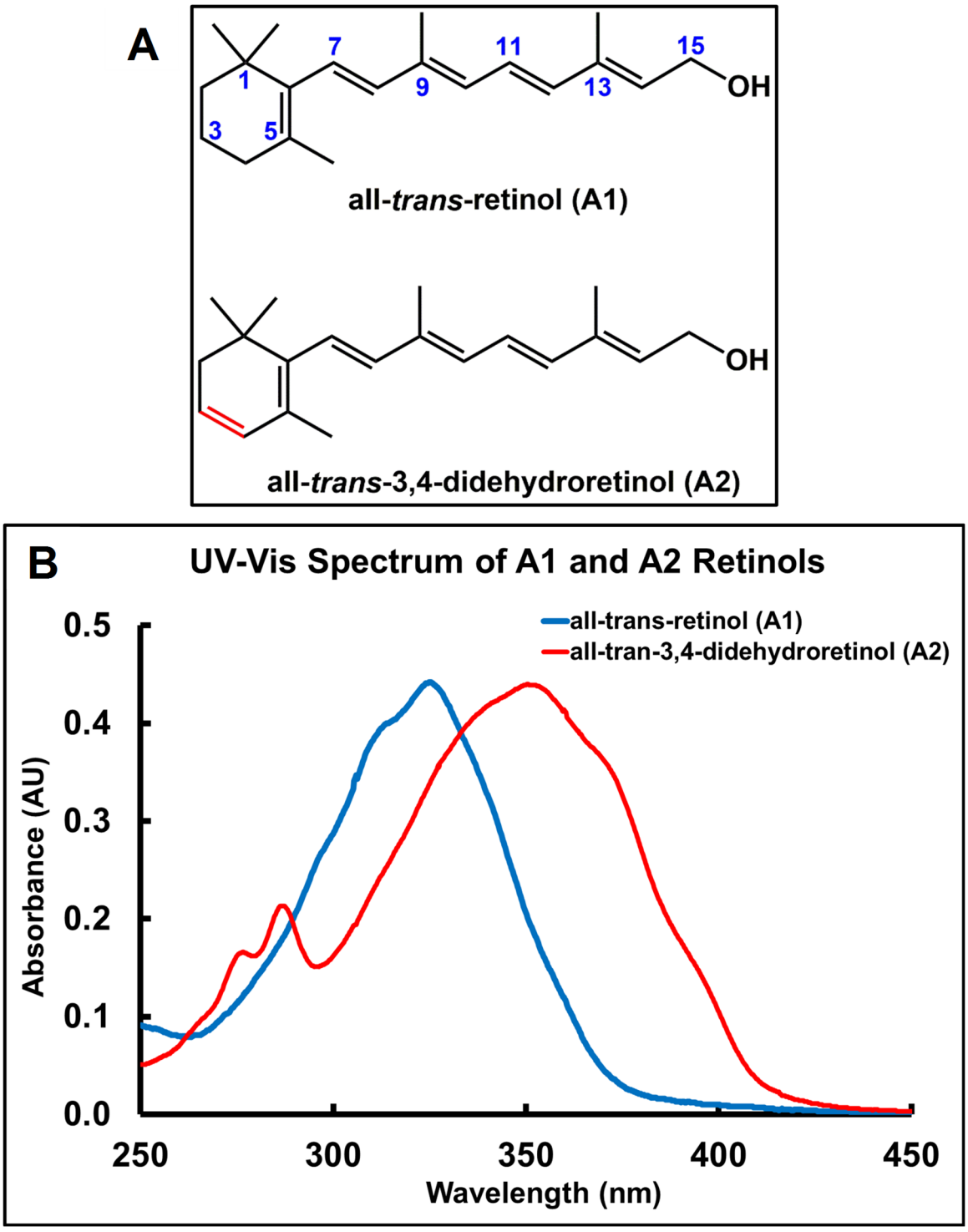

Figure 2.1-7. Structures and UV-Vis spectra of A1 and A2 retinols. (A) Chemical structures of A1 and A2 retinols. Note the extra double band (marked red) at the 3,4-position in the β-ionone ring in A2 retinol. **(B)** UV-Vis spectra of A1 and A2 retinols in ethanol. The λ_{max} of A1 retinol is ~325 nm while the λ_{max} of A2 retinol is ~350 nm.

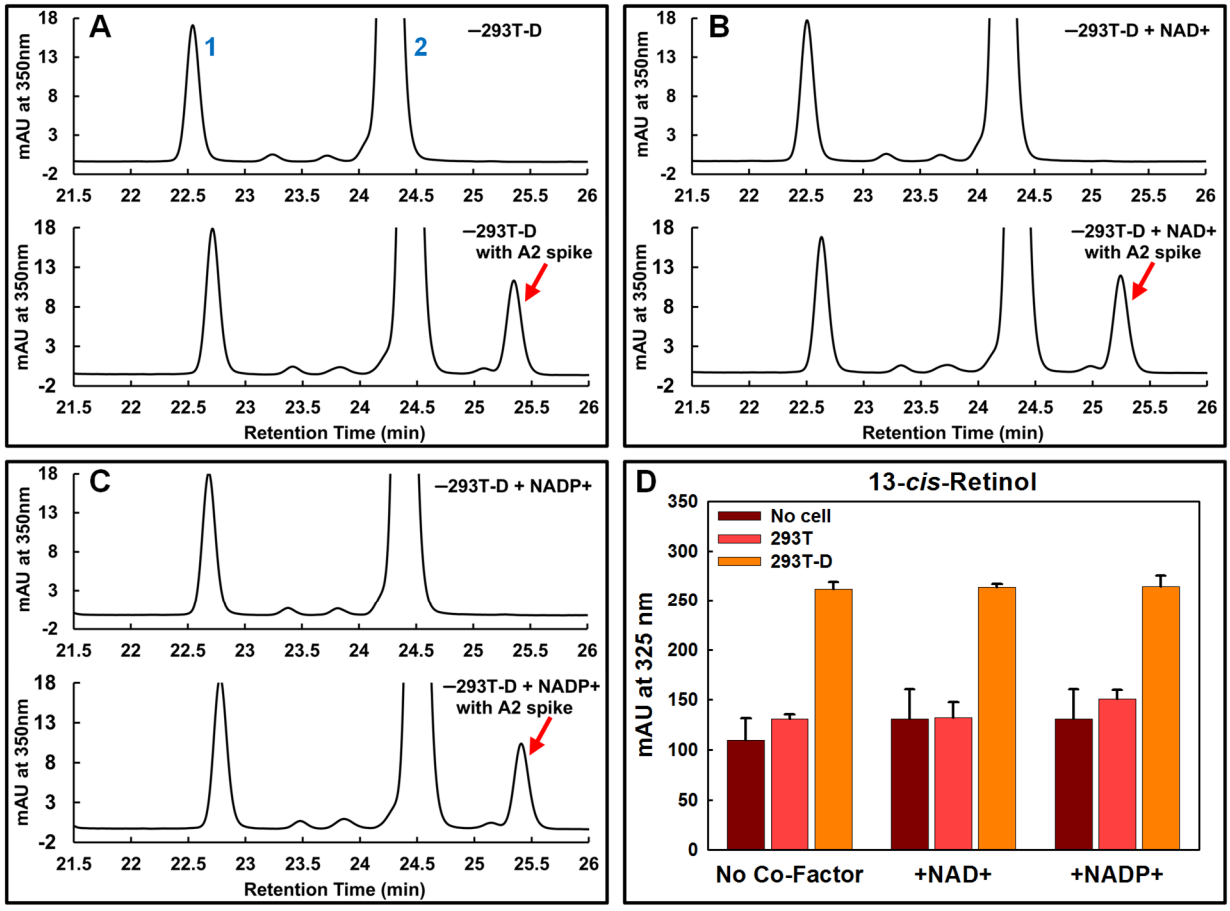

Figure 2.1-8. DES1 did not seem to convert A1 retinol to A2. Enzymatic activity assay was performed using assay buffer without cell homogenate (No cell), or homogenate of 293T or 293T-D cells, with A1 retinol as the substrate. **(A-C Top)** Representative HPLC chromatograms of DES1 dehydrogenase activity assay using 293T-D cell homogenate and A1 retinol, in the absence **(A)** or presence of NAD^+ **(B)** or $NADP^+$ **(C)**. Corresponding HPLC chromatograms of aliquots from the same samples but supplemented with small amounts of external A2 retinol as references ("A2 spike", red arrows) were shown at the **Bottom**. No significant A2 peak was observed in the top panels in any condition, indicating DES1 does not have robust enzymatic activity for converting A1 to A2 retinol. Peak 1: 13-*cis*-retinol; Peak 2: all-*trans*-retinol (A1). **(D)** DES1 isomerase activity was observed in the same experiment. 13-*cis*-retinol was quantitated to represent DES1 isomerase activity. The significant increase of 13-*cis*-retinol in samples containing 293T-D cell homogenate compared to the others in all the conditions indicates the active protein. Data were plotted as Mean ± S.D., n=3 for 293T and 293T-D samples and n=2 for no cell homogenate (No cell) control samples.

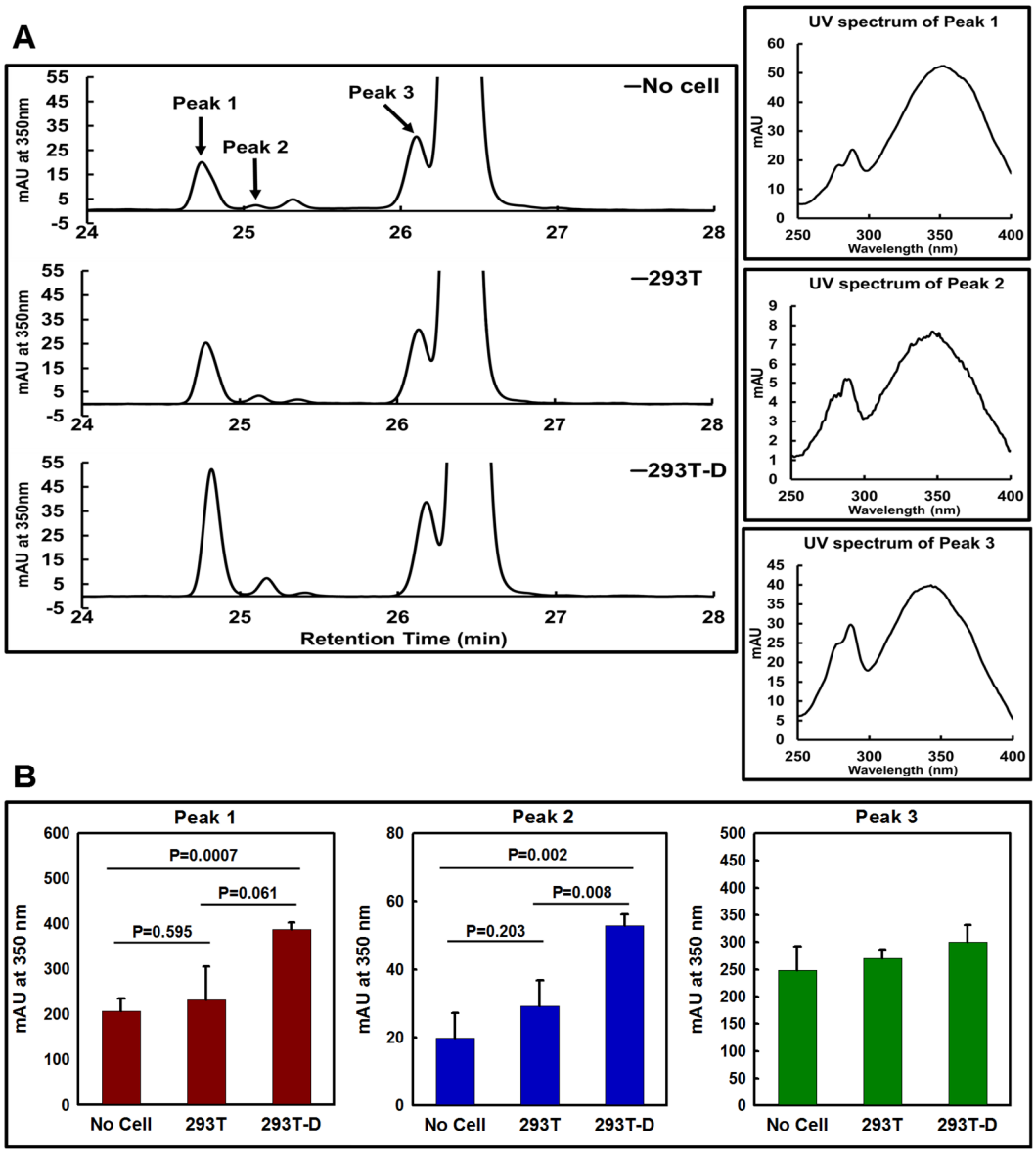

Figure 2.1-9. DES1 isomerized A2 retinol. DES1 isomerase activity was tested using assay buffer without cell homogenate (No cell), or homogenate of 293T or 293T-D cells, with A2 retinol as the substrate. **(A)** Representative HPLC chromatograms of samples with no cell homogenate (top panel), 293T cell homogenate (middle panel) and 293T-D cell homogenate (bottom panel). In the chromatograms, three peaks (peaks 1-3) that were believed to be *cis*-isomers of A2 retinol were observed. Their UV spectra were similar to that of A2 retinol (see **Fig.2.1-7B**), with their λ_{max} around 350 nm and characteristic secondary peaks between 250 nm and 300 nm (**Right panels in A**). **(D)** Quantitation of peaks 1-3, in mAU read at 350 nm from the HPLC chromatograms. Data were plotted as Mean ± S.D., n=3. P=0.006 for Peak 1, p=0.002 for Peak 2, p=0.230 for Peak 3 by single factor ANOVA tests. P-values of two-tailed *t*-tests on each pair of internal groups for Peak 1 and Peak 2 were determined. Such p-values were not determined for Peak 3 because there was no significant difference by a single factor ANOVA test.

References

Bavik, C. O., F. Levy, U. Hellman, C. Wernstedt and U. Eriksson (1993). "The retinal pigment epithelial membrane receptor for plasma retinol-binding protein. Isolation and cDNA cloning of the 63-kDa protein." J Biol Chem **268**(27): 20540-20546.

Beauchamp, E., D. Goenaga, J. Le Bloc'h, D. Catheline, P. Legrand and V. Rioux (2007). "Myristic acid increases the activity of dihydroceramide Delta 4-desaturase 1 through its N-terminal myristoylation." Biochimie **89**(12): 1553-1561.

Beauchamp, E., X. Tekpli, G. Marteil, D. Lagadic-Gossmann, P. Legrand and V. Rioux (2009). "N-Myristoylation targets dihydroceramide Delta 4-desaturase 1 to mitochondria: Partial involvement in the apoptotic effect of myristic acid." Biochimie **91**(11-12): 1411-1419.

Bhatt, M. R., Y. Khatri, R. J. Rodgers and L. L. Martin (2017). "Role of cytochrome b5 in the modulation of the enzymatic activities of cytochrome P450 17alpha-hydroxylase/17,20-lyase (P450 17A1)." J Steroid Biochem Mol Biol **170**: 2-18.

Buist, P. H. and B. Behrouzian (1998). "Deciphering the cryptoregiochemistry of oleate Delta(12) desaturase: A kinetic isotope effect study." Journal of the American Chemical Society **120**(5): 871-876.

Bunt-Milam, A. H. and J. C. Saari (1983). "Immunocytochemical localization of two retinoid-binding proteins in vertebrate retina." J Cell Biol **97**(3): 703-712.

Cadena, D. L., R. C. Kurten and G. N. Gill (1997). "The product of the MLD gene is a member of the membrane fatty acid desaturase family: Overexpression of MLD inhibits EGF receptor biosynthesis." Biochemistry **36**(23): 6960-6967.

Casasampere, M., Y. F. Ordonez, A. Pou and J. Casas (2016). "Inhibitors of dihydroceramide desaturase 1: Therapeutic agents and pharmacological tools to decipher the role of dihydroceramides in cell biology." Chem Phys Lipids **197**: 33-44.

Causeret, C., L. Geeraert, G. Van der Hoeven, G. P. Mannaerts and P. P. Van Veldhoven (2000). "Further characterization of rat dihydroceramide desaturase: Tissue distribution, subcellular localization, and substrate specificity." Lipids **35**(10): 1117-1125.

Chander, P., S. Gentleman, E. Poliakov and T. M. Redmond (2012). "Aromatic residues in the substrate cleft of RPE65 protein govern retinol isomerization and modulate its progression." J Biol Chem **287**(36): 30552-30559.

Dean, R. L. and E. Miskiewicz (2003). "Rates of electron transport in the thylakoid membranes of isolated, illuminated chloroplasts are enhanced in the presence of ammonium chloride." Biochemistry and Molecular Biology Education **31**(6): 410-417.

Deigner, P. S., W. C. Law, F. J. Canada and R. R. Rando (1989). "Membranes as the energy source in the endergonic transformation of vitamin A to 11-cis-retinol." Science **244**(4907): 968-971.

Endo, K., T. Akiyama, S. Kobayashi and M. Okada (1996). "Degenerative spermatocyte, a novel gene encoding a transmembrane protein required for the initiation of meiosis in Drosophila spermatogenesis." Mol Gen Genet **253**(1-2): 157-165.

Enright, J. M., M. B. Toomey, S. Y. Sato, S. E. Temple, J. R. Allen, R. Fujiwara, V. M. Kramlinger, L. D. Nagy, K. M. Johnson, Y. Xiao, M. J. How, S. L. Johnson, N. W. Roberts, V. J. Kefalov, F. P. Guengerich and J. C. Corbo (2015). "Cyp27c1 Red-Shifts the Spectral Sensitivity of Photoreceptors by Converting Vitamin A1 into A2." Curr Biol **25**(23): 3048-3057.

Ezanno, H., J. le Bloc'h, E. Beauchamp, D. Lagadic-Gossmann, P. Legrand and V. Rioux (2012). "Myristic acid increases dihydroceramide Delta4-desaturase 1 (DES1) activity in cultured rat hepatocytes." Lipids **47**(2): 117-128.

Fabrias, G., J. Munoz-Olaya, F. Cingolani, P. Signorelli, J. Casas, V. Gagliostro and R. Ghidoni (2012). "Dihydroceramide desaturase and dihydrosphingolipids: Debutant players in the sphingolipid arena." Progress in Lipid Research **51**(2): 82-94.

Gan, L., L. L. von Moltke, L. A. Trepanier, J. S. Harmatz, D. J. Greenblatt and M. H. Court (2009). "Role of NADPH-cytochrome P450 reductase and cytochrome-b5/NADH-b5 reductase in variability of CYP3A activity in human liver microsomes." Drug Metab Dispos **37**(1): 90-96.

Geeraert, L., G. P. Mannaerts and P. P. VanVeldhoven (1997). "Conversion of dihydroceramide into ceramide: involvement of a desaturase." Biochemical Journal **327**: 125-132.

Golczak, M., P. D. Kiser, D. T. Lodowski, A. Maeda and K. Palczewski (2010). "Importance of membrane structural integrity for RPE65 retinoid isomerization activity." J Biol Chem **285**(13): 9667-9682.

Golovleva, I., S. Bhattacharya, Z. Wu, N. Shaw, Y. Yang, K. Andrabi, K. A. West, M. S. Burstedt, K. Forsman, G. Holmgren, O. Sandgren, N. Noy, J. Qin and J. W. Crabb (2003). "Disease-causing mutations in the cellular retinaldehyde binding protein tighten and abolish ligand interactions." J Biol Chem **278**(14): 12397-12402.

Hamel, C. P., E. Tsilou, B. A. Pfeffer, J. J. Hooks, B. Detrick and T. M. Redmond (1993). "Molecular cloning and expression of RPE65, a novel retinal pigment epithelium-specific microsomal protein that is post-transcriptionally regulated in vitro." J Biol Chem **268**(21): 15751-15757.

Honjo, K., T. Ishibashi and Y. Imai (1985). "Partial purification and characterization of lathosterol 5-desaturase from rat liver microsomes." J Biochem **97**(3): 955-959.

Jahng, W. J., C. David, N. Nesnas, K. Nakanishi and R. R. Rando (2003). "A cleavable affinity biotinylating agent reveals a retinoid binding role for RPE65." Biochemistry **42**(20): 6159-6168.

Jokela, M., A. Vartio, L. Paulin, N. Fyhrquist-Vanni and K. Donner (2003). "Polymorphism of the rod visual pigment between allopatric populations of the sand goby (Pomatoschistus minutus): a microspectrophotometric study." Journal of Experimental Biology **206**(15): 2611-2617.

Kaylor, J. J., J. D. Cook, J. Makshanoff, N. Bischoff, J. Yong and G. H. Travis (2014). "Identification of the 11-cis-specific retinyl-ester synthase in retinal Muller cells as multifunctional O-acyltransferase (MFAT)." Proc Natl Acad Sci U S A **111**(20): 7302-7307.

Kaylor, J. J., T. Xu, N. T. Ingram, A. Tsan, H. Hakobyan, G. L. Fain and G. H. Travis (2017). "Blue light regenerates functional visual pigments in mammals through a retinyl-phospholipid intermediate." Nat Commun **8**(1): 16.

Kaylor, J. J., Q. Yuan, J. Cook, S. Sarfare, J. Makshanoff, A. Miu, A. Kim, P. Kim, S. Habib, C. N. Roybal, T. Xu, S. Nusinowitz and G. H. Travis (2013). "Identification of DES1 as a vitamin A isomerase in Muller glial cells of the retina." Nat Chem Biol **9**(1): 30-36.

Kiser, P. D., E. R. Farquhar, W. Shi, X. Sui, M. R. Chance and K. Palczewski (2012). "Structure of RPE65 isomerase in a lipidic matrix reveals roles for phospholipids and iron in catalysis." Proc Natl Acad Sci U S A **109**(41): E2747-2756.

Kiser, P. D., M. Golczak, D. T. Lodowski, M. R. Chance and K. Palczewski (2009). "Crystal structure of native RPE65, the retinoid isomerase of the visual cycle." Proc Natl Acad Sci U S A **106**(41): 17325-17330.

Kiser, P. D., M. Golczak and K. Palczewski (2014). "Chemistry of the retinoid (visual) cycle." Chem Rev **114**(1): 194-232.

Kiser, P. D. and K. Palczewski (2010). "Membrane-binding and enzymatic properties of RPE65." Prog Retin Eye Res **29**(5): 428-442.

Kiser, P. D. and K. Palczewski (2016). "Retinoids and Retinal Diseases." Annu Rev Vis Sci **2**: 197-234.

Kiser, P. D., J. Zhang, M. Badiee, Q. Li, W. Shi, X. Sui, M. Golczak, G. P. Tochtrop and K. Palczewski (2015). "Catalytic mechanism of a retinoid isomerase essential for vertebrate vision." Nat Chem Biol **11**(6): 409-415.

Larsen, P. J. and N. Tennagels (2014). "On ceramides, other sphingolipids and impaired glucose homeostasis." Mol Metab **3**(3): 252-260.

Lee, E. and K. Kariya (1986). "Propylthiouracil, a selective inhibitor of NADH-cytochrome b5 reductase." FEBS Lett **209**(1): 49-51.

Leenheer, A. P. d., W. E. Lambert and J. F. Van Bocxlaer (2000). Modern chromatographic analysis of vitamins. New York, Marcel Dekker.

McBee, J. K., V. Kuksa, R. Alvarez, A. R. de Lera, O. Prezhdo, F. Haeseleer, I. Sokal and K. Palczewski (2000). "Isomerization of all-trans-retinol to cis-retinols in bovine retinal pigment epithelial cells: dependence on the specificity of retinoid-binding proteins." Biochemistry **39**(37): 11370-11380.

Michel, C., G. van Echten-Deckert, J. Rother, K. Sandhoff, E. Wang and A. H. Merrill, Jr. (1997). "Characterization of ceramide synthesis. A dihydroceramide desaturase introduces the 4,5-trans-double bond of sphingosine at the level of dihydroceramide." J Biol Chem **272**(36): 22432-22437.

Moiseyev, G., Y. Takahashi, Y. Chen, S. Gentleman, T. M. Redmond, R. K. Crouch and J. X. Ma (2006). "RPE65 is an iron(II)-dependent isomerohydrolase in the retinoid visual cycle." J Biol Chem **281**(5): 2835-2840.

Morshedian, A., M. B. Toomey, G. E. Pollock, R. Frederiksen, J. M. Enright, S. D. McCormick, M. C. Cornwall, G. L. Fain and J. C. Corbo (2017). "Cambrian origin of the CYP27C1-mediated vitamin A1-to-A2 switch, a key mechanism of vertebrate sensory plasticity." R Soc Open Sci **4**(7): 170362.

Poliakov, E., T. Parikh, M. Ayele, S. Kuo, P. Chander, S. Gentleman and T. M. Redmond (2011). "Aromatic lipophilic spin traps effectively inhibit RPE65 isomerohydrolase activity." Biochemistry **50**(32): 6739-6741.

Porter, T. D. (2015). "Electron Transfer Pathways in Cholesterol Synthesis." Lipids **50**(10): 927-936.

Provencio, I., E. R. Loew and R. G. Foster (1992). "Vitamin A2-based visual pigments in fully terrestrial vertebrates." Vision Res **32**(12): 2201-2208.

Reuter, T. E., R. H. White and G. Wald (1971). "Rhodopsin and porphyropsin fields in the adult bullfrog retina." J Gen Physiol **58**(4): 351-371.

Rioux, V., F. Pedrono and P. Legrand (2011). "Regulation of mammalian desaturases by myristic acid: N-terminal myristoylation and other modulations." Biochimica Et Biophysica Acta-Molecular and Cell Biology of Lipids **1811**(1): 1-8.

Romeo, A. M., L. Christen, E. G. Niles and D. J. Kosman (2001). "Intracellular chelation of iron by bipyridyl inhibits DNA virus replication: ribonucleotide reductase maturation as a probe of intracellular iron pools." J Biol Chem **276**(26): 24301-24308.

Saari, J. C. and D. L. Bredberg (1987). "Photochemistry and stereoselectivity of cellular retinaldehyde-binding protein from bovine retina." J Biol Chem **262**(16): 7618-7622.

Sagara, H. and K. Hirosawa (1991). "Monoclonal-Antibodies Which Recognize Endoplasmic-Reticulum in the Retinal-Pigment Epithelium." Experimental Eye Research **53**(6): 765-771.

Saulter, J. Y., J. R. Kurian, L. A. Trepanier, R. R. Tidwell, A. S. Bridges, D. W. Boykin, C. E. Stephens, M. Anbazhagan and J. E. Hall (2005). "Unusual dehydroxylation of antimicrobial amidoxime prodrugs by cytochrome b5 and NADH cytochrome b5 reductase." Drug Metab Dispos **33**(12): 1886-1893.

Savile, C. K., G. Fabrias and P. H. Buist (2001). "Dihydroceramide delta(4) desaturase initiates substrate oxidation at C-4." J Am Chem Soc **123**(19): 4382-4385.

Schulze, H., C. Michel and G. van Echten-Deckert (2000). "Dihydroceramide desaturase." Sphingolipid Metabolism and Cell Signaling, Pt A **311**: 22-30.

Shanklin, J., E. Whittle and B. G. Fox (1994). "8 Histidine-Residues Are Catalytically Essential in a Membrane-Associated Iron Enzyme, Stearoyl-Coa Desaturase, and Are Conserved in Alkane Hydroxylase and Xylene Monooxygenase." Biochemistry **33**(43): 12787-12794.

Sun, H. and G. H. Travis (2010). "Retinoids: Methods and Protocols." Retinoids: Methods and Protocols **652**: 1-365.

Temple, S. E., E. M. Plate, S. Ramsden, T. J. Haimberger, W. M. Roth and C. W. Hawryshyn (2006). "Seasonal cycle in vitamin A1/A2-based visual pigment composition during the life history of coho salmon (Oncorhynchus kisutch)." J Comp Physiol A Neuroethol Sens Neural Behav Physiol **192**(3): 301-313.

Ternes, P., S. Franke, U. Zahringer, P. Sperling and E. Heinz (2002). "Identification and characterization of a sphingolipid Delta 4-desaturase family." Journal of Biological Chemistry **277**(28): 25512-25518.

Toyama, M., M. Hironaka, Y. Yamahama, H. Horiguchi, O. Tsukada, N. Uto, Y. Ueno, F. Tokunaga, K. Seno and T. Hariyama (2008). "Presence of rhodopsin and porphyropsin in the eyes of 164 fishes, representing marine, diadromous, coastal and freshwater species--a qualitative and comparative study." Photochem Photobiol **84**(4): 996-1002.

Triola, G., G. Fabrias, J. Casas and A. Llebaria (2003). "Synthesis of cyclopropene analogues of ceramide and their effect on dihydroceramide desaturase." J Org Chem **68**(26): 9924-9932.

Vitolo, L. M. W., G. T. Hefter, B. W. Clare and J. Webb (1990). "Iron Chelators of the Pyridoxal Isonicotinoyl Hydrazone Class .2. Formation-Constants with Iron(Iii) and Iron(Ii)." Inorganica Chimica Acta **170**(2): 171-176.

Wright, C. B., T. M. Redmond and J. M. Nickerson (2015). "A History of the Classical Visual Cycle." Molecular Biology of Eye Disease **134**: 433-448.

Wu, B. X., G. Moiseyev, Y. Chen, B. Rohrer, R. K. Crouch and J. X. Ma (2004). "Identification of RDH10, an All-trans Retinol Dehydrogenase, in Retinal Muller Cells." Invest Ophthalmol Vis Sci **45**(11): 3857-3862.

2.2 Characterization of DES1 with a DES1 knockout mouse model

2.2.1 Introduction

As discussed in **Chapter 1**, the maintenance of sustained vision in vertebrates relies on a constant supply of chromophore for the opsin visual pigments. This chromophore is provided by the canonical and alternate visual cycles. The canonical visual cycle is well understood with RPE65 as its retinoid isomerase (Redmond, Yu et al. 1998, Jin, Li et al. 2005, Moiseyev, Chen et al. 2005, Redmond, Poliakov et al. 2005). The alternate visual cycle is, however, relatively less characterized. Recently, we have identified DES1 as a strong candidate for the isomerase in the alternate visual cycle (Isomerase II). DES1 catalyzes equilibrium isomerization of retinol (Kaylor, Yuan et al. 2013). At equilibrium, 11-*cis*-retinoids are present as a small fraction of other retinoid isomers (Rando and Chang 1983). Production of chromophore is thought to be driven by mass action through two proteins that exhibit high 11-*cis* specificity. One of them is CRALBP, which binds to 11-*cis*-retinol with high affinity (Saari and Bredberg 1987, Golovleva, Bhattacharya et al. 2003) and has been shown to physically interact with DES1 **(Chapter 2.1.2.1)**. The other is MFAT, which is an 11-*cis*-specific retinyl-ester synthase and has been suggested to cooperate with DES1 (Kaylor, Cook et al. 2014). Although we have performed many biochemical studies (such as those in **Chapter 2.1** and (Kaylor, Yuan et al. 2013)), comprehensive *in vivo* evidence is needed to confirm the role of DES1 as the Isomerase II in physiological conditions.

In our biochemical studies, we predominantly used chicken DES1 ((Kaylor, Yuan et al. 2013) and **Chapter 2.1**), but chickens are not ideal for *in vivo* studies for apparent

reasons. Mice, on the other hand, are more suitable for this purpose. The expression of DES1 in mouse retina has been confirmed (Kaylor, Yuan et al. 2013). A functional alternate visual cycle in mouse retina has also been confirmed by physiological studies such as (Wang, Estevez et al. 2009, Wang and Kefalov 2009). Thus, a DES1 knockout mouse model will be a powerful tool to answer the question whether DES1 is the Isomerase II. In parallel, the disruption of Isomerase I, Rpe65, has been shown to cause a severe phenotype in mice, such as the absence of rhodopsin, the disorganization of ROS, an abnormal accumulation of all-*trans*-retinyl esters in the RPE (Redmond, Yu et al. 1998) and the early degeneration of cones (Znoiko, Rohrer et al. 2005). If DES1 is indeed Isomerase II, a significant phenotype in mice is also expected, especially when it comes to the retinoid processing in the retina and the functions of cone photoreceptors.

A DES1 deficient mouse model has been established from Des1 mutated mouse embryonic stem cells (Zambrowicz, Friedrich et al. 1998) and studied, mainly focusing on its role as a dihydroceramide desaturase (Holland, Brozinick et al. 2007). A series of phenotypes in those Des1-/- mice were observed, such as a poor birth/survival rate, a short lifespan (usually die within 8-10 weeks), a markedly reduced body size, significantly reduced ceremide but increased dihydroceramide contents in the body, and various abnormalities in blood biochemistry (Holland, Brozinick et al. 2007). Visual function in Des1-/- mice has not been characterized.

As a first step to determine if DES1 is isomerase II, we studied retina morphology, retinoid profiles in retina and RPE after overnight dark-adaptation, and the expression levels of multiple visual cycle-related genes in Des1-/- mice.

2.2.2 Results

2.2.2.1 Confirmation of the successful disruption of DES1 expression

To establish a Des1-/- mouse line, we obtained Des1+/- mice that were generated using mouse embryonic stem cells (corresponding to Omnibank clone OST368559 cell line) with Des1 gene (accession No. NM_007853) disrupted by gene trapping (gene trapping vector VICTR48), the same embryonic stem cell line as previously reported (Zambrowicz, Friedrich et al. 1998, Holland, Brozinick et al. 2007). These Des1+/- animals were then crossed with wild type (129) mice for several generations. To promote the survival of Des1-/- mice, Des1+/- offspring were outcrossed with CAST/EiJ mice. Their Des1+/- offspring were screened for the Leu450/Leu450 variant of the Rpe65 gene and wild-type for the spontaneous retinal degenerative *rd*8 mutation and selected for subsequent breeding.

Several methods were used to ensure the successful disruption of Des1 expression in Des1-/- mice. Mouse pups were genotyped to distinguish Des1+/+, Des1+/- or Des1 -/- mice **(Fig.2.2-1A)**. Reverse transcription-polymerase chain reactions (RT-PCR) were performed using RNA extracted from the retinas of Des1+/+ and Des1-/- mice, followed by gel electrophoresis analysis to ensure the absence of Des1 mRNA in Des1-/- mice **(Fig.2.2-1B)**. The absence of normal DES1 protein in Des1-/- mice was confirmed by immunoblotting using livers from Des1+/+ and Des1-/- mice **(Fig.2.2-1C)**. Also, our Des1-/- mice showed significant phenotypes including a dramatically smaller body size compared to that of age-matched Des1+/+ and Des1+/- mice, consistent with what was

previously described (Holland, Brozinick et al. 2007) **(Fig.2.2-1D)**. These results confirm the successful disruption of DES1 expression in our Des1-/- mice.

2.2.2.2 No obvious retina abnormality was observed in the retina of Des1-/- mice compared to that of age-matched Des1+/+ and Des1+/- mice by light microscopic analysis

To determine whether there are significant retina abnormalities in Des1-/- mice, such as photoreceptor degeneration and disorganization of photoreceptor outer segments, light microscopic analysis on retinas of about 1-month-old Des1+/+, Des1+/- and Des1-/- mice were performed. The general retina structures and laminations were similar between mice of these three genotypes. The structures of photoreceptor outer segments were also similar between these mice **(Fig.2.2-2)**. No significant loss of photoreceptor nuclei was observed in the retina of Des1-/- mice compared to that of age-matched Des1+/+ and Des1+/- mice **(Fig.2.2-2)**. These observations suggest that the retina of Des1-/- mice are healthy at this age.

2.2.2.3 Des1-/- mice had a similar amount of visual chromophore to that of age-matched Des1+/+ and Des1+/- mice

Although the morphological analysis did not reveal significant alterations in the retina of Des1-/- mice, it is important to know whether these mice contain a normal amount of visual pigments. This is intriguing given that Rpe65-/- mice showed an absence of rhodopsin (Redmond, Yu et al. 1998). The amount of visual pigments can be reflected by the quantitation of the visual chromophore, 11-*cis*-retinal. To address this question,

we first overnight dark-adapted Des1+/+, Des1+/- and Des1-/- mice, and then dissected their retinas and RPEs and extracted the retinoid contents in these tissues. The amounts of 11-*cis*-retinal, as well as other major retinoids, were analyzed by HPLC. As shown in **Fig.2.2-3**, the retinoid profiles between the retinas of Des1+/+ (WT), Des1+/- (Het) and Des1-/- (KO) mice were similar. No significant reduction of 11-*cis*-retinal was observed in Des1-/- retina, even though they had a reduced body size (thus a possibly reduced retina size as well) **(Fig.2.1-1D)**. These indicate that the formation of visual pigments and the dark-adaptation of photoreceptors are not significantly affected despite the disruption of Des1 gene. In parallel, the retinoid contents in the RPEs were also analyzed **(Fig.2.2-4)**. In general, they were also similar between mice of different genotypes **(Fig.2.2-4)**, except that the amounts of retinyl esters seem to be lower in the RPE of Des1-/- mice **(Fig.2.2-4C, F and G)**. However, large variations of the amounts of retinyl esters were observed, which could probably be due to the high background variability of these mice (our mice were outcrossed with CAST/EiJ mice to facilitate the survival of the Des1-/- pups, so a homogenous background was not established). We were not able to draw a confident conclusion in this regard.

2.2.2.4 The expression levels of several visual cycle-related genes were largely unaffected in the retina and RPE of Des1-/- mice compared to that of age-matched Des1+/+ and Des1+/- mice

If DES1 is Isomerase II, its deficiency could affect the expression levels of genes in the alternate visual cycle, such as CRALBP and MFAT in the retina. Both CRALBP and MFAT are at the downstream of DES1 and are thought to facilitate 11-*cis*-retinoid

formation (Kaylor, Yuan et al. 2013, Kaylor, Cook et al. 2014). Therefore, we determined the mRNA expression levels of these genes by qRT-PCR using RNA extracted from the retinas of about 1-month-old Des1+/+ and Des1-/- mice. The expression level of CRALBP is slightly higher in the retina of Des1-/- mice compared to that of Des1+/+ mice (p=0.049) **(Fig.2.2-5A)**. No significant difference of MFAT expression was observed in these retinas **(Fig.2.2-5B)**. We then asked whether the machinery of the canonical visual cycle was upregulated as a result of a compensatory mechanism to the impaired putative Isomerase II. To address that, I determined the expression levels of Rpe65, CRALBP, LRAT and RDH5 in the RPEs of Des1+/+ and Des1-/- mice by qRT-PCR **(Fig.2.2-5C-F)**. Only the expression level of RDH5 showed a mild increase in the RPE of Des1-/- mice compared to that of Des1+/+ mice (p=0.012) **(Fig.2.2-5F)**. No significant difference was seen in the other genes **(Fig.2.2-5C-E)**.

The expression of genes at the transcriptional level may not always correlate with that at the protein level (Maier, Guell et al. 2009). For this reason, we collected retinas and RPEs from Des1-/- and age-matched Des1+/+ mice and determined the expression levels of several genes at their protein level. Due to the availability and quality of antibodies, we were able to perform immunoblotting on the expression level of CRALBP in the retina, as well as that of RPE65, CRALBP and LRAT in RPE. The protein expression levels of CRALBP showed a minor decrease in both the retina (p=0.033) **(Fig.2.2-6A and E)** and RPE (p=0.002) **(Fig.2.2-6B and E)** of Des1-/- mice compared to that of Des1+/+ mice. The protein expression levels of RPE65 and LRAT were similar in the RPEs of Des1+/+ and Des1-/- mice **(Fig.2.2-6C, C', D, D' and E)**.

Although a statistically significant difference was reached for the expression levels of certain genes, such as the expression levels of CRALBP mRNA in retina, RDH5 mRNA in RPE and CRALBP protein in both retina and RPE, these differences were small. Furthermore, both of the expression levels of the mRNA and protein of CRALBP showed mild differences between the retina of Des1+/+ and Des1-/- mice, but in opposite directions **(Fig.2.2-5A and Fig.2.2-6E)**. A similar trend was also seen for CRALBP expression in the RPE **(Fig.2.2-5C and Fig.2.2-6E)**. Therefore, taking both the qRT-PCR and immunoblotting results collectively, we concluded that the expression levels of these visual cycle-related genes are similar between the retinas and RPEs of Des1-/- and Des1+/+ mice.

2.2.3 Discussion

In vivo studies are crucial to determine whether DES1 is the Isomerase II in the retina. Utilizing biochemical resources and methods, we have performed the above characterization of the Des1 knockout mouse model. However, no apparent vision-related abnormities of Des1-/- mice have been found so far. The morphology of the Des1-/- retina seemed to be normal compared to that of the Des1+/+ and Des1+/- retinas **(Fig.2.2-2)**. The amounts of 11-*cis*-retinal after overnight dark-adaptation were comparable between Des1+/+, Des1+/- and Des1-/- mice **(Figs.2.2-3 and -4)**. The expression levels of several visual cycle-related genes, including Rpe65, CRALBP, LRAT, RDH5 and MFAT, were also not dramatically different between Des1+/+ and Des1-/- mice **(Figs.2.2-5 and -6)**.

Although the above preliminary studies did not reveal a dramatic difference between Des1+/+ and Des1-/- mice, there are multiple reasons why this would be the case. (1) Cones only account for a small population of total photoreceptors in mouse retina (Carter-Dawson and LaVail 1979). As discussed in **Chapter 1**, the alternate visual cycle powered by Isomerase II almost exclusively support cones. In this case, even if there are significant changes of cone visual pigments and cone functions, in the presence of an overwhelming number of rods, the difference would not be easily observed. (2) The animals studied (about 1-month old) might be too young to show a significant impairment of visual function. (3) The biochemical studies we performed may not be sensitive enough to observe a phenotype. In this case, electrophysiological characterization might be helpful. (4) Although not observed in our preliminary studies, it is completely possible that a strong visual phenotype will be apparent under extensive bright light illumination.

To sum up, although preliminary studies have been performed, the effects of Des1 gene disruption on the function and photosensitivity recovery of cones after bleach, which is our key hypothesis, have not been tested. Therefore, our current data do not lead to a clear conclusion whether DES1 is the Isomerase II or not. Further studies focusing on the cone functions of Des1-/- mice are needed to address this question.

2.2.4 Materials and Methods

2.2.4.1 Animal use and care

As previously described (Kaylor, Xu et al. 2017), our animal usage conforms with the policies of “the guide for the care and use of laboratory animals of the National Institutes

of Health, and the Association for Research in Vision and Ophthalmology Statement for the use of animals in ophthalmic and vision research". Our protocol was approved by the Animal Research Committee at University of California, Los Angeles (permit No.: A3196-01).

2.2.4.2 Des1 mouse strain

The experimental animals were all reared in cyclic light. Des1+/- mice with disrupted Des1 gene (by gene trapping) were purchased from Texas A&M System Health Science Center/Texas A&M Institute of Genomic Medicine. These mice were generated with mouse embryonic stem cells that correspond to Omnibank clone OST368559 cell line (accession number of DES1 is NM_007853), the same as previously reported (Zambrowicz, Friedrich et al. 1998, Holland, Brozinick et al. 2007). The obtained Des1+/- animals were crossed with wild type (129) mice for several generations. To increase the survival rate of Des1-/- mice, the Des1+/- offspring were outcrossed with wild-derived CAST/EiJ mice (Jackson Laboratory). Their Des1+/- offspring with Leu/Leu at codon 450 for Rpe65 gene and absence of *rd*8 mutation were selected for subsequent breeding. Both breeders were Des1+/- mice and the pups were genotyped.
Primers for determining the 450 codon of Rpe65 (Kaylor, Xu et al. 2017):
Forward: 5' CCTTTGAATTTCCTCAAATCAATTA
Reverse: 5' TTCCAGAGCATCTGGTTGAG
Primers for determining *rd*8 mutation (Kaylor, Xu et al. 2017):
Forward: 5' GGTGACCAATCTGTTGACAATCC
Reverse: 5' GCCCCATTTGCACACTGATGAC

The amplicons were subjected to sequencing analysis afterwards.

The genotyping of Des1 was performed in a multiplex reaction using primers of

Forward: 5’ AAATTGTTGGGTATGAGCTTTGC (gene-specific);

Reverse: 5’ CCATTTGAACGGCAGCTAGTC (gene-specific) and

5’ ATAAACCCTCTTGCAGTTGCATC (LTR Reverse detecting the gene trapping vector, sequence suggested by the Des1 mice provider).

Primers were synthesized by Integrated DNA Technologies. The PCR amplicons were subjected to gel electrophoresis using 1.5% agarose gels. A Des1 wild type allele shows a band of ~391 bp while the KO allele carrying the gene trapping vector shows a band of ~257 bp.

2.2.4.3 Retina morphological studies by light microscopy

These studies were performed using a similar method previously described (Lenis, Sarfare et al. 2017). Briefly, Des1+/+, Des1+/- and Des1-/- mice of about 1-month old were anesthetized, euthanized and then intracardially perfused with fixing solution (2% formaldehyde and 2.5% glutaraldehyde in 0.1 M sodium phosphate buffer (pH 7.2)). Their eyeballs were enucleated with the superior part marked. Eyeballs were fixed in 1% osmium tetroxide (in 0.1 M sodium phosphate, pH 7.2) followed by dehydration using an alcohol gradient. 1-μm-thick sections were cut and stained with toluidine blue after embedding. Images were taken by a CoolSNAP camera (Photometrics) using a 40x objective lens on a light microscope (Zeiss Axiophot).

2.2.4.4 Analysis of retinoid contents in retina and RPE

Des1+/+, Des1+/- and Des1-/- mice of about 1-month old were dark-adapted overnight (more than 16 hours in the dark) and euthanized the next day by cervical dislocation. Their retina and RPE tissues were immediately dissected in ice-cold PBS (1X) pH 7.2, snap-frozen in liquid nitrogen and kept at -80 ºC in the dark until use. On the day of extraction, the tissues were gently thawed on ice and homogenized in 600 µL of 2M hydroxylamine hydrochloride (Sigma-Aldrich) (dissolved in PBS, pH 7.0) in glass-to-glass homogenizers on ice. The homogenates were incubated at room temperature for 20 minutes to allow oximation of the retinaldehydes. 25 µL of 5% SDS and 50 µL brine were added to each homogenate. After 20 minutes, retinoids were extracted into chilled hexane (2ml, twice, separated by centrifugation at 3500g for 5min) after the addition of 2 mL chilled methanol, dried and resuspended in 100 µL of chilled hexane similarly as described (see **Chapter 2.1,** and (Kaylor, Yuan et al. 2013, Kaylor, Xu et al. 2017)). The retinoids were analyzed by HPLC as previously described (Kaylor, Yuan et al. 2013, Kaylor, Xu et al. 2017). Retinal isomer component was quantitated based on their corresponding *syn*- and *anti*-retinaldehyde oximes (ROXs) unless otherwise indicated (see (Kaylor, Xu et al. 2017), also **Fig.3.1-2** in **Chapter 3.1**). It is worth mentioning that the amounts of certain retinoids shown here were very low. In these cases, significant quantitation inaccuracies may occur due to technical limitations. These low values were reported because they might be useful for certain general comparisons, but extra caution should be taken if using them for absolute significance.

2.2.4.5 Determination of the expression levels of several visual cycle-related genes by qRT-PCR

Retina and RPE tissues from mice of about 1-month old were dissected in ice-cold PBS (1X) pH 7.2 (Gibco/Thermo Fisher Scientific). The dissected tissues were treated with Ambion RNAlater solution (Ambion) on ice for at least one hour. The RNAlater solution was then removed following a brief centrifugation, and the tissues were stored at -80 ºC until use. RNA was extracted using Absolutely RNA Miniprep Kit (Agilent Technologies) according to the protocol suggested by the manufacturer. CDNA was synthesized with equal amounts of RNA from the same type of tissue using SuperScript III First-Strand Synthesis SuperMix for qRT-PCR (Invitrogen) according to the protocol suggested by the manufacturer. Quantitative real-time PCR reactions were performed in a total volume of 10 µL using iTaq Universal SYBR Green Supermix (BioRad) in a CFX96 Real-Time system (BioRad) with the following cycling condition: 95 °C for 30 s followed by 40 cycles of 95 °C for 5 s; 60 °C for 30 s. The primers used are as listed below.

Rpe65, Forward: 5’ CCCAACTATATCGTTTTTGTGGA;

Reverse: 5’ GATTGAAAGGGGAAGTCCTG.

CRALBP, Forward: 5’ CCCTGGTGTCCTTTCCAGTC;

Reverse: 5’ CTGGGAATGAATCCTGGAGCA.

LRAT, Forward: 5’ ATACAGCCTACTGTGGAACA;

Reverse: 5’ CAGCCGAAGCAAGACTGCTT, according to previously published sequences (Masuda, Wahlin et al. 2014).

RDH5, Forward: 5’ GAAAGCTACAGCTTCACACATTG;

Reverse: 5’ CACATGATGGGATGAGATGC, according to previously published sequences (Masuda, Wahlin et al. 2014).

MFAT, Forward: 5’ CGCACAGCCCTTAAACATGG;

Reverse: 5’ TGGTAGAGGTTCTCCAACAACAG.

Des1, Forward: 5’ TGTAGCCATGATGCTTCTCG;

Reverse: 5’ GAGTTGTAGTGCGGGAGGTC, according to previously published sequences (Kaylor, Yuan et al. 2013). The quantitation of Des1 expression was not shown, but the amplicons were subjected to gel electrophoresis and the image was shown in **Fig.2.2-1B**.

β-actin was used as the reference gene and amplified by primers previously published (Kaylor, Yuan et al. 2013) with a minor modification:

Forward: 5’ CTGGCACCACACCTTCTACAATGAGC;

Reverse: 5’ GTGGTGGTGAAGCTGTAGCCACG.

The qRT-PCR data were analyzed by the $2^{-\Delta\Delta Ct}$ method as previously published (Livak and Schmittgen 2001). The expression levels of the genes of interest were normalized to those of Des1+/+ mice. Two-tailed *t*-tests (either Welch’s or Student’s, based on F-tests) were performed on the ΔCt values of the genes of interest relative to actin (calculated within each biological sample) to determine the statistical significance between the Des1+/+ and Des1-/- tissue samples. A p-value of less than 0.05 was considered significant.

2.2.4.6 Immunoblot analysis

Immunoblot analysis was performed using similar methods as previously published (Kaylor, Yuan et al. 2013, Lenis, Sarfare et al. 2017). Retina and RPE tissues from about 1-month-old mice were dissected in ice-cold PBS (1X) pH 7.2 with EDTA-free Halt protease inhibitor cocktail (Thermo Fisher Scientific), snap-frozen in liquid nitrogen immediately, and kept at -80 ºC until use. Livers were collected from about 1-month old mice, snap-frozen in liquid nitrogen and stored at -80 ºC until use (**Fig.2.2-1C**). Tissues were homogenized by sonication (Branson sonifier 450) in ice-cold PBS (1X) pH 7.2 with protease inhibitor cocktail. The homogenates were treated with benzonase nuclease (Sigma-Aldrich) at room temperature for 75 minutes followed by the treatment of SDS (final concentration 1%) for 20 minutes at 4 ºC. The treated homogenates were centrifuged at 3000 g for 5 minutes to pellet cellular debris, and the supernatants were collected for further tests. Aliquots were taken for protein concentration determination. The supernatants were stored at -80 ºC until use. Protein concentrations were determined by a protein assay using a Micro BCA protein assay kit (Thermo Scientific) according to the protocol suggested by the manufacturer. Equal amounts of protein from each sample were separated by 12% Novex NuPAGE Bis-Tris gels (Invitrogen) and transferred as previously described (Kaylor, Yuan et al. 2013). Membranes were blocked with Odyssey Blocking Buffer (LI-COR Biosciences) and probed with primary antibodies in the Blocking Buffer with 0.1% Tween 20 and 0.5% donkey serum as described (Kaylor, Yuan et al. 2013). Primary antibodies used included: anti-RPE65, the same custom antibody (from rabbit) as previously published (Mata, Moghrabi et al. 2004); anti-CRALBP, a mouse monoclonal antibody (1H7, Sigma-Aldrich); anti-LRAT, a

generous gift from Dr. Krzysztof Palczewski, the same as previously published (Batten, Imanishi et al. 2004); anti-β-actin, a mouse monoclonal antibody (8H10D10, Thermo Fisher Scientific); anti-GAPDH, a rabbit polyclonal antibody (FL-335, Santa Cruz Biotechnology); anti-DES1, a generous gift from Dr. Scott A. Summers, the same as previously published (Holland, Brozinick et al. 2007). After primary antibody incubation, the membranes were then incubated in cognate secondary antibodies (1:20,000) labeled with IR-dye (LI-COR) and scanned by an Odyssey CLx Infrared Imaging System (LI-COR) (Kaylor, Yuan et al. 2013, Lenis, Sarfare et al. 2017). LI-COR Odyssey analysis software was used for quantitative analyses with the proteins of interest normalized to β-actin or GAPDH. Two-tailed *t*-tests (either Welch's or Student's) were performed and a p-value of less than 0.05 was considered significant.

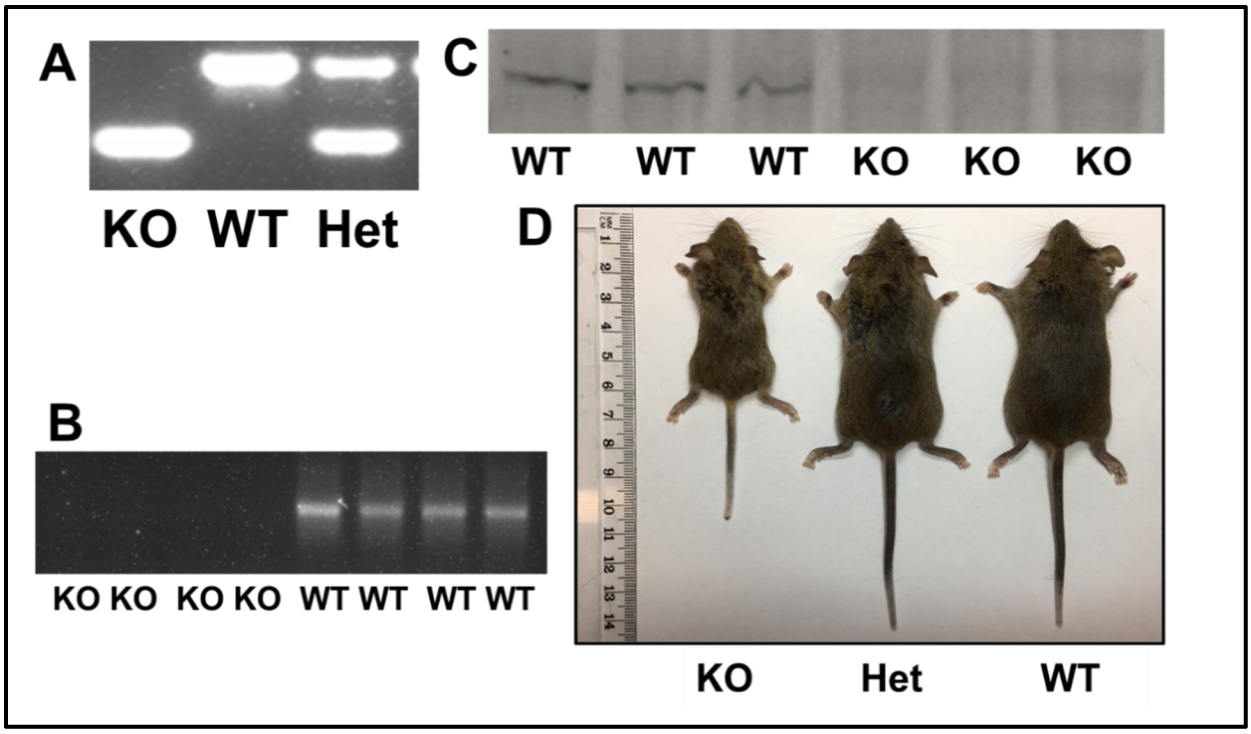

Figure 2.2-1. Validation of the successful disruption of DES1 expression in Des1 knockout mice. (A) A representative genotyping gel image. The absence of the normal Des1 gene amplicon (top band) and the presence of the amplicon from the gene trapping vector disrupting normal Des1 expression (bottom band) indicate a Des1 knockout (KO) mouse. The wild type (WT) mouse only showed the top band while the heterozygous (Het) mouse showed both bands. **(B)** A gel image of the amplicons from the RT-PCR reactions detecting Des1 mRNA expression in the retinas of four Des1 knockout (KO) (no band) and four Des1 wild type (WT) mice (all showed bands) of about 1-month old. **(C)** Immunoblot analysis of livers from three Des1 wild type (all showed bands) and three Des1 knockout (none showed band) mice of about 1-month old (75 µg total protein/lane). Livers instead of eye tissues were used due to their easy availability and abundance of proteins. **(D)** A representative picture of the gross appearances of about 1-month old Des1-/- (KO), Des1+/- (Het) and Des1+/+ (WT) mice. The Des1 knockout (KO) mouse had a significantly smaller body size.

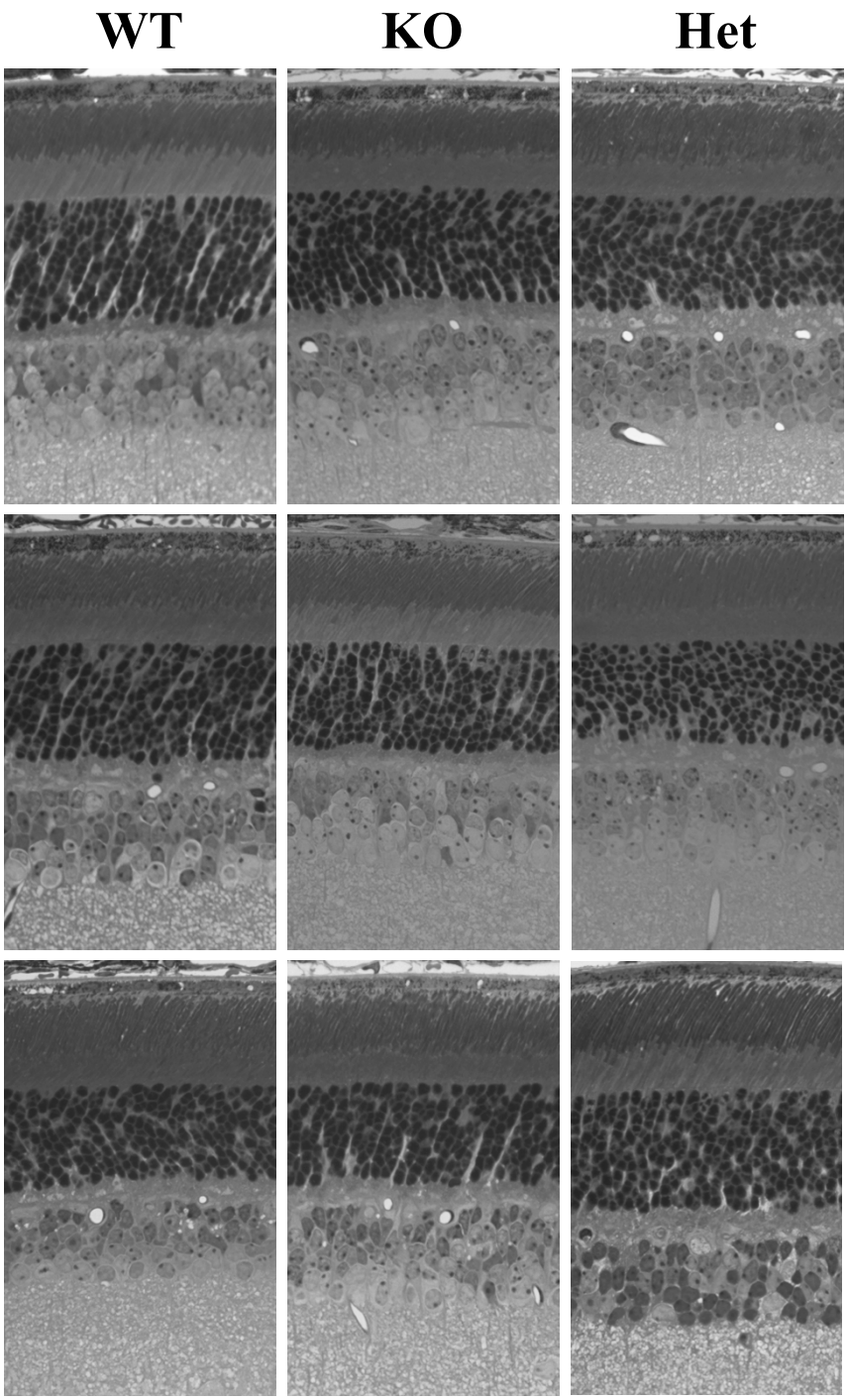

Figure 2.2-2. DES1-/- mouse retina did not exhibit significant morphological abnormality. Representative light microscopic images of the retinas from three Des1+/+ (WT, left column), three Des1-/- (KO, middle column) and three Des1+/- (Het, right column) mice. These mice were all about 1-month old. Images were taken with a 40X lens.

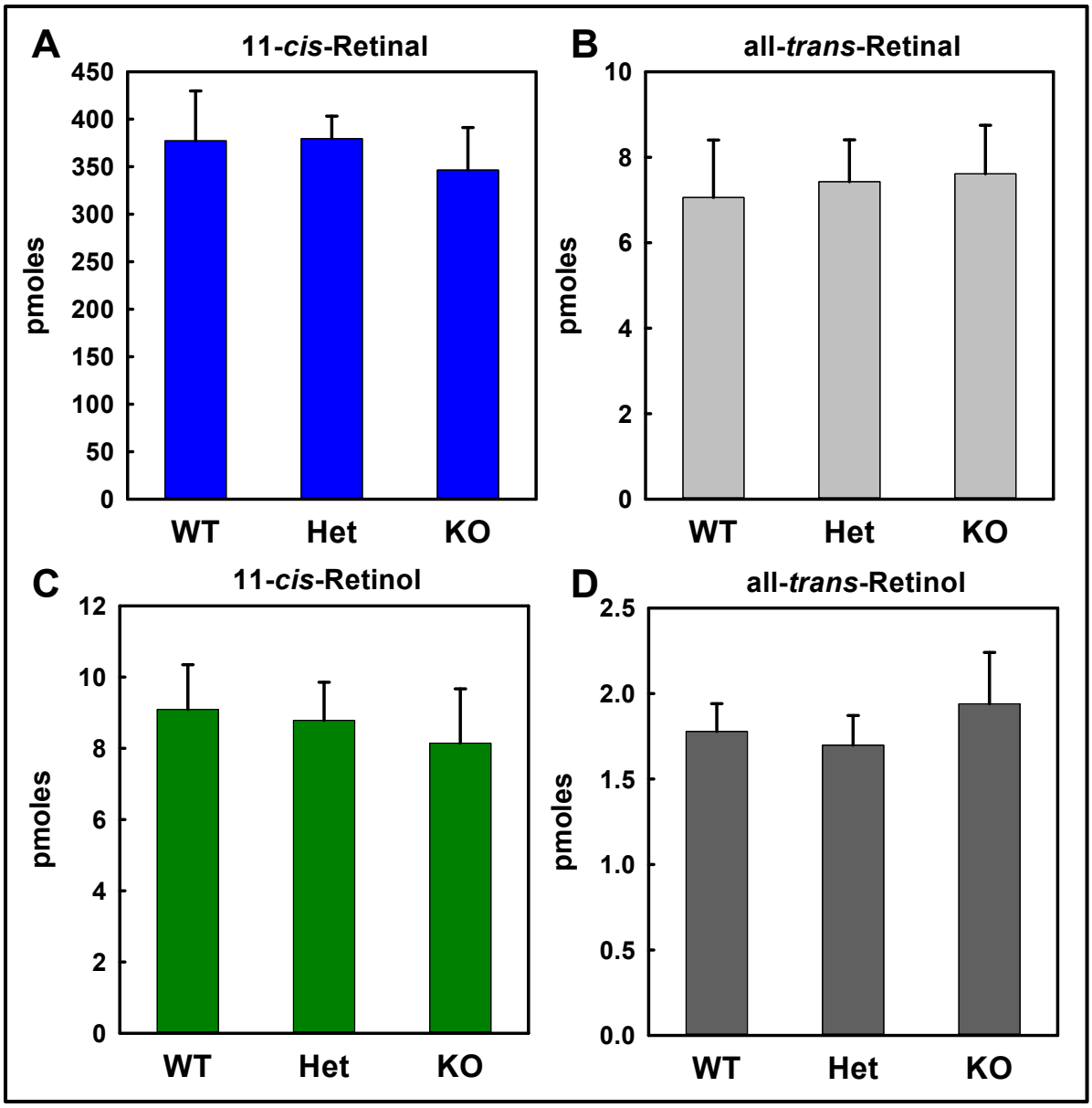

Figure 2.2-3. The retina of Des1-/- mice contained similar amounts of visual chromophore and other retinoids compared to that of Des1+/+ and Des1+/- mice. Des1+/+ (WT), Des1+/- (Het) and Des1-/- (KO) mice of about 1-month old were sacrificed after overnight dark-adaptation. Their retinas and RPEs were dissected and the retinoid contents in these tissues were analyzed by HPLC. The amounts of 11-*cis*-retinal **(A)**, all-*trans*-retinal **(B),** 11-*cis*-retinol **(C)** and all-*trans*-retinol **(D)** in the retinas of these mice as indicated are shown in this figure. In general, the amounts of visual chromophore (11-*cis*-retinal) were similar between mice of all the genotypes, as well as the other three types of retinoids. Data were plotted as Mean ± S.D., n=6 (6 retinas from three mice) for Des1+/+ (WT) and Des1-/- (KO) mice and n=8 (8 retinas from four mice) for Des1+/- (Het) mice.

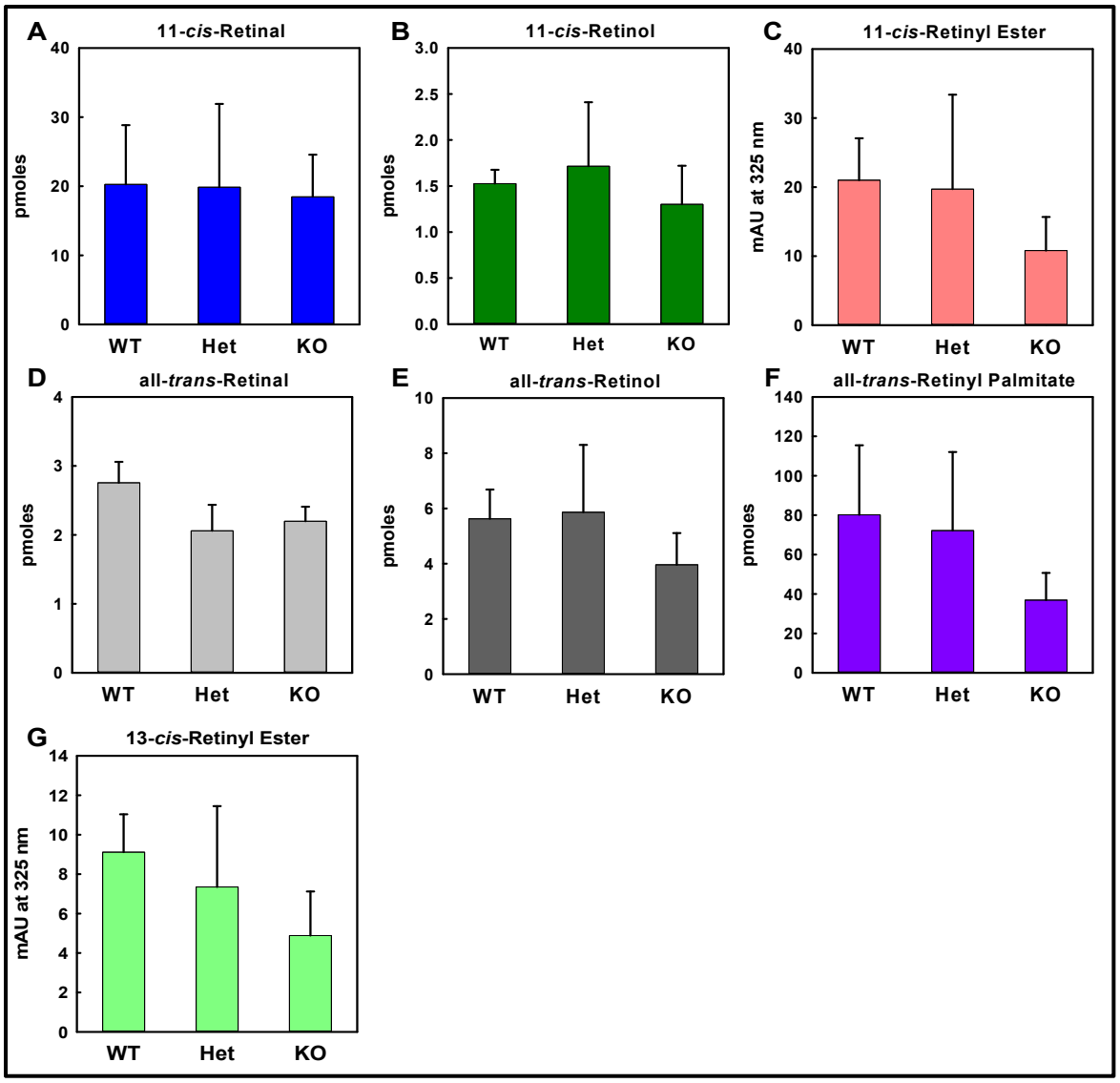

Figure 2.2-4. The RPE of Des1-/- mice contained similar amounts of retinals and retinols but seemingly lower amounts of retinyl esters compared to that of Des1+/+ and Des1+/- mice. The retinoid contents of the RPEs from the same mice in **Figure 2.2-3** were analyzed by HPLC and shown in this figure. Retinoids quantitated include: 11-*cis*-retinal **(A)**, 11-*cis*-retinol **(B),** 11-*cis*-retinyl ester **(C)**, all-*trans*-retinal **(D)**, all-*trans*-retinol **(E)**, all-*trans*-retinyl ester (mainly retinyl palmitate) **(F)** and 13-*cis*-retinyl ester **(G)**. The amount of 11-*cis*-retinal was quantitated only from *syn*-11-*cis*-ROX (see **Fig.3.1-2** in **Chapter 3.1** for a detailed explanation). *Anti*-11-*cis*-ROX had co-eluted with a peak of impurity in this experiment, so it was not included in the quantitation of 11-*cis*-retinal. The amounts of retinals and retinols were similar between the RPEs of Des1+/+ (WT), Des1+/- (Het) and Des1-/- (KO) mice. The amounts of retinyl esters seem to be lower in the RPE of Des1-/- but had large variations. Data were plotted as Mean ± S.D., n=6 (6 RPEs from three mice) for Des1+/+ (WT) and Des1-/- (KO) mice and n=8 (8 RPEs from four mice) for Des1+/- (Het) mice.

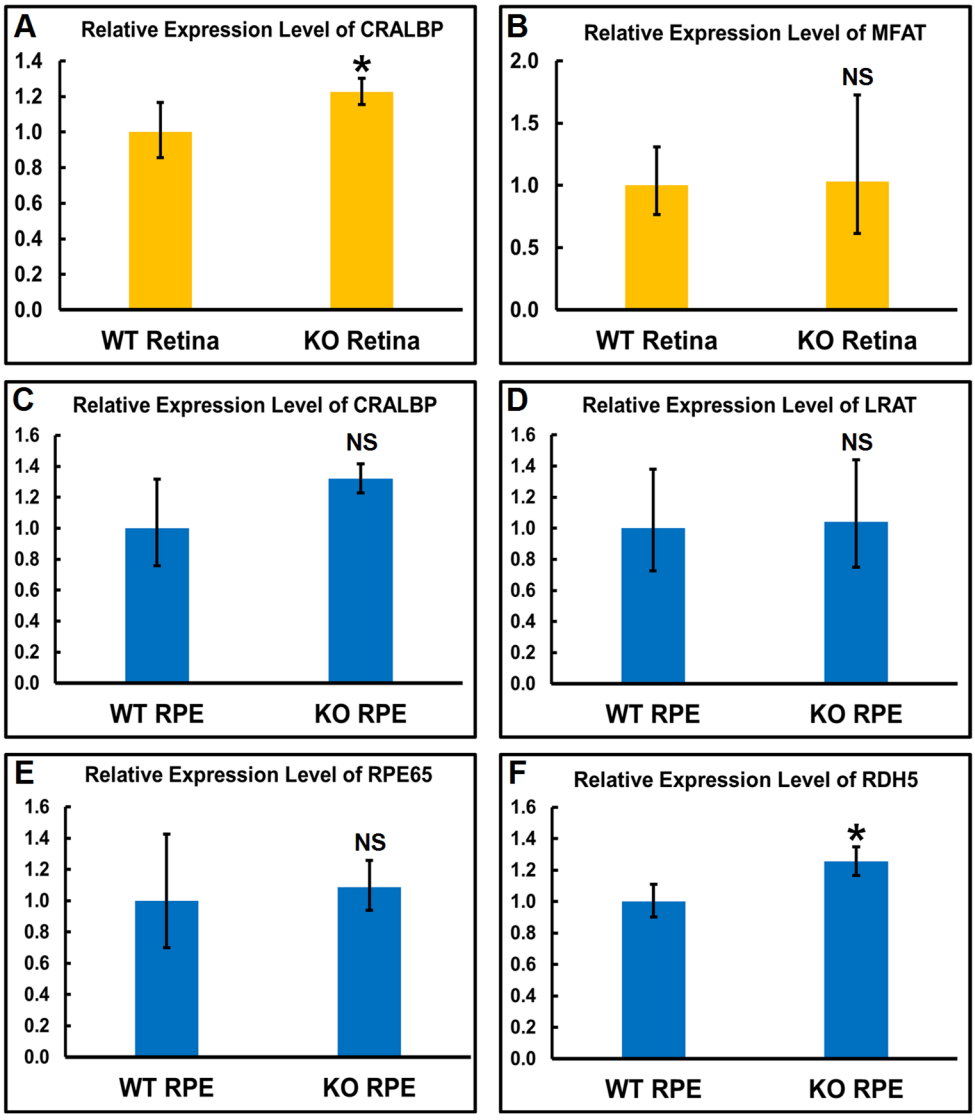

Figure 2.2-5. The mRNA expression levels of several visual cycle-related genes were generally similar in the retinas and RPEs of Des1+/+ and Des1-/- mice. RNA from retinas and RPEs of about 1-month old Des1+/+ (WT) and Des1-/- (KO) mice (four mice each genotype) were extracted. Equal amounts of RNA from each type of tissue were used to make cDNA. The expression levels of the mRNA of several visual-cycle related genes were determined by qRT-PCR with β-actin as the reference gene. Tested mRNA included CRALBP **(A)** and MFAT **(B)** in retina, and CRALBP **(C)**, LRAT **(D)**, RPE65 **(E)** and RDH5 **(F)** in RPE. The relative expression levels of these genes were calculated by the $2^{-\Delta\Delta Ct}$ method and normalized to that of the WT tissues, following a published method (Livak and Schmittgen 2001). Data were plotted as Mean ± Confidence Intervals (RQ_{min} to RQ_{max}), n=4. *p<0.05; NS, non-significant, compared to WT by a two-tailed *t*-test on ΔCt values (the difference of Ct values between the gene of interest and the reference gene) with equal variances for all except **(C)** (unequal variances). P=0.049 for the expression of CRALBP in retina **(A)** and p=0.012 for the expression of RDH5 in RPE **(F)**.

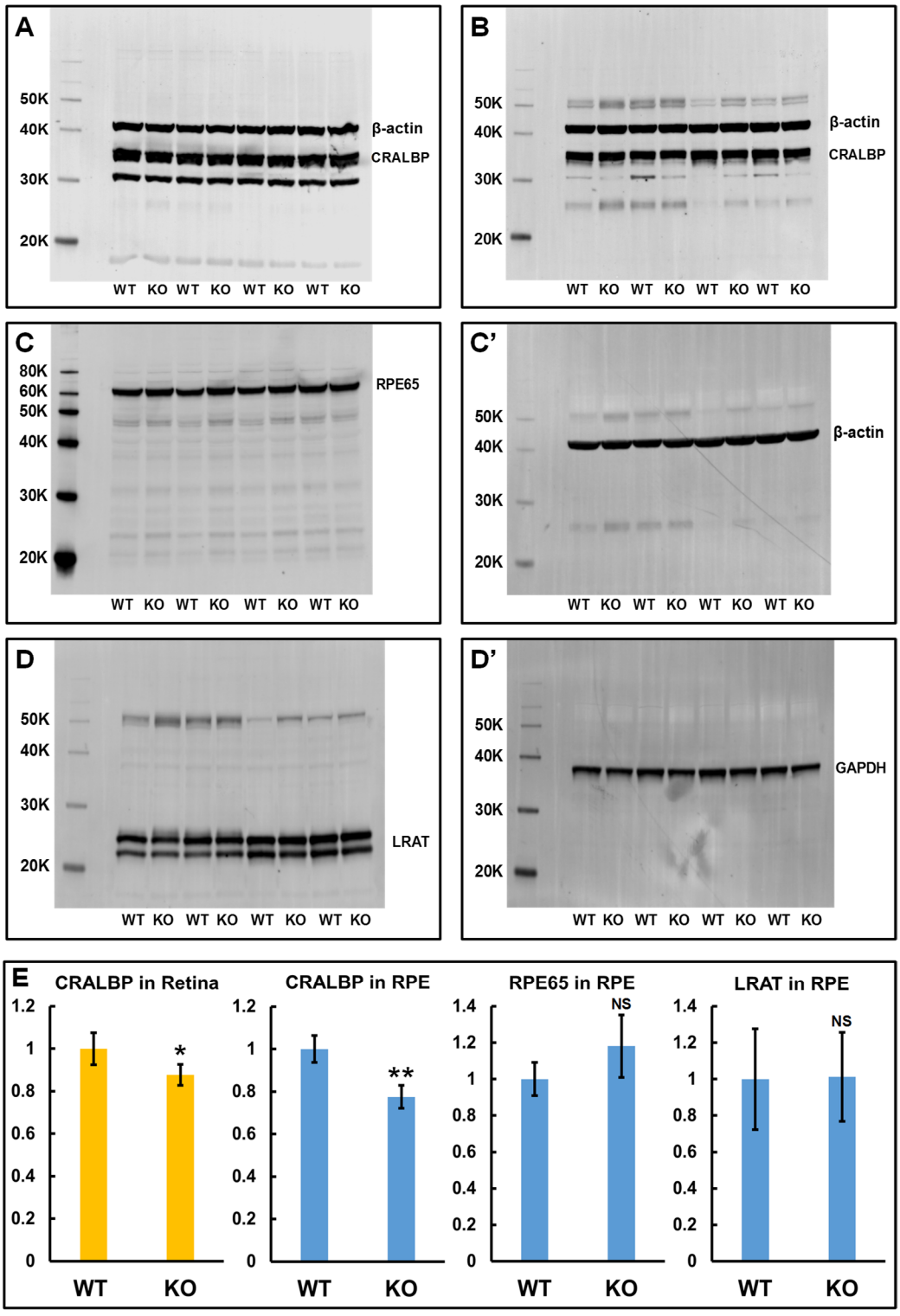

Figure 2.2-6. The protein expression levels of several visual cycle-related genes were generally similar in the retinas and RPEs of Des1+/+ and Des1-/- mice. Retina and RPE homogenates were prepared from about 1-month old Des1+/+ (WT) and Des1-/- (KO) mice (four mice each genotype, as indicated), and analyzed by

immunoblot. Equal amounts of total protein (15-40 μg) per lane were loaded within each gel. Shown above were immunoblots of: the expressions of CRALBP in retina **(A)** and RPE **(B)** with β-actin as the loading control; the expression of RPE65 in RPE **(C)** with β-actin **(C')** as the loading control detected on the same membrane but in a separate channel; the expression of LRAT in RPE **(D)** with GAPDH **(D')** as the loading control detected on the same membrane but in a separate channel. **(E)** Quantitation of the expression levels of the indicated proteins from these immunoblots. The expression levels were determined as ratios of the proteins of interest relative to the loading controls and normalized to the expression levels of the WT mice. For LRAT expressed in RPE, the quantitation included both bands **(D)**. Data were plotted as Mean ± S.D., n=4. * $p<0.05$; ** $p<0.01$; NS, non-significant, compared to WT by a two-tailed *t*-test with equal variances. P=0.033 for the expression of CRALBP in retina and P=0.002 for the expression of CRALBP in RPE.

References

Batten, M. L., Y. Imanishi, T. Maeda, D. C. Tu, A. R. Moise, D. Bronson, D. Possin, R. N. Van Gelder, W. Baehr and K. Palczewski (2004). "Lecithin-retinol acyltransferase is essential for accumulation of all-trans-retinyl esters in the eye and in the liver." J Biol Chem **279**(11): 10422-10432.

Carter-Dawson, L. D. and M. M. LaVail (1979). "Rods and cones in the mouse retina. I. Structural analysis using light and electron microscopy." J Comp Neurol **188**(2): 245-262.

Golovleva, I., S. Bhattacharya, Z. Wu, N. Shaw, Y. Yang, K. Andrabi, K. A. West, M. S. Burstedt, K. Forsman, G. Holmgren, O. Sandgren, N. Noy, J. Qin and J. W. Crabb (2003). "Disease-causing mutations in the cellular retinaldehyde binding protein tighten and abolish ligand interactions." J Biol Chem **278**(14): 12397-12402.

Holland, W. L., J. T. Brozinick, L. P. Wang, E. D. Hawkins, K. M. Sargent, Y. Liu, K. Narra, K. L. Hoehn, T. A. Knotts, A. Siesky, D. H. Nelson, S. K. Karathanasis, G. K. Fontenot, M. J. Birnbaum and S. A. Summers (2007). "Inhibition of ceramide synthesis ameliorates glucocorticoid-, saturated-fat-, and obesity-induced insulin resistance." Cell Metab **5**(3): 167-179.

Jin, M., S. Li, W. N. Moghrabi, H. Sun and G. H. Travis (2005). "Rpe65 is the retinoid isomerase in bovine retinal pigment epithelium." Cell **122**(3): 449-459.

Kaylor, J. J., J. D. Cook, J. Makshanoff, N. Bischoff, J. Yong and G. H. Travis (2014). "Identification of the 11-cis-specific retinyl-ester synthase in retinal Muller cells as multifunctional O-acyltransferase (MFAT)." Proc Natl Acad Sci U S A **111**(20): 7302-7307.

Kaylor, J. J., T. Xu, N. T. Ingram, A. Tsan, H. Hakobyan, G. L. Fain and G. H. Travis (2017). "Blue light regenerates functional visual pigments in mammals through a retinyl-phospholipid intermediate." Nat Commun **8**(1): 16.

Kaylor, J. J., Q. Yuan, J. Cook, S. Sarfare, J. Makshanoff, A. Miu, A. Kim, P. Kim, S. Habib, C. N. Roybal, T. Xu, S. Nusinowitz and G. H. Travis (2013). "Identification of DES1 as a vitamin A isomerase in Muller glial cells of the retina." Nat Chem Biol **9**(1): 30-36.

Lenis, T. L., S. Sarfare, Z. Jiang, M. B. Lloyd, D. Bok and R. A. Radu (2017). "Complement modulation in the retinal pigment epithelium rescues photoreceptor degeneration in a mouse model of Stargardt disease." Proc Natl Acad Sci U S A **114**(15): 3987-3992.

Livak, K. J. and T. D. Schmittgen (2001). "Analysis of relative gene expression data using real-time quantitative PCR and the 2(T)(-Delta Delta C) method." Methods **25**(4): 402-408.

Maier, T., M. Guell and L. Serrano (2009). "Correlation of mRNA and protein in complex biological samples." FEBS Lett **583**(24): 3966-3973.

Masuda, T., K. Wahlin, J. Wan, J. Hu, J. Maruotti, X. Yang, J. Iacovelli, N. Wolkow, R. Kist, J. L. Dunaief, J. Qian, D. J. Zack and N. Esumi (2014). "Transcription factor SOX9 plays a key role in the regulation of visual cycle gene expression in the retinal pigment epithelium." J Biol Chem **289**(18): 12908-12921.

Mata, N. L., W. N. Moghrabi, J. S. Lee, T. V. Bui, R. A. Radu, J. Horwitz and G. H. Travis (2004). "Rpe65 is a retinyl ester binding protein that presents insoluble substrate to the isomerase in retinal pigment epithelial cells." J Biol Chem **279**(1): 635-643.

Moiseyev, G., Y. Chen, Y. Takahashi, B. X. Wu and J. X. Ma (2005). "RPE65 is the isomerohydrolase in the retinoid visual cycle." Proc Natl Acad Sci U S A **102**(35): 12413-12418.

Rando, R. R. and A. Chang (1983). "Studies on the Catalyzed Interconversions of Vitamin-a Derivatives." Journal of the American Chemical Society **105**(9): 2879-2882.

Redmond, T. M., E. Poliakov, S. Yu, J. Y. Tsai, Z. Lu and S. Gentleman (2005). "Mutation of key residues of RPE65 abolishes its enzymatic role as isomerohydrolase in the visual cycle." Proc Natl Acad Sci U S A **102**(38): 13658-13663.

Redmond, T. M., S. Yu, E. Lee, D. Bok, D. Hamasaki, N. Chen, P. Goletz, J. X. Ma, R. K. Crouch and K. Pfeifer (1998). "Rpe65 is necessary for production of 11-cis-vitamin A in the retinal visual cycle." Nat Genet **20**(4): 344-351.

Saari, J. C. and D. L. Bredberg (1987). "Photochemistry and stereoselectivity of cellular retinaldehyde-binding protein from bovine retina." J Biol Chem **262**(16): 7618-7622.

Wang, J. S., M. E. Estevez, M. C. Cornwall and V. J. Kefalov (2009). "Intra-retinal visual cycle required for rapid and complete cone dark adaptation." Nat Neurosci **12**(3): 295-302.

Wang, J. S. and V. J. Kefalov (2009). "An alternative pathway mediates the mouse and human cone visual cycle." Curr Biol **19**(19): 1665-1669.

Zambrowicz, B. P., G. A. Friedrich, E. C. Buxton, S. L. Lilleberg, C. Person and A. T. Sands (1998). "Disruption and sequence identification of 2,000 genes in mouse embryonic stem cells." Nature **392**(6676): 608-611.

Znoiko, S. L., B. Rohrer, K. Lu, H. R. Lohr, R. K. Crouch and J. X. Ma (2005). "Downregulation of cone-specific gene expression and degeneration of cone photoreceptors in the Rpe65-/- mouse at early ages." Invest Ophthalmol Vis Sci **46**(4): 1473-1479.

2.3 Search for a specific cone retinol dehydrogenase in the alternate visual cycle

2.3.1 Introduction

An early study by Jones et al. suggested that the chromophore precursor, 11-*cis*-retinol, can be utilized only by cones but not rods (Jones, Crouch et al. 1989). Later, Mata et al. found a novel $NADP^+$ based 11-*cis*-retinol dehydrogenase activity in the cone-dominant chicken and ground squirrel retinas and reported that its activity strongly correlates with the percentage of cones in the retinas of different species, suggesting cone photoreceptors might be its primary location (Mata, Radu et al. 2002). Physiological recordings performed by Kefalov and colleagues demonstrated that cones but not rods recover sensitivity in isolated retina without RPE in several different species (Wang, Estevez et al. 2009, Wang and Kefalov 2009). Observations made by Ala-Laurila et al. in salamander have agreed that 11-*cis*-retinol could only be utilized by cone photoreceptors (Ala-Laurila, Cornwall et al. 2009). Most recent studies from Sato and Kefalov have confirmed that the utilization of the alternate visual cycle is restricted to cones and suggest that this restriction is regulated by the ability of cones to oxidize *cis*-retinols (Sato and Kefalov 2016).

Despite the established cone-specificity of the alternate visual cycle, the underlying biochemical mechanism, a putative retinol dehydrogenase (RDH) (described in papers such as (Mata, Radu et al. 2002, Ala-Laurila, Cornwall et al. 2009, Wang and Kefalov 2009, Parker, Wang et al. 2011, Wang and Kefalov 2011, Sato and Kefalov 2016)) that enables cones, but not rods, to oxidize 11-*cis*-retinol to 11-*cis*-retinal, has still yet to be

identified (See **Fig.1-2**, RDH?). After the identification of DES1 as a candidate for Isomerase II, we were dedicated to seeking this specific RDH to deepen our understanding of the alternate visual cycle.

If the different capabilities of cones and rods to utilize 11-*cis*-retinol is due to such an RDH (referred to as “the cone RDH” for simplicity hereafter), we hypothesized that it should meet at least two criteria: (1) Expression in cones but not rods. (2) Exhibition of 11-*cis* specific retinol oxidase activity.

Considering the high redundancy of RDHs (see **Chapter 1.3**), an unbiased library screening might be an ideal method but is very tedious, costly and technically difficult in practice. A candidate-based approach, in contrast, may be more efficient, economical and effective. Therefore, we adopted the latter and performed biochemical studies on several proteins that we deemed to be the top candidates.

2.3.2 Results

2.3.2.1 Candidates of the cone RDH

Based on a literature search as well as previous works from our lab and others, five candidates were proposed. (1) Dehydrogenase/reductase member 1 (DHRS1, also known as SDR19C1), a member of the SDR19C family (Persson, Kallberg et al. 2009). Relatively little is known regarding its localization in retina and activity towards retinoids. Its expression was indicated to be higher in the macula than the peripheral retina, thus it is probably expressed in cones ((Bowes Rickman, Ebright et al. 2006) and personal communications with Dr. Catherine Bowes Rickman (Duke University), data not shown).

(2) Dehydrogenase/reductase member 3 (DHRS3, also known as retSDR1). It is a member of the short-chain dehydrogenase/reductase (SDR) 16C family (also designated as SDR16C1) (Persson, Kallberg et al. 2009, Lundova, Zemanova et al. 2015) and has been shown to be expressed predominantly in COS at both mRNA and protein levels (Haeseleer, Huang et al. 1998). It is a highly conserved integral membrane protein located in the ER (Deisenroth, Itahana et al. 2011, Lundova, Zemanova et al. 2015). Sf9 cell-expressed DHRS3 reduces all-*trans*- but not 11-*cis*-retinal (Haeseleer, Huang et al. 1998). Its enzymatic activity is generally NADP(H)-dependent (Haeseleer, Huang et al. 1998, Lundova, Zemanova et al. 2015). However, its specificity for retinol oxidation has not been extensively characterized. (3) Short chain dehydrogenase/reductase family 9C, member 7 (SDR9C7). Based on a previous *in situ* hybridization study using mouse retina sections, SDR9C7 was suggested to be expressed in retina and probably also in cones (previous work in our lab by Dr. Minghao Jin, unpublished data, data not shown). (4) Retinol dehydrogenase 10 (RDH10). It belongs to the SDR16C family (Persson, Kallberg et al. 2009, Kedishvili 2013) and contains highly conserved amino acid sequences between human, mouse and bovine (Wu, Chen et al. 2002). It is a membrane-associated protein localized in the microsomes (Wu, Chen et al. 2002, Wu, Moiseyev et al. 2004, Takahashi, Moiseyev et al. 2009, Lhor and Salesse 2014). It is expressed predominantly in the RPE (Wu, Chen et al. 2002) but is also found in retinal Müller cells (Wu, Moiseyev et al. 2004). Although RDH10 exhibits retinoid oxidoreductase activity at both directions *in vitro* (Takahashi, Moiseyev et al. 2009), oxidation has been reported to be the favored reaction (Belyaeva, Johnson et al. 2008, Takahashi, Moiseyev et al. 2009). It oxidizes both *cis*-

and *trans*-retinols (Belyaeva, Johnson et al. 2008, Sahu, Sun et al. 2015). The cofactor preference of NAD(H) or NADP(H) for RDH10 has been described in several papers, such as (Wu, Chen et al. 2002, Wu, Moiseyev et al. 2004, Belyaeva, Johnson et al. 2008, Farjo, Moiseyev et al. 2009, Takahashi, Moiseyev et al. 2009, Sahu, Sun et al. 2015), but has not yet been completely clarified, indicating the complexity in this area. Interestingly, RDH10 has been shown to interact with CRALBP and RPE65 (Farjo, Moiseyev et al. 2009). Visual chromophore regeneration is affected with the loss of RDH10 function in RPE (Sahu, Sun et al. 2015). (5) Alcohol dehydrogenase 7 (class IV), mu or sigma polypeptide (ADH7) (listed as ADH4 in some literature). It seems to be expressed in both retina and RPE (Martras, Alvarez et al. 2004). More interestingly, recent kinetic characterizations of both recombinant human and mouse ADH7 (listed as ADH4 in the original paper) using retinoids as substrate and NAD/NADH as cofactor showed that it oxidizes 9-*cis*- and 11-*cis*-retinol efficiently with a much higher K_{cat}/K_M than all-*trans*- and 13-*cis*-retinol. Moreover, its K_{cat}/K_M values of oxidizing 11-*cis*-retinol is several-fold higher than that of reducing 11-*cis*-retinal for both human and mouse ADH7 (Allali-Hassani, Peralba et al. 1998, Martras, Alvarez et al. 2004). These results, together with other studies of human (Yang, Davis et al. 1994) and rat (Boleda, Saubi et al. 1993, Crosas, Allali-Hassani et al. 2000) ADH7, all suggest that ADH7 has high enzymatic activity towards retinoids, therefore making it a good candidate for the cone RDH.

Several other interesting proteins were also considered as potential candidates but were excluded because of their presence in rods. Examples include RDH8 (Rattner, Smallwood et al. 2000, Maeda, Maeda et al. 2005), RDH11 (Kasus-Jacobi, Ou et al.

2003, Kasus-Jacobi, Ou et al. 2005, Parker and Crouch 2010), RDH12 (Haeseleer, Jang et al. 2002, Maeda, Maeda et al. 2006), RDH13 (Haeseleer, Jang et al. 2002), and RDH14 (Haeseleer, Jang et al. 2002).

After the identification of the five candidates, we obtained their cDNA clones, which include mouse DHRS3 (Accession No. BC010972), mouse DHRS1 (Accession No. BC003930), mouse SDR9C7 (accession No. NM_027301), human RDH10 (accession No. NM_172037) and human ADH7 (Accession No. BC131512). mDHRS3, mDHRS1, mSDR9C7 and hADH7 were then subcloned into pcDNA3.1, a eukaryotic expression vector. HRDH10 was originally in the vector of pcDNA6, a vector similar to pcDNA3.1, so was not subcloned. When necessary, a single nucleotide mutation was made to ensure the protein-coding nucleotide sequences of the clones match those in the National Center for Biotechnology Information (NCBI) database.

2.3.2.2 Expression of the cone RDH candidates in mouse retina

If the cone RDH candidates are expressed in cones, they should be detected in retina homogenates. The presence of SDR9C7 in the retina has been shown by previous work in our lab. To confirm the presence of the other candidates in the retina, immunoblot analysis was performed using tissues from wild type (129) as well as retinal degeneration 7 (*rd*7) mice. The *rd*7 strain carries a mutation in the Nr2e3 gene and has “hybrid” rods that can also oxidize 11-*cis*-retinol (Wang, Nymark et al. 2014). As shown in **Fig.2.3-1**, (putative) immunoblot signals from all four RDH candidates were observed in mouse retina, with seemingly similar intensities between the wild type (129) and *rd*7 mice.

2.3.2.3 RDH activity assays of the cone RDH candidates

Another crucial feature of the putative cone RDH is its capability to oxidize 11-*cis*-retinol. To test if these candidates have this ability, their plasmids were transiently transfected into HEK 293T cells. Homogenates of these transfected cells were prepared and used for assays of their 11-*cis*-retinol oxidase activity in the presence of both NAD^+ and $NADP^+$. Two out of the five candidates, namely hRDH10 and hADH7, showed robust activities which were significantly higher than that of the other candidates and the controls (samples without cell homogenate ("no cell") and with the homogenate of cells transfected with the pcDNA empty vector ("pcDNA")) **(Fig.2.3-2)**. MDHRS3, mDHRS1 and mSDR9C7, however, did not exhibit robust oxidase activity compared to the pcDNA control in this experiment.

The all-*trans*-retinol oxidation abilities of these candidates were also tested in a similar condition **(Fig.2.3-3)**. HRDH10 and hADH7 again exhibited robust all-*trans*-retinol oxidase activities that were several-fold higher than that of the "no cell" and "pcDNA" controls. MDHRS3 also exhibited moderate oxidase activity towards all-*trans*-retinol. It is worth mentioning that a previous study showed that 11-*cis*-retinal was not reduced by DHRS3 while all-*trans*-retinal was (Haeseleer, Huang et al. 1998). However, such all-*trans*-retinal reductase activity was low (as pointed out by Lundova et al. (Lundova, Zemanova et al. 2015)), only a few picomole/min. This activity was not detected by the study of Lundova et al (Lundova, Zemanova et al. 2015). Also, bidirectional catalytic activity is not uncommon in short-and medium-chain dehydrogenases/reductases (Yang, Davis et al. 1994, Haeseleer, Jang et al. 2002, Pares, Farres et al. 2008).

Therefore, our results regarding the oxidase activity of mDHRS3 towards 11-*cis*- and all-*trans*-retinols are in line with the above reports. No robust all-*trans*-retinol oxidase activity of mDHRS1 or mSDR9C7 was observed in this experiment. The successful transfections of the candidates were later confirmed by qRT-PCR tests using RNA extracted from aliquots of the cell homogenates, excluding the possibility that the inactivity of certain candidates was due to a transfection failure.

2.3.2.4 Further tests with RDH10 and ADH7

Based on the enzymatic activity tests **(Figs.2.2-2 and -3)**, hRDH10 and hADH7 were the most robust RDHs and gained priority for our further investigation. To determine the cellular localization of these two candidates in the retina, we tried to perform an immunofluorescent test with mouse retina slides. However, due to some technical challenges, such as the possibly insufficient affinities of the antibodies, the autofluorescence of photoreceptors and the low population of cones, these tests did not yield a definite conclusion (data not shown).

Considering the enrichment of cone photoreceptors in a cone-dominant chicken retina compared to a rod-dominant mouse retina, we hypothesized that the expression of the cone RDH may also be higher in the retina of chickens than that of mice. Accordingly, if RDH10 or ADH7 is the cone RDH, its expression may also be higher in chicken retina. To test this, retinas of chicken and wild type (129) mice were dissected and their RNA were extracted. I then designed three sets of primers against mouse and chicken RDH10 respectively. ADH7 (ADH class IV) is not highly conserved between mammals and birds. Based on our knowledge, it is still unclear what the chicken orthologue to that

of human or mouse is (Duester 2000, Gonzalez-Duarte and Albalat 2005). Considering the close phylogenetic relationship between ADH1 (class I) and ADH7 (class IV) (Gonzalez-Duarte and Albalat 2005, Persson, Hedlund et al. 2008, Hoog and Ostberg 2011), as well as the hit of the similar (predicted) chicken protein sequence (accession No. XP_001234263.2) to human ADH7 when searched using UniGene in the NCBI website (https://www.ncbi.nlm.nih.gov/UniGene/clust.cgi?ORG=Hs&CID=389&ALLPROT=1), our best guess for the gene closest to human ADH7 is chicken “alcohol dehydrogenase 1” (or “ADH1C” (class I, gamma polypeptide)). The amino acid sequences of human ADH7 (accession No. NP_000664 or NP_001159976) and chicken ADH1(C) (accession No. NP_001292112, updated from the predicted version, XP_001234263) shares about 68-69% identity. Therefore, primers were designed against mouse ADH7 and chicken ADH1C. To measure the expression levels of these genes, qRT-PCR reactions were performed and the expression levels of the genes of interest were calculated relative to the reference gene,18S ribosomal RNA, from the same species. Disappointingly, the expression level of RDH10 was not elevated in the chicken retina compared to that in the mouse retina in this test **(Fig.2.3-4A)**. The expression level of chicken ADH1C in the chicken retina was not significantly higher than that of mouse ADH7 in the mouse retina either **(Fig.2.3-4B)**. It should be noted that the ΔCt values of both ADH7 and ADH1C were very high (around 35-37) in the qRT-PCR reactions, yet amplicons of proper sizes were visualized later by gel electrophoresis **(Fig.2.3-4C)**. These indicate that although the mRNA (cDNA) was correctly amplified, their abundance might be very low in the retina tissues. We do not have a good explanation as to why this was the case, but the

immunoblot seems to show a relatively strong signal in the mouse retina **(Fig.2.3-1)**, although the gene expressions at these two levels do not always agree (Maier, Guell et al. 2009).

Later, data from other studies were accessed, which reduced our interest to advance this project further (see “Discussion” for details).

2.3.3 Discussion

In our attempt to identify the cone RDH, five candidates were proposed based on our best knowledge of the literature and previous studies. According to our enzymatic assays, two of them (hRDH10 and hADH7) showed robust oxidase activities towards 11-*cis*- and all-*trans*-retinols **(Figs.2.3-2 and -3)**. For this project, measuring the enzymatic activity of these candidates was relatively easy, while determining the precise cellular localization of them in the retina was much harder, especially in the rod-dominant mouse retina. Our attempt to address the localization of hRDH10 and hADH7 faced technical challenges and were not successful, leaving this question unanswered. Although the other candidates (DHRS3, DHRS1 and SDR9C7) did not exhibit robust 11-*cis*-oxidase activity in my assay, it is possible that the conditions of these activity assays were not optimal for each candidate, reducing or eliminating the oxidase activities that they might have had otherwise. The time and resources to perform exhaustive condition optimization for each candidate were determined to be prohibitive, especially when their cellular localizations were still in question.

After these attempts failed, other possible methods were considered. One of them would be to perform high throughput experiments like RNA sequencing analysis on purified rods and cones (or rod- and cone-rich preparations). Isolation of rods and cones in the carp retina (Tachibanaki, Tsushima et al. 2001, Miyazono, Shimauchi-Matsukawa et al. 2008) and isolation of cones in the rat retina (Skaper 2012) were examples of such a purification. Another method would be to perform analysis on single cell level, such as single cell RT-PCR of photoreceptors, to determine whether the candidates are selectively expressed in cones. These experiments did not seem to be trivial and straightforward, so we did not perform. However, they could potentially help to identify the cone RDH in the future.

As part of the alternate visual cycle, the identity of the cone RDH is an intriguing question not only to us but also to others. In 2008, Miyazono et al. reported a novel robust enzymatic activity in carp (*Cyprinus carpio*) cone membranes, which oxidizes 11-*cis*-retinol to 11-*cis*-retinal with the simultaneous reduction of all-*trans*-retinal (Miyazono, Shimauchi-Matsukawa et al. 2008). Follow-up studies by Sato et al. confirmed that this activity is a retinal-retinol redox coupling reaction and determined its subcellular localization to be in the cone inner segments. The oxidation of this activity showed high specificity towards 11-*cis*- and 9-*cis*-retinols (Sato, Fukagawa et al. 2013). Subsequently, carp retinol dehydrogenase 13-like (RDH13L) was identified as the protein partially responsible for this activity. A mouse functional homolog, RDH14, also showed a similar activity. They were thought to be involved in cone pigment regeneration (Sato, Miyazono et al. 2015). However, no further evidence has confirmed this hypothesis.

Another interesting observation is that the ability of mouse M-cones to oxidize exogenous 9-*cis*-retinol (an 11-*cis*-retinol analog) is affected by the disruption of RDH8 and ABCA4, suggesting that RDH8 may be involved in the cone RDH activity (Kolesnikov, Maeda et al. 2015). However, more evidence is needed to support this hypothesis, especially given the fact that RDH8 is also present in the ROS and has been reported as an all-*trans*-retinal reductase (Rattner, Smallwood et al. 2000, Maeda, Maeda et al. 2005).

Most recently, the subcellular localization of this cone RDH activity has been finally determined to be in the COS (Sato, Frederiksen et al. 2017). Interestingly, a closely followed paper from the same lab investigated the possibility of RDH10 as the cone RDH (Xue, Sato et al. 2017). RDH10 was proposed because its expression level in the *rd*7 mouse retina (which has “hybrid” rods that can also use *cis*-retinols (Wang, Nymark et al. 2014)) was about three-fold of that in a wild type mouse retina and was the only known RDH out of the over 400 upregulated genes in *rd*7 retina identified by RNA-seq analysis (Xue, Sato et al. 2017). However, after comprehensive characterization of multiple mouse strains with RDH10 deficiency in different tissues within the retina, as well as transgenic mice with RDH0 expressed in rods, the authors concluded that it was “not required for the function of the retina visual cycle” (Xue, Sato et al. 2017). This conclusion also excluded RDH10 from our top candidate list. Their RNA-seq data was also made to the public (Xue, Sato et al. 2017). Besides RDH10, only one of our candidates was listed in the genes that had significantly different expressions between *rd*7 and wild type mouse retinas. It was DHRS3 but not ADH7. However, DHRS3 was actually downregulated rather than upregulated in *rd*7 mouse retina, consistent with a

previous study (Corbo and Cepko 2005). In addition, RDH8, RDH13 or RDH14 were not on the list. An earlier study also analyzed the gene expressions in wild type and Nrl mutant mouse retinas (Corbo, Myers et al. 2007). The photoreceptors in the Nrl-/- retina are cone-like without rod function (Mears, Kondo et al. 2001), and are able to use the cone visual cycle (Parker, Wang et al. 2011). However, the expression of DHRS3 was reported to be downregulated in the Nrl-/- retina, together with RDH12. No RDH was found in the list of genes upregulated in the Nrl-/- retina (Corbo, Myers et al. 2007).

So far, the reason for the exclusive ability of cones to utilize 11-*cis*-retinol for their visual pigment regeneration is still an open question. Several possibilities exist: (1) There indeed is a cone-specific RDH. This is logical and reasonable, and currently under active investigation. The challenge for identifying such a cone RDH may be due to technical difficulties for their characterizations, especially considering the redundancies of RDHs in the retina (see **Chapter 1.3**. For an RDH review, see (Sahu and Maeda 2016)) and the low population of cones in a rod-dominant retina. (2) A second possibility is that this oxidase activity may depend on a coupled enzyme complex but not a single protein. It has been reported that RDH10 and DHRS3 reciprocally activate each other (Adams, Belyaeva et al. 2014). This is particularly interesting considering both enzymes were in our candidate list. Although it is unlikely that this reciprocal activation is responsible for the cone RDH activity in this case given the extensive studies of RDH10 deficient and transgenic mice (Xue, Sato et al. 2017), a similar mechanism used by other proteins is completely possible. However, identifying such an enzyme complex may be even more difficult than identifying a single enzyme. (3) A third possibility is that this unique ability of cones is not due to a specific enzyme or an enzyme complex, but

lies in the distinct structures and/or functions between cones and rods, for instance, their outer segment architectural and longitudinal diffusion difference (Holcman and Korenbrot 2004).

Due to the limitations of our resources and the limited observed effects, we did not continue with this project. Future studies are needed to address this open question.

2.3.4 Materials and Methods

2.3.4.1 CDNA clones of the cone RDH candidates

The plasmids of mouse DHRS3 (Accession No. BC010972, Catalog No. MC204257) and mouse DHRS1 (Accession No. BC003930, Catalog No. MC200338) were purchased from OriGene. The plasmid of human ADH7 (Accession No. BC131512, Catalog No. MHS6278-211690510) was purchased from Thermo Scientific. The plasmid of mouse SDR9C7 (Accession No. NM_027301) was a generous gift from Dr. Minghao Jin (previously in our lab, currently at the Louisiana State University Health Sciences Center). The plasmid of human RDH10 (accession No. NM_172037) was a generous gift from Dr. Jian-Xing Ma (University of Oklahoma Health Sciences Center). These cDNA clones except hRDH10 were subcloned into the mammalian expression vector, pcDNA3.1. Human RDH10 was not subcloned because it was in the vector of pcDNA6, a mammalian vector similar to pcDNA3.1. Single nucleotide mutations were made if necessary to ensure the protein-coding nucleotide sequences of the clones match those in the NCBI database. Specifically, such mutations were made to SDR9C7, as well as to hRDH10 (introducing a stop codon before a tag). The mutations were carried out using a QuickChange Site-Directed Mutagenesis Kit (Agilent) according to the protocol

suggested by the manufacturer. Sequences in the protein-coding regions of these clones were confirmed by plasmid sequencing with big dye terminator (obtained from UCLA Genotyping and Sequencing Core) and an ABI 3130XL genetic analyzer (Applied Biosystems).

2.3.4.2 Immunoblot analysis

Immunoblot analysis was performed similarly as described in **Chapter 2.2.4.6**. Retinas from wild type (129) and *rd7* (Wang, Nymark et al. 2014) mice were dissected in ice-cold PBS (1X) pH 7.2 with EDTA-free protease inhibitors, snap-frozen in liquid nitrogen and stored at -80 ºC until use. The *rd7* mice were generous gifts from Dr. Vladimir J. Kefalov (Washington University in St Louis). On the day of use, the tissues were gently thawed on ice and homogenized by sonication in PBS pH 7.2 with EDTA-free protease inhibitor cocktail on ice. The homogenates were treated with benzonase nuclease (Sigma-Aldrich) at room temperature for 75-90 minutes followed by the addition of SDS (final concentration 1%) and the incubation at 4 ºC for 30 minutes. Cellular debris was pelleted by a brielf centrifugation and the supernatants were collected and stored at -80 ºC. Aliquots of the supernatants were taken and their protein concentrations were determined by a Micro BCA protein assay. On the day of use, equal amounts of total protein (25-40 µg) per lane (within each gel) were separated by 12% Novex NuPAGE Bis-Tris gels (Invitrogen), transferred and blocked. Membranes were probed with primary antibodies followed by the incubation with cognate secondary antibodies labeled with IR-dye (LI-COR), all in Odyssey Blocking Buffer with 0.1% Tween 20 and 0.5% donkey serum. Membranes were imaged with an Odyssey infrared imaging

system (LI-COR). Primary antibodies used included: anti-DHRS3, a rabbit polyclonal antibody (NBP1-80846, Novus Biologicals); anti-DHRS1, a rabbit polyclonal antibody (16275-1-AP, Proteintech); anti-RDH10, a rabbit polyclonal antibody (AP4738c, Abgent); anti-ADH7, a rabbit polyclonal antibody (AP9703b, Abgent (distributed by One World Lab)).

2.3.4.3 Retinol dehydrogenase activity assays.

Plasmids of cone RDH candidates, mDHRS3, mDHRS1, mSDR9C7, hRDH10, hADH7 and pcDNA 3.1 (empty vector, control) were transfected into HEK 293T cells maintained in 100 mm dishes using PolyFect transfection reagent (Qiagen) according to the protocol suggested by the manufacturer. Cells were harvested about 48 hours after the transfection and homogenized in 40 mM Tris buffer pH 7.2 with 1 mM DTT on ice using glass-to-glass homogenizers. Aliquots of homogenates were taken and the protein concentrations were determined by a micro BCA assay using a Pierce BCA protein assay kit (reducing agent compatible, Thermo Scientific). The main homogenate stocks were snap-frozen in liquid nitrogen and stored at -80 ºC until use. Retinol dehydrogenase activity assays were performed using the above cell homogenates with equal amounts of total protein (0.5-0.6 mg/reaction) in 40 mM Tris buffer pH 7.2 with 1 mM DTT, supplemented with 1% BSA, 500 μM of NAD^+ and 500 μM of $NADP^+$. The reactions were initiated with the addition of 10 μM 11-*cis*-retinol or all-*trans*-retinol (in DMSO) and incubated at 37 ºC for 15-20 minutes. 25 μL of 5% SDS was added to each 500 μL reaction mixture to quench the reactions immediately after the incubation. 500 μL of 2M hydroxylamine hydrochloride (Sigma-Aldrich) (dissolved in PBS, pH 7.0) was

then added and the mixtures were incubated at room temperature for 10-15 minutes to allow the oximation of retinals. Retinoids were extracted twice into 2 ml hexane after the addition of 50 µL brine and 2 ml methanol, and analyzed by HPLC subsequently. 11-*cis*-retinol was prepared from 11-*cis*-retinal (a generous gift from Dr. Rosalie K. Crouch) as described (Kaylor, Yuan et al. 2013). The concentration of 11-*cis*-retinol was determined using a molar extinction coefficient of 34890 $M^{-1}cm^{-1}$ at 319 nm in ethanol (Leenheer, Lambert et al. 2000). The concentration of all-*trans*-retinol was determined using a molar extinction coefficient of 52770 $M^{-1}cm^{-1}$ at 325 nm in ethanol (Leenheer, Lambert et al. 2000).

2.3.4.4 Immunofluorescence of RDH10 and ADH7 in mouse retina

Immunofluorescence tests of RDH10 and ADH7 in mouse retina were performed with a similar method as previously described (Kaylor, Cook et al. 2014), with modifications. Wild type (129) mice were sacrificed and the eyeballs were enucleated and fixed in 4% paraformaldehyde (Electron Microscopy Sciences) in PBS at 4 ºC for 30 minutes. The anterior part of the eyeball including the cornea was removed and the remaining portion was returned to the above fixative at 4 ºC overnight. The eyecups were then rinsed by three 5-minute washes in PBS and infiltrated by 10% sucrose (in PBS pH 7.2) for 1 hour, 30% sucrose for 2 hours and finally O.C.T compound (Tissue-Tek) for 1 hour at room temperature (RT). The eyecups were oriented and embedded in O.C.T compound, frozen in liquid nitrogen and stored at -80 ºC. Eight-µm-thick sections were cut and stored at -80 ºC until use. On the day of use, the slides were gently thawed and further fixed in 4% paraformaldehyde at RT for 20 minutes, followed by three 5-minute

rinses in PBS. Sections were reduced in 0.1 M $NaBH_4$ (Sigma-Aldrich) (in PBS) for 10 minutes twice at RT, rinsed with PBS, and permeabilized and blocked in 0.1% Triton X-100 (Fisher Scientific) with1% BSA and 2% normal donkey serum in PBS at RT for 1 hour. Sections were probed with primary antibodies of RDH10 (AP4738c, Abgent) or ADH7 (AP9703b, Abgent (distributed by One World Lab)) at 1:100 dilution at 4 ºC overnight, followed by washing and incubation with lectin peanut agglutinin (PNA) 488 and donkey anti-Rabbit 568 (AlexaFluor) at 1:150 dilution at RT for 80 minutes. Sections were then rinsed, dried, and mounted in ProLong Gold antifade reagent with DAPI (Life Technologies) at RT overnight. Slides were imaged by an Olympus FluoView FV1000 confocal laser-scanning microscope system.

2.3.4.5 Analysis of the expression levels of RDH10 and ADH7 (ADH1C) in mouse and chicken retinas by qRT-PCR

QRT-PCR analysis was performed similarly as described in **Chapter 2.2.4.5** and (Kaylor, Yuan et al. 2013, Kaylor, Cook et al. 2014). For qRT-PCR analysis of RDH10 and ADH7 (or ADH1C) expression levels in the mouse and chicken retinas, heads from freshly slaughtered chicken (provided by Al Salam Polleria) were delivered on ice in the dark within two hours similarly as described. Eyeballs were removed and cut open by a scalpel. Retinas were dissected in 1X PBS pH 7.2 on ice after an approximately 45 minutes dark-adaptation (for easy separation of the retina from RPE). Dissected retinas were immediately frozen in liquid nitrogen and stored at -80 ºC until use. Mouse retina was dissected from euthanized wild type (129) mouse and treated with RNAlater solution (Ambion) on ice for 3 hours before frozen at -80 ºC. RNA of mouse and chicken

retinas were extracted using Absolutely RNA Miniprep Kit (Agilent Technologies) according to the protocol suggested by the manufacturer. CDNA was synthesized with equal amounts of RNA (~223 ng) from mouse and chicken retinas using SuperScript III First-Strand Synthesis SuperMix for qRT-PCR (Invitrogen). Quantitative real-time PCR reactions were performed in a total volume of 20 µL using iTaq Universal SYBR Green Supermix (BioRad) in a StepOne Real-Time PCR System (48-well platform, Applied Biosystems) with its attached StepOne software. Cycling condition: 94 °C for 3 minutes followed by 40 cycles of 94 °C for 30 s; 60 °C for 40 s; 72 °C for 60 s and then extended at 72 °C for 5 minutes. In this experiment, the same cDNA of each species was used for triplicate qRT-PCR reactions (technical triplicates). The primers used are as listed below.

Mouse 18S ribosomal RNA (Kaylor, Yuan et al. 2013),

Forward: 5’ TTTGTTGGTTTTCGGAACTGA

Reverse: 5’ CGTTTATGGTCGGAACTACGA

Chicken 18S ribosomal RNA (Kaylor, Yuan et al. 2013),

Forward: 5’ ATCCATTGGAGGGCAAGTCT

Reverse: 5’ CCAGCCTGCTTTGAACACTC

Mouse RDH10 Pair 1, Forward: 5’ ATGGTTCGCCACATCTACCG

Reverse: 5’ GCCTTAGTGGTCCAGAAGTGT

Mouse RDH10 Pair 2, Forward: 5’ CAGAGGCTGCCGAATCAGAA

Reverse: 5’ TACTGATTGATGCGCACGGA

Mouse RDH10 Pair 3, Forward: 5’ ACGCACACTTCTGGACCACT

Reverse: 5’ ATACATGCACACGACGGCTT

Mouse ADH7, Forward: 5’ GAACCGTGCCTCAGTCAGAA

Reverse: 5’ GCCTGTCAGATCGCTCCTAA

Chicken RDH10 Pair 1, Forward: 5’ CGCGCATTTCTGGACCACT

Reverse: 5’ ATACATGAGGCGAGGTGTGC

Chicken RDH10 Pair 2, Forward: 5’ GCACTGCTGGAGTAGAGGATTA

Reverse: 5’ CCGGTACATGCACACAACTG

Chicken RDH10 Pair 3, Forward: 5’ CACGAGTCTTTGAGCCATGA

Reverse: 5’ AACTGCTTCAAAGGGCAGAA

Chicken ADH1C, Forward: 5’ GCTTGACTCGGCACAAGAAAC

Reverse: 5’ GCGTCTCCTGGCTTTAACGAA

The chicken ADH1C primers were designed based on a predicted mRNA sequence of XM_001234262.3, which has been replaced by NM_001305183.

The expression levels of the genes of interest were calculated using a relative quantitation to the expression levels of the reference gene,18S ribosomal RNA of the corresponding species, similarly as described (Kaylor, Yuan et al. 2013, Kaylor, Cook et al. 2014).

The qRT-PCR reaction mixtures were loaded onto 2% agarose gels after the addition of 1/5 volume (final concentration 1X) of Load 6X Loading Dye Bromophenol Blue (Abnova) and visualized under UV light to confirm the presence of the proper amplicons.

For qRT-PCR analysis to confirm the successful transfection of cone RDH candidates, cell homogenate aliquots of 293T cells transfected with the cone RDH candidates or

pcDNA (stored at -80°C) were gently thawed, and their RNA were extracted using the same kit and protocol as above. Equal amounts of RNA (~600 ng) were used to make cDNA. Quantitative real-time PCR reactions were performed with the following cycling condition: 94 °C for 3 minutes followed by 40 cycles of 94 °C for 20 s; 60 °C for 30 s; 72 °C for 40 s and then extended at 72 °C for 5 minutes. The primers used are listed below.

Mouse DHRS3, Forward: 5' CCTCAAGGAGACGACAGAGG

Reverse: 5' ACAATATGGCCGTTCTGGAG

Mouse DHRS1, Forward: 5' GGCCAAGTGTGTGTGGTAAC

Reverse: 5' TAGTGGCCTCTGAGTCCAAC

Mouse SDR9C7, Forward: 5' TGCAGACCTTCCTCCTAGATG

Reverse: 5' GTTCCCTGGCTCAATGATGC

Human RDH10, Forward: 5' GACACTGGCATGTTCAGAGG

Reverse (BGH Reverse, not gene specific, detecting a sequence in the vector): 5' TAGAAGGCACAGTCGAGG

Human ADH7, Forward: 5' TCGTGGAGTACTGGCTGATG

Reverse: 5' TTAACAGCAGCGCCATATCC

Human/Mouse 18S ribosomal RNA, Forward: 5' TTTGTTGGTTTTCGGAACTGA

Reverse: 5' CGTTTATGGTCGGAACTACGA

The qRT-PCR data were analyzed by the $2^{-\Delta\Delta Ct}$ method (Livak and Schmittgen 2001) using the StepOne software (Applied Biosystems) attached to the instrument. 18S ribosomal RNA was used as the reference gene and 293T cells transfected with pcDNA3.1 was used as the control. The relative expression levels of the genes of

interest were several orders of magnitude higher in homogenates of cells transfected with the candidates compared to those transfected with pcDNA (specific number varied due to different genes and their different endogenous levels in the control samples). The successful transfections of these candidates were therefore confirmed.

2.3.4.6 Statistical analysis

As described in **Chapter 2.1.4.5**, statistical significance between two groups was determined by either a two-tailed Welch's or a two-tailed Student's *t*-test (based on an F-test). A p-value of less than 0.05 was considered significant.

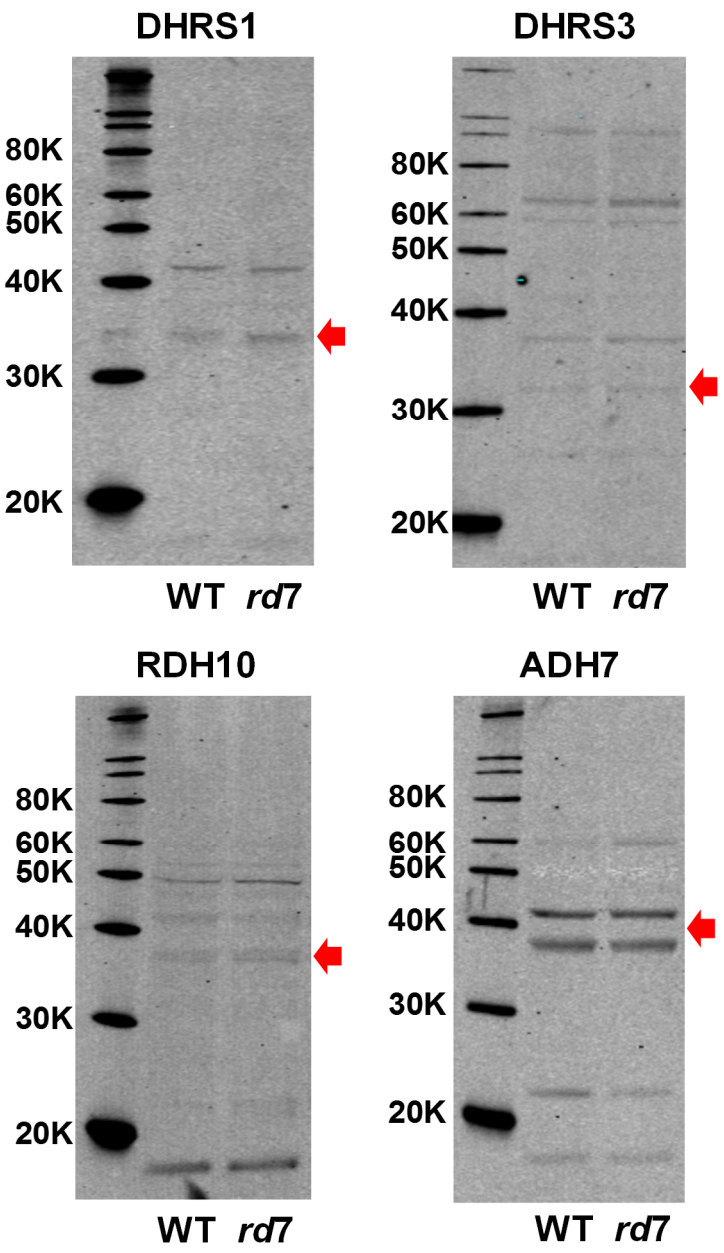

Figure 2.3-1. Expression of DHRS1, DHRS3, RDH10 and ADH7 in mouse retina. Retina homogenates were prepared from wild type129 (WT) and *rd7* mice and detected by the antibodies of DHRS1, DHRS3, RDH10 and ADH7 as indicated. Equal amounts of total protein (25-40 μg) per lane (within each gel) were loaded. Bands showing the proteins of interest were indicated by red arrows. In the immunoblot of ADH7, two bands around 40 kDa were observed. Either or both could be ADH7 based on their molecular weight, although we could not distinguish whether or which was/were ADH7.

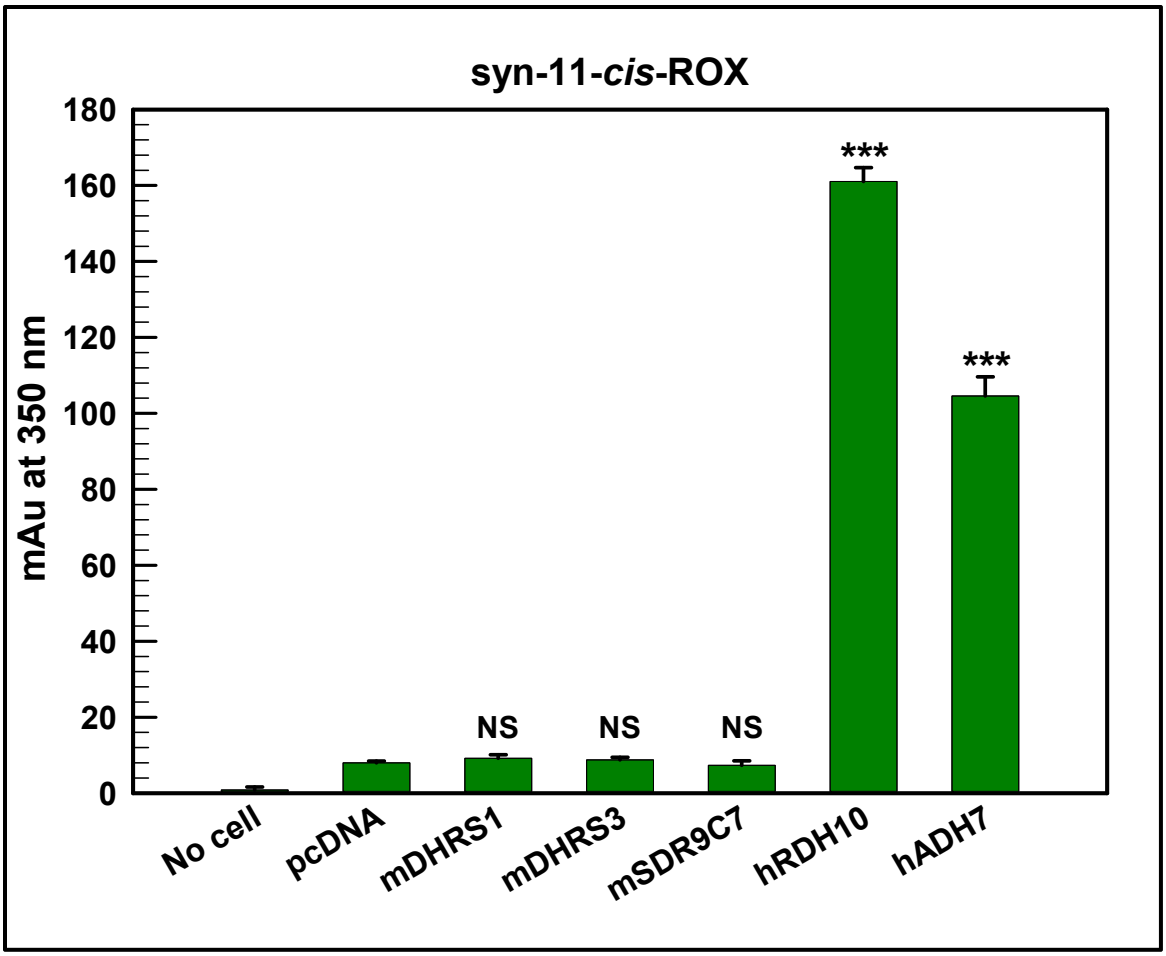

Figure 2.3-2. 11-*cis*-retinol oxidase activity of the cone RDH candidates. The 11-*cis*-retinol oxidase activity of the cone RDH candidates was tested using homogenates of 293T cells transfected with each candidate including mouse DHRS1, mouse DHRS3, mouse SDR9C7, human RDH10 and human ADH7 as indicated. 293T cells transfected with pcDNA and samples containing no cell homogenate (No cell) were also included as controls. The oxidase activity was represented by the production of *syn*-11-*cis*-retinaldehyde oximes (ROX) in mAU read at 350 nm (representing a portion of total 11-*cis*-retinal, see **Fig.3.1-2** for a detailed explanation). Data were plotted as Mean ± S.D., n=3. ***p<0.001; NS, non-significant, compared to the pcDNA control.

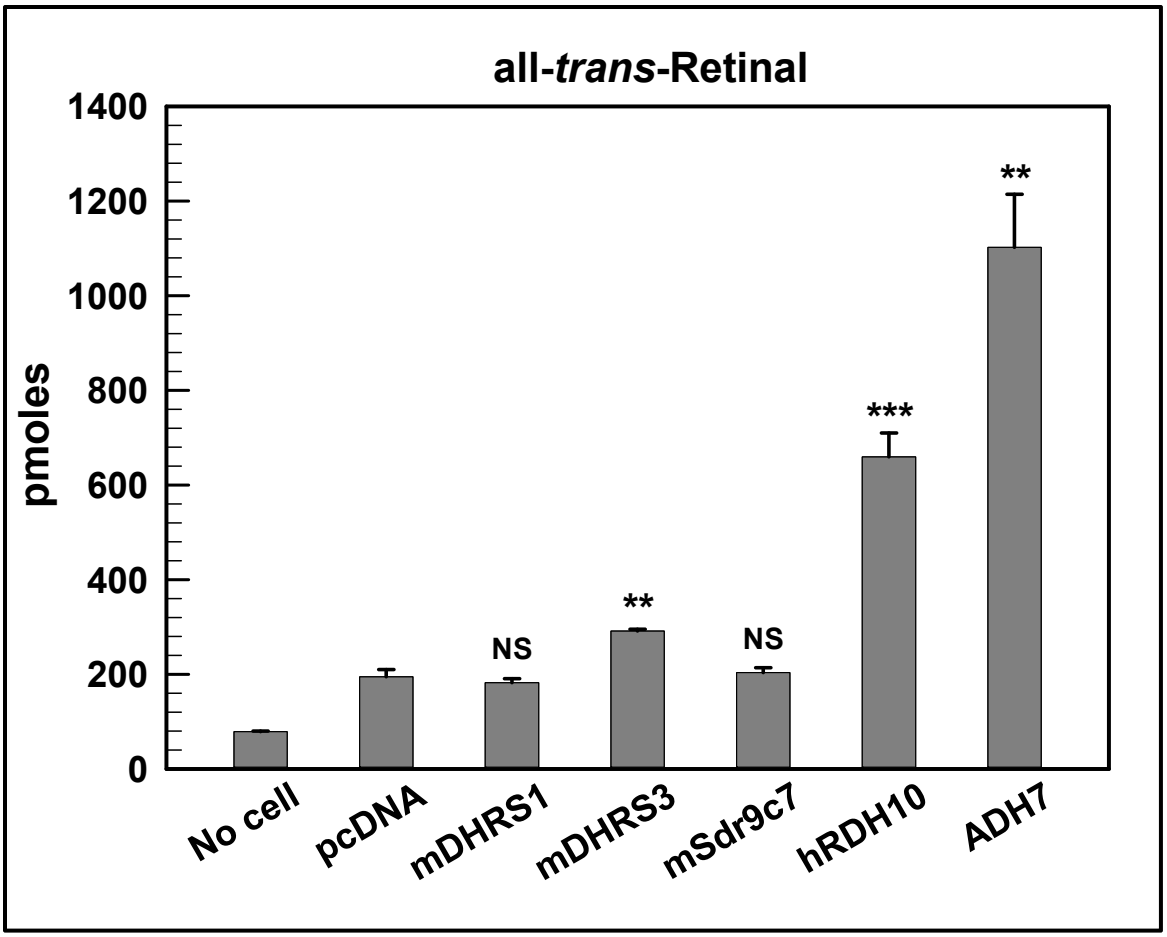

Figure 2.3-3. all-*tans*-retinol oxidase activity of the cone RDH candidates. The all-*trans*-retinol oxidase activity of the cone RDH candidates was tested using homogenates of 293T cells transfected with each candidate similar to **Fig.2.3-2**. 293T cells transfected with pcDNA and samples containing no cell homogenate (No cell) were also included as controls. The oxidase activity was represented by the production of all-*trans*-retinal in pmoles. Data were plotted as Mean ± S.D., n=3. **p<0.01; ***p<0.001; NS, non-significant, compared to the pcDNA control.

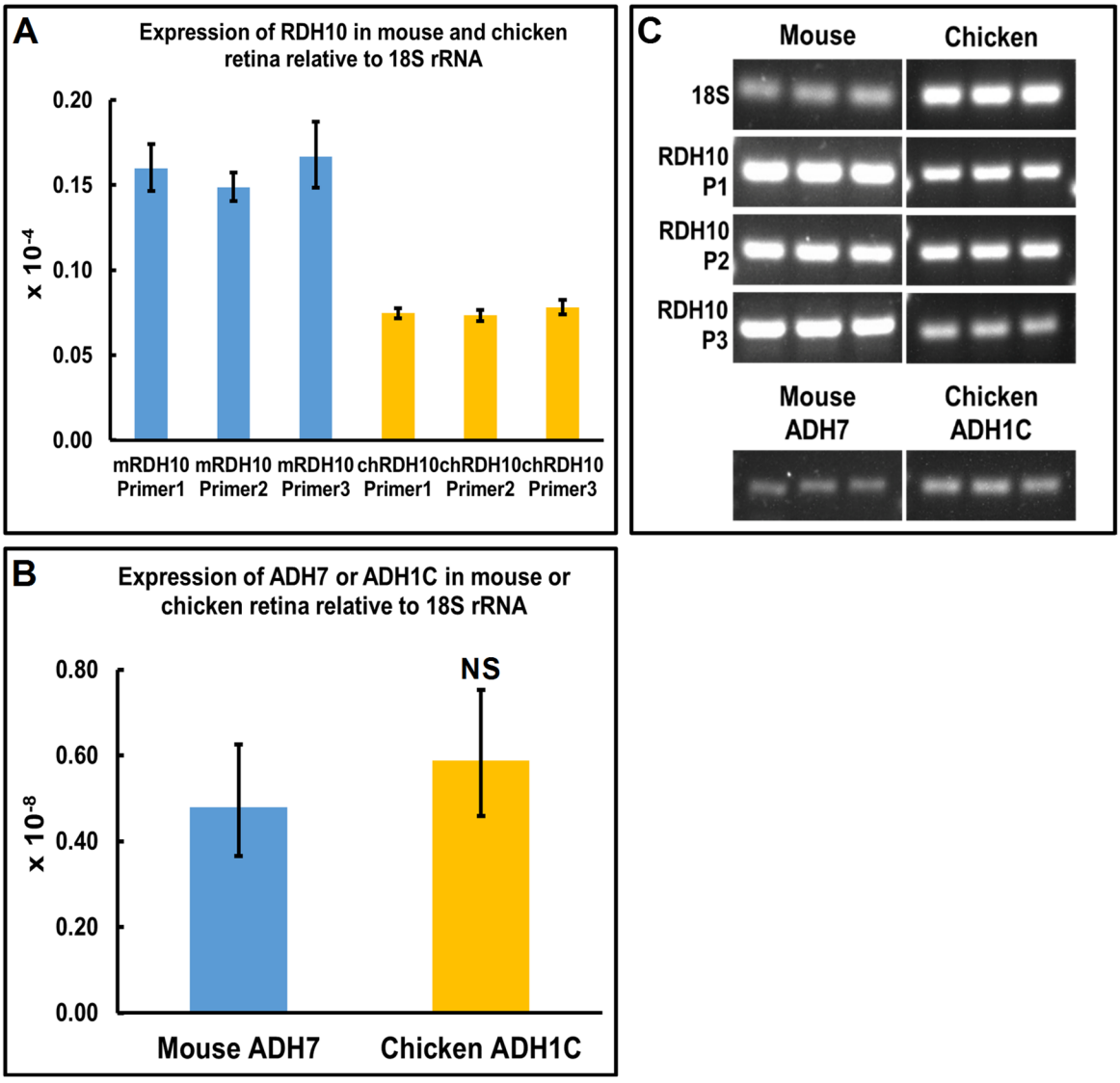

Figure 2.3-4. Expression levels of the mRNA of RDH10, ADH7 and ADH1C in mouse and chicken retinas. The expression levels of RDH10 mRNA were measured by qRT-PCR with three different sets of primers for the retina of each species **(A)**. The expression levels of mouse ADH7 and chicken ADH1C were determined by one set of primers for each **(B)**. All expression levels were relative to 18S ribosomal RNA of the corresponding species. Data were plotted as Mean ± Confidence Intervals (RQ_{min} to RQ_{max}), n=3 (technical triplicates from the same cDNA of each species). NS, non-significant, by a two-tailed student's *t*-test (on the ΔCt values) compared to mouse ADH7 **(B)**. **(C)** Gel images of qRT-PCR amplicons confirming the proper amplification of the genes of interest. Amplicons of mouse ADH7 and chicken ADH1C were observed, but the original Ct values from qRT-PCR were very high (about 35-37), indicating the mRNA was correctly amplified but the abundance was low.

References

Adams, M. K., O. V. Belyaeva, L. Wu and N. Y. Kedishvili (2014). "The retinaldehyde reductase activity of DHRS3 is reciprocally activated by retinol dehydrogenase 10 to control retinoid homeostasis." J Biol Chem **289**(21): 14868-14880.

Ala-Laurila, P., M. C. Cornwall, R. K. Crouch and M. Kono (2009). "The action of 11-cis-retinol on cone opsins and intact cone photoreceptors." J Biol Chem **284**(24): 16492-16500.

Allali-Hassani, A., J. M. Peralba, S. Martras, J. Farres and X. Pares (1998). "Retinoids, omega-hydroxyfatty acids and cytotoxic aldehydes as physiological substrates, and H2-receptor antagonists as pharmacological inhibitors, of human class IV alcohol dehydrogenase." FEBS Lett **426**(3): 362-366.

Belyaeva, O. V., M. P. Johnson and N. Y. Kedishvili (2008). "Kinetic analysis of human enzyme RDH10 defines the characteristics of a physiologically relevant retinol dehydrogenase." J Biol Chem **283**(29): 20299-20308.

Boleda, M. D., N. Saubi, J. Farres and X. Pares (1993). "Physiological substrates for rat alcohol dehydrogenase classes: aldehydes of lipid peroxidation, omega-hydroxyfatty acids, and retinoids." Arch Biochem Biophys **307**(1): 85-90.

Bowes Rickman, C., J. N. Ebright, Z. J. Zavodni, L. Yu, T. Wang, S. P. Daiger, G. Wistow, K. Boon and M. A. Hauser (2006). "Defining the human macula transcriptome and candidate retinal disease genes using EyeSAGE." Invest Ophthalmol Vis Sci **47**(6): 2305-2316.

Corbo, J. C. and C. L. Cepko (2005). "A hybrid photoreceptor expressing both rod and cone genes in a mouse model of enhanced S-cone syndrome." Plos Genetics **1**(2): 140-153.

Corbo, J. C., C. A. Myers, K. A. Lawrence, A. P. Jadhav and C. L. Cepko (2007). "A typology of photoreceptor gene expression patterns in the mouse." Proc Natl Acad Sci U S A **104**(29): 12069-12074.

Crosas, B., A. Allali-Hassani, S. E. Martinez, S. Martras, B. Persson, H. Jornvall, X. Pares and J. Farres (2000). "Molecular basis for differential substrate specificity in class IV alcohol dehydrogenases: a conserved function in retinoid metabolism but not in ethanol oxidation." J Biol Chem **275**(33): 25180-25187.

Deisenroth, C., Y. Itahana, L. Tollini, A. Jin and Y. Zhang (2011). "p53-Inducible DHRS3 is an endoplasmic reticulum protein associated with lipid droplet accumulation." J Biol Chem **286**(32): 28343-28356.

Duester, G. (2000). "Families of retinoid dehydrogenases regulating vitamin A function: production of visual pigment and retinoic acid." Eur J Biochem **267**(14): 4315-4324.

Farjo, K. M., G. Moiseyev, Y. Takahashi, R. K. Crouch and J. X. Ma (2009). "The 11-cis-retinol dehydrogenase activity of RDH10 and its interaction with visual cycle proteins." Invest Ophthalmol Vis Sci **50**(11): 5089-5097.

Gonzalez-Duarte, R. and R. Albalat (2005). "Merging protein, gene and genomic data: the evolution of the MDR-ADH family." Heredity (Edinb) **95**(3): 184-197.

Haeseleer, F., J. Huang, L. Lebioda, J. C. Saari and K. Palczewski (1998). "Molecular characterization of a novel short-chain dehydrogenase/reductase that reduces all-trans-retinal." J Biol Chem **273**(34): 21790-21799.

Haeseleer, F., G. F. Jang, Y. Imanishi, C. A. Driessen, M. Matsumura, P. S. Nelson and K. Palczewski (2002). "Dual-substrate specificity short chain retinol dehydrogenases from the vertebrate retina." J Biol Chem **277**(47): 45537-45546.

Holcman, D. and J. I. Korenbrot (2004). "Longitudinal diffusion in retinal rod and cone outer segment cytoplasm: the consequence of cell structure." Biophys J **86**(4): 2566-2582.

Hoog, J. O. and L. J. Ostberg (2011). "Mammalian alcohol dehydrogenases--a comparative investigation at gene and protein levels." Chem Biol Interact **191**(1-3): 2-7.

Jones, G. J., R. K. Crouch, B. Wiggert, M. C. Cornwall and G. J. Chader (1989). "Retinoid requirements for recovery of sensitivity after visual-pigment bleaching in isolated photoreceptors." Proc Natl Acad Sci U S A **86**(23): 9606-9610.

Kasus-Jacobi, A., J. Ou, Y. K. Bashmakov, J. M. Shelton, J. A. Richardson, J. L. Goldstein and M. S. Brown (2003). "Characterization of mouse short-chain aldehyde reductase (SCALD), an enzyme regulated by sterol regulatory element-binding proteins." J Biol Chem **278**(34): 32380-32389.

Kasus-Jacobi, A., J. Ou, D. G. Birch, K. G. Locke, J. M. Shelton, J. A. Richardson, A. J. Murphy, D. M. Valenzuela, G. D. Yancopoulos and A. O. Edwards (2005). "Functional characterization of mouse RDH11 as a retinol dehydrogenase involved in dark adaptation in vivo." J Biol Chem **280**(21): 20413-20420.

Kaylor, J. J., J. D. Cook, J. Makshanoff, N. Bischoff, J. Yong and G. H. Travis (2014). "Identification of the 11-cis-specific retinyl-ester synthase in retinal Muller cells as multifunctional O-acyltransferase (MFAT)." Proc Natl Acad Sci U S A **111**(20): 7302-7307.

Kaylor, J. J., Q. Yuan, J. Cook, S. Sarfare, J. Makshanoff, A. Miu, A. Kim, P. Kim, S. Habib, C. N. Roybal, T. Xu, S. Nusinowitz and G. H. Travis (2013). "Identification of DES1 as a vitamin A isomerase in Muller glial cells of the retina." Nat Chem Biol **9**(1): 30-36.

Kedishvili, N. Y. (2013). "Enzymology of retinoic acid biosynthesis and degradation." J Lipid Res **54**(7): 1744-1760.

Kolesnikov, A. V., A. Maeda, P. H. Tang, Y. Imanishi, K. Palczewski and V. J. Kefalov (2015). "Retinol dehydrogenase 8 and ATP-binding cassette transporter 4 modulate dark adaptation of M-cones in mammalian retina." J Physiol **593**(22): 4923-4941.

Leenheer, A. P. d., W. E. Lambert and J. F. Van Bocxlaer (2000). Modern chromatographic analysis of vitamins. New York, Marcel Dekker.

Lhor, M. and C. Salesse (2014). "Retinol dehydrogenases: membrane-bound enzymes for the visual function." Biochem Cell Biol **92**(6): 510-523.

Livak, K. J. and T. D. Schmittgen (2001). "Analysis of relative gene expression data using real-time quantitative PCR and the 2(T)(-Delta Delta C) method." Methods **25**(4): 402-408.

Lundova, T., L. Zemanova, B. Malcekova, A. Skarka, H. Stambergova, J. Havrankova, M. Safr and V. Wsol (2015). "Molecular and biochemical characterisation of human short-chain dehydrogenase/reductase member 3 (DHRS3)." Chem Biol Interact **234**: 178-187.

Maeda, A., T. Maeda, Y. Imanishi, V. Kuksa, A. Alekseev, J. D. Bronson, H. Zhang, L. Zhu, W. Sun, D. A. Saperstein, F. Rieke, W. Baehr and K. Palczewski (2005). "Role of photoreceptor-specific retinol dehydrogenase in the retinoid cycle in vivo." J Biol Chem **280**(19): 18822-18832.

Maeda, A., T. Maeda, Y. Imanishi, W. Sun, B. Jastrzebska, D. A. Hatala, H. J. Winkens, K. P. Hofmann, J. J. Janssen, W. Baehr, C. A. Driessen and K. Palczewski (2006). "Retinol dehydrogenase (RDH12) protects photoreceptors from light-induced degeneration in mice." J Biol Chem **281**(49): 37697-37704.

Maier, T., M. Guell and L. Serrano (2009). "Correlation of mRNA and protein in complex biological samples." FEBS Lett **583**(24): 3966-3973.

Martras, S., R. Alvarez, S. E. Martinez, D. Torres, O. Gallego, G. Duester, J. Farres, A. R. de Lera and X. Pares (2004). "The specificity of alcohol dehydrogenase with cis-retinoids. Activity with 11-cis-retinol and localization in retina." Eur J Biochem **271**(9): 1660-1670.

Mata, N. L., R. A. Radu, R. C. Clemmons and G. H. Travis (2002). "Isomerization and oxidation of vitamin a in cone-dominant retinas: a novel pathway for visual-pigment regeneration in daylight." Neuron **36**(1): 69-80.

Mears, A. J., M. Kondo, P. K. Swain, Y. Takada, R. A. Bush, T. L. Saunders, P. A. Sieving and A. Swaroop (2001). "Nrl is required for rod photoreceptor development." Nat Genet **29**(4): 447-452.

Miyazono, S., Y. Shimauchi-Matsukawa, S. Tachibanaki and S. Kawamura (2008). "Highly efficient retinal metabolism in cones." Proc Natl Acad Sci U S A **105**(41): 16051-16056.

Pares, X., J. Farres, N. Kedishvili and G. Duester (2008). "Medium- and short-chain dehydrogenase/reductase gene and protein families : Medium-chain and short-chain dehydrogenases/reductases in retinoid metabolism." Cell Mol Life Sci **65**(24): 3936-3949.

Parker, R., J. S. Wang, V. J. Kefalov and R. K. Crouch (2011). "Interphotoreceptor retinoid-binding protein as the physiologically relevant carrier of 11-cis-retinol in the cone visual cycle." J Neurosci **31**(12): 4714-4719.

Parker, R. O. and R. K. Crouch (2010). "Retinol dehydrogenases (RDHs) in the visual cycle." Exp Eye Res **91**(6): 788-792.

Persson, B., J. Hedlund and H. Jornvall (2008). "Medium- and short-chain dehydrogenase/reductase gene and protein families : the MDR superfamily." Cell Mol Life Sci **65**(24): 3879-3894.

Persson, B., Y. Kallberg, J. E. Bray, E. Bruford, S. L. Dellaporta, A. D. Favia, R. G. Duarte, H. Jornvall, K. L. Kavanagh, N. Kedishvili, M. Kisiela, E. Maser, R. Mindnich, S. Orchard, T. M. Penning, J. M. Thornton, J. Adamski and U. Oppermann (2009). "The SDR (short-chain dehydrogenase/reductase and related enzymes) nomenclature initiative." Chem Biol Interact **178**(1-3): 94-98.

Rattner, A., P. M. Smallwood and J. Nathans (2000). "Identification and characterization of all-trans-retinol dehydrogenase from photoreceptor outer segments, the visual cycle enzyme that reduces all-trans-retinal to all-trans-retinol." J Biol Chem **275**(15): 11034-11043.

Sahu, B. and A. Maeda (2016). "Retinol Dehydrogenases Regulate Vitamin A Metabolism for Visual Function." Nutrients **8**(11).

Sahu, B., W. Sun, L. Perusek, V. Parmar, Y. Z. Le, M. D. Griswold, K. Palczewski and A. Maeda (2015). "Conditional Ablation of Retinol Dehydrogenase 10 in the Retinal Pigmented Epithelium Causes Delayed Dark Adaption in Mice." J Biol Chem **290**(45): 27239-27247.

Sato, S., R. Frederiksen, M. C. Cornwall and V. J. Kefalov (2017). "The retina visual cycle is driven by cis retinol oxidation in the outer segments of cones." Vis Neurosci **34**: E004.

Sato, S., T. Fukagawa, S. Tachibanaki, Y. Yamano, A. Wada and S. Kawamura (2013). "Substrate specificity and subcellular localization of the aldehyde-alcohol redox-coupling reaction in carp cones." J Biol Chem **288**(51): 36589-36597.

Sato, S. and V. J. Kefalov (2016). "cis Retinol oxidation regulates photoreceptor access to the retina visual cycle and cone pigment regeneration." J Physiol **594**(22): 6753-6765.

Sato, S., S. Miyazono, S. Tachibanaki and S. Kawamura (2015). "RDH13L, an enzyme responsible for the aldehyde-alcohol redox coupling reaction (AL-OL coupling reaction) to supply 11-cis retinal in the carp cone retinoid cycle." J Biol Chem **290**(5): 2983-2992.

Skaper, S. D. (2012). "Isolation and culture of rat cone photoreceptor cells." Methods Mol Biol **846**: 147-158.

Tachibanaki, S., S. Tsushima and S. Kawamura (2001). "Low amplification and fast visual pigment phosphorylation as mechanisms characterizing cone photoresponses." Proc Natl Acad Sci U S A **98**(24): 14044-14049.

Takahashi, Y., G. Moiseyev, K. Farjo and J. X. Ma (2009). "Characterization of key residues and membrane association domains in retinol dehydrogenase 10." Biochem J **419**(1): 113-122, 111 p following 122.

Wang, J. S., M. E. Estevez, M. C. Cornwall and V. J. Kefalov (2009). "Intra-retinal visual cycle required for rapid and complete cone dark adaptation." Nat Neurosci **12**(3): 295-302.

Wang, J. S. and V. J. Kefalov (2009). "An alternative pathway mediates the mouse and human cone visual cycle." Curr Biol **19**(19): 1665-1669.

Wang, J. S. and V. J. Kefalov (2011). "The cone-specific visual cycle." Prog Retin Eye Res **30**(2): 115-128.

Wang, J. S., S. Nymark, R. Frederiksen, M. E. Estevez, S. Q. Shen, J. C. Corbo, M. C. Cornwall and V. J. Kefalov (2014). "Chromophore supply rate-limits mammalian photoreceptor dark adaptation." J Neurosci **34**(34): 11212-11221.

Wu, B. X., Y. Chen, Y. Chen, J. Fan, B. Rohrer, R. K. Crouch and J. X. Ma (2002). "Cloning and characterization of a novel all-trans retinol short-chain dehydrogenase/reductase from the RPE." Invest Ophthalmol Vis Sci **43**(11): 3365-3372.

Wu, B. X., G. Moiseyev, Y. Chen, B. Rohrer, R. K. Crouch and J. X. Ma (2004). "Identification of RDH10, an All-trans Retinol Dehydrogenase, in Retinal Muller Cells." Invest Ophthalmol Vis Sci **45**(11): 3857-3862.

Xue, Y., S. Sato, D. Razafsky, B. Sahu, S. Q. Shen, C. Potter, L. L. Sandell, J. C. Corbo, K. Palczewski, A. Maeda, D. Hodzic and V. J. Kefalov (2017). "The role of retinol dehydrogenase 10 in the cone visual cycle." Sci Rep **7**(1): 2390.

Yang, Z. N., G. J. Davis, T. D. Hurley, C. L. Stone, T. K. Li and W. F. Bosron (1994). "Catalytic efficiency of human alcohol dehydrogenases for retinol oxidation and retinal reduction." Alcohol Clin Exp Res **18**(3): 587-591.

Chapter 3: Identification of a novel non-enzymatic pathway for functional visual pigment regeneration under blue light through a retinyl-phospholipid intermediate

3.1 Preliminary studies on the photoisomerization of retinaldehyde and N-retinylidene-phosphatidylethanolamine (N-ret-PE)

A small portion of this section is adapted from the publication: Joanna J. Kaylor, Tongzhou Xu, Norianne T. Ingram, Avian Tsan, Hayk Hakobyan, Gordon L. Fain and Gabriel H. Travis (2017). Blue light regenerates functional visual pigments in mammals through a retinyl-phospholipid intermediate. *Nat Commun*. 8(1):16. doi:10.1038/s41467-017-00018-4. Author contributions are listed on the Acknowledgement page of this dissertation.

3.1.1 Introduction

As discussed in **Chapter 1**, light detection is mediated by the visual pigments in the photoreceptors. In most vertebrate visual pigments, the light-sensitive chromophore is 11-*cis*-retinal (Nakanishi 1991, Zhong, Kawaguchi et al. 2012), which is covalently bound to the opsin through a protonated Schiff base (Filipek, Stenkamp et al. 2003). Upon the absorption of a photon, 11-*cis*-retinal is isomerized to all-*trans*-retinal, triggering the conversion of the pigment to its active signaling state (Meta II) (Okada, Ernst et al. 2001). In ciliary photoreceptors in chordates, after a transient activation, the visual pigment decays to apo-opsin and free all-*trans*-retinal (Wald 1968, Okada, Ernst et al. 2001). In contrast to ciliary photoreceptors, visual chromophore in rhabdomeric photoreceptors of certain invertebrates remains covalently bound to opsin even after having been photoisomerized to the all-*trans*-isomer. More interestingly, the bound all-*trans*-isomer can be reversed to its 11-*cis*-form when it absorbs another photon, exhibiting a bistable feature (Lamb 2013). Although in ciliary photoreceptors, a similar

“photoreversal” process can occur in certain short-lived intermediates immediately following photon absorption (such as metarhodopsin I), such ability is rapidly lost after the formation of Meta II (Williams 1964, Arnis and Hofmann 1995, Grimm, Reme et al. 2000, Furutani, Kandori et al. 2003, Lamb 2009). Therefore, regeneration of 11-*cis*-retinal in ciliary photoreceptors predominantly relies on the enzymatic visual cycles.

Although two visual cycle pathways have been established (see **Chapter 1**), shortcomings in this field still exist. For example, the canonical visual is thought to be too slow (“50-fold slower”) for adequate chromophore regeneration in bright light (Mata, Radu et al. 2002). On the other hand, DES1 catalyzes retinoid isomerization at high speed, but the production of 11-*cis*-retinol is highly limited by itself, since the reaction features an equilibrium isomerization similar to that catalyzed by iodine (Kaylor, Yuan et al. 2013). The further enhancement of 11-*cis*-retinol ratio is thought to rely on the driving force of other proteins such as CRALBP and MFAT through mass action (Kaylor, Yuan et al. 2013, Kaylor, Cook et al. 2014). Although the alternate visual cycle is thought to be “20-fold faster”, even with the joint efforts of the two visual cycles, the requirement of chromophore regeneration under bright light condition may still not be completely met (Mata, Radu et al. 2002). Furthermore, a recent physiological study suggests that the rate of the alternate visual cycle is only comparable to but not much faster than that of the canonical visual cycle (Wang, Estevez et al. 2009).

Although used as the chromophore, 11-*cis*-retinal is relatively unstable compared to other isomers. At the equilibrium state of retinal catalyzed by iodine or trifluoroacetic acid (TFA), the mixtures contained ~60% all-*trans*-retinal, followed by 13-*cis*-retinal

(~22-23%), 9-*cis*-retinal (~11-14%) and 9,13-di-*cis*-retinal (~4-5%), while 11-*cis*-retinal only accounts for less than 0.2% (Rando and Chang 1983). On the contrary, when retinoids were exposed to light, the fraction of 11-*cis* isomer was much higher. For example, in aqueous sodium dodecyl sulfate, 11-*cis*-retinal accounted for 16.0% at the photostationary status following the illumination of all-*trans*-retinal with the light of 380 nm or above. Such ratio even reached 19.0% in ethanol (Deval and Singh 1988). In another earlier study, 11-*cis*-retinal reached 43% in acetonitrile, 37% in DMSO and 35% in pyridine and 19.5-20% in ethanol upon the irradiation of all-*trans*-retinal in a few light conditions (Liu and Asato 1984). Observations of the 11-*cis*-retinal production after the illumination of all-*trans*-retinal could be traced back to studies at an even earlier time, such as those by Hubbard and Wald (Hubbard and Wald 1952), Brown and Wald (Brown and Wald 1956), and Denny et al.(Denny, Chun et al. 1981). A higher ratio of 11-*cis* isomer relative to iodine-catalyzed equilibrium could also be achieved from photoisomerization of protonated and unprotonated Schiff base of retinal (with n-butylamine) under certain conditions (Koyama, Kubo et al. 1991).

More interestingly, retinylidene phospholipid formed by all-*trans*-retinal and phosphatidylethanolamine (PE) was reported to be possibly involved in the conversion of all-*trans*- to 11-*cis*-retinal in rod outer segments under light (Shichi and Somers 1974). This isomerization activity was not significantly affected by heat treatment (thus not enzymatic) and its efficiency was light wavelength dependent, with 450-460 nm light being the most effective (Shichi and Somers 1974).

Daylight vision is important to many vertebrates, especially humans. Given the aforementioned phenomena as well as the fact that retina is exposed to light constantly during the visual process, an intriguing question arises: does light also promote the vision of vertebrates, as it does to certain invertebrates, by accelerating their visual chromophore regeneration?

Considering the following facts: (1) the report of Shichi and Somers above (Shichi and Somers 1974); (2) the fact that retinaldehydes are hydrophobic (Szuts and Harosi 1991) and readily and reversibly forms the retinyl-lipid, N-retinylidene-PE (N-ret-PE) with PE (Pitt, Collins et al. 1955, Poincelot, Millar et al. 1969, Anderson and Maude 1970, Beharry, Zhong et al. 2004, Quazi, Lenevich et al. 2012), (3) PE accounts for ~35%-38% of total lipids in human, bovine and rat ROS (Fliesler and Anderson 1983) and (4) the λ_{max} of protonated N-ret-PE is around 450 nm (Anderson and Maude 1970, Beharry, Zhong et al. 2004), which is within the optimal wavelength range from Shichi and Somers' report (Shichi and Somers 1974) and transparent through optic media (Boettner and Wolter 1962, Laube, Apel et al. 2004), we hypothesized that light may promote vertebrate vision and N-ret-PE may be a photoactive intermediate.

Retinoid studies are usually carried out in darkness to protect 11-*cis*-retinoids, so our hypothesis that light may facilitate its production seems unusual. To set a solid ground for further studies, I performed preliminary *in vitro* tests for the photoisomerization features of all-*trans*-retinal and N-ret-PE.

3.1.2 Results

3.1.2.1 Synthesis, purification and quantitative analysis of N-ret-PE

To study the photoisomerization properties, N-ret-PE was synthesized using all-*trans*-retinal and 1-oleoyl-2-hydroxy-*sn*-glycero-3-phosphoethanol, and purified in its protonated form in acidified methanol by reverse-phase HPLC **(Fig.3.1-1)**. 1-oleoyl-2-hydroxy-*sn*-glycero-3-phosphoethanolamine was used as the PE source due to its ease in incorporating into membrane phospholipid bilayers compared to dioleoyl-PEs. To quantitate different isomer components of N-ret-PE in isomerization experiments, we decided to adopt an oximation method, by which stable retinaldehyde oximes were made by reacting N-ret-PE (and also retinaldehydes) with hydroxylamine. The isomer compositions of tested samples could then be determined with normal-phase HPLC using the same method as quantitating retinaldehydes **(Fig.3.1-2)**.

3.1.2.2 Photoisomerization of non-protonated and protonated N-ret-PE in methanol

To test the photoisomerization features of N-ret-PE, purified all-*trans*-N-ret-PE (at-N-ret-PE) was dissolved in either alkalized or acidified methanol to maintain their non-protonated or protonated forms, respectively. They were then exposed to monochromatic light of 370 nm or 450 nm, or kept in the dark. Light-induced formations of *cis*-N-ret-PEs were observed **(Fig.3.1-3)**. The wavelengths that lead to maximum amounts of *cis*-isomers formed were 370 nm for non-protonated N-ret-PE and 450 nm for protonated N-ret-PE. These wavelengths of light coincide with the λ_{max} of non-protonated (~365 nm) and protonated (~450 nm) N-ret-PE in methanol (Kaylor, Xu et al.

2017). Moreover, the amounts of 11-*cis*-isomer formed (tens of picomoles) under optimal wavelength were much higher than what would be expected from an iodine-catalyzed all-*trans*-retinal thermal isomerization, which would only be <0.2% of total isomers (< 4 picomoles in this case) (Rando and Chang 1983). On the other hand, based on rough estimations from *anti*-13-*cis*-ROX and *syn*-9-*cis*-ROX (see the legend of **Fig.3.1-3**), the light-dependent formation of 13-*cis*- and 9-*cis*-isomers seemed to be comparable to or lower than that of 11-*cis*-isomer, especially for the protonated N-ret-PE **(Fig.3.1-3)**. This was also dramatically different from what would be expected from the iodine-catalyzed isomerization of all-*trans*-retinal, at the equilibrium of which 13-*cis*- and 9-*cis*-isomers account for more than 20% or 10% of the total isomers, respectively (Rando and Chang 1983).

These observations confirm the photoisomerization feature of N-ret-PE as previously reported (Shichi and Somers 1974). The relatively higher amount of 11-*cis*-N-ret-PE formed compared to the iodine-catalyzed thermal isomerization, indicates a high potential of N-ret-PE to contribute to the chromophore regeneration in light.

3.1.2.3 Photoisomerization of all-*trans*-retinal and N-ret-PE in liposomes under different light conditions

To test if the photoisomerization of N-ret-PE takes place in aqueous phase and under normal light condition, at-N-ret-PE was delivered in acidified methanol to liposomes made from porcine brain polar lipids in PBS. These liposomes were exposed to UV-filtered laboratory room light (white) for 15 minutes at room temperature (RT). Similar light-dependent formation of *cis*-isomers (those isomers could be in the form of either

free retinal or N-ret-PE in liposomes, same below) was observed and the dominant isomer formed seemed to be the 11-*cis*-isomer (comparing the “net” increase of *cis*-isomers between samples in the light and in the dark) **(Fig.3.1-4)**.

Photoisomerization of 11-*cis*-retinal in a visual pigment occurs in a very short period of time (Manathunga, Yang et al. 2017). It is reasonable to assume that photoisomerization of N-ret-PE also occurs in a similar timescale. If that is the case, photoisomerization of N-ret-PE could be induced by very brief light exposure. To test this, at-N-ret-PE was incorporated into liposomes of porcine brain polar lipids in PBS and exposed up to 5 times to a UV-filtered white strobe light flash of 750 Watt. A steady increase of 11-*cis*-N-ret-PE with each flash was observed. On the other hand, 13-*cis*-N-ret-PE, the thermally preferred *cis*-isomer (Rando and Chang 1983), did not show such increase compared to samples in the dark, nor did 9-*cis*-N-ret-PE **(Fig.3.1-5)**. These data suggest that the photoisomerization of N-ret-PE occurs in a very short period of light exposure and that 11-*cis*-N-ret-PE seems to be the preferred *cis*-isomer formed in light, whose formation is light dosage-dependent.

At-N-ret-PE could be formed by the condensation of all-*trans*-retinal and PE (Pitt, Collins et al. 1955, Poincelot, Millar et al. 1969, Anderson and Maude 1970, Beharry, Zhong et al. 2004, Quazi, Lenevich et al. 2012). To confirm that this process occurs efficiently in lipid membranes and the formed N-ret-PE undergoes photoisomerization, I incorporated all-*trans*-retinal into liposomes of 100% DOPC (1,2-dioleoyl-sn-glycero-3-phosphocholine) or 65% DOPC/35% DOPE (1,2-dioleoyl-*sn*-glycero-3-phosphoethanolamine) (mol %) in slightly acidified PBS (pH 6.5) (the apparent pK_a of

protonated N-ret-PE is 6.9 (Quazi, Lenevich et al. 2012)). The percentage of PE in these liposomes reflects its composition in ROS (Fliesler and Anderson 1983). These liposomes were then exposed to monochromatic light of 450 nm (close to the λ_{max} of protonated N-ret-PE), 375 nm (close to the λ_{max} of all-*trans*-retinal (383 nm in ethanol (Leenheer, Lambert et al. 2000)) and non-protonated N-ret-PE) with equal photon fluxes, or kept in the dark for 80 seconds at RT. As shown in **Fig.3.1-6**, under 375 nm light, the 11-*cis*- and 13-*cis*-isomers formed were comparable in both types of liposomes. However, under 450 nm light, a significantly higher amount of 11-*cis*-isomer was formed in liposomes of 65%DOPC/35%DOPE compared to that of 100% DOPC. These strongly indicate that N-ret-PE can be successfully formed in the presence of all-*trans*-retinal and PE in lipid membranes, and that the formed N-ret-PE undergoes photoisomerization as expected.

3.1.2.4 Comparison of the inhibitory effects of spin traps/probes on the retinoid isomerization induced by iodine or light

As mentioned in the introduction, the *cis*-isomer compositions of iodine-catalyzed versus light-induced isomerization of retinoids could be quite different under certain conditions, suggesting different isomerization mechanisms in these processes. If any of the isomerization mechanism involves a radical intermediate, the isomerization process may be inhibited by spin trap and/or spin probe reagents (Poliakov, Parikh et al. 2011).

To address that, I first tested the isomerization of all-*trans*-retinal catalyzed by molecular iodine in *n*-heptane in the presence of 1 mM spin traps/probes, which included (4-hydroxy-2,2,6,6-tetramethylpiperidine-1-oxyl (4-hydroxy-TEMPO); 5,5-dimethyl-1-

pyrroline-N-oxide (DMPO); 2,2-dimethyl-4-phenyl-2H-imidazole-1-oxide (DMPIO); N-tert-butyl-α-phenylnitrone (PBN) and 4-phenyl-2,2,5,5-tetramethyl-3-imidazoline-1-oxyl nitroxide (PTMIO). I also tested the photoisomerization of all-*trans*-retinal in methanol exposed to monochromatic light of 380 nm in the presence of 1 mM of the same spin traps/probes. For iodine-catalyzed isomerization, after a 10-minute incubation at 37 ºC, a significant increase of 13-*cis*-retinal was observed in samples with iodine and without spin trap/probe reagents ($+I_2$ -SPTP), compared to the control samples without either ($-I_2$ -SPTP). Such an increase can be seen even in samples at 0-minute time point (not actual 0 min due to sample handling time), indicating the fast speed of the iodine-catalyzed isomerization **(Fig.3.1-7)**. This iodine-catalyzed isomerization was significantly inhibited by all the tested spin trap/probe agents except DMPIO **(Fig.3.1-7)**.

On the other hand, when all-*trans*-retinal in methanol was exposed to 380 nm light in the presence of these spin trap/probe reagents for up to 9 minutes, the photoisomerization of all-*trans*-retinal was largely unaffected by any of these reagents (compared to the dramatic degree of inhibition observed in **Fig.3.1-7**) **(Fig.3.1-8)**.

A similar inhibition test was also performed on the photoisomerization of protonated N-ret-PE in acidified methanol exposed to 450 nm light. Consistent with the result of the inhibition test on the photoisomerization of all-*trans*-retinal, in general, the photoisomerization of protonated N-ret-PE did not seem to be inhibited by these spin trap/probe reagents either **(Fig.3.1-9)**.

These observations indicate that the mechanisms of the photoisomerization and iodine-catalyzed thermal isomerization of retinoids might be radically different. The former

probably does not involve a free radical intermediate, while the latter probably does, as mentioned by previous publications such as (Benson, Egger et al. 1965, Hepperle, Li et al. 2005).

3.1.2.5 Action spectrum analysis of the photoisomerization of all-*trans*-retinal and N-ret-PE

The above data strongly suggest that photoisomerization may be a promising mechanism to accelerate 11-*cis*-retinal formation. To study the photoisomerization properties of retinoids systematically, I performed “action spectrum” experiments of all-*trans*-retinal, non-protonated N-ret-PE and protonated N-ret-PE.

In these tests, retinoids were dissolved in regular (for all-*trans*-retinal), alkalized (for non-protonated N-ret-PE) or acidified (for protonated N-ret-PE) methanol. These retinoids were illuminated with monochromatic light of the same photon flux from 325 nm to 650 nm with 25-nm increments for 80 seconds at RT. The action spectrum of all-*trans*-retinal is shown in **Fig.3.1-10**. A significant light-induced formation of *cis*-retinals was observed following light exposure. The 11-*cis*- and 13-*cis*-isomers formed were at comparable levels. The formation of *cis*-isomers reached their maxima around 375 nm (350 nm – 400 nm), close to the λ_{max} of all-*trans*-retinal in methanol (~380 nm in our experience, the λ_{max} of all-*trans*-retinal is ~383 nm in ethanol (Leenheer, Lambert et al. 2000)). The substrate, all-*trans*-retinal, exhibited a corresponding depletion.

The action spectrum of non-protonated N-ret-PE exhibited a similar pattern to that of all-*trans*-retinal, with the maximal photoisomerization observed around 375 nm (350 nm – 375 nm), also close to its λ_{max} (~365 nm) **(Fig.3.1-11)**. However, the 11-*cis*-isomer formed seemed to be more abundant than the 13-*cis*- and 9-*cis*-isomers.

The action spectrum of protonated N-ret-PE exhibited significant 11-*cis*-isomer formation, the amount of which was much higher than that of 13-*cis*- and 9-*cis*-isomers. The ratio of 11-*cis*-/13-*cis*-isomers formed was about 37:1 (121 picomoles/3.3 picomoles) and the ratio of 11-*cis*-/9-*cis*-isomers was about 6.7:1 (121 picomoles/18 picomoles). The pattern of the action spectrum resembles the absorbance spectrum of protonated N-ret-PE, with 450 nm the optimal wavelength. The at-N-ret-PE substrate exhibited a corresponding depletion **(**see **Chapter 3.2, Fig.1 and Supplementary Fig.1)**.

3.1.3 Discussion

The data presented here suggest that N-ret-PE undergoes robust photoisomerization, and in contrast to the thermal equilibrium,11-*cis*-isomer is a major *cis*-isomer formed in light. This photoisomerization occurs not only in monochromatic light but also in white room light or strobe light **(Figs.3.1-3 to 5, and Chapter 3.2 Fig.1)**.

Although all-*trans*-retinal and non-protonated N-ret-PE also showed a significant formation of 11-*cis*-isomers in light **(Figs.3.1-3, -10 and -11)**, their contributions to visual chromophore regeneration are likely limited due to the poor transmission of UV light by the optic media (Boettner and Wolter 1962, Laube, Apel et al. 2004). However, protonated N-ret-PE, which has its λ_{max} in the visible light range (~450nm)

and exhibits high 11-*cis*-specificity in its photoisomerization, is a very promising candidate for a photosensitive intermediate that could contribute to light-dependent chromophore regeneration in ciliary photoreceptors.

In liposome experiments **(Figs.3.1-4 to 6)**, high amounts of 13-*cis*-isomer were always present in samples containing N-ret-PE or PE, even in the control samples kept in the dark. This might be attributed to the impurity of the substrate and the thermal isomerization during the experimental period. However, I believe the major reason was the catalytic effect of PE, which has been previously reported (Groenendijk, Jacobs et al. 1980). In this case, it could be argued that the smaller net increase of 13-*cis*-isomer (thus the better 11-*cis*-specificity) was due to its already elevated level in the dark. However, the action spectrum experiment of protonated N-ret-PE in acidified methanol **(Chapter 3.2, Fig.1)** confirmed that 11-*cis*-N-ret-PE is the major *cis*-isomer formed in its photoisomerization.

All the above data were obtained by *in vitro* biochemical tests. Although the phenomena were exciting and promising, some of them were quite preliminary. Therefore, more detailed studies, including *in vivo* experiments in animals, were essential to validate our hypothesis. If photoisomerization of N-ret-PE does facilitate 11-*cis*-retinal regeneration in physiological conditions, the extent of its contribution, which could be reflected by its quantum efficiency, is also an important question to answer.

In the next section **(Chapter 3.2)**, the accelerated regeneration of rhodopsin under blue light than darkness will be confirmed by studies using both photoreceptor OS membranes and live mice. The quantum efficiency of N-ret-PE will be determined (which is comparable to that of rhodopsin). Both transretinal electroretinogram (ERG) and isolated cone suction electrode recordings will be performed to address that cones show higher photosensitivity when exposed to 450-nm versus 560-nm light. All these *in vitro* and *in vivo* studies finally confirm our hypothesis and establish a novel non-enzymatic visual cycle pathway. A detailed model will also been proposed **(**see **Chapter 3.2, Fig.6)**.

3.1.4 Materials and Methods

3.1.4.1 Synthesis and purification of at-N-Ret-PE

The synthesis and purification processes of at-N-ret-PE have been described in detail in our recent publication (Kaylor, Xu et al. 2017) (reprinted in **Chapter 3.2**).

3.1.4.2 Retinoid analysis by normal-phase HPLC

Retinoids were quantitated using our published method (Kaylor, Xu et al. 2017) with minor modifications. Briefly, each 200 µL sample was treated with 10-25 µL of 5% SDS (for liposome samples only), 20-50 µL brine and 200 µL of 2 M hydroxylamine hydrochloride (pH 7.0-7.2) (Sigma-Aldrich). The mixtures were incubated at RT for 10-20 minutes to allow oximation of retinaldehydes or N-ret-PE. Retinoids were then extracted and analyzed as described (Kaylor, Yuan et al. 2013, Kaylor, Xu et al. 2017) (for retinoid analysis, also see **Fig.3.1-2**).

3.1.4.3 Preparation of liposomes

Desired amounts of lipids in chloroform solutions were dried under a stream of nitrogen gas in a glass test tube. Dried lipids were hydrated by adding one ml of argon gas bubbled PBS (pH 7.2 or 6.5 as indicated below) and incubated in the dark for one hour with agitation, followed by vortexing. The hydrated multilamellar vesicles were extruded through two stacked polycarbonate membranes (Whatman Nuclepore Track-Etched Membrane, diameter 19 mm, pore size 0.2 μm) for 45 passes using a LiposoFast extruder (Avestin, designed based on (MacDonald, MacDonald et al. 1991)). Desired amounts of the extrusion were taken and diluted with the same hydration buffer (argon gas bubbled PBS, pH 7.2 or 6.5) to the final concentrations needed. The prepared liposomes were either used the same day or kept at 4 ºC overnight and used the next day. All-*trans*-retinal or at-N-ret-PE was delivered in small volumes of ethanol or acidified methanol respectively to liposomes and incubated in the dark for at least 15 minutes (preferably under argon gas) with agitation to allow their incorporation into liposome membranes. Methanol was acidified by TFA, with pH values of ~1-2.5 measured by a pH meter in our preliminary tests, which has been standardized to 20 μL TFA per liter methanol in our later tests including these published (Kaylor, Xu et al. 2017). Lipids used to prepare liposomes included: 1,2-dioleoyl-sn-glycero-3-phosphocholine (DOPC) (25 mg/ml, Avanti Polar Lipids, Cat. No.850375C), 1,2-dioleoyl-*sn*-glycero-3-phosphoethanolamine (DOPE) (10 mg/ml, Sigma Aldrich, Cat. No.42490), brain polar lipid extract (porcine) (25 mg/ml, Avanti Polar Lipids, Cat. No.141101C). All of them were in chloroform solutions.

3.1.4.4 Photoisomerization of non-protonated and protonated N-ret-PE in methanol

For the experiment of the photoisomerization of non-protonated and protonated N-ret-PE in methanol **(Fig.3.1-3)**, purified N-ret-PE (final concentration 10 μM) was added to alkalized (with sodium hydroxide crystals) or acidified (with TFA) methanol to maintain their non-protonated or protonated form, respectively. The protonation status of each form was confirmed by measuring the UV-Vis spectrum of an aliquot of each sample using a spectrophotometer (UV-2401(PC), Shimazu Corporation). Samples of each form were added to quartz 10 mm cuvettes covered in black paper except the front side (same below, unless otherwise mentioned). These samples were exposed to "monochromatic" light of either 370 nm or 450 nm (with approximately equal photon fluxes) from a custom monochromator (Newport Instruments) or kept in the dark, all for 5 minutes at RT. After the treatment, samples were placed in the dark immediately (same below) and three replicates of 200 μL samples under each condition were used for retinoid analysis. It is worth mentioning that the light source of the monochromator was a xenon arc lamp, not a laser, so the "monochromatic" light was technically not composed of a single wavelength of photons, and is thus not 'real' monochromatic. The "monochromatic" light was measured by a spectroradiometer (Black-comet CXR-SR-50, StellarNet Inc) and the peak wavelength was reported as the wavelength of the light. The bandwidth of the monochromatic light was within 20 nm in most cases (except for UV light close to 325 nm, which may be a bit wider). Due to the current technical challenges to obtain "real monochromatic light" at multiple wavelengths and

to accurately quantitate the photon flux or energy, errors exist in the measurements of wavelengths and intensities of the light used in our experiments.

3.1.4.5 Photoisomerization of retinoids in liposomes under different light conditions.

For photoisomerization of N-ret-PE in liposomes of brain polar lipids under laboratory room light (**Fig.3.1-4**), N-ret-PE (final concentration 10 μM) was delivered in TFA acidified methanol (<3.5% of total volume) to liposomes of 2 mg/ml brain polar lipids in PBS pH 7.2. Samples were either kept in the dark or placed into cuvettes covered in aluminum foil except for the front sides which were placed behind a 400-nm cut-on glass filter (Newport, FSQ-GG400, same below) and exposed to laboratory room light (white, everyday light condition, intensity undefined). The dark/light treatments were performed at RT for 15 minutes with agitation. Three replicates of 200 μL samples from each condition were used for retinoid analysis.

For photoisomerization of N-ret-PE in liposomes of brain polar lipids under a strobe light **(Fig.3.1-5)**, N-ret-PE (final concentration 10 μM) was delivered in acidified methanol (~ 1% of total volume) to liposomes of 2 mg/ml brain polar lipids in PBS pH 7.2. The N-ret-PE containing liposomes were placed in black paper-covered (except the front side) cuvettes behind a 400-nm cut-on glass filter and exposed to zero (dark) to five flashes of a 750-watt strobe light at about one meter away. Two replicates of 200 μL samples from each condition were used for retinoid analysis.

For the comparison of all-*trans*-retinal photoisomerization in liposomes of 100% DOPC or 65% DOPC/35% DOPE (mol %) **(Fig.3.1-6)**, all-*trans*-retinal (final concentration 10 μM) was delivered in ethanol (<0.5% of total volume) to each type of liposomes containing 1 mM total lipids in PBS, pH 6.5. Samples were either kept in the dark or exposed to the monochromatic light of 375 nm (at 0.30 W/m^2) or 450 nm (at 0.25 W/m^2) with the same photon flux for 80 seconds at RT (same method as described in "action spectrum of at-N-ret-PE" in (Kaylor, Xu et al. 2017)). Three replicates of 200 μL samples of each condition were used for retinoid analysis after the treatment.

3.1.4.6 The inhibitory effects of spin traps/probes on the retinoid isomerization induced by iodine or light

For the inhibition test of iodine-catalyzed all-*trans*-retinal thermal isomerization **(Fig.3.1-7)**, 10 μM all-*trans*-retinal ± 1 mM spin traps/probes were dissolved in *n*-heptane (Sigma-Aldrich) and kept on ice. 2.5 μM iodine (I_2) in heptane (or an equal volume of heptane for no iodine control) was added subsequently to initiate the isomerization. After mixing, samples at 0-minute time point were immediately quenched by mixing 20 μL of 2 M NaS_2O_3 with each 200 μL reaction mixture. Samples at the 10-minute time point were incubated at 37 ºC in a water bath for 10 minutes, followed by immediately moved onto ice and quenched with the same method. The quenched reaction mixtures were dried under a strong stream of nitrogen gas for at least 15 minutes, followed by resuspension with 200 μL methanol. The methanol resuspensions were then treated with 200 μL of 2 M hydroxylamine hydrochloride and 50 μL brine, extracted and analyzed for retinoid contents as described above.

For the inhibition test of all-*trans*-retinal photoisomerization **(Fig.3.1-8)**, samples containing 10 μM all-*trans*-retinal ± 1 mM spin traps/probes were dissolved in methanol and exposed to monochromatic light of 380 nm at 0.1 W/m^2 in black paper-covered (except front side) cuvettes for 0 (dark control), 1, 3 or 9 minutes at RT. Three replicates of 200 μL samples from each condition were used for retinoid analysis.

For the inhibition of at-N-ret-PE photoisomerization **(Fig.3.1-9)**, equal volumes of 20 μM protonated at-N-ret-PE in acidified methanol (20 μL TFA per liter methanol) and 2 mM spin traps/probes in methanol (or methanol only for the controls) were mixed to reach a final concentration of 10 μM at-N-ret-PE ± 1 mM spin traps/probes shortly before light exposure. Samples were exposed to monochromatic light of 450 nm at 0.14 W/m^2 for 0 (dark control), 1,2 or 4 minutes in black paper-covered (except front side) cuvettes at RT. Three replicates of 200 μL samples from each condition were used for retinoid analysis. The photoisomerization activity was represented by the formation of the 11-*cis*-isomer.

The spin trap/probes used in these studies included: 4-hydroxy-2,2,6,6-tetramethylpiperidine-1-oxyl (4-hydroxy-TEMPO) (Aldrich); 5,5-dimethyl-1-pyrroline-N-oxide (DMPO) (Sigma); 2,2-dimethyl-4-phenyl-2H-imidazole-1-oxide (DMPIO) (Enzo Life Sciences and Alexis Biochemicals); N-tert-butyl-α-phenylnitrone (PBN) (Sigma) and 4-phenyl-2,2,5,5-tetramethyl-3-imidazoline-1-oxyl nitroxide (PTMIO) (Enzo Life Sciences).

3.1.4.7 Action spectrum analysis of all-*trans*-retinal and N-ret-PE

10 μM all-*trans*-retinal was dissolved in regular methanol. 10 μM all-*trans*-*N*-ret-PE was dissolved in alkalized (0.4 g sodium hydroxide (EM Science) per liter methanol) or acidified methanol (20 μL TFA per liter methanol) to maintain the non-protonated or protonated form, respectively. Concentrations of both were determined in their protonated form with a molar extinction coefficient of 31,300 $M^{-1}cm^{-1}$ (Anderson and Maude 1970) (the concentration of non-protonated N-ret-PE was determined before the replacement of the solvent from acidified methanol to alkalized methanol). The rest of the action spectrum studies were performed using the same method as described (Kaylor, Xu et al. 2017). For the action spectrum of all-*trans*-retinal, minor amounts of UV light contamination might be present in monochromatic light above 550 nm, possibly caused by second-harmonic generation from the light source.

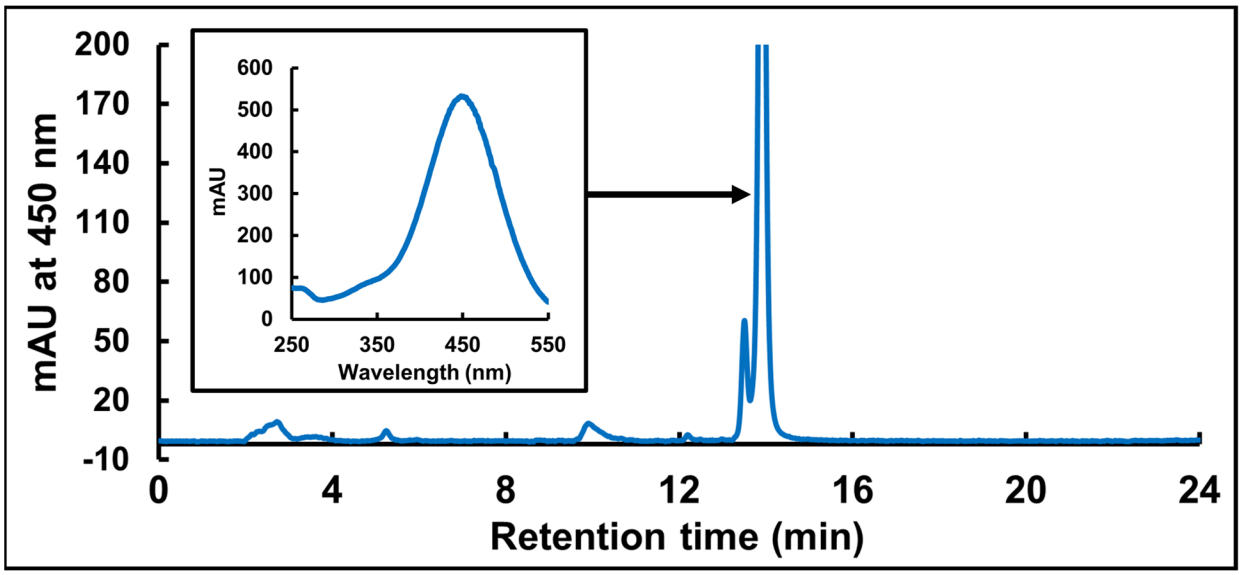

Figure 3.1-1. A representative reverse-phase HPLC chromatogram for at-N-ret-PE purification. At-N-ret-PE was dissolved in acidified methanol and purified in its protonated form by reverse-phase HPLC. Its retention time is about 14 minutes. Its UV-vis spectrum is shown in the inset.

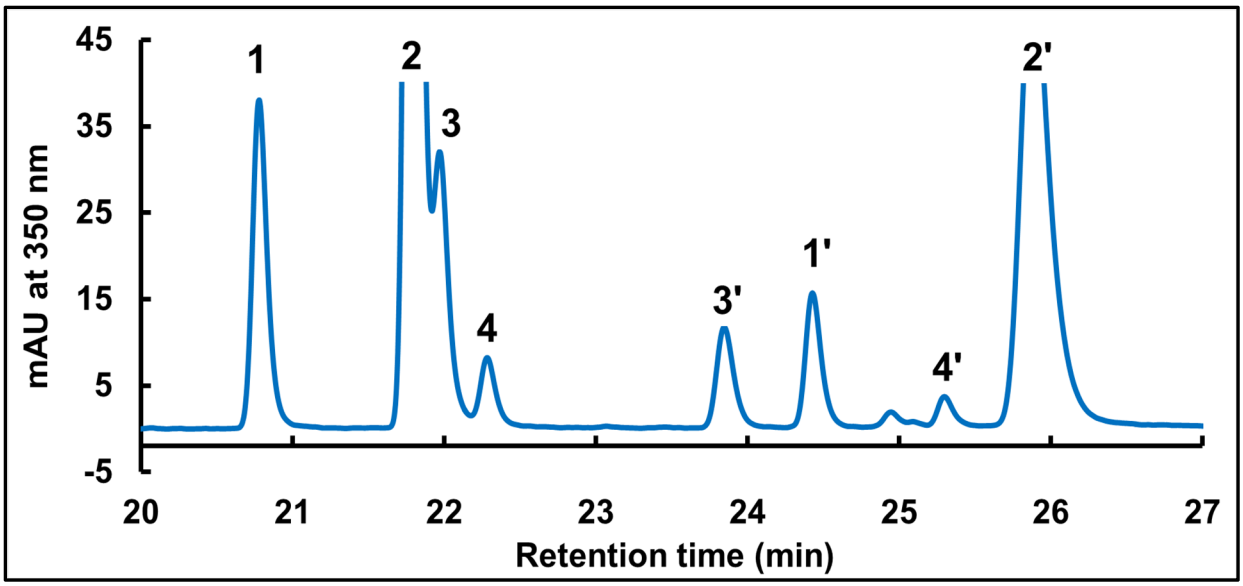

Figure 3.1-2. A representative normal-phase HPLC chromatogram for the analysis of retinaldehyde oximes. For the analysis of retinaldehydes (retinals) or N-ret-PEs, stable retinaldehyde oximes (ROX) were made by oximation of samples with hydroxylamine and quantitated by normal-phase HPLC. The corresponding *syn*-oximes and *anti*-oximes were summed to quantitate each retinaldehyde (retinal) or N-ret-PE isomer unless otherwise indicated. A representative chromatogram is presented with peak identities. Peak 1: *syn*-11-*cis*-ROX, Peak 2: *syn*-all-*trans*-ROX, Peak 3: *syn*-13-*cis*-ROX, Peak 4: *syn*-9-*cis*-ROX, Peak 1': *anti*-11-*cis*-ROX, Peak 2': *anti*-all-*trans*-ROX, Peak 3': *anti*-13-*cis*-ROX, Peak 4': *anti*-9-*cis*-ROX. It should be noted that under certain conditions, some ROXs may partially co-elute with others, especially peaks 2 and 3, introducing errors for the analysis. In case of low retinoid abundance, significant quantitation inaccuracy may occur due to technical limitations. ROXs were quantitated by peak areas under the curve (in mAU) and converted to picomoles in some experiments (as indicated) using calibration curves obtained from ROX standards (Kaylor, Yuan et al. 2013, Kaylor, Xu et al. 2017). The calibration curves may artificially introduce a small number of picomoles (usually below five) in certain cases even if the raw peak area was zero. When data are presented, such small numbers may be included. However, they do not affect the interpretation of the results.

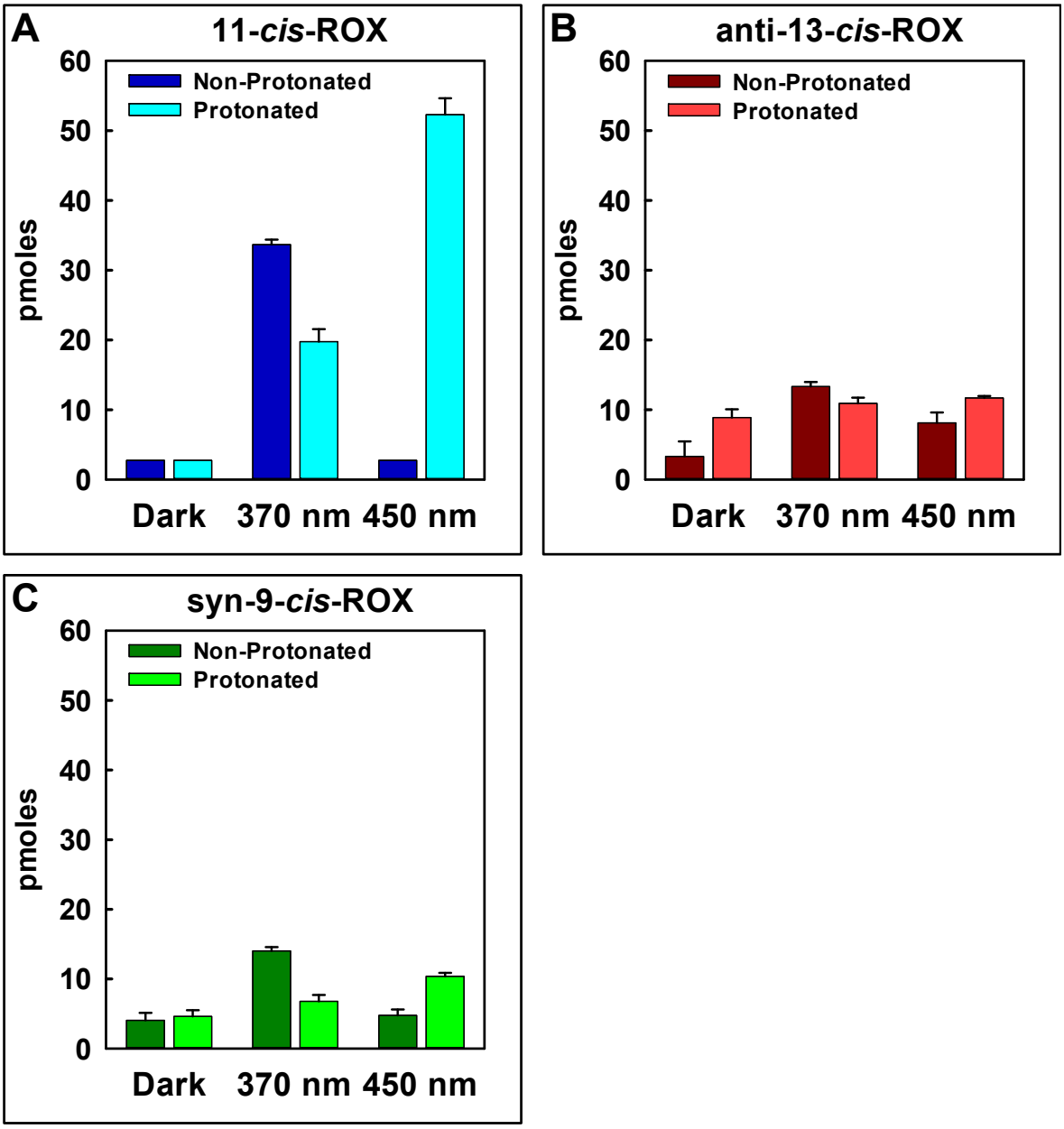

Figure 3.1-3. Photoisomerization of non-protonated and protonated N-ret-PE in methanol. Non-protonated or protonated forms of N-ret-PE dissolved in alkalized or acidified methanol respectively were exposed to monochromatic light at 370 nm, 450 nm or kept in the dark. The formation of 11-*cis*-ROX (quantitated from both *syn*- and *anti*-11-cis-ROX) **(A)**, *anti*-13-*cis*-ROX **(B)** and *syn*-9-*cis*-ROX **(C)** were quantitated. The *syn*-13-*cis*-ROX or *anti*-9-*cis*-ROX was not quantitated due to technical difficulties, but the total amounts of 13-*cis*- and 9-*cis*-ROX could be roughly estimated from the *anti*-13-*cis*-ROX and *syn*-9-*cis*-ROX. The *syn*-ROX usually accounts for 50-80% of the total ROXs of the same isomer, with the rest the *anti*-ROX, in most of our experience. Also, the ratio of *syn*-/*anti*-ROX of the same isomer was usually unchanged in the same experiment. Data were plotted as Mean ± S.D., n=3.

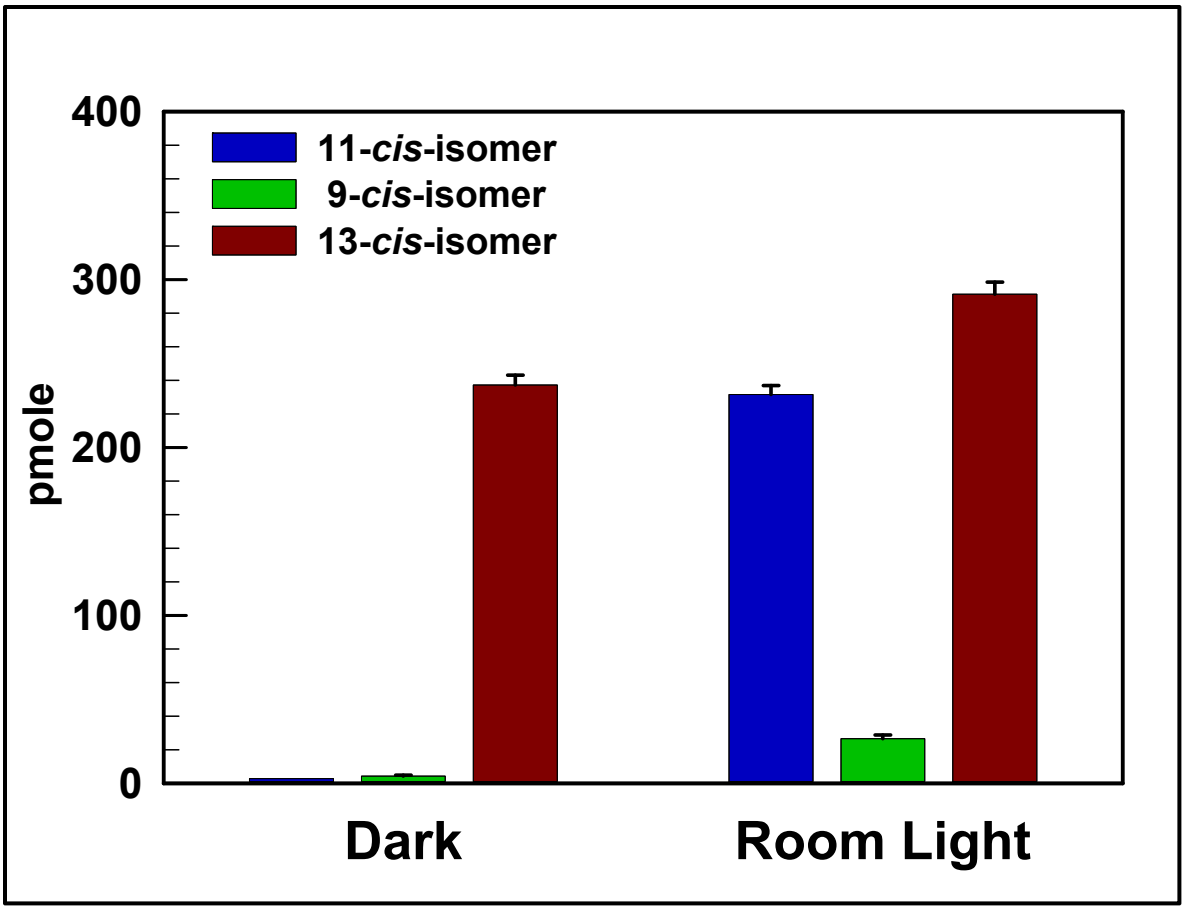

Figure 3.1-4. Photoisomerization of N-ret-PE in liposomes under room light. Purified at-N-ret-PE was delivered in acidified methanol to liposomes of porcine brain polar lipids in PBS, pH 7.2. The liposomes were either kept in the dark or exposed to UV-filtered laboratory room light for 15 minutes at RT. The formation of *cis*-isomers (could be in the form of either free retinal or N-ret-PE) was quantitated. Note the significant formation of 11-*cis*-isomer after light exposure. Data were plotted as Mean ± S.D., n=3.

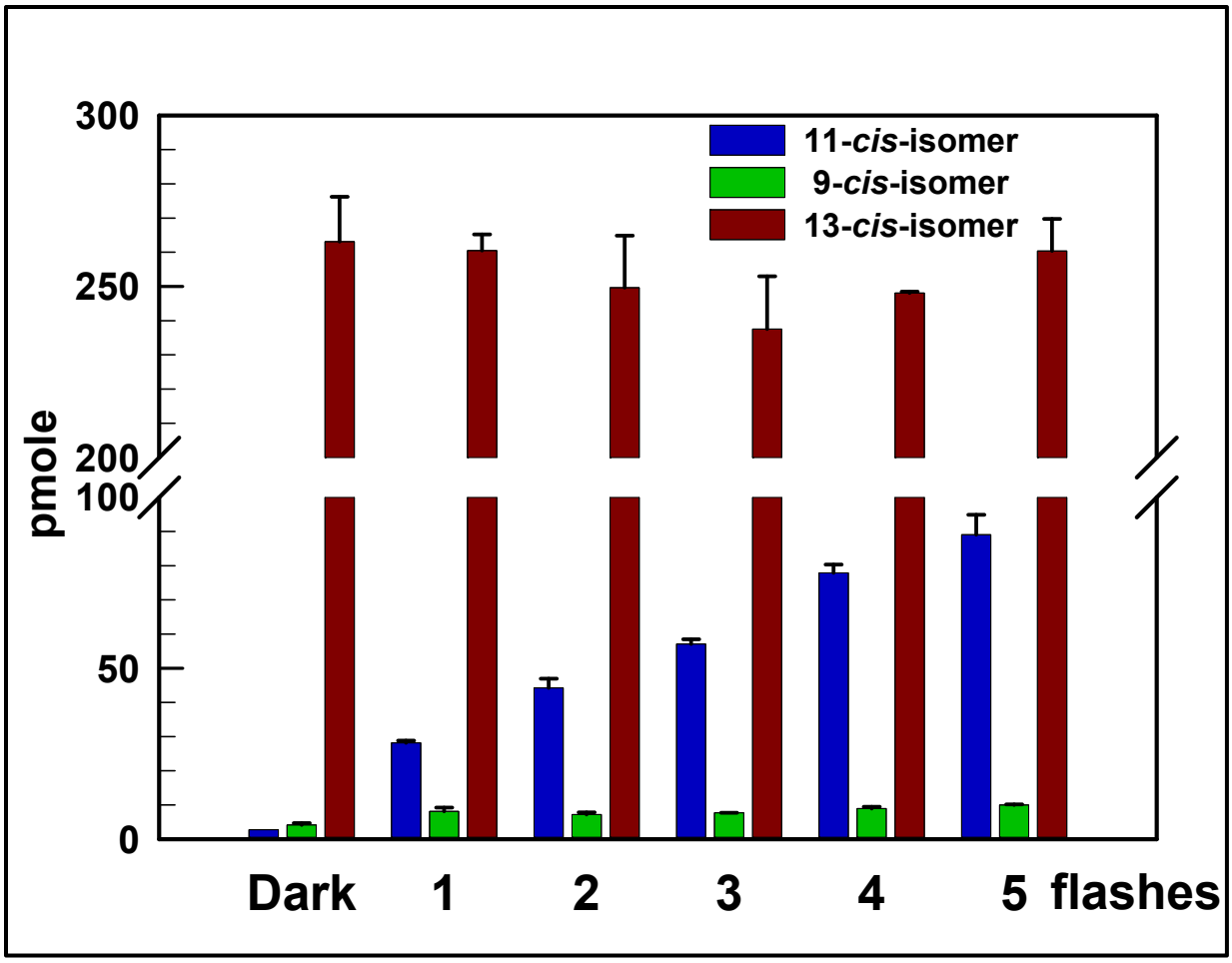

Figure 3.1-5. Photoisomerization of N-ret-PE in liposomes exposed to strobe light. Purified at-N-ret-PE was delivered in acidified methanol to liposomes of porcine brain polar lipids in PBS, pH 7.2. The liposomes were either kept in the dark or exposed to a 750-watt strobe light for up to five flashes. The formation of *cis*-isomers was quantitated. For the 9-*cis*-isomer, only *syn*-9-*cis*-ROX was quantitated (the *anti*-9-*cis*-ROX was too low to be confidently quantitated). Note the significant increase of 11-*cis*-isomer with the increase of flashes. Data were plotted as Mean ± S.D., n=2.

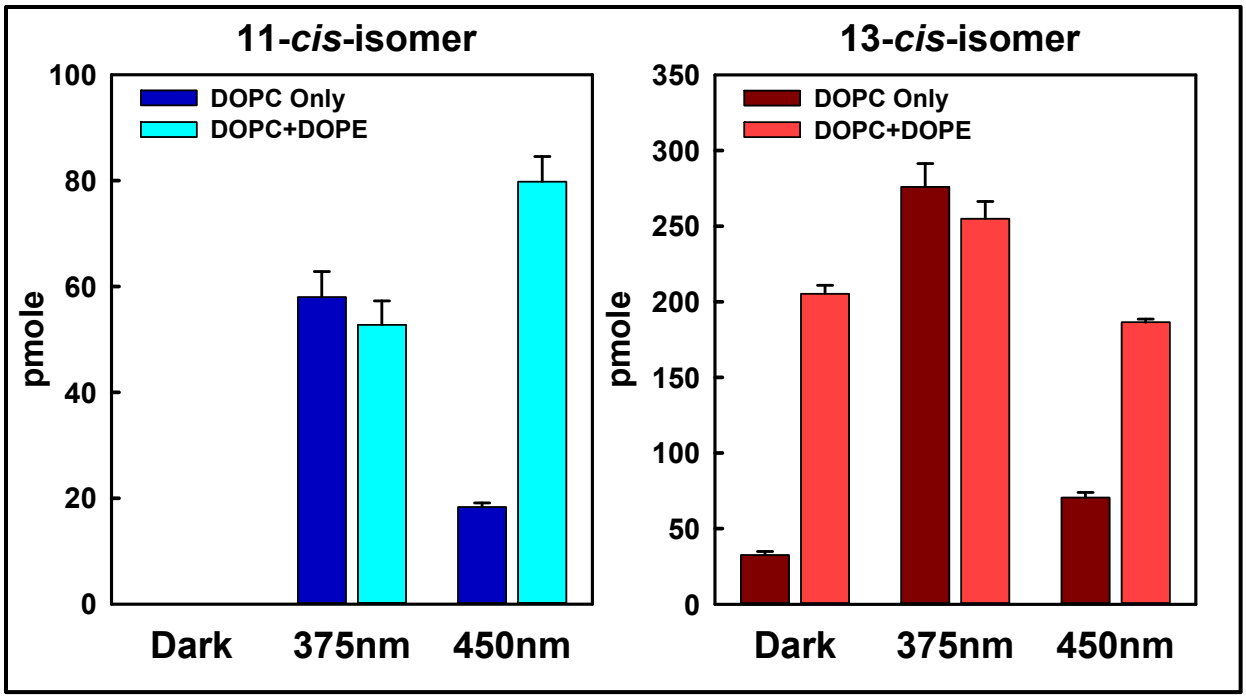

Figure 3.1-6. Photoisomerization of all-*trans*-retinal in liposomes of 100% DOPC or 65% DOPC/35% DOPE. All-*trans*-retinal was delivered in ethanol to liposomes of 100% DOPC (DOPC Only) or 65% DOPC/35% DOPE (DOPC+DPOE) in PBS, pH 6.5. These liposomes were either kept in the dark or exposed to monochromatic light of 375 nm or 450 nm with the same photon flux for 80 seconds at RT. The dominant *cis*-isomers, 11-*cis*- and 13-*cis*-isomers, were quantitated (the 13-*cis*-ROX might contain a minor amount of 9-*cis*-ROX). Note the difference of all-*trans*-retinal photoisomerization in the different types of liposomes. Data were plotted as Mean ± S.D., n=3.

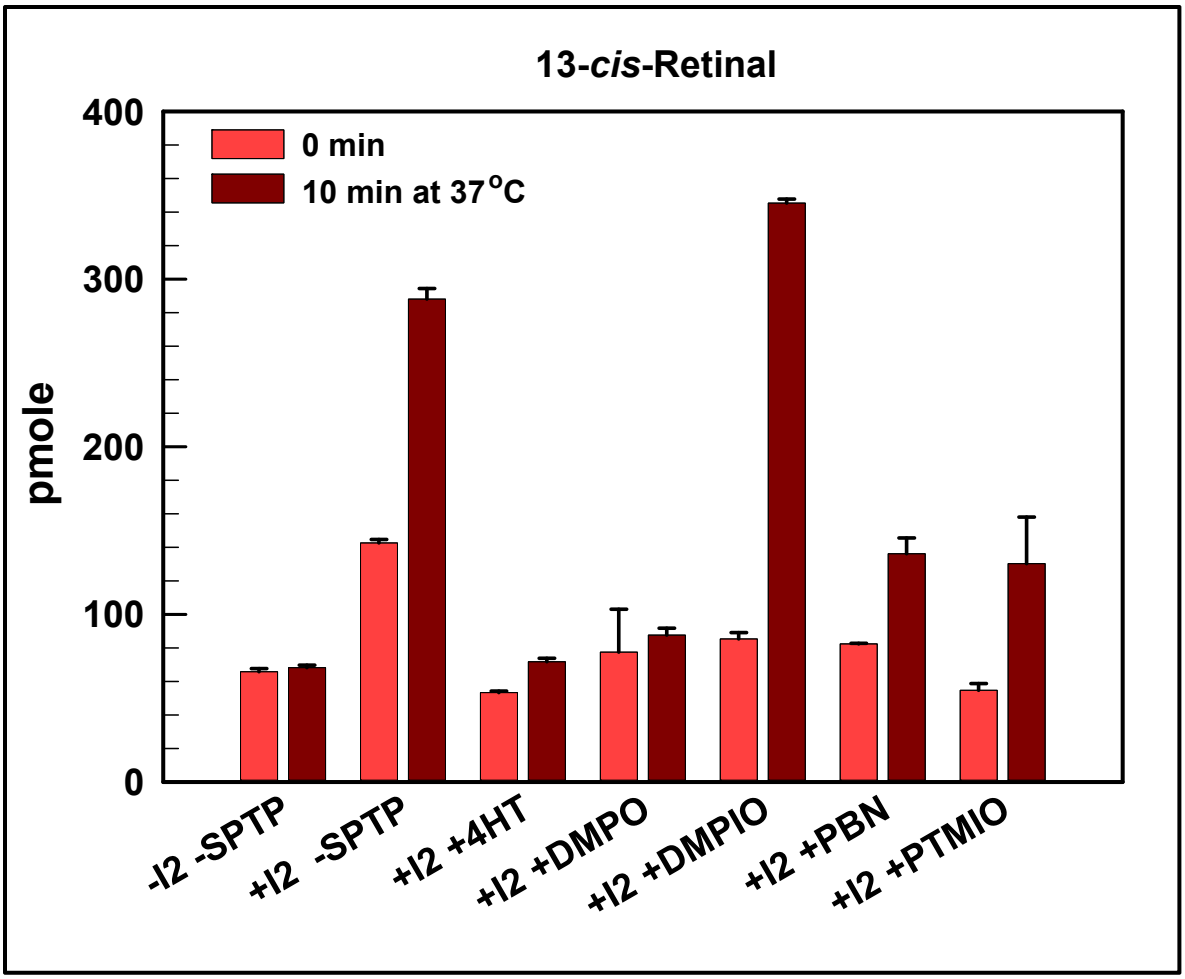

Figure 3.1-7. Iodine-catalyzed all-*trans*-retinal isomerization was inhibited by spin trap/probe reagents. All-*trans*-retinal dissolved in *n*-heptane was incubated at 37 ºC for 0 or 10 minutes with (+I_2) or without (-I_2) iodine in the absence (-SPTP) or presence of 1 mM spin traps/probes reagents, including 4-hydroxy-TEMPO (4HT), DMPO, DMPIO, PBN or PTMIO, as indicated. The isomerization rate was represented by the formation of 13-*cis*-retinal. Data were plotted as Mean ± S.D., n=3.

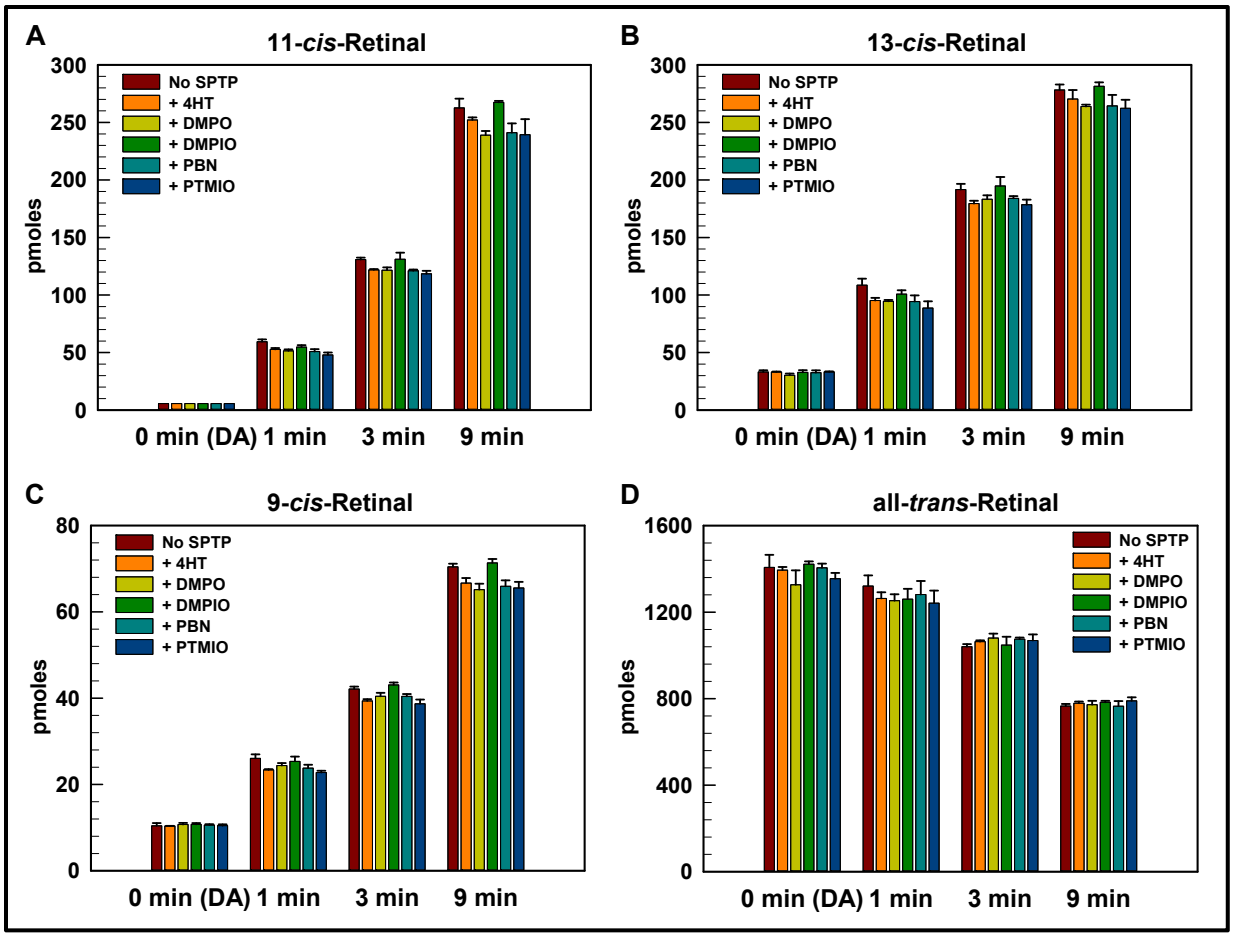

Figure 3.1-8. Photoisomerization of all-*trans*-retinal was largely not inhibited by the spin traps/probe reagents tested. Inhibition of photoisomerization of all-*trans*-retinal was tested in the absence (No SPTP) or presence of 1 mM indicated spin traps/probes reagents. Samples were exposed to monochromatic light of 380 nm at RT for 0 (kept in the dark), 1, 3 and 9 minutes as indicated. The 11-*cis*- **(A)**, 13-*cis*- **(B)**, 9-*cis*- **(C)** and all-*trans*-isomers **(D)** were quantitated. In general, there seemed to be no significant inhibition of the light-dependent formation of *cis*-isomers by these spin trap/probe reagents. The substrate, all-*trans*-retinal, showed a time-dependent depletion **(D)** and corresponds to the formation of *cis*-isomers **(A-C)**. Data were plotted as Mean ± S.D., n=3.

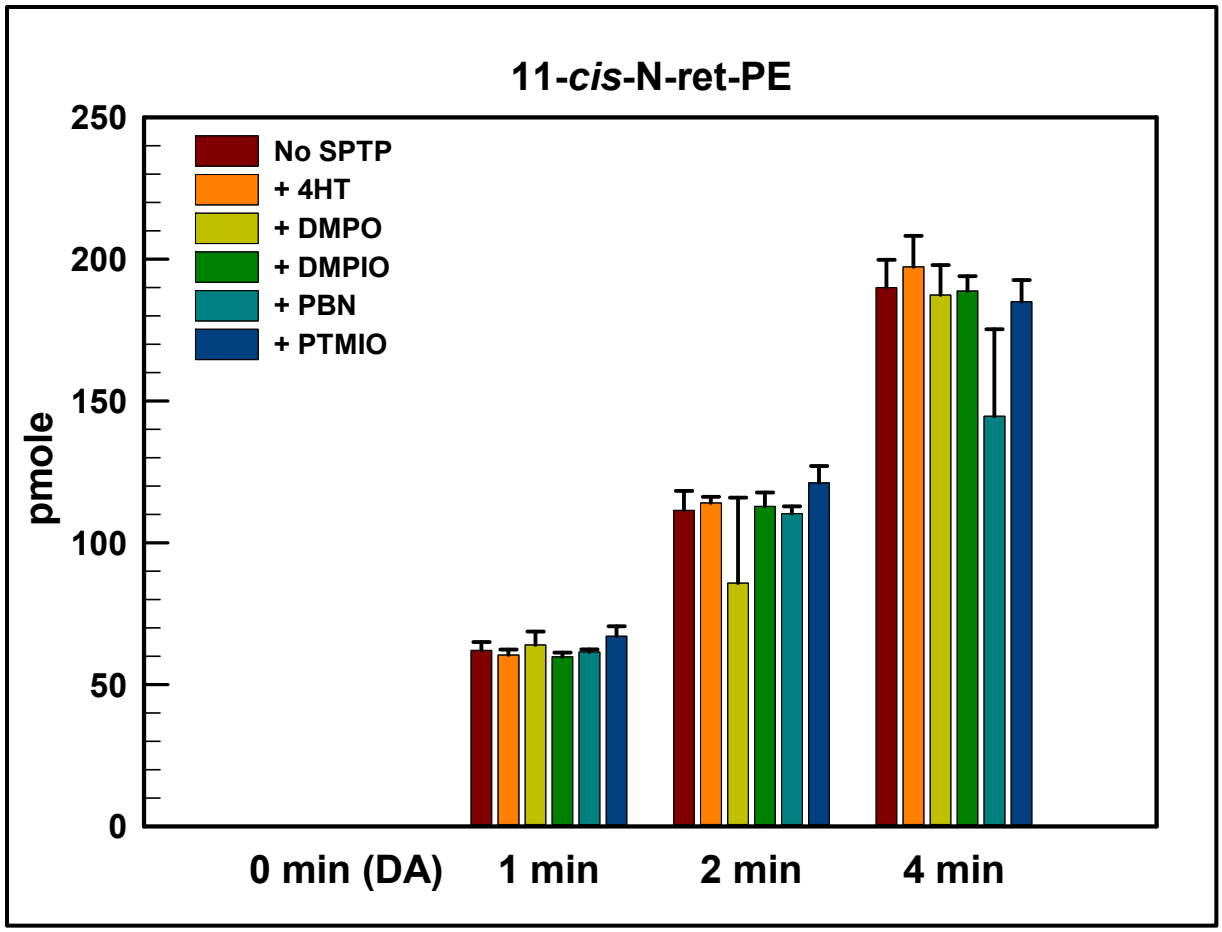

Figure 3.1-9. Photoisomerization of protonated at-N-ret-PE was largely not inhibited by the spin traps/probe reagents tested. At-N-ret-PE with or without (No SPTP) 1 mM indicated spin traps/probes in acidified methanol were exposed to monochromatic light of 450 nm at RT for 0 (kept in the dark), 1, 2 and 4 minutes. The dominant *cis*-isomer formed in photoisomerization, 11-*cis*-isomer, was quantitated. There seemed to be no significant inhibition of photoisomerization by the tested spin trap/probe agents. Data were plotted as Mean ± S.D., n=3.

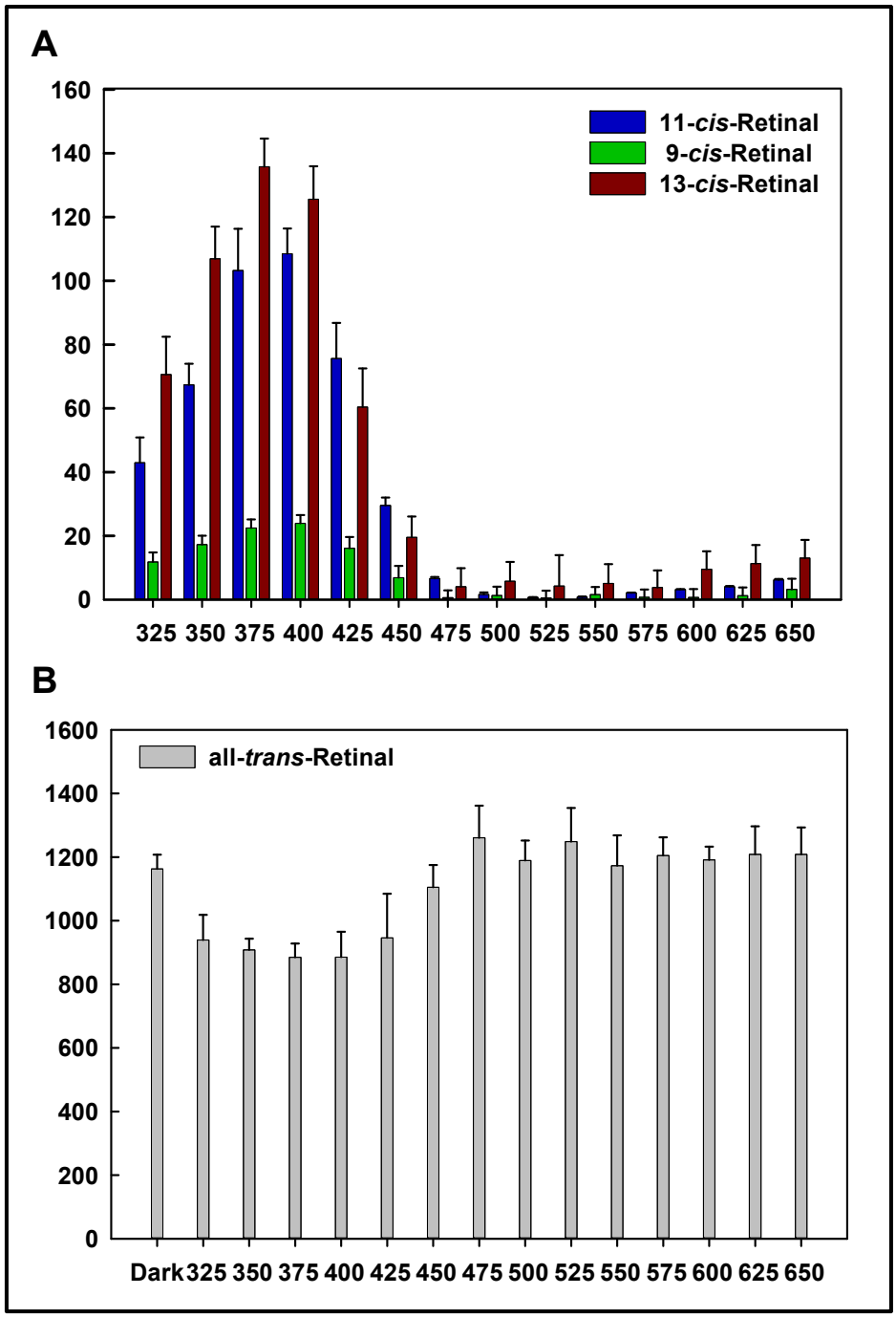

Figure 3.1-10. Action spectrum of all-*trans*-retinal photoisomerization. All-*trans*-retinal in methanol was either kept in the dark or exposed to monochromatic light from 325 nm to 650 nm as indicated with the same photon flux at RT for 80 seconds. The formation of the *cis*-isomers **(A)** and the amount of the all-*trans*-retinal substrate **(B)** after the treatment were quantitated. The background level of each *cis*-isomer in the dark was subtracted in **(A)**. Data were plotted as Mean ± S.D., n=3. The S.D. of the samples in the dark was included in the error propagations of the samples exposed to light in **(A)**.

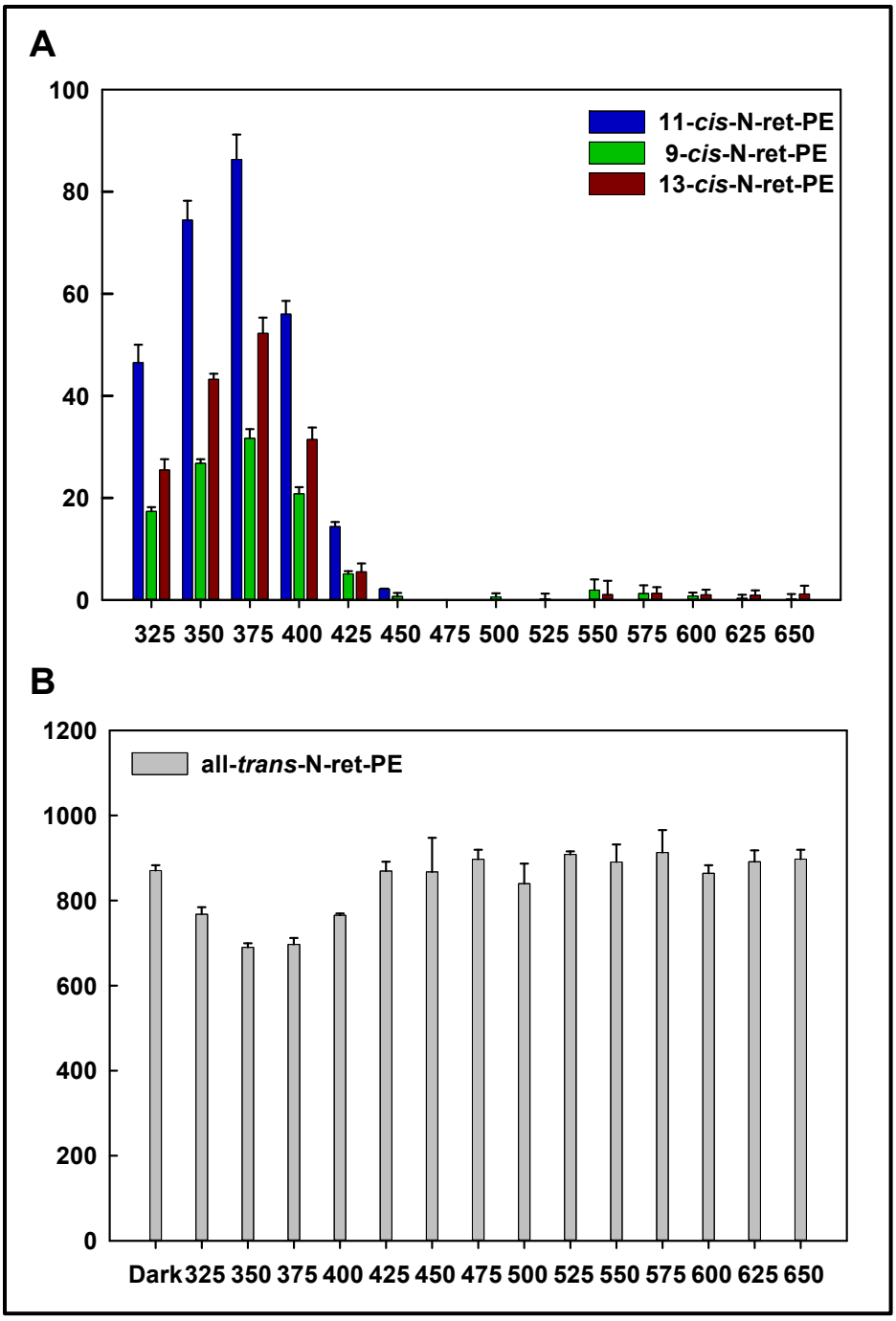

Figure 3.1-11. Action spectrum of non-protonated N-ret-PE photoisomerization. Non-protonated N-ret-PE in alkalized methanol was either kept in the dark or exposed to monochromatic light from 325 nm to 650 nm as indicated with the same photon flux at RT for 80 seconds. The formation of the *cis*-isomers **(A)** and the amount of the all-*trans*-N-ret-PE substrate **(B)** after treatment were quantitated. The background level of each *cis*-isomer in the dark was subtracted in **(A)**. Data were plotted as Mean ± S.D., n=3. The S.D. of the samples in the dark was included in the error propagations of the samples exposed to light in **(A)**.

References

Anderson, R. E. and M. B. Maude (1970). "Phospholipids of bovine outer segments." Biochemistry **9**(18): 3624-3628.

Arnis, S. and K. P. Hofmann (1995). "Photoregeneration of bovine rhodopsin from its signaling state." Biochemistry **34**(29): 9333-9340.

Beharry, S., M. Zhong and R. S. Molday (2004). "N-retinylidene-phosphatidylethanolamine is the preferred retinoid substrate for the photoreceptor-specific ABC transporter ABCA4 (ABCR)." J Biol Chem **279**(52): 53972-53979.

Benson, S. W., K. W. Egger and D. M. Golden (1965). "Iodine-Catalyzed Isomerization of Olefins .3. Kinetics of Geometrical Isomerization of Butene-2 and Rate of Rotation About a Single Bond." Journal of the American Chemical Society **87**(3): 468-&.

Boettner, E. A. and J. R. Wolter (1962). "Transmission of the Ocular Media." Investigative Ophthalmology **1**(6): 776-783.

Brown, P. K. and G. Wald (1956). "The neo-b isomer of vitamin A and retinene." J Biol Chem **222**(2): 865-877.

Denny, M., M. Chun and R. S. H. Liu (1981). "9-Cis,11-Cis-Retinal from Direct Irradiation of All-Trans-Retinal - New Geometric Isomers of Vitamin-a and Carotenoids 9." Photochemistry and Photobiology **33**(2): 267-269.

Deval, P. and A. K. Singh (1988). "Photoisomerization of All-Trans-Retinal in Organic-Solvents and Organized Media." Journal of Photochemistry and Photobiology a-Chemistry **42**(2-3): 329-336.

Filipek, S., R. E. Stenkamp, D. C. Teller and K. Palczewski (2003). "G protein-coupled receptor rhodopsin: a prospectus." Annu Rev Physiol **65**: 851-879.

Fliesler, S. J. and R. E. Anderson (1983). "Chemistry and metabolism of lipids in the vertebrate retina." Prog Lipid Res **22**(2): 79-131.

Furutani, Y., H. Kandori and Y. Shichida (2003). "Structural changes in lumirhodopsin and metarhodopsin I studied by their photoreactions at 77 K." Biochemistry **42**(28): 8494-8500.

Grimm, C., C. E. Reme, P. O. Rol and T. P. Williams (2000). "Blue light's effects on rhodopsin: photoreversal of bleaching in living rat eyes." Invest Ophthalmol Vis Sci **41**(12): 3984-3990.

Groenendijk, G. W., C. W. Jacobs, S. L. Bonting and F. J. Daemen (1980). "Dark isomerization of retinals in the presence of phosphatidylethanolamine." Eur J Biochem **106**(1): 119-128.

Hepperle, S. S., Q. Li and A. L. East (2005). "Mechanism of cis/trans equilibration of alkenes via iodine catalysis." J Phys Chem A **109**(48): 10975-10981.

Hubbard, R. and G. Wald (1952). "Cis-trans isomers of vitamin A and retinene in the rhodopsin system." J Gen Physiol **36**(2): 269-315.

Kaylor, J. J., J. D. Cook, J. Makshanoff, N. Bischoff, J. Yong and G. H. Travis (2014). "Identification of the 11-cis-specific retinyl-ester synthase in retinal Muller cells as multifunctional O-acyltransferase (MFAT)." Proc Natl Acad Sci U S A **111**(20): 7302-7307.

Kaylor, J. J., T. Xu, N. T. Ingram, A. Tsan, H. Hakobyan, G. L. Fain and G. H. Travis (2017). "Blue light regenerates functional visual pigments in mammals through a retinyl-phospholipid intermediate." Nat Commun **8**(1): 16.

Kaylor, J. J., Q. Yuan, J. Cook, S. Sarfare, J. Makshanoff, A. Miu, A. Kim, P. Kim, S. Habib, C. N. Roybal, T. Xu, S. Nusinowitz and G. H. Travis (2013). "Identification of DES1 as a vitamin A isomerase in Muller glial cells of the retina." Nat Chem Biol **9**(1): 30-36.

Koyama, Y., K. Kubo, M. Komori, H. Yasuda and Y. Mukai (1991). "Effect of protonation on the isomerization properties of n-butylamine Schiff base of isomeric retinal as revealed by direct HPLC analyses: selection of isomerization pathways by retinal proteins." Photochem Photobiol **54**(3): 433-443.

Lamb, T. D. (2009). "Evolution of vertebrate retinal photoreception." Philos Trans R Soc Lond B Biol Sci **364**(1531): 2911-2924.

Lamb, T. D. (2013). "Evolution of phototransduction, vertebrate photoreceptors and retina." Progress in Retinal and Eye Research **36**: 52-119.

Laube, T., H. Apel and H. R. Koch (2004). "Ultraviolet radiation absorption of intraocular lenses." Ophthalmology **111**(5): 880-885.

Leenheer, A. P. d., W. E. Lambert and J. F. Van Bocxlaer (2000). Modern chromatographic analysis of vitamins. New York, Marcel Dekker.

Liu, R. S. H. and A. E. Asato (1984). "Photochemistry and Synthesis of Stereoisomers of Vitamin-A." Tetrahedron **40**(11): 1931-1969.

MacDonald, R. C., R. I. MacDonald, B. P. Menco, K. Takeshita, N. K. Subbarao and L. R. Hu (1991). "Small-volume extrusion apparatus for preparation of large, unilamellar vesicles." Biochim Biophys Acta **1061**(2): 297-303.

Manathunga, M., X. Yang, Y. Orozco-Gonzalez and M. Olivucci (2017). "Impact of Electronic State Mixing on the Photoisomerization Time Scale of the Retinal Chromophore." J Phys Chem Lett: 5222-5227.

Mata, N. L., R. A. Radu, R. C. Clemmons and G. H. Travis (2002). "Isomerization and oxidation of vitamin a in cone-dominant retinas: a novel pathway for visual-pigment regeneration in daylight." Neuron **36**(1): 69-80.

Nakanishi, K. (1991). "Why 11-Cis-Retinal." American Zoologist **31**(3): 479-489.

Okada, T., O. P. Ernst, K. Palczewski and K. P. Hofmann (2001). "Activation of rhodopsin: new insights from structural and biochemical studies." Trends Biochem Sci **26**(5): 318-324.

Pitt, G. A., F. D. Collins, R. A. Morton and P. Stok (1955). "Studies on rhodopsin. VIII. Retinylidenemethylamine, an indicator yellow analogue." Biochem J **59**(1): 122-128.

Poincelot, R. P., P. G. Millar, R. L. Kimbel, Jr. and E. W. Abrahamson (1969). "Lipid to protein chromophore transfer in the photolysis of visual pigments." Nature **221**(5177): 256-257.

Poliakov, E., T. Parikh, M. Ayele, S. Kuo, P. Chander, S. Gentleman and T. M. Redmond (2011). "Aromatic lipophilic spin traps effectively inhibit RPE65 isomerohydrolase activity." Biochemistry **50**(32): 6739-6741.

Quazi, F., S. Lenevich and R. S. Molday (2012). "ABCA4 is an N-retinylidene-phosphatidylethanolamine and phosphatidylethanolamine importer." Nat Commun **3**: 925.

Rando, R. R. and A. Chang (1983). "Studies on the Catalyzed Interconversions of Vitamin-a Derivatives." Journal of the American Chemical Society **105**(9): 2879-2882.

Shichi, H. and R. L. Somers (1974). "Possible involvement of retinylidene phospholipid in photoisomerization of all-trans-retinal to 11-cis-retinal." J Biol Chem **249**(20): 6570-6577.

Szuts, E. Z. and F. I. Harosi (1991). "Solubility of retinoids in water." Arch Biochem Biophys **287**(2): 297-304.

Wald, G. (1968). "Molecular basis of visual excitation." Science **162**(3850): 230-239.

Wang, J. S., M. E. Estevez, M. C. Cornwall and V. J. Kefalov (2009). "Intra-retinal visual cycle required for rapid and complete cone dark adaptation." Nat Neurosci **12**(3): 295-302.

Williams, T. P. (1964). "Photoreversal of Rhodopsin Bleaching." J Gen Physiol **47**: 679-689.

Zhong, M., R. Kawaguchi, M. Kassai and H. Sun (2012). "Retina, retinol, retinal and the natural history of vitamin A as a light sensor." Nutrients **4**(12): 2069-2096.

3.2 Blue light regenerates functional visual pigments in mammals through a retinyl-phospholipid intermediate

This section is a reprint of the publication: Joanna J. Kaylor, Tongzhou Xu, Norianne T. Ingram, Avian Tsan, Hayk Hakobyan, Gordon L. Fain and Gabriel H. Travis (2017). Blue light regenerates functional visual pigments in mammals through a retinyl-phospholipid intermediate. *Nat Commun*. 8(1):16. doi:10.1038/s41467-017-00018-4. Author contributions are listed on the Acknowledgement page of this dissertation.

nature COMMUNICATIONS

ARTICLE

DOI: 10.1038/s41467-017-00018-4 OPEN

Blue light regenerates functional visual pigments in mammals through a retinyl-phospholipid intermediate

Joanna J. Kaylor[1], Tongzhou Xu[1,2], Norianne T. Ingram[1,2], Avian Tsan[1], Hayk Hakobyan[1], Gordon L. Fain[1,3] & Gabriel H. Travis[1,4]

The light absorbing chromophore in opsin visual pigments is the protonated Schiff base of 11-*cis*-retinaldehyde (11cRAL). Absorption of a photon isomerizes 11cRAL to all-*trans*-retinaldehyde (atRAL), briefly activating the pigment before it dissociates. Light sensitivity is restored when apo-opsin combines with another 11cRAL to form a new visual pigment. Conversion of atRAL to 11cRAL is carried out by enzyme pathways in neighboring cells. Here we show that blue (450-nm) light converts atRAL specifically to 11cRAL through a retinyl-phospholipid intermediate in photoreceptor membranes. The quantum efficiency of this photoconversion is similar to rhodopsin. Photoreceptor membranes synthesize 11cRAL chromophore faster under blue light than in darkness. Live mice regenerate rhodopsin more rapidly in blue light. Finally, whole retinas and isolated cone cells show increased photosensitivity following exposure to blue light. These results indicate that light contributes to visual-pigment renewal in mammalian rods and cones through a non-enzymatic process involving retinyl-phospholipids.

[1] Jules Stein Eye Institute, University of California Los Angeles School of Medicine, Los Angeles, California 90095, USA. [2] Molecular, Cellular and Integrative Physiology Graduate Program, University of California Los Angeles School of Medicine, Los Angeles, California 90095, USA. [3] Department of Integrative Biology and Physiology, University of California Los Angeles School of Medicine, Los Angeles, California 90095, USA. [4] Department of Biological Chemistry, University of California Los Angeles School of Medicine, Los Angeles, California 90095, USA. Correspondence and requests for materials should be addressed to G.H.T. (email: travis@jsei.ucla.edu)

Light perception in metazoans is mediated by two types of photosensitive cells, rhabdomeric and ciliary photoreceptors. Both contain membranous structures filled with opsin pigments. Ciliary photoreceptors, such as human rods and cones, contain an outer segment (OS) comprising a stack of membranous disks. The first event in light perception is capture of a photon by an opsin pigment. The light-absorbing chromophore in most opsins is 11-*cis*-retinaldehyde (11cRAL) coupled to a lysine residue through a protonated Schiff-base linkage. Absorption of a photon isomerizes the 11cRAL to all-*trans*-retinaldehyde (atRAL), transiently converting the pigment to its active (metarhodopsin II/III) signaling state. In the rhabdomeric photoreceptors of insects, atRAL remains covalently coupled to the opsin following activation. Absorption of a second photon flips the atRAL back to 11cRAL, restoring light sensitivity through photoregeneration[1]. For this reason, rhabdomeric opsins are called bistable pigments. In bright light they flicker between signaling and light-sensitive forms.

The opsin pigments of ciliary photoreceptors decay following photoactivation to yield unliganded apo-opsin and free atRAL[2]. Ciliary opsins are hence called bleaching pigments. Immediately following photon absorption by a ciliary opsin, the resulting metarhodopsin I may absorb a second photon, converting the atRAL back to 11cRAL, and the pigment to its light sensitive state[3, 4]. Thus, during the first millisecond of the rhodopsin cycle, ciliary rhodopsin behaves as a bistable pigment. After deprotonation of the Schiff base with activation of the pigment, photoreversal no longer occurs[5, 6]. Photoreversal therefore contributes negligibly to pigment regeneration in ciliary photoreceptors. Light sensitivity is restored to apo-opsin when it combines with another 11cRAL to form rhodopsin. The conversion of atRAL back to 11cRAL is carried out by multi-step enzyme pathways in cells of the retinal pigment epithelium (RPE)[7] and Müller glial cells in the retina[8, 9, 10]. Thus, rods and cones rely on enzymatic reactions in neighboring cells to synthesize visual chromophore, and appear not to benefit from the faster photoregeneration employed by "lower" metazoan species. For sustained vision in daylight, ciliary photoreceptors must be supplied with fresh 11cRAL at a rate that matches the rate of chromophore consumption through photoisomerization of opsins.

Retinaldehydes are lipophilic with low aqueous solubility[11]. They are present at high concentrations in OS disk membranes, which serve as conduits for 11cRAL and atRAL flowing to and from the opsins. Opsin crystal structures show openings to the ligand-binding cavity between pairs of transmembrane helices[12, 13]. Retinaldehydes are thought to enter and exit the chromophore-binding site of opsin via these openings. In the disk bilayer, retinaldehydes rapidly and reversibly condense with phosphatidylethanolamine (PE) to form the retinyl-lipid, *N*-retinylidene-PE (*N*-ret-PE)[14, 15]. Importantly, it was previously shown that all-*trans*- (at-) *N*-ret-PE undergoes photoisomerization to 11-*cis*- (11c-) *N*-ret-PE in visible light[16], and that 11c-*N*-ret-PE transfers 11cRAL to apo-opsin[14, 17]. Photoregeneration of visual pigments has never been reported in vertebrates. It is currently thought that visual pigments in vertebrate photoreceptors are regenerated exclusively by the enzymatic visual cycles. Here, we show that mammalian photoreceptors possess a mechanism for light-driven regeneration of opsin pigments, employing *N*-ret-PE as a light-sensitive intermediate. This mechanism is distinct from both photoregeneration of bistable opsins in rhabdomeric photoreceptors and the enzymatic visual cycles in RPE and Müller cells of vertebrates.

Results

Photoisomerization of *N*-ret-PE. We synthesized at-*N*-ret-PE and determined its absorbance spectra in acidified or alkalized methanol. The maximum absorption wavelength (λ_{max}) of protonated at-*N*-ret-PE was 450 nm, while the λ_{max} of non-protonated at-*N*-ret-PE was 365 nm (Supplementary Fig. 1). The pK_a of *N*-ret-PE is 6.9[18]. Since the pH near the surface of biological membranes is approximately one pH-unit lower than the surrounding aqueous medium[19], most *N*-ret-PE is protonated in vivo. Non-protonated *N*-ret-PE probably contributes little to chromophore photoregeneration because of its low abundance, and because the optic media blocks transmission of light below 400 nm[20].

We tested whether *N*-ret-PE undergoes at-to-11c photoisomerization in light, as previously observed[16]. To this end, we exposed samples of protonated at-*N*-ret-PE to monochromatic light of wavelengths 325–650 nm for 80 s, each with a photon flux of 0.95 µmol photons/m^2 s. We determined the isomer composition of *N*-ret-PE for each wavelength by reacting the samples with hydroxylamine to form stable retinaldehyde oximes and quantitating by normal-phase liquid chromatography (LC).

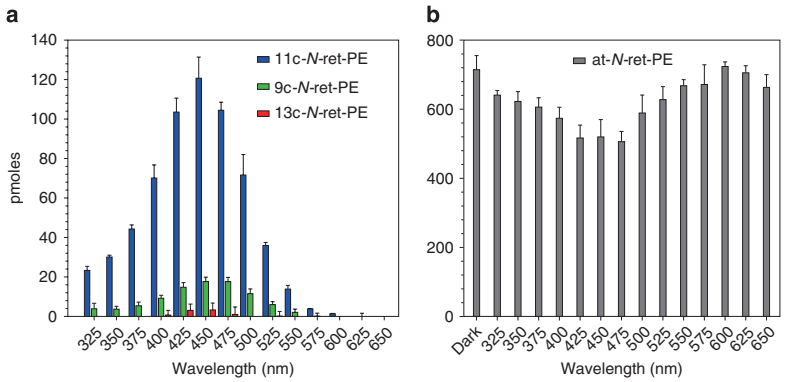

Fig. 1 Action spectrum for photoisomerization of protonated at-*N*-ret-PE. Protonated at-*N*-ret-PE in acidified methanol was incubated in the dark or under monochromatic light of the indicated wavelengths and the same photon flux. **a** Molar composition of 11c-, 9c- and 13c-*N*-ret-PE isomers following the incubation in light. The dark background level of each isomer was subtracted. Note the 37-fold higher level of 11c- versus 13c-*N*-ret-PE in the 450-nm samples. **b** Molar amounts of at-*N*-ret-PE remaining after incubation in the dark or in light of the indicated wavelengths. Data are plotted as mean ± s.d. ($n = 3$)

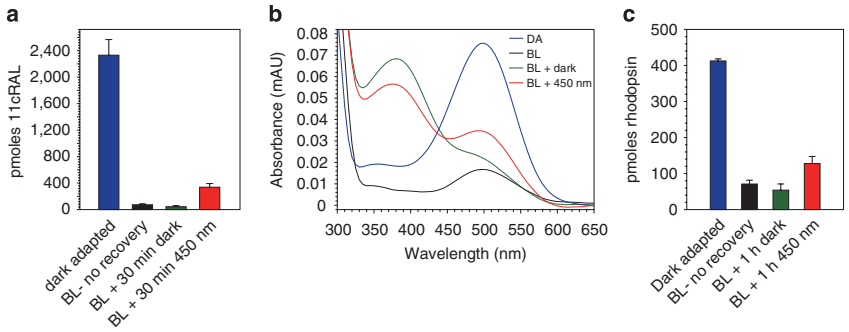

Fig. 2 Light-dependent regeneration of 11cRAL and rhodopsin in bovine OS. Aliquots of rod OS from dark-adapted bovine retinas were analyzed before and after a deep photobleach. After addition of atRAL, the remaining aliquots were incubated in the dark or in 450-nm light at 0.5 W/m^2 for the indicated times. **a** Levels of 11cRAL in dark-adapted (DA), immediate post-bleach (BL—no recovery), post-bleach plus 30 min incubation with atRAL in the dark (BL + 30 min dark), or post-bleach plus 30 min incubation with atRAL in 450-nm light (BL + 30 min 450 nm) OS. Data are plotted as mean ± s.d. ($n = 3$). **b** Representative UV-visible spectra of affinity-purified rhodopsin from bovine OS treated as described in panel **c**. The prominent 360-370-nm shoulders in the rhodopsin spectra from the (BL + 1 h dark) and (BL + 1 h. 450 nm) samples represent the added atRAL. **c** Levels of rhodopsin in bovine OS from dark-adapted bovine eyes (DA), immediately following a photobleach (BL - no recovery), incubated for 1 h in the dark with atRAL following the photobleach (BL + 1 h dark), or incubated for 1 h in 450-nm light with atRAL following the photobleach (BL + 1 h 450 nm). Data are plotted as mean ± s.d. ($n = 3$)

Table 1 Retinaldehydes in N-ret-PE and total retinaldehydes in DA mouse retinas (pmoles per retina)

	11cRAL	atRAL	13cRAL	9cRAL	Combined RALs
Retinaldehydes in *N*-ret-PE	10.0 ± 0.7	18.1 ± 1.3	8.0 ± 0.6	0.9 ± 0.1	37.0 ± 2.7
Total retinaldehydes	454.0 ± 25	72.3 ± 6.1	22.1 ± 3.6	7.9 ± 1.4	556.3 ± 35

We observed dramatic light-dependent conversion of at-*N*-ret-PE to its 11c-isomer (Fig. 1). The action spectrum for synthesis of 11c-*N*-ret-PE was nearly identical to the UV-visible absorbance spectrum of protonated at-*N*-ret-PE, both exhibiting maxima at ~450 nm (Fig. 1 and Supplementary Fig. 1). Light-dependent synthesis of the 9c-isomer and 13c-isomer also exhibited maxima at 450 nm, but were formed in much lower amounts than the 11c-isomer (Fig. 1a). Consistently, at-*N*-ret-PE showed light-dependent depletion, with an inverted action spectrum, also centered at 450 nm (Fig. 1b). To quantitate light-dependent formation of *cis*-isomers, we subtracted the amount of each *cis*-isomer in the dark-incubated samples from that in the 450-nm light-exposed samples (Fig. 1a). This yielded 121 pmol of 11c-, 18 pmol of 9-*cis*- (9c-), and 3.3 pmol of 13-*cis*- (13c-) *N*-ret-PE, balanced by 195 pmol of at-*N*-ret-PE consumed. These pmole values have relative but not absolute meaning. The ratio of 11cRAL to 13cRAL following photoisomerization of *N*-ret-PE was 37:1. Efficient photoconversion of at- to 11c-*N*-ret-PE suggests that *N*-ret-PE in OS may be a source of chromophore for the visual opsins in light-exposed retinas.

Synthesis of rhodopsin by OS membranes exposed to blue light. Next, we tested whether 450-nm light could induce synthesis of 11cRAL in native OS membranes. We prepared rod OS from the retinas of fresh, ex vivo dark-adapted bovine eyes. Equal aliquots of fresh OS membranes were exposed to UV-filtered white light (400-nm cutoff) to bleach the rhodopsin. Following addition of atRAL, one set of OS samples was placed in the dark while a second set was exposed to 450-nm monochromatic light for 30 min. The OS samples were extracted and analyzed for retinoid content by normal-phase LC. The UV-filtered white light photobleached approximately 95% of 11cRAL in the OS samples, indicating that most was in the form of rhodopsin since it was sensitive to visible light (Fig. 2a). OS samples exposed to 450-nm light for 30 min yielded a 7.8-fold increase in total 11cRAL over samples kept in the dark (Fig. 2a). These data suggest that OS membranes support light-driven synthesis of visual chromophore.

To test for light-dependent synthesis of rhodopsin, we again prepared fresh, dark-adapted bovine OS membranes. We divided the OS into samples containing two nmoles of rhodopsin. Some were photobleached by exposure to UV-filtered white light for 45 min while the remaining samples were kept in the dark. Ten nmoles of atRAL substrate was added to the photobleached samples. One set was incubated for 1 h in the dark while the other set was exposed to 450-nm light. We purified opsin protein from the OS samples by immunoaffinity chromatography and quantitated rhodopsin pigment by UV-visible absorbance spectroscopy (Figs 2b and c). The initial exposure to white light bleached 83% of the rhodopsin. No recovery of rhodopsin was observed following 1-h incubation in the dark. This was expected since the required chromophore-regenerating enzymes are not present in OS. In contrast, rhodopsin increased 2.4-fold in OS samples exposed to 450-nm light (Fig. 2c). These data show that free atRAL efficiently combines with PE to form at-*N*-ret-PE, and that following photoisomerization, 11c-*N*-ret-PE efficiently donates 11cRAL to regenerate rhodopsin in OS membranes.

***N*-ret-PE in dark-adapted mouse retinas**. Here we measured *N*-ret-PE in retinas from dark-adapted wild type (strain 129/Sv) mice. We extracted phospholipids from retina homogenates and separated them by reverse-phase LC. Three doublet peaks, all with λ_{max} near 450 nm, eluted between 21 and 38 min (Supplementary Fig. 2a). These peaks likely represent different fatty-acyl forms of *N*-ret-PE. We collected the eluates corresponding to these peaks, reacted the pooled fractions with hydroxylamine to form retinaldehyde oximes, and separated the oximes by normal-phase LC (Supplementary Fig. 2b). This allowed us to quantitate the retinaldehyde isomers of *N*-ret-PE in dark-adapted mouse retinas (Table 1). We also quantitated total

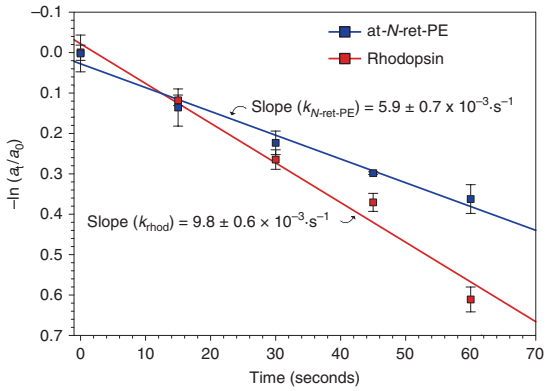

Fig. 3 Kinetics of rhodopsin and *N*-ret-PE photoisomerization. Protonated at-*N*-ret-PE and rhodopsin were exposed to 450-nm or 500-nm monochromatic light respectively at the same photon flux for the indicated times. The initial amounts of at-*N*-ret-PE and rhodopsin are represented by a_0, and the amounts at time *t* by a_t. The first-order rate constant (*k*) is described by: $kt = -\ln(a_t/a_0)$. Here, the slopes of the plots $-\ln(a_t/a_0)$ versus *t* yield the rate constants $k_{(N\text{-ret-PE})}$ and $k_{(rhod)}$. Each data point is shown as the mean ± s.e.m. ($n = 3$). The rate constants are also shown as mean ± s.e.m

retinaldehydes in dark-adapted (DA) 129/Sv mouse retinas (Table 1). Total retinaldehydes, representing mainly rhodopsin, contained predominantly 11cRAL, while *N*-ret-PE contained higher fractions of 13cRAL and atRAL (Table 1) reflecting the much lower thermal stability of *N*-ret-PE versus rhodopsin[21]. By combining the retinaldehyde isomers in *N*-ret-PE, we quantitated total *N*-ret-PE per dark-adapted mouse retina as 37 pmol (Table 1), or approximately 7% of the total retinaldehyde pool.

Quantum efficiency of *N*-Ret-PE. Upon exposure to 450-nm light, at-*N*-ret-PE is specifically converted to 11c-*N*-ret-PE (Fig. 1). Accordingly, we compared the rates of protonated at-*N*-ret-PE disappearance in 450-nm light to rhodopsin disappearance in 500-nm light, both with photon fluxes of 1.0 µmol/m^2 s. We plotted $-\ln(a_t / a_0)$ versus time, where a_t = amount of at-*N*-ret-PE or rhodopsin after illumination for *t* seconds and a_0 = initial amount without illumination ($t = 0$). This plot yielded the first-order rate constants, $k_{N\text{-ret-PE}}$ and k_{rhod} (Fig. 3). We determined the quantum efficiency[22] for *N*-ret-PE ($\Phi_{N\text{-ret-PE}}$) by the relationship shown in Eq. 1, as previously described[23, 24].

$$\Phi_{N-\text{ret}-\text{PE}} = \frac{\varepsilon_{\text{rhod}}}{\varepsilon_{N-\text{ret}-\text{PE}}} \times \frac{k_{N-\text{ret}-\text{PE}}}{k_{\text{rhod}}} \times \Phi_{\text{rhod}} \quad (1)$$

By inserting the molar extinction coefficients ($\mathcal{E}$) for rhodopsin at 500 nm (40,600 M^{-1} cm^{-1})[25] and *N*-ret-PE at 450 nm (31,300 M^{-1} cm^{-1}),[15] and the published quantum efficiency for rhodopsin ($\Phi_{rhod} = 0.65$),[26] we determined that $\Phi_{N\text{-ret-PE}} = 0.51 \pm 0.07$ (mean ± s.e.m.). The quantum efficiencies of rhodopsin and protonated *N*-ret-PE are therefore similar. The quantum efficiencies of cone opsins are similar to that of rhodopsin[27] and hence also to *N*-ret-PE.

Light-stimulated synthesis of chromophore by mouse retinas. Retinal G protein coupled receptor (RGR) opsin is a non-visual opsin in RPE and Müller cells of the retina[28]. Based on its similarity to squid retinochrome, and the phenotype of delayed rhodopsin regeneration in $Rgr^{-/-}$ mutant mice, RGR-opsin was proposed to function as a "reverse" photoisomerase for synthesis of visual chromophore[29]. The λ_{max} of protonated RGR-opsin is 469 nm[30], close to the λ_{max} of protonated *N*-ret-PE. Here we tested whether RGR-opsin contributes to the observed 450-nm light-dependent synthesis of 11cRAL. We prepared retina homogenates from wild type (strain 129/Sv) and $Rgr^{-/-}$ mutant (strain 129/Sv background) mice. After photobleaching the homogenates in UV-filtered (400 nm cutoff) white light, we added all-*trans*-retinol (atROL) substrate and incubated the homogenates in the dark or under 450-nm monochromatic light. Retinaldehydes formed during these incubations were quantitated by normal phase LC. As with bovine OS membranes (Fig. 2), the concentration of 11cRAL was approximately eight-fold higher in wild-type mouse retina homogenates exposed to 450-nm light compared to homogenates kept in the dark (Supplementary Fig. 3a). We observed no light-dependent stimulation of 9cRAL or 13cRAL (Supplementary Figs 3b,c), and the expected light dependent consumption of atRAL (Supplementary Fig. 3d). The high levels of 9cRAL and 13cRAL versus 11cRAL in retinal homogenates kept in the dark (Supplementary Figs 3b–d) is due to thermal isomerization of atRAL during the incubations[9]. Loss of RGR-opsin in $Rgr^{-/-}$ mouse retina homogenates had no effect on light-dependent formation of 11cRAL, in fact levels of 11cRAL were marginally higher in $Rgr^{-/-}$ versus wild-type retina homogenates exposed to 450-nm light (Supplementary Fig. 3a). As with wild-type mouse retinas, levels of 9cRAL and 13cRAL were not increased in $Rgr^{-/-}$ retinas following exposure to 450-nm light (Supplementary Figs 3b,c), while levels of atRAL exhibited a similar compensatory reduction (Supplementary Fig. 3d). These data suggest that RGR-opsin is not responsible for the observed blue light-dependent synthesis of visual chromophore.

Accelerated recovery of rhodopsin in live mice by blue light. To determine whether blue-light stimulates rhodopsin regeneration in vivo, we dark-adapted wild type (129/Sv) mice overnight. The mice were anesthetized and exposed to UV-filtered strobe light to bleach approximately 90% of the rhodopsin. We allowed one group of mice to recover in darkness, exposed another group to 450-nm light, and exposed the third group to 540-nm light, all for 10 min. Photon fluxes were the same for the 450-nm and 540-nm light (1.8 µmol/m^2 s). We chose 540 nm to complement 450 nm because these wavelengths bracket the λ_{max} of rhodopsin (500 nm) and are equally efficient at photoisomerizing rhodopsin. Immediately after the recovery period, we euthanized the mice, collected and homogenized their retinas, and performed immunoaffinity separation to isolate rhodopsin protein. To confirm similar recoveries of affinity purified rhodopsin protein independent of its ligand state, we determined the protein concentration of each supernatant fraction. The concentrations were similar, with a global average of 162 ± 18 µg/ml (s.e.m., $n = 15$). Next, we measured the amounts of functional rhodopsin in the same eluates by measuring the difference in 500-nm absorbance before and after bleaching with a strobe (Figs 4a, b).

Functional rhodopsin approximately doubled in samples from mice allowed to recover in the dark for 10 min versus samples from mice collected immediately following the bleach (Fig. 4b). Mice exposed to 450-nm light during post-bleach recovery showed an additional 1.5-fold increase in percent rhodopsin above the amount in mice that recovered in darkness (Fig. 4b). Finally, retinas from mice exposed to 540-nm light during recovery contained a lower percent of rhodopsin than retinas from mice that either recovered in the dark or were exposed to 450-nm light (Fig. 4b). The difference in rhodopsin levels

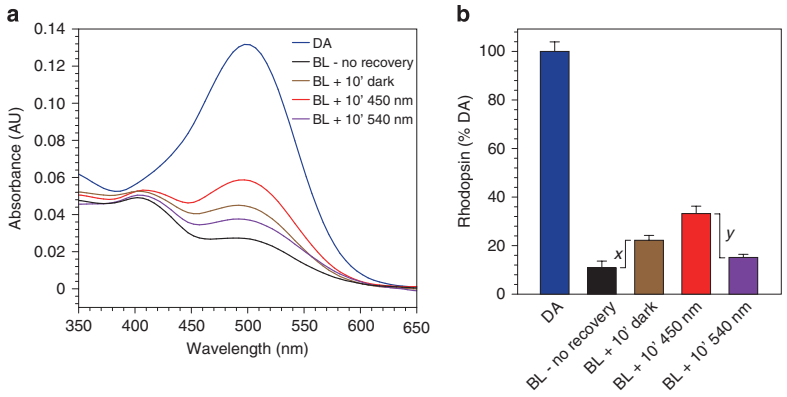

Fig. 4 Light dependent regeneration of rhodopsin in live mice. Wild-type mice were dark adapted overnight and exposed to the following light conditions: dark-adapted (DA); 90% strobe bleach with no recovery time (BL – no recovery); strobe bleach with 10 min recovery in the dark (BL + 10′ dark); strobe bleach with 10 min recovery in 450-nm light (BL + 10′ 450 nm); or strobe bleach with 10 min recovery in 540-nm light (BL + 540 nm). The photon fluxes of the 450-nm and 540-nm light were identical. The mice were euthanized, their retinas collected, and affinity purification of rhodopsin was carried out on the retina homogenates. **a** Representative baseline-normalized UV-Vis spectra of purified rhodopsin from mice exposed to the indicated light conditions. **b** Levels of rhodopsin visual pigment in retinas from mice exposed to the indicated light conditions, expressed as percent of dark-adapted rhodopsin. The value *x* represents the increase in rhodopsin during post-bleach recovery. The value *y* represents the difference in rhodopsin between mice exposed to 450-nm versus 540-nm light during recovery. Error bars show ± s.d. (n = 3)

between mice bleached with no recovery period and mice bleached with 10 min recovery in the dark represents rhodopsin regenerated by the enzymatic visual cycles (*x* in Fig. 4b). The difference in rhodopsin levels between mice that recovered in 450-nm light and mice that recovered in 540-nm light represents rhodopsin regenerated through photoisomerization of *N*-ret-PE (*y* in Fig. 4b). This applies because the 450-nm and 540-nm light photoisomerize rhodopsin with similar efficiency (Fig. 4a), while 540-nm light has little effect on protonated *N*-ret-PE (Fig. 1 and Supplementary Fig. 1). The radiant energies used in this experiment were 0.5 W/m^2 and 0.42 W/m^2 for the 450-nm and 540-nm light, respectively, yielding identical photon fluxes (1.8 µmol photons/m^2 s), similar to the radiant energy in a typical office environment. These results establish that blue-light dependent regeneration of rhodopsin occurs in live mice.

Increased photosensitivity of cones exposed to blue light. Rods comprise > 90% of photoreceptors in retinas from most mammalian species including mice, cattle and humans[31, 32]. Given the small percentage of cones, the blue light-dependent synthesis of 11cRAL observed in bovine OS and mouse retinas (Figs 2, 4) mainly reflects retinyl-lipid photoisomerization in rods. To test if photoisomerization of *N*-ret-PE contributes to regeneration of cone opsins, we made electrical recordings of cone photoresponses before and after bleaching with 450 nm or 560 nm monochromatic light. We chose these two wavelengths because the M-cones are equally sensitive to 450-nm and 560-nm light, while at-*N*-ret-PE is only photoisomerized to 11c-*N*-ret-PE by 450-nm light (Figs 1, 2). To do these experiments, we used a white-light LED and narrow-band interference filters. The absolute intensities at 450 nm and 560 nm (as measured with a calibrated photodiode) were nearly identical at all LED voltages. To demonstrate their equivalence, we measured the response of single M-cones at these two wavelengths as a function of LED intensity (Fig. 5a). Because the maximum amplitude of the current responses varied somewhat from cell to cell, primarily as the result of small differences in the seal of the suction pipette around the cell, we normalized responses (*R*) to maximum response amplitudes (R_{max}) at each of the two wavelengths. After normalization, response amplitudes as a function of flash intensity were nearly identical.

We then recorded photovoltages from M-cone enriched whole dorsal retinas (Fig. 5b) and suction-electrode responses from single M-cones (Fig. 5c). All of our M-cone recordings (including those in Fig. 5a) were made from *Gnat1*$^{-/-}$ mice lacking rod α-transducin, which exhibit normal cone photoresponses but no detectable rod response[33]. We exposed retinas or groups of cells to either 450-nm or 560-nm monochromatic light for 15 sec at the same photon fluxes calculated to bleach 85% of cone M opsin[34, 35], assuming a pigment photosensitivity of 6×10^9 µm^2. After bleaching with either wavelength, M-cones were stimulated at 500 nm, near the λ_{max} of M-cone opsin (508 nm).

The results of these experiments are shown in Fig. 5b for whole-retina recordings and Fig. 5c for suction-electrode recordings. These figures give the value of $I_{½}$ from fits of response amplitudes to the Michaelis–Menten function (see Methods). The value of $I_{½}$ quantifies the amount of light necessary to produce a half-maximal response. Thus the greater the value of $I_{½}$, the more light required to produce a half-maximal response and the lower the sensitivity. Our recordings show that $I_{½}$ was not significantly different in darkness for either whole-retina recordings ($p = 0.357$) or suction-electrode recordings ($p = 0.675$), as would be expected from the results of Fig. 5a. The value of $I_{½}$ increased after both 450-nm and 560-nm bleaches, indicating a drop in sensitivity. The amplitude of this decrease in sensitivity was smaller after the 450-nm bleach compared to the 560-nm bleach by a factor of approximately two. Although we observed small changes in sensitivity with time especially for the 560-nm bleaches, these changes were not significant. We therefore averaged measurements from all the time points, which gave mean $I_{½}$ values for the suction-electrode recordings of $2.6 \pm 0.2 \times 10^4$ after the 450-nm bleach ($n = 75$), and $5.9 \pm 0.9 \times 10^4$ after the 560-nm bleach ($n = 60$). This sensitivity difference was highly significant (Student's *t*, $p < 0.001$). A similar comparison for the whole-retina recordings was also statistically significant (Student's *t*, $p < 0.005$). Thus, with

two different preparations and recording techniques, we observed higher sensitivity in mouse cones after exposure to 450-nm versus 560-nm light. Since M cones were equally sensitive to our 450-nm and 560-nm lights (Fig. 5a), the two illuminations should have produced nearly equal bleaches. The smaller decrease in sensitivity after the 450-nm bleach is consistent with a role for retinyl-lipid photoisomerization in cone pigment regeneration.

Discussion

Rhodopsin and the cone opsin pigments require a continuous supply of visual chromophore to maintain photosensitivity in bright light. One molecule of 11cRAL is required for each photon absorbed. The endergonic conversion of atRAL to 11cRAL is carried out by multi-step enzyme pathways in RPE and Müller cells. Estimates of the maximum turnover rates suggest that the visual cycles cannot keep up with the high rates of rhodopsin and cone-opsin photoisomerization occurring in daylight[36]. Here we demonstrate a non-enzymatic mechanism for visual pigment regeneration involving photoisomerization of retinyl phospholipids in OS disk membranes (Fig. 6).

The OS membranes conduct 11cRAL and atRAL to and from the opsins during light exposure. Both retinaldehyde isomers reversibly condense with PE to form *N*-ret-PE. Protonated at-*N*-ret-PE was converted with remarkable specificity to 11c-*N*-ret-PE by blue light (Fig. 1). As an indication of this specificity, the ratio of 11cRAL to 13cRAL after exposure of at-*N*-ret-PE to 450-nm light was 37:1 (Fig. 1a). In contrast, the ratio of 11cRAL to 13cRAL at thermal equilibrium is 1:240[37]. Therefore, the 11c-isomer was enriched nearly 9000-fold by light over its equilibrium concentration during exposure to 450-nm light. This property of *N*-ret-PE[16] allows it to serve as a source of visual chromophore. The retinoid isomerases, Rpe65 and DES1 of the canonical and non-canonical visual cycles both exhibit much lower 11c-specificity[9, 38]. The difference in free energy between atRAL and 11cRAL is 4.1 kcal/mole[37]. Both Rpe65 and DES1 use hydrolysis of a retinyl ester to drive retinoid isomerization[9, 10, 39]. The actual metabolic cost of retinoid isomerization is 7.5 kcal/mol from hydrolysis of an activated fatty acid. In contrast, the energy of a 450-nm photon is 64 kcal/mol, far more than required to convert at-*N*-ret-PE to 11c-*N*-ret-PE. Regeneration of visual chromophore through retinyl-lipid photoisomerization is a unique example of an energy-requiring metabolic reaction in mammals being powered by visible light.

The membranes of most mammalian cells contain 15–25% PE[40], while OS disk membranes contain 38% PE[15]. The ratio of phospholipids to rhodopsin is 100:1 in OS membranes[41], hence PE is at 38-fold molar excess over rhodopsin. This abundance of PE in OS disks promotes formation of *N*-ret-PE from free retinaldehyde released by rhodopsin, and thereby photoregeneration of visual chromophore. *N*-ret-PE is the translocated substrate for the ABCA4 flippase in OS discs[18]. ABCA4 is the product of the gene affected in recessive Stargardt macular degeneration[42]. Loss of ABCA4 in Stargardt patients and *Abca4*$^{-/-}$ mice causes accumulation of bisretinoids that arise

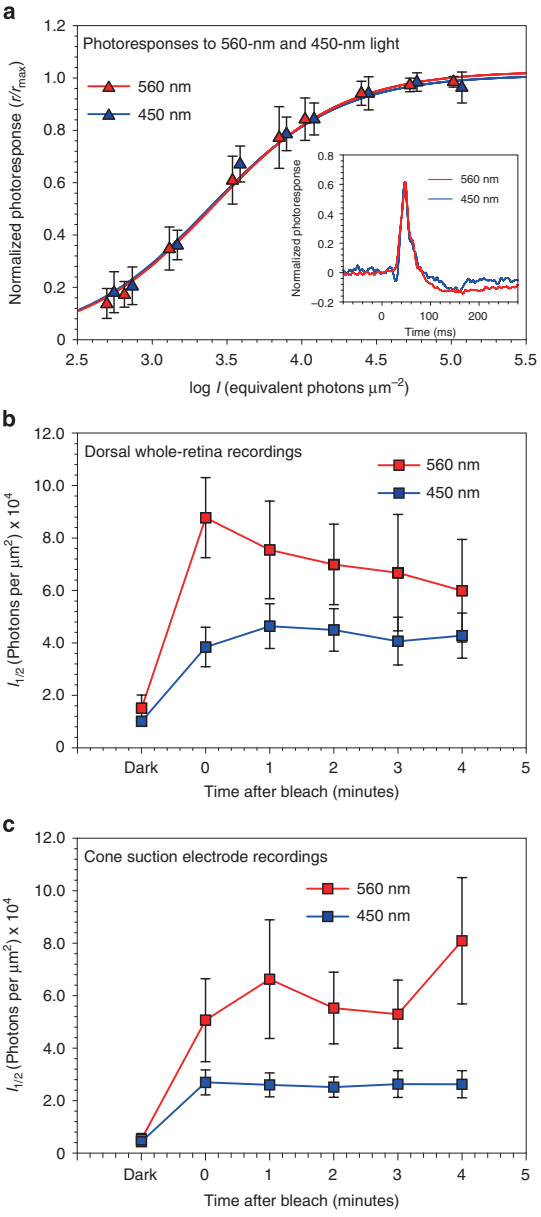

Fig. 5 Photosensitivity in *Gnat1*$^{-/-}$ cones after exposure to 450-nm or 560-nm light. Photoresponses were recorded from M (508-nm) cones in *Gnat1*$^{-/-}$ retinas before and after 15-second exposures to 450-nm or 560-nm light calculated to bleach 85% of the M-cone pigment. **a** Mean suction-electrode responses (±s.e.m.) from dark-adapted M cones as a function of flash intensity to 450-nm ($n = 7$) and 560-nm ($n = 10$) light at the same LED current and flash durations. Peak response amplitudes (r) were separately normalized to maximum peak response amplitudes at saturating light intensities (r_{max}) for the two wavelengths, and intensities were multiplied by 0.6 to give equivalent intensities at the λ_{max} of the M-cone pigment. Curves are Michaelis-Menten equation with values of $I_{1/2}$ of 2410 for 450 nm and 2560 for 560 nm (in equivalent photons µm^{-2}). Inset: mean responses to 450-nm and 560-nm light of flashes 2.5 ms in duration at intensities of approximately 3600 equivalent photons µm^{-2}. **b**,**c** Mean M-cone responses (±s.e.m.) before and after bleaching 85% of the cone visual pigment from **b** whole dorsal *Gnat1*$^{-/-}$ retinas from five mice and **c** suction-electrode recordings from single *Gnat1*$^{-/-}$ cones ($n = 14$ for 450-nm bleach, $n = 12$ for 560-nm bleach). Bleaching was performed with the same 450-nm and 560-nm light sources used in **a**. Cones and whole retinas were stimulated before and after the photobleach with three 500-nm flash intensities spanning the range of cone responses from small to nearly saturating. Mean response amplitudes were used to estimate the intensity required to produce a half-maximal response from fits to the Michaelis–Menten equation

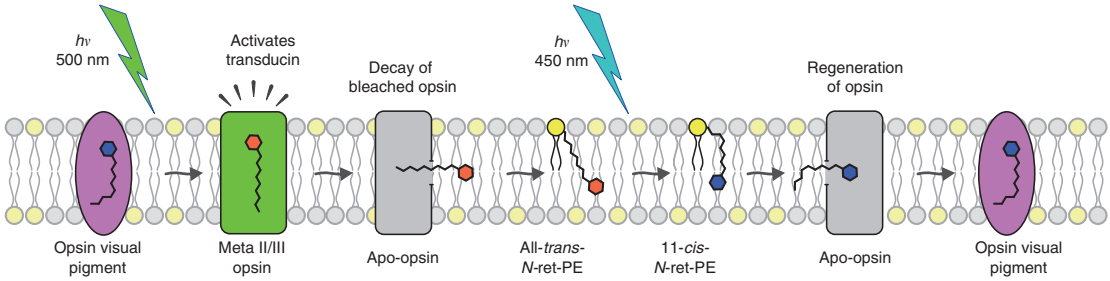

Fig. 6 Retinyl-lipid photoregeneration of opsins in rod or cone OS. The results presented here suggest the existence of a light-driven mechanism to regenerate visual pigments in rod and cone OS through photoisomerization of retinyl-lipids. This diagram shows the phospholipid bilayer of a rod OS disk. Rhodopsin absorbs a 500-nm photon (*hv*) that photoisomerizes its 11cRAL chromophore to atRAL, converting the pigment to its active metarhodopsin II/III (meta II/III) state. After a brief signaling period, the bleached opsin decays, releasing free atRAL into the bilayer. The atRAL reversibly condenses with PE (yellow circles) to form at-*N*-ret-PE. Protonated at-*N*-ret-PE is converted specifically to 11c-*N*-ret-PE upon absorption of a 450-nm photon. Spontaneous hydrolysis of 11c-*N*-ret-PE yields free 11cRAL, which irreversibly combines with unliganded apo-opsin to form a new rhodopsin pigment. A similar process occurs in cone OS to regenerate cone opsin pigments

through delayed clearance and secondary condensation of *N*-ret-PE with another retinaldehyde[43, 44]. We quantitated *N*-ret-PE in dark-adapted mouse retinas by comparing retinaldehydes contained in *N*-ret-PE to total retinaldehydes, which are mostly 11cRAL in rhodopsin (Supplementary Figs 2a,b and Table 1). *N*-ret-PE comprised ~7% of total retinaldehydes in a dark-adapted retina. 11cRAL not associated with rhodopsin undergoes thermal isomerization to its lower-energy isomers in the dark. This is exemplified by the higher fraction of atRAL and 13cRAL in *N*-ret-PE versus total retina following overnight dark adaptation (Table 1). Within the OS, any 11cRAL that thermally isomerizes to atRAL or 13cRAL would be quickly restored to the 11c-configuration through photoisomerization of *N*-ret-PE. Thus, 11c-*N*-ret-PE represents a protected and readily available pool of visual chromophore in photoreceptor OS.

While rods are single-photon detectors with a photoresponse that saturates in bright light, cones are less sensitive, providing color vision in bright light with a photoresponse that never saturates. Accordingly, cones seem better suited than rods to benefit from chromophore photoregeneration. We employed two experimental systems to test whether photoisomerization of *N*-ret-PE contributes to cone opsin regeneration. First, we recorded cone photovoltages from whole dorsal retinas of *Gnat1*$^{-/-}$ mice. We observed approximately two-fold greater sensitivity of M cones in the explants following exposure to 450-nm versus 560-nm light at the same photon flux (Fig. 5b). We also performed suction recording from isolated M-cone photoreceptors. Here again, we observed approximately two-fold greater sensitivity following a photobleach with 450-nm versus 560-nm light (Fig. 5c). These differences in cone photosensitivity are consistent with the higher levels of rhodopsin in mouse retinas following in vivo exposure to 450-nm versus 540-nm light (Fig. 4b). Hence, cones as well as rods appear to use photoisomerization of retinyl-lipids to regenerate visual pigments.

Although we used 450-nm light to uncover *N*-ret-PE photoisomerization, monochromatic light is not required for retinyl-lipid photoregeneration. In fact, white light is far more effective at photoisomerizing *N*-ret-PE than narrow-band 450-nm light, as indicated by the broad absorbance spectrum of protonated *N*-ret-PE (Supplementary Fig. 1). Given their overlapping spectra (Supplementary Fig. 1 and Fig. 4a), photoisomerization of *N*-ret-PE and bleaching of rhodopsin occur simultaneously in natural light. The rate of rhodopsin bleaching was slightly faster than the rate of *N*-ret-PE photoisomerization (Fig. 3), consistent with the observation that light exposure causes net depletion of visual pigments in retina membranes. Photoisomerization of *N*-ret-PE is therefore in the "kinetic shadow" of rhodopsin bleaching and difficult to observe.

The bleach/recovery experiment in mice (Fig. 4) allowed us to compare contributions of the enzymatic visual cycles to retinyl-lipid photoregeneration. Rhodopsin increased above its immediate post-bleach levels during the 10-min recovery period in the dark (Fig. 4b). This increase, shown by *x* in Fig. 4b, is due to the chromophore-synthesis activities of the enzymatic visual cycles. Significantly higher rhodopsin levels were seen in retinas from mice that recovered under 450-nm light, while lower rhodopsin levels were seen in retinas from mice that recovered under 540-nm light (Fig. 4b). Rhodopsin was bleached to the same extent by the 450-nm and 540-nm lights, while only 450-nm light significantly photoisomerized *N*-ret-PE (Fig. 1 and Supplementary Fig. 1). Accordingly, three factors affected rhodopsin levels in retinas from mice that recovered under 450-nm light: (i) the enzymatic visual cycles, (ii) photoisomerization of rhodopsin and (iii) photoisomerization of *N*-ret-PE; while only two factors affected rhodopsin levels in samples from mice that recovered under 540-nm light: (i) the enzymatic visual cycles and (ii) photoisomerization of rhodopsin. The contribution of *N*-ret-PE photoisomerization to rhodopsin regeneration is therefore represented by the difference in rhodopsin levels between samples that recovered under 450-nm and 540-nm light (*y* in Fig. 4b). Since $y > x$, photoisomerization of *N*-ret-PE contributed more to rhodopsin regeneration than did the enzymatic visual cycles under these light conditions.

The cone suction-recording experiment provided additional information about the contribution of retinyl-lipid photoisomerization to opsin pigment levels. Using the relationships in Eq. 3 and 4 (Methods), we estimated that cones exposed to 450-nm light behaved as if they contained approximately 15% more pigment than cones exposed to 560-nm light, suggesting a 15% contribution of *N*-ret-PE photoisomerization to cone opsin regeneration under these conditions. In nature, the contribution of retinyl-lipid photoisomerization to opsin pigment regeneration probably increases with intensifying ambient light. Retinyl-lipid photoregeneration may be required for sustained vision in daylight.

Methods

Animal use and care statement. This study was carried out in accordance with recommendations in the guide for the care and use of laboratory animals of the National Institutes of Health, and the Association for Research in Vision and

Ophthalmology Statement for the use of animals in ophthalmic and vision research. The animal use protocol was approved by the University of California, Los Angeles Animal Research Committee (permit number: A3196-01). Euthanasia was performed by cervical dislocation on deeply anesthetized (xylazine 10 mg/kg and ketamine 100 mg/kg) mice. All steps were taken to minimize pain and distress in the mice.

Synthesis and purification of at-N-Ret-PE. All reactions were performed under dim red light. We synthesized at-*N*-ret-PE according to published methods[45] with modifications. Briefly, atRAL (Sigma-Aldrich) was mixed with 5.6 mg 1-oleoyl-2-hydroxy-*sn*-glycero-3-phosphoethanolamine (18:1 lyso PE, Avanti Polar Lipids) in three ml of a solution containing six volumes of methanol (Fisher Scientific), 12 volumes of chloroform (Sigma-Aldrich) and one volume of triethylamine (Sigma-Aldrich). The solution was incubated at room temperature for 1 h with gentle mixing in the dark. Three ml of one-M hydrochloric acid (EM Science) was added and the mixture was centrifuged at 3500 × *g* for 5 min. The lower organic phase (chloroform) containing at-*N*-ret-PE was collected and the upper phase was extracted again with 2 ml chloroform. The pooled extracts were further rinsed with 3 ml of one-M hydrochloric acid, and the final chloroform extracts were dried under a stream of nitrogen and dissolved in acidified methanol (20-µl trifluoroacetic acid (TFA) per liter methanol). The at-*N*-ret-PE was purified in its protonated form by reverse-phase LC (see below) with an elution time of approximately 14 min. By this method, free atRAL eluted at approximately 10 min.

Action spectrum of at-N-Ret-PE. Ten µM at-*N*-ret-PE was dissolved in acidified methanol (20 µl TFA per liter) to maintain the protonated state. Its concentration was determined by absorption at 450 nm using a Shimadzu UV-2401PC UV-Vis spectrophotometer and a molar extinction coefficient of 31,300 $M^{-1}cm^{-1}$ [15]. Triplicate samples were placed into quartz 10 mm cuvettes (SCC) covered in black paper with only the front side exposed to light. The samples were either kept in the dark or illuminated with monochromatic light at wavelengths of 325 to 650 nm with 25-nm increments at room temperature for 80 s. The monochromatic light was generated by a custom monochromator (Newport Instruments) with a xenon arc lamp. The light intensities were measured with a spectroradiometer (Black-comet CXR-SR-50, StellarNet Inc.) and adjusted (from 0.35 W/m^2 at 325 nm to 0.18 W/m^2 at 650 nm) such that each wavelength delivered a photon flux of 0.95 µmol photons/(m^2 s). Two hundred µl from each sample were analyzed by normal-phase LC.

Normal-phase LC analysis of retinoids. Retinoids were treated with 20–25 µl 5% sodium dodecyl sulfate (SDS) (for samples of at-*N*-ret-PE in methanol, SDS was not added) and 50 µl brine. To quantitate retinaldehydes in *N*-ret-PE and opsin pigments, retinaldehyde oximes were generated by addition of hydroxylamine hydrochloride (200–500 µl of 2 M solution, pH 7.0) (Sigma). The samples were mixed by vortexing and incubated at room temperature for 15 min. 2 ml of methanol were added and the samples were extracted twice with 2 ml hexane as previously described[9]. The identity of each eluted peak was established by comparing the spectra and elution times with those of authentic retinoid standards. Sample peaks were quantitated by comparing peak areas to calibration curves established with retinoid standards. Peak areas for the corresponding *syn*-oximes and *anti*-oximes were summed to quantitate each retinaldehyde isomer.

Determination of the decay constants. Bovine rod OS were purified by published methods[46] and used as the source of rhodopsin. Purified rod OS were dissolved in 20 mM sodium phosphate (Fisher Scientific) buffer pH 7.2 with 100 mM sodium chloride (Fisher Scientific), 2.5% sucrose (Fisher Scientific) and 2% CHAPS (Calbiochem), and diluted to an absorbance of 0.22 AU at 500 nm (the λ_{max} of rhodopsin). Purified protonated at-*N*-ret-PE was diluted in acidified methanol to yield an absorbance of 0.22 AU at 450 nm (the λ_{max} of at-*N*-ret-PE). Triplicate aliquots of purified rod OS were exposed to 500-nm monochromatic light at 0.25 W/m^2 (1.0 µmol photons/m^2 s) at room temperature for 0, 15, 30, 45, and 60 s. Triplicate aliquots of protonated *N*-ret-PE were exposed to 450-nm monochromatic light at 0.28 W/m^2 (1.0 µmol photons/m^2 s) and otherwise treated identically as the rhodopsin samples. Two hundred µl from each sample were removed and analyzed for retinoid content by normal-phase LC. The amount of rhodopsin at each time point was determined by quantitation of 11cRAL.

Reverse-phase LC of phospholipids. Phospholipid extraction was performed with modifications to a previously published protocol[47]. All extractions were performed under dim red light. Retina homogenates from 8-week-old strain 129/Sv mice or bovine OS were extracted by the addition of 3 ml of 1:2 (vol/vol) mixture of chloroform (Sigma) and acidified methanol (Fisher) (one L methanol + 8 µl trifluroacetic acid (Sigma)) followed by brief vortexing and incubation on ice for 10 min. Next, 1.3 ml of 0.3 M NaCl were added and the samples extracted twice into one ml chloroform with centrifugation at 1750 × g for 10 min at 10 °C to separate phases. The pooled chloroform layers were transferred to 16 × 100 mm borosilicate glass test tubes and evaporated to dryness under a stream of nitrogen. Samples were dissolved in 100 µl of acidified methanol and analyzed by reverse-phase LC[48] on an Agilent 1100 series chromatograph equipped with a photodiode-array detector using an Phenomenex Primeshere C18-HC 110 A column (250 × 4.6 mm) and a 15–0% water gradient in acidified methanol (8 µl TFA/L methanol) at a flow rate of 1.0 (gradient) to 2.4 (isocratic) ml per min. Spectra (190–550 nm) were acquired for all eluted peaks. The identity of each eluted peak was established by comparing the spectra and elution times with those of authentic retinoid and *N*-ret-PE standards. Sample peaks were quantitated by peak area.

Mice and genotyping. All mice were reared in cyclic light. The 129/Sv wild-type control mice were purchased from Taconic Biosciences, Inc. Retinal G protein-coupled receptor knockout ($Rgr^{-/-}$) mice[29] were generously provided by Henry Fong, genotyping protocols and strain background information were reported previously[49]. $Gnat1^{-/-}$ mice lacking rod α-transduc in[33] were generously provided by Janis Lem. All mice were genotyped to exclude the *rd8* and *rpe65* L450M mutations. The primers for each genotyping: *rd8*, F: 5′GGTGACCAATCTGTTG ACAATCC, R: 5′GCCCCATTTGCACACTGATGAC; *rpe65* codon 450, F: 5′CCTTTGAATTTCCTCAAATCAATTA, R: 5′TTCCAGAGCATCTGGTTGAG.

Rhodopsin purification from mouse retinas. Retinas from 8-week-old wild-type (strain 129/Sv) mice were dissected under dim red light and homogenized in a glass to glass tissue grinder (Kontes) in solubilization buffer (40 mM Tris (Fisher) pH 7.2, 1% CHAPS (Fisher), and 0.1 mg/ml PMSF (Sigma)). The homogenates were spun at 17,000 × g for 15 min at 4 °C to pellet cell debris. Collected supernatants were added to 100 µl agarose beads coupled to the 1D4 antibody against rhodopsin (PureCube Rho1D4 Agarose), washed with solubilization buffer, and incubated overnight with agitation at 4 °C. Beads were combined with elution buffer (40 mM Tris pH 7.2, 1% CHAPS, 200 µM 1D4 peptide (Cube Biotech)) for 1 h at room temperature. The beads were then pelleted by centrifugation (3000 RPM for 5 min, Eppendorf 5415D centrifuge) and the rhodopsin-containing supernatants were collected. Rhodopsin was quantified spectrophotometrically at 500 nm (Shimadzu UV-2401PC UV-Vis spectrophotometer) using the molar extinction coefficient of 40,600 $M^{-1}cm^{-1}$ [25].

Rhodopsin purification from bovine rod OS. Bovine rod OS were prepared from the eyes of freshly slaughtered cattle using published procedures[46]. Purified OS in 50 µl aliquots containing 2-nmoles rhodopsin were prepared in triplicate for each light condition. OS samples for rhodopsin regenerative studies were bleached on ice (12,000 lux for 45 min with a halogen lamp) to remove endogenous retinoids. The OS were supplemented with 50 µM atRAL in dimethyl sulfoxide and diluted to 200 µl with pH 6.0 phosphate-citrate buffer containing 0.1 mg/ml PMSF. Samples were incubated overnight at 4.0 °C with gentle agitation. The following day, samples were incubated at 37 °C for 30 or 60 min with gentle agitation in the dark or under 450-nm monochromatic light (20-nm bandwidth) at 0.5 W/m^2. Samples incubated for 30 min were extracted and analyzed for retinoid content by normal-phase LC to measure production of 11cRAL. Rhodopsin was purified from samples incubated for 1 h using Rho 1D4-agarose (Cube Biotech) as described above. Absorbance spectra were acquired for all samples using a Shimadzu UV-2401PC UV-Vis spectrophotometer. Difference spectra were acquired after bleaching the samples in the same cuvette with a Novatron strobe light (3 × 1500 W). The difference spectra were normalized to the baseline (A_{650}) and protein content (A_{280}). Additional OS samples (dark and 450-nm light-treated) were examined for *N*-ret-PE content by reverse-phase LC, as described above. Peaks identified as *N*-ret-PE by their absorbance spectra were collected, reacted with hydroxylamine to form retinaldehyde oximes, and re-analyzed by normal-phase LC to determine the retinaldehyde content of *N*-ret-PEs.

Photoisomerization in retina homogenates from mice. Eight to 10-week-old wild type (strain 129/Sv) and $Rgr^{-/-}$ (129/Sv background) mice were euthanized and their eyes collected. Retinas from mice of each genotype were pooled and disrupted by glass/glass homogenization (Kontes) in 6.0 ml 40 mM Tris buffer pH 7.2. The homogenates were extensively bleached (20,000 lux from a xenon arc lamp with a 400-nm UV cutoff filter for 45 min) to destroy endogenous retinoids. Protein concentrations were determined (Pierce BCA Protein Assay Kit, Thermofisher) and used for normalization of pre- and post-bleach retinoid content. Photoisomerization assays were performed on similar homogenate samples in 500 µl reactions with addition of 5% BSA, 25 µM all-*trans*-retinol, and 500 µM $NADP^+$ (all from Sigma). Samples were placed in cuvettes and agitated in the dark or during exposure to 450-nm light (10-nm bandwidth with an irradiance of 0.2 W/m^2) for 25 min at 37 °C. Retinoids were extracted from samples and analyzed by normal-phase LC, as described above.

Blue-light dependent regeneration of rhodopsin in live mice. Triplicate sets of 8-week-old wild type (129/Sv) mice were dark adapted overnight. All mice were anesthetized as described above and their pupils dilated with one drop of 1.5% tropicamide and 2.5 % phenylephrine. Three sets of six mice were kept in the dark for the dark-adapted (DA) rhodopsin determinations (90 mice total). The remaining mice were bleached by exposure to ten 1500-W flashes of a Novatron strobe. We observed no change in the thickness of any retina layer by optical coherence

tomography at one and 7 days post-exposure, indicating that the strobe light caused no retinal damage in mice. Immediately post-bleach, three sets of six mice were euthanized, their retinas collected (12 retinas per sample) and homogenized, as described above. The remaining nine sets of six mice were exposed for 10 min to one of three different light conditions: (i) darkness, (ii) 450-nm light, or (iii) 540-nm light. Both "monochromatic" light sources had a 10-nm bandwidth. The irradiances on the corneal surfaces were 0.5 W/m^2 for the 450-nm light and 0.42 W/m^2 for 540-nm light, to yield identical photon fluxes of 1.8 µmol photons/m^2 s. Immediately following the 10-min recovery periods, the mice were euthanized in the dark, their retinas dissected (12 retinas per sample) and homogenized, as described above. Rhodopsin was purified from mouse retina homogenates by immunoaffinity chromatography, also as described above. After purification, rhodopsin was quantitated by difference spectra analysis. The purified rhodopsin samples were also analyzed for 11cRAL and atRAL content by normal-phase LC.

Whole-retina and cone-suction recordings from mouse cones. *Gnat1*$^{-/-}$ mice (8-week-old) reared under cyclic light were dark-adapted overnight then euthanized. Their eyes were marked with a cauterization tool at the ventral pole, enucleated, and only the dorsal retina, which contains predominantly middle-wavelength sensitive (M) cones[50], was collected. The dorsal retinas were isolated from the RPE and perfused with Ames solution (Sigma) containing an additional 1.9 g/l $NaHCO_3$ and bubbled with 95% O_2 / 5% CO_2. For whole-retina recordings of cone responses, dorsal retinas were placed photoreceptors up on Whatman Anodisc filter membranes (Sigma) in a custom built recording chamber. Retinas were isolated and perfused with 2 mM aspartic acid and 40 µM DL-AP4 (Tocris, Bristol, UK) on the photoreceptor side and 2 mM aspartic acid and 1 mM barium chloride (Sigma) on the ganglion-cell surface. Photovoltages were measured with a DP-311 differential amplifier (Warner Instruments, Hamden, CT). For suction recordings, retinas were sliced into pieces and recordings were made from individual cone inner segments[51]. Both preparations were stimulated with an LED optical system (Cairn Research, Faversham, UK) coupled to an inverted microscope. Test flashes were delivered with a 505-nm LED through a 500-nm interference filter. Cones were bleached with either 450-nm or 560-nm illumination from a white-light LED and interference filters at 450 nm and 560 nm. The intensities of the test and bleaching lights were calibrated with a photodiode (United Detector Technology, San Diego, CA). The intensities of the 450-nm and 560-nm illuminations from the LED were nearly the same at the same diode currents, and M-cones were equally sensitive to these two wavelengths at the same diode intensities and flash durations (see Fig. 5a). Recordings were filtered with an 8-pole Bessel filter and sampled at 100 Hz. Data were displayed and analyzed with PCLAMP (Molecular Devices, Sunnyvale, CA) and Origin plotting software (OriginLabs, Cambridge, MA).

Estimation of sensitivity. Sensitivities for Fig. 5b and c were estimated by measuring responses to two dim light intensities and to a nearly saturating bright light. The test-flash intensities were (photons µm^{-2}) 2840, 9690, 200,000 before bleaches and 19,000, 43,200, 200,000 following bleaches for Fig. 5b (whole retina); and 2200, 3500, and 66,600 before bleaches and 6900, 15,500, and 66,600 after bleaches for one series of experiments, and 650, 5,410, and 95,000 before the bleaches and 9200, 40,500, and 220,000 after bleaches for a second series for Fig. 5c (suction-electrode recordings). At each intensity, 10 flashes were given at 1-s intervals for the dim flashes, or every 1.5 s for the nearly saturating flashes, and response amplitudes were averaged. The determinations at 0 min were begun 10 sec after the bleach; recovery of photoresponse and maximum response amplitude was virtually complete after 10 s, even for these large bleaches[52]. Determinations at 1–4 min were begun one to 4 min after the bleach. Each determination took a total of about 40 s. Sensitivities were then determined by fitting each series of three mean response amplitudes to the Michaelis–Menten equation (Eq. 2),

$$r = r_{\max}\frac{I}{I + I_{1/2}} \quad (2)$$

where r is response amplitude in pA, $r_{\max}$ is the maximum value of r, I is intensity in 500-nm photons µm^{-2}, and $I_{1/2}$ is a constant equal to the intensity of the flash producing a half-maximal response. The Michaelis–Menten relation predicts that responses at dim light intensities ($I << I_{1/2}$) are directly proportional to light intensity, with a proportionality constant equal to $r_{\max}/I_{1/2}$. This proportionality constant gives the response per unit light intensity at dim light intensities in the linear range of the Michaelis–Menten relation and is therefore equal to the sensitivity of the photoreceptor. Sensitivity is thus inversely related to $I_{1/2}$, and plotting the value of $I_{1/2}$ is therefore a meaningful and appropriate way to display differences in cone sensitivity provided there are no changes in $r_{\max}$. In Fig. 5 we therefore show the changes in the value of $I_{1/2}$ after the 450-nm and 560-nm bleaches. There were no significant changes in $r_{\max}$.

Estimation of cone pigment regenerated from N-Ret-PE. Previous experiments have shown that photoreceptor desensitization after strong bleaches is the result of two mechanisms: (i) the decrease in quantum catch produced by the decrease in concentration of unbleached pigment, and (ii) adaptation produced by activation of the cascade by bleached pigment[53, 54, 55]. These two mechanisms sum to produce a decrease in sensitivity that is well described by the equation (Eq. 3)

$$\frac{S_F}{S_F^D} = \frac{1 - F}{1 + kF} \quad (3)$$

where S_F is the sensitivity of the photoreceptor, S_F^D is the sensitivity in darkness, F is the fraction bleached, and k is a constant, equal to 34–35 for mouse rods[56] but 8.6 for salamander cones[53].

Although no similar measurements have been made for bleached mouse cones, we can estimate the value of k from our data if we assume that, following the 560-nm bleach, no pigment regeneration occurred. We need first to use the values of $I_{1/2}$ before and after bleaching to estimate S_F/S_F^D. We observe that the Michaelis–Menten equation (Eq. 2) provides an adequate description of the responses of cones to increasing flash intensity (Fig. 5a); and that for dim flash intensities ($I << I_{1/2}$), the amplitude of the response (and therefore the sensitivity of the cone) is inversely proportional to $I_{1/2}$. Therefore, we can estimate S_F^D as 2560/59,000 or 0.043 after the 560-nm bleach, and 2410/26,000 or 0.093 after the 450-nm bleach.

Now, if no pigment regeneration had occurred after the 560-nm bleach, $F = 0.85$ and we can solve equation in Eq. 3 for k and obtain a value of 2.9, considerably lower than for salamander cones. We now insert this value into Eq. 3 and solve for the fraction bleached (Eq. 4).

$$F = \frac{1 - \frac{S_F}{S_F^D}}{1 + k\frac{S_F}{S_F^D}} \quad (4)$$

If k is 2.9 and, after the 450-nm bleach, S_F/S_F^D is 0.093, then F is 0.71 instead of 0.85. The cones are behaving as if the 450-nm light had produced approximately 15% less bleached pigment than the 560-nm bleach, presumably because of retinyl-lipid photoisomerization. We note that if we have underestimated the value of k, and it is in fact larger and nearer to that for salamander cones or mouse rods, the value of F from Eq. 4 would have been smaller and the amount of pigment regenerated through *N*-ret-PE photoisomerization even larger.

Reproducibility and statistical analysis of mouse studies. No power studies were performed on mouse experiments. No experimental animals were excluded from analysis. No randomization or blinding was used in the mouse studies. Statistical significance (p-values) were determined either with a two-tailed Welch's t-test or Student's t. p-values of less than 0.05 were considered significant.

Data availability. All data generated and analyzed during this study are included in this published article and its Supplementary Information files, and available from the corresponding author upon request.

Received: 28 December 2016 Accepted: 15 February 2017
Published online: 04 May 2017

References

1. Montell, C. *Drosophila* visual transduction. *Trends. Neurosci.* **35**, 356–363 (2012).
2. Ebrey, T. & Koutalos, Y. Vertebrate photoreceptors. *Prog. Retin. Eye Res.* **20**, 49–94 (2001).
3. Williams, T. P. Photoreversal of rhodopsin bleaching. *J. Gen. Physiol.* **47**, 679–689 (1964).
4. Grimm, C., Reme, C. E., Rol, P. O. & Williams, T. P. Blue light's effects on rhodopsin: photoreversal of bleaching in living rat eyes. *Invest Ophthalmol. Vis. Sci.* **41**, 3984–3990 (2000).
5. Arnis, S. & Hofmann, K. P. Photoregeneration of bovine rhodopsin from its signaling state. *Biochemistry* **34**, 9333–9340 (1995).
6. Furutani, Y., Kandori, H. & Shichida, Y. Structural changes in lumirhodopsin and metarhodopsin I studied by their photoreactions at 77 K. *Biochemistry* **42**, 8494–8500 (2003).
7. Wright, C. B., Redmond, T. M. & Nickerson, J. M. A history of the classical visual cycle. *Prog. Mol. Biol. Transl. Sci.* **134**, 433–448 (2015).
8. Wang, J. S. & Kefalov, V. J. The cone-specific visual cycle. *Prog. Retin. Eye. Res.* **30**, 115–128 (2011).
9. Kaylor, J. J. *et al.* Identification of DES1 as a vitamin a isomerase in Muller glial cells of the retina. *Nat. Chem. Biol.* **9**, 30–36 (2013).
10. Kaylor, J. J. *et al.* Identification of the 11-*cis*-specific retinyl-ester synthase in retinal Muller cells as multifunctional *O*-acyltransferase (MFAT). *Proc. Natl. Acad. Sci. USA* **111**, 7302–7307 (2014).
11. Szuts, E. Z. & Harosi, F. I. Solubility of retinoids in water. *Arch. Biochem. Biophys.* **287**, 297–304 (1991).
12. Hildebrand, P. W. *et al.* A ligand channel through the G protein coupled receptor opsin. *PLoS ONE* **4**, e4382 (2009).
13. Wang, T. & Duan, Y. Retinal release from opsin in molecular dynamics simulations. *J. Mol. Recognit.* **24**, 350–358 (2011).

14. Poincelot, R. P., Millar, P. G., Kimbel, R. L. Jr. & Abrahamson, E. W. Lipid to protein chromophore transfer in the photolysis of visual pigments. *Nature* **221**, 256–257 (1969).
15. Anderson, R. E. & Maude, M. B. Phospholipids of bovine outer segments. *Biochemistry* **9**, 3624–3628 (1970).
16. Shichi, H. & Somers, R. L. Possible involvement of retinylidene phospholipid in photoisomerization of all-*trans*-retinal to 11-*cis*-retinal. *J. Biol. Chem.* **249**, 6570–6577 (1974).
17. Kimbel, R. L. Jr., Poincelot, R. P. & Abramhamson, E. W. Chromophore transfer from lipid to protein in bovine rhodopsin. *Biochemistry* **9**, 1817–1820 (1970).
18. Quazi, F., Lenevich, S. & Molday, R. S. ABCA4 is an N-retinylidene-phosphatidylethanolamine and phosphatidylethanolamine importer. *Nat. Commun.* **3**, 925 (2012).
19. Tsui, F. C., Ojcius, D. M. & Hubbell, W. L. The intrinsic pKa values for phosphatidylserine and phosphatidylethanolamine in phosphatidylcholine host bilayers. *Biophys. J.* **49**, 459–468 (1986).
20. Boettner, E. A. & Wolter, J. R. Transmission of the ocular media. *Invest. Ophthalmol. Vis. Sci.* **1**, 776–783 (1962).
21. Groenendijk, G. W., Jacobs, C. W., Bonting, S. L. & Daemen, F. J. Dark isomerization of retinals in the presence of phosphatidylethanolamine. *Eur. J. Biochem.* **106**, 119–128 (1980).
22. Dartnall, H. J. The photosensitivities of visual pigments in the presence of hydroxylamine. *Vis. Res.* **8**, 339–358 (1968).
23. Saari, J. C. & Bredberg, D. L. Photochemistry and stereoselectivity of cellular retinaldehyde-binding protein from bovine retina. *J. Biol. Chem.* **262**, 7618–7622 (1987).
24. Hao, W. S. & Fong, H. K. W. The endogenous chromophore of retinal G protein-coupled receptor opsin from the pigment epithelium. *J. Biol. Chem.* **274**, 6085–6090 (1999).
25. Wald, G. & Brown, P. K. The molar extinction of rhodopsin. *J. Gen. Physiol.* **37**, 189–200 (1953).
26. Kim, J. E., Tauber, M. J. & Mathies, R. A. Wavelength dependent *cis-trans* isomerization in vision. *Biochemistry* **40**, 13774–13778 (2001).
27. Okano, T., Fukada, Y., Shichida, Y. & Yoshizawa, T. Photosensitivities of iodopsin and rhodopsins. *Photochem. Photobiol.* **56**, 995–1001 (1992).
28. Pandey, S., Blanks, J. C., Spee, C., Jiang, M. & Fong, H. K. Cytoplasmic retinal localization of an evolutionary homolog of the visual pigments. *Exp. Eye. Res.* **58**, 605–613 (1994).
29. Chen, P. *et al.* A photic visual cycle of rhodopsin regeneration is dependent on Rgr. *Nat. Genet.* **28**, 256–260 (2001).
30. Hao, W. & Fong, H. K. Blue and ultraviolet light-absorbing opsin from the retinal pigment epithelium. *Biochemistry* **35**, 6251–6256 (1996).
31. Krebs W. & Krebs I. P. in *The Structure of the Eye* (eds Hollyfield, J. G.) (Elsevier Biomedical, Amsterdam, Netherlands, 1982).
32. Carter-Dawson, L. D. & LaVail, M. M. Rods and cones in the mouse retina. I. Structural analysis using light and electron microscopy. *J. Comp. Neurol.* **188**, 245–262 (1979).
33. Calvert, P. D. *et al.* Phototransduction in transgenic mice after targeted deletion of the rod transducin alpha-subunit. *Proc. Natl. Acad. Sci. USA* **97**, 13913–13918 (2000).
34. Woodruff, M. L., Lem, J. & Fain, G. L. Early receptor current of wild-type and transducin knockout mice: photosensitivity and light-induced Ca^{2+}release. *J. Physiol.* **557**, 821–828 (2004).
35. Nymark, S., Frederiksen, R., Woodruff, M. L., Cornwall, M. C. & Fain, G. L. Bleaching of mouse rods: microspectrophotometry and suction-electrode recording. *J. Physiol.* **590**, 2353–2364 (2012).
36. Mata, N. L., Radu, R. A., Clemmons, R. & Travis, G. H. Isomerization and oxidation of vitamin a in cone-dominant retinas. A novel pathway for visual-pigment regeneration in daylight. *Neuron* **36**, 69–80 (2002).
37. Rando, R. R. & Chang, A. Studies on the catalyzed interconversion of vitamin A derivatives. *J. Am. Chem. Soc.* **105**, 2879–2882 (1983).
38. Redmond, T. M., Poliakov, E., Kuo, S., Chander, P. & Gentleman, S. RPE65, visual cycle retinol isomerase, is not inherently 11-*cis*-specific: support for a carbocation mechanism of retinol isomerization. *J. Biol. Chem.* **285**, 1919–1927 (2010).
39. Deigner, P. S., Law, W. C., Canada, F. J. & Rando, R. R. Membranes as the energy source in the endergonic transformation of vitamin A to 11-*cis*-retinol. *Science* **244**, 968–971 (1989).
40. Vance, J. E. Phospholipid synthesis and transport in mammalian cells. *Traffic* **16**, 1–18 (2015).
41. Shichi, H. & Shelton, E. Assessment of physiological integrity of sonicated retinal rod membranes. *J. Supramol. Struct.* **2**, 7–16 (1974).
42. Allikmets, R. *et al.* A photoreceptor cell-specific ATP-binding transporter gene (*ABCR*) is mutated in recessive Stargardt macular dystrophy. *Nat. Genet.* **15**, 236–246 (1997).
43. Weng, J. *et al.* Insights into the function of Rim protein in photoreceptors and etiology of Stargardt's disease from the phenotype in *abcr* knockout mice. *Cell* **98**, 13–23 (1999).
44. Mata, N. L., Weng, J. & Travis, G. H. Biosynthesis of a major lipofuscin fluorophore in mice and humans with ABCR-mediated retinal and macular degeneration. *Proc. Natl. Acad. Sci. USA* **97**, 7154–7159 (2000).
45. Ahn, J., Wong, J. T. & Molday, R. S. The effect of lipid environment and retinoids on the ATPase activity of ABCR, the photoreceptor ABC transporter responsible for Stargardt macular dystrophy. *J. Biol. Chem.* **275**, 20399–20405 (2000).
46. Pentia, D. C., Hosier, S., Collupy, R. A., Valeriani, B. A. & Cote, R. H. Purification of PDE6 isozymes from mammalian retina. *Methods. Mol. Biol.* **307**, 125–140 (2005).
47. Bligh, D. G. & Dyer, W. J. A rapid method for total lipid extraction and purification. *Can. J. Biochem. Physiol.* **37**, 911–917 (1959).
48. Parish, C. A., Hashimoto, M., Nakanishi, K., Dillon, J. & Sparrow, J. Isolation and one-step preparation of A2E and iso-A2E, fluorophores from human retinal pigment epithelium. *Proc. Natl. Acad. Sci. USA* **95**, 14609–14613 (1998).
49. Radu, R. A. *et al.* Retinal pigment epithelium-retinal G protein receptor-opsin mediates light-dependent translocation of all-*trans*-retinyl esters for synthesis of visual chromophore in retinal pigment epithelial cells. *J. Biol. Chem.* **283**, 19730–19738 (2008).
50. Szel, A. *et al.* Unique topographic separation of two spectral classes of cones in the mouse retina. *J. Comp. Neurol.* **325**, 327–342 (1992).
51. Nikonov, S. S. *et al.* Jr. Photoreceptors of $Nrl^{-/-}$ mice coexpress functional S- and M-cone opsins having distinct inactivation mechanisms. *J. Gen. Physiol.* **125**, 287–304 (2005).
52. Nikonov, S. S., Kholodenko, R., Lem, J. & Pugh, E. N. Jr. Physiological features of the S- and M-cone photoreceptors of wild-type mice from single-cell recordings. *J. Gen. Physiol.* **127**, 359–374 (2006).
53. Jones, G. J., Fein, A., MacNichol, E. F. Jr. & Cornwall, M. C. Visual pigment bleaching in isolated salamander retinal cones. Microspectrophotometry and light adaptation. *J. Gen. Physiol.* **102**, 483–502 (1993).
54. Cornwall, M. C. & Fain, G. L. Bleached pigment activates transduction in isolated rods of the salamander retina. *J. Physiol.* **480**, 261–279 (1994).
55. Jones, G. J., Cornwall, M. C. & Fain, G. L. Equivalence of background and bleaching desensitization in isolated rod photoreceptors of the larval tiger salamander. *J. Gen. Physiol.* **108**, 333–340 (1996).
56. Fan, J., Woodruff, M. L., Cilluffo, M. C., Crouch, R. K. & Fain, G. L. Opsin activation of transduction in the rods of dark-reared *Rpe65* knockout mice. *J. Physiol.* **568**, 83–95 (2005).

Acknowledgements

This work was supported by NIH R01 Grants EY011713, EY024379 (G.H.T.) and EY0001844 (G.L.F.), the Charles Kenneth Endowed Professorship (G.H.T.), the National Eye Institute Core Grant P30EY00331, and a Research to Prevent Blindness Unrestricted Grant to the Jules Stein Eye Institute. T.X. was supported in part by a China Scholarship Council scholarship. We thank Wayne Hubbell and Alapakkam Sampath for helpful discussions. We also thank Roxana Radu, Tamara Lenis and Jeremy Cook for their useful comments on the manuscript. Finally, we thank Nicholas Bischoff for his technical assistance.

Author contributions

J.J.K. designed and performed the experiments on bovine OS, mouse retinas, and live mice. T.X. designed and performed experiments on photoisomerization of *N*-ret-PE in solution and the quantum efficiency determination. N.T.I. helped design and performed whole-retina and suction-electrode cone recording experiments. A.T. performed experiments on OS and in live mice. H.H. performed experiments on OS and mouse retinas. G. L.F. helped design the experiments in Fig. 5, analyzed data from whole-retina and suction-electrode cone recording experiments, and wrote this section of the manuscript. G.H.T. conceptualized the study, analyzed the data, and wrote the manuscript.

Additional information

Supplementary Information accompanies this paper at doi:10.1038/s41467-017-00018-4.

Competing interests: The authors declare no competing financial interests.

Reprints and permission information is available online at http://npg.nature.com/reprintsandpermissions/

Publisher's note: Springer Nature remains neutral with regard to jurisdictional claims in published maps and institutional affiliations.

SUPPLEMENTARY INFORMATION

SUPPLEMENTARY FIGURES

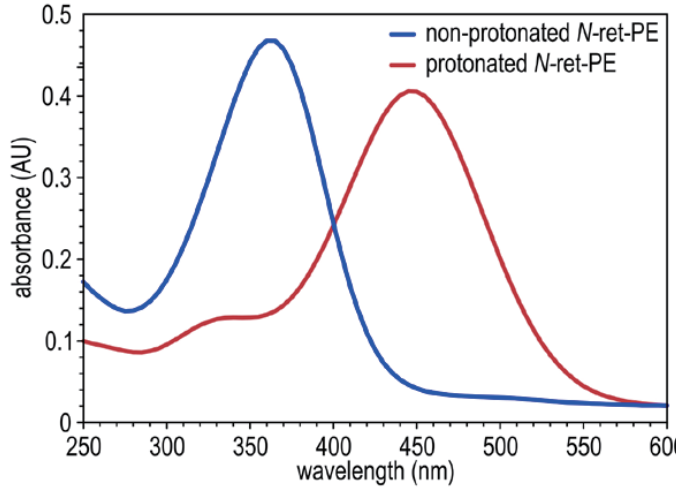

Supplementary Figure 1. Absorbance spectra of protonated and non-protonated *N*-ret-PE. Absorbance spectra for synthetic *N*-ret-PE were acquired in acidified (red curve) or alkalinized (blue curve) methanol. The λ_{max} is 450 nm for protonated- and 365 nm for non-protonated-*N*-ret-PE.

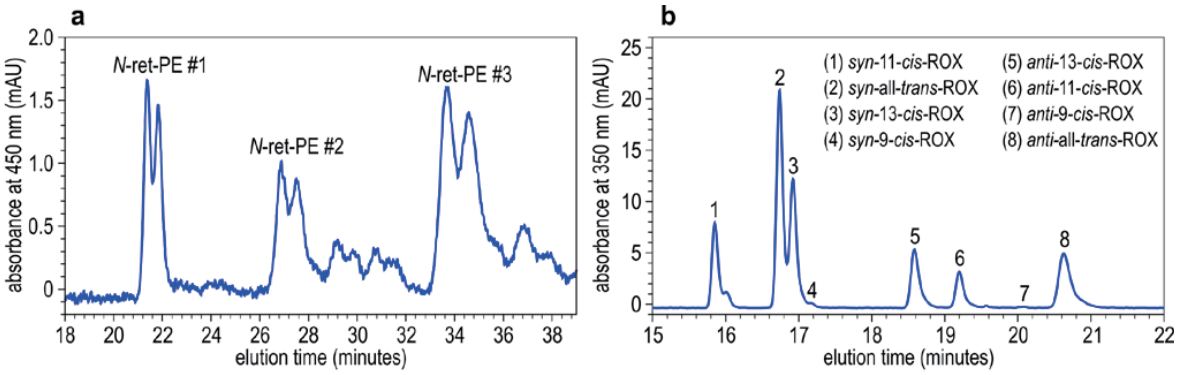

Supplementary Figure 2. Quantitation of *N*-ret-PE and constituent retinaldehydes in dark-adapted mouse retinas. (a) Reverse-phase chromatogram. Phospholipids were extracted from dark-adapted mouse retinas and separated by reverse-phase LC. An excerpt of the chromatogram is shown here. Three doublet peaks were identified with λ_{max} = 450 nm (*N*-ret-PE #1, *N*-ret-PE #2 and *N*-ret-PE #3), representing different fatty-acyl forms. Fractions containing these peaks were collected and pooled. **(b)** Normal-phase chromatogram. The pooled *N*-ret-PE sample was reacted with hydroxylamine to form retinaldehyde oximes, which were separated by normal-phase LC. An excerpt of the chromatogram containing the retinaldehyde oximes is shown. The *syn*- and *anti*-oximes of the four retinaldehyde isomers found are identified in the inset. Retinaldehyde levels are shown in Table 1.

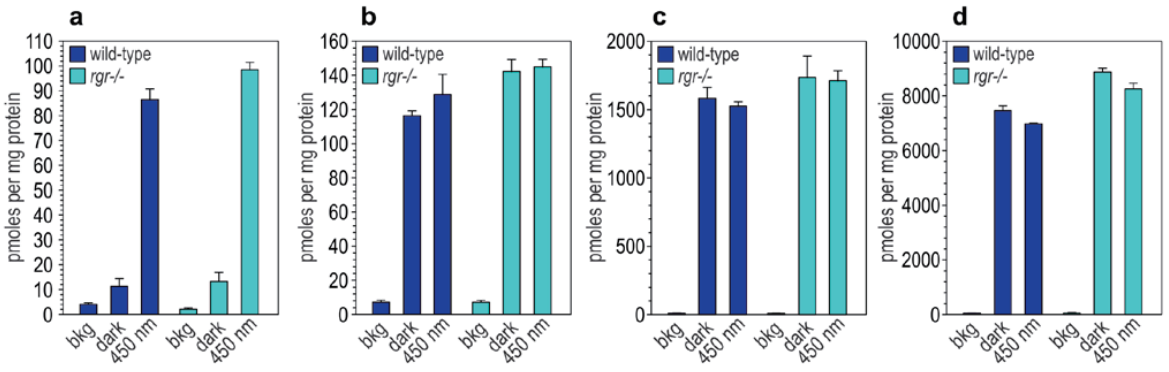

Supplementary Figure 3. Blue-light dependent synthesis of 11cRAL by wild type and *Rgr-/-* mouse retinas. Homogenates of retinas from wild type and *Rgr-/-* mice were photobleached to remove endogenous retinoids and incubated with atROL in the dark or during exposure to 450-nm light. Homogenates then were extracted into hexane and analyzed by normal phase LC. The retinaldehyde isomers: **(A)** 11cRAL, **(B)** 9cRAL, **(C)** 13cRAL, and **(D)** atRAL are shown as pmoles per mg protein in retinas immediately post-bleach (bkg), following incubation in the dark (dark), and following incubation in 450-nm light (450 nm). The dark and 450-nm light exposed samples were incubated with at-retinol. Error bars show mean ± S.D. (n=4). Note the approximately eight-fold higher 11cRAL in wild type and *Rgr-/-* retina homogenates incubated in 450-nm light versus darkness. Also note the similar levels of 11cRAL in wild type and *Rgr-/-* homogenates incubated in 450-nm light.

Chapter 4: General discussion: Significance of the current study, its limitations and future research directions

As one of the primary senses, vision is crucial to human beings and many vertebrates. A continuous supply of visual chromophore is essential for proper visual function. The disruption of visual cycle(s) components has been related to a variety of retinopathies, including retinitis pigmentosa, Stargardt disease, Leber congenital amaurosis, etc.(Liu, Chen et al. 2016). Strategies for the treatment of these diseases include but are not limited to: (1) gene therapy, (2) stem cell-based therapy, (3) pharmacological chromophore (or its analogs or derivatives) supplementation, (4) reducing toxic product formations (such as all-*trans*-retinal and N-retinylidene-N-retinylethanolamine (A2E)) by a controlled inhibition of visual cycle, chemical sequestration of toxic products or the administration of deuterium-enriched vitamin A (isotope effect) (Travis, Golczak et al. 2007, Kiser and Palczewski 2016, Zarbin 2016). As discussed (Kiser and Palczewski 2016), several chemicals are under active research to treat these diseases, such as 9-*cis*-retinoids (as a pharmacological supplement for 11-*cis*-retinal) (Van Hooser, Aleman et al. 2000, Koenekoop, Sui et al. 2014), retinylamine (a visual cycle inhibitor) (Golczak, Kuksa et al. 2005), primary amines (as all-*trans*-retinal sequesters) (Maeda, Golczak et al. 2011).

In this study, we performed both *in vitro* characterization of DES1 using biochemical methods **(Chapter 2.1)** and *in vivo* studies using a DES1 knockout mouse model **(Chapter 2.2)**. DES1 has been identified as a retinoid isomerase and a strong candidate for Isomerase II (Kaylor, Yuan et al. 2013). These studies promote our understanding of the alternate visual cycle and may provide potential therapeutic targets for retina diseases caused by pathological retinoid metabolism. In this study, competent DES1 inhibitors, such as ascorbic acid, NEM, DCPIP, HMB, 4-hydroxy-TEMPO and

PTMIO have also been identified **(Chapter 2.1)**, which could have the potential to be used as novel visual cycle inhibitors and facilitate new drug development.

Based on current knowledge, visual chromophore regeneration in vertebrates is predominantly mediated by enzymes, such as those in the canonical and alternate visual cycles. In this study, we demonstrate that functional visual pigment can also be regenerated in mammals under blue light through the formation of a photoactive intermediate, N-ret-PE **(Chapter 3)**. Possible involvement of N-ret-PE in visual chromophore regeneration has been described in the early literature (Shichi and Somers 1974, Shichi and Somers 1975). However, due to the limited knowledge at the time, these studies were not complete. Different from photoreversal (Williams 1964, Arnis and Hofmann 1995, Grimm, Reme et al. 2000, Furutani, Kandori et al. 2003), such an N-ret-PE-mediated photoregeneration pathway in this study is, to our knowledge, a new finding. It demonstrates that, like certain insects, vertebrates can also take advantage of photoisomerization for chromophore regeneration, albeit through a different mechanism. Interestingly, blue light was thought to be hazardous, causing photochemical damage to the retina (Algvere, Marshall et al. 2006). Our new finding may promote the comprehensive understanding of the role of blue light from a different angle. Furthermore, this finding also highlights that light should be taken into consideration in future retinoid and visual cycle studies, which are currently performed in the dark (under dim red light) most of the time. Also, how the supply of chromophore to photoreceptors can keep up with the fast consumption rate in bright light condition is a difficult question to answer. This photoregeneration mechanism, with a quantum efficiency of N-ret-PE comparable to that of opsins **(Chapter 3.2, Fig.3)**, may provide a

partial but adequate answer, as the contribution of this mechanism can increase in parallel with the light intensity and occurs very fast.

However, we also realize that limitations do exist in this study. (1) Although we have identified DES1 as a strong candidate for the Isomerase II in the retina (Kaylor, Yuan et al. 2013), the evidence was mainly obtained from *in vitro* biochemical studies. Efforts to confirm such a role of DES1 in the retina have been made by characterizing a Des1 knockout mouse model **(Chapter 2.2)**. However, the key point, their abilities to recover cone sensitivity following a bleach, has not been tested. Future studies are needed to fully address this. (2) In our experiments to characterize the biochemical properties of DES1, multiple inhibitors were used, such as cytochrome b5 electron transfer inhibitors, spin trap/probe reagents and iron chelators. However, it is possible that due to specificity issues and other "off-target" effects of these inhibitors, alternative interpretations of the results exist. (3) When it comes to the question whether or not a carbocation or a radical intermediate is involved in the catalytic process of DES1, although our data support a possible radical intermediate **(Chapter 2.1)**, the exact species of the intermediate cannot be confidently determined. (4) In this study, attempts to identify a specific cone RDH were made **(Chapter 2.3)**. However, the identification of such an enzyme remains a mystery. In our study, due to limited resources, exhaustive investigations were not completely performed. (5) We have demonstrated that blue light promotes the regeneration of functional visual pigments in mammals **(Chapter 3.2)**, but the extent to which this pathway contributes to visual pigment regeneration remains to be fully investigated. Although the quantum efficiency of N-ret-PE was determined and an estimation of 15% contribution to cone pigment regeneration was estimated

(Chapter 3.2), the estimation was only based on a limited number of physiological tests. Further detailed and more sophisticated determinations are still needed. (6) Other limitations of this study may include unoptimized experimental conditions, technical imperfections, shortage of complete knowledge for experiment design as well as limited replicates and high variations in certain tests, etc.

In this dissertation, several questions remain unanswered, requiring future research. Examples of these open questions include but not are limited to: (1) Determining whether DES1 is indeed the Isomerase II. This is a fundamental question. Electrophysiological studies may be highly helpful in this regard. Possible future experiments may include the generation of a rod α-transducin (Gnat1) and Des1 double knockout mouse line, whose rod photoreceptors do not generate light photoresponses due to the deficiency of Gnat1 (Calvert, Krasnoperova et al. 2000). This allows for the differentiation of cone photoresponses from an overwhelming number of rods. With this powerful genetic mouse model, *ex vivo* transretinal ERG can be performed on the retinas of Gnat1-/- Des1-/- and Gnat1-/- Des1+/+ mice. A significantly reduced recovery of photosensitivity following a bleach in Des1-/- mice is expected if DES1 is the Isomerase II. (2) After confirming the role of DES1 in the alternate visual cycle, further biochemical characterizations regarding its mechanisms would be interesting to carry out. Electron paramagnetic resonance (EPR) and electron-nuclear double resonance (ENDOR) spectroscopies on purified DES1 protein may be among the most interesting studies to determine the species of the intermediates in DES1 catalyzed isomerization process (Kispert, Konovalova et al. 2004, Ligia Focsan, Magyar et al. 2015). (3) Crystallizing DES1 and performing structural analysis. (4) Generating Rpe65-/- and

Des1-/- double knockout, Gnat1-/-, Rpe65-/- Des1-/- triple knockout mice and performing biochemical and electrophysiological experiments to address the contributions of different visual cycle pathways, including the N-ret-PE photoregeneration pathway. (5) Performing a more intensive candidate search or a high throughput analysis to identify more cone RDH candidates and characterize their functions and roles in the cone pigment regeneration. (6) Since ABCA4, a member of the A-subfamily of ATP-binding cassette (ABC), is an N-ret-PE importer (Quazi, Lenevich et al. 2012), it is also worth investigating the effect of N-ret-PE photoregeneration in wild type and ACBA4 deficient mice.

In summary, the findings presented in this study greatly advance our comprehension of chromophore regeneration mechanisms in vertebrates. This study may also provide valuable insights for retinoid studies, clinical practice on visual cycle-related retina diseases, and the development of novel treatments for these diseases. However, as always, this study has its limitations and further research is needed to address these unanswered questions.

References

Algvere, P. V., J. Marshall and S. Seregard (2006). "Age-related maculopathy and the impact of blue light hazard." Acta Ophthalmol Scand **84**(1): 4-15.

Arnis, S. and K. P. Hofmann (1995). "Photoregeneration of bovine rhodopsin from its signaling state." Biochemistry **34**(29): 9333-9340.

Calvert, P. D., N. V. Krasnoperova, A. L. Lyubarsky, T. Isayama, M. Nicolo, B. Kosaras, G. Wong, K. S. Gannon, R. F. Margolskee, R. L. Sidman, E. N. Pugh, Jr., C. L. Makino and J. Lem (2000). "Phototransduction in transgenic mice after targeted deletion of the rod transducin alpha -subunit." Proc Natl Acad Sci U S A **97**(25): 13913-13918.

Furutani, Y., H. Kandori and Y. Shichida (2003). "Structural changes in lumirhodopsin and metarhodopsin I studied by their photoreactions at 77 K." Biochemistry **42**(28): 8494-8500.

Golczak, M., V. Kuksa, T. Maeda, A. R. Moise and K. Palczewski (2005). "Positively charged retinoids are potent and selective inhibitors of the trans-cis isomerization in the retinoid (visual) cycle." Proc Natl Acad Sci U S A **102**(23): 8162-8167.

Grimm, C., C. E. Reme, P. O. Rol and T. P. Williams (2000). "Blue light's effects on rhodopsin: photoreversal of bleaching in living rat eyes." Invest Ophthalmol Vis Sci **41**(12): 3984-3990.

Kaylor, J. J., Q. Yuan, J. Cook, S. Sarfare, J. Makshanoff, A. Miu, A. Kim, P. Kim, S. Habib, C. N. Roybal, T. Xu, S. Nusinowitz and G. H. Travis (2013). "Identification of DES1 as a vitamin A isomerase in Muller glial cells of the retina." Nat Chem Biol **9**(1): 30-36.

Kiser, P. D. and K. Palczewski (2016). "Retinoids and Retinal Diseases." Annu Rev Vis Sci **2**: 197-234.

Kispert, L. D., T. Konovalova and Y. Gao (2004). "Carotenoid radical cations and dications: EPR, optical, and electrochemical studies." Arch Biochem Biophys **430**(1): 49-60.

Koenekoop, R. K., R. F. Sui, J. Sallum, L. I. van den Born, R. Ajlan, A. Khan, A. I. den Hollander, F. P. M. Cremers, J. D. Mendola, A. K. Bittner, G. Dagnelie, R. A. Schuchard and D. A. Saperstein (2014). "Oral 9-cis retinoid for childhood blindness due to Leber congenital amaurosis caused by RPE65 or LRAT mutations: an open-label phase 1b trial." Lancet **384**(9953): 1513-1520.

Ligia Focsan, A., A. Magyar and L. D. Kispert (2015). "Chemistry of carotenoid neutral radicals." Arch Biochem Biophys **572**: 167-174.

Liu, X., J. Chen, Z. Liu, J. Li, K. Yao and Y. Wu (2016). "Potential Therapeutic Agents Against Retinal Diseases Caused by Aberrant Metabolism of Retinoids." Invest Ophthalmol Vis Sci **57**(3): 1017-1030.

Maeda, A., M. Golczak, Y. Chen, K. Okano, H. Kohno, S. Shiose, K. Ishikawa, W. Harte, G. Palczewska, T. Maeda and K. Palczewski (2011). "Primary amines protect against retinal degeneration in mouse models of retinopathies." Nat Chem Biol **8**(2): 170-178.

Quazi, F., S. Lenevich and R. S. Molday (2012). "ABCA4 is an N-retinylidene-phosphatidylethanolamine and phosphatidylethanolamine importer." Nat Commun **3**: 925.

Shichi, H. and R. L. Somers (1974). "Possible involvement of retinylidene phospholipid in photoisomerization of all-trans-retinal to 11-cis-retinal." J Biol Chem **249**(20): 6570-6577.

Shichi, H. and R. L. Somers (1975). "Effect of the physical state of phospholipid on rhodopsin regeneration from retinylidene phospholipid." Photochem Photobiol **22**(5): 187-191.

Travis, G. H., M. Golczak, A. R. Moise and K. Palczewski (2007). "Diseases caused by defects in the visual cycle: retinoids as potential therapeutic agents." Annu Rev Pharmacol Toxicol **47**: 469-512.

Van Hooser, J. P., T. S. Aleman, Y. G. He, A. V. Cideciyan, V. Kuksa, S. J. Pittler, E. M. Stone, S. G. Jacobson and K. Palczewski (2000). "Rapid restoration of visual pigment and function with oral retinoid in a mouse model of childhood blindness." Proc Natl Acad Sci U S A **97**(15): 8623-8628.

Williams, T. P. (1964). "Photoreversal of Rhodopsin Bleaching." J Gen Physiol **47**: 679-689.

Zarbin, M. (2016). "Cell-Based Therapy for Degenerative Retinal Disease." Trends Mol Med **22**(2): 115-134.